Republic of Iraq
Ministry of Higher Education and
Scientific Research
University of Baghdad
College of Education for Pure Science
(Ibn -Al-Haitham)

Stopping Power and range of heavy ions in human body tissues

A Thesis Submitted To

The Council of College of Education for Pure Science Ibn Al- Hatham /Baghdad University in Partial Fulfillment of the Requirements for the Degree of Doctor of Philosophy (Ph.D) in Physics

By

Zeena Jameel Raheem

B.Sc. in Physics, College of Education for Pure Science Ibn Al - Haitham, University of Baghdad in 2007
M.Sc. in Nuclear Physics, College of Education for Pure Science Ibn Al - Haitham, University of Baghdad in 2010

Supervised By

Prof. Dr. Bashair Mohammed Saied

2019A.D.   **1440 A.H.**

بِسْمِ اللَّهِ الرَّحْمَٰنِ الرَّحِيمِ

قَالُوا۟ سُبْحَٰنَكَ لَا عِلْمَ لَنَآ إِلَّا مَا عَلَّمْتَنَآ إِنَّكَ أَنتَ ٱلْعَلِيمُ ٱلْحَكِيمُ ﴿٣٢﴾

صدق الله العظيم

(سورة البقرة الآية / ٣٢)

<u>**Supervisor's Certification**</u>

I certify that this thesis titled " *Stopping Power and Range of Heavy Ions in Human Body* " was prepared by (*Zeena Jameel Raheem*), under my supervision at the Certification University of Baghdad/ Education College for Pure Science Ibn Al-Haitham / Department of Physics in partial fulfillment of the requirements for the degree of Doctor of philosophy in Physics.

Signature:

Supervisor: Prof. Dr. Bashair Mohammed Saied

University of Baghdad/ College of Education for Pure Science (Ibn-Al-Haitham) / Department of Physics

Date. 28 / 7 /2019

In view of the available recommendations, I forward this thesis for debate by the examination committee.

Signature: S . A . Maki

Name: Dr. Samir Ata Maki

Titel: Professor.

University of Baghdad/ College of Education for Pure Science (Ibn-Al-Haitham) / Department of Physics
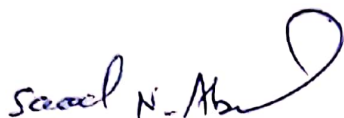
Date: 28 / 7 / 2019

<u>Certification of Examiners</u>

We certify, that we have read the thesis titled " *Stopping Power and Range of Heavy Ions in Human Body* " presented by *Zeena Jameel Raheem* and as an examining committee, we examined the student on its contents, and in what is related to it, and that in our opinion it meets the standard of a thesis for the degree of Doctor of Philosophy (Ph.D) in Physics.

<u>**(Chairman)**</u>
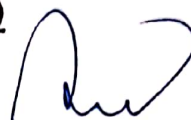
Signature: *Saad N. Ab*

Name: Prof. Dr. Saad Naji Abood

Title: University of Nahrain

Date: 1 /12/ 2019

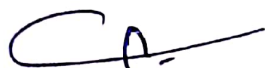<u>**(Member)**</u>

Signature:

Name: Prof. Dr. Raad Hmeed

Title: University of Baghdad

Date: 26 / 11 / 2019

<u>**(Member)**</u>

Signature:

Name: Prof. Dr. Asia H.Al-Mashhadani

Address: University of Baghdad

Date: 1 / 12/ 2019

<u>**(Member)**</u>

Signature:

Name: Assist. Prof. Dr. Nada F. Kadhim

Address: University of Al- Mustansiriyah

Date: 28/11/ 2019

<u>**(Member)**</u>

Signature: Ahmed

Name: Assist. Prof. Dr. Ahmed Fadhil Mkhaiber

Address: University of Baghdad

Date: 27/11 / 2019

<u>**(Supervisor)**</u>

Signature:
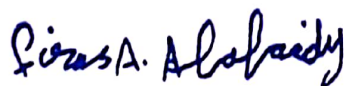
Name: Prof. Dr. Bashair Mohammed Saied

Address: University of Baghdad

Date: 27/ 11 2019

Approved by the Dean of College of Education for Pure Science (Ibn Al-Haitham) / University of Bagdad

Signature: *Firas A. Alobaidy*

Name: Assist Prof. Dr. Firas Abdulhmeed Abdullatif

Behalf / the dean of Education College for pure science /Ibn Al Haitham University of Baghdad

Dedication

To my parents ....

Symbol of love and sacrifice

To my family...............

My beloved husband (Ali), companion of my

life .and my daughters (Naya and Lana).

To The spirit of my martyr brother and sisters.........

Springs of love and affection.

Zeena

<u>Acknowledgements</u>

Abstract

Nuclear physics science has participated significantly to the development of the use of heavy ions in the treatment of tumors due to their ability to kill the abnormal tissues with high accuracy without affecting the surrounding healthy tissues for tumor. Moreover, their ability to ionize the infected tissue and thus destroy the cancer cells with the small dose absorbed from radiation. Therefore an accurate description of the energy loss for heavy ion and its range within the tissue should be provided.

In this study, the stopping power and range for heavy ions (^{7}Li , ^{12}C , ^{16}O,^{19}F) that interaction with eighth tissues of the Human body (Adipose , Blood, Breast, Brain ,Lung , Muscle, Bone, Skin) tissues were calculated using six methods (SRIM , SRIM Dictionary, CasP program , PASS program , MSATR program, and Bethe formula) in energy range (0.025-1000)MeV. Some small differences in the stopping power values were observed by using the six methods and the necessary explanations causing these differences are explained , Using the Matlab 2015 program, the semi-empirical formula for calculating the total energy loss of heavy ions and their range in these tissues were produced through knowing heavy ions energy, as were calculated the Liner Energy Transfer (LET), thickness of these tissues and the stopping time of heavy ion in these tissues. As well as were calculated dose, equivalent and effective dose for these heavy ions.

The results are displayed that the increasing of values of total energy loss with the increase of atomic number z for the falling particle, this is due to the mass stopping power is proportional to z^2 of falling particle. As well as when heavy ions are used, the acute Bragg peak can be formed to deposit most of the heavy ion energy in the tumor mass in order to achieve the best treatment and less damage to tissues surrounding the tumor.

Comparing our results of the calculated mass stopping power of adipose tissue and bone tissue with ICRU-73 was found very good agreement between them.

List of some Symbols

Symbols	Description
δ – rays	Dealta –ray
RBE	The relative biological efficacy
LET	Linear energy transfer
i	The number of ion pairs produced per unit path
W	The average amount of energy lost from heavy particles in the production of a pair of ion
WAT	White adipose tissue
BAT	Brown adipose tissue
α	Alpha particle
ICRU	International commission on radiation units and measurement
a	the classical atomic radius
b	the size of the classical impact parameter
σ	specific cross section (probability)
$(-dE/\rho dx)$	Mass stopping power
ρ	Density of material or target or tissue
ν	the frequency
$\bar{\nu}$	the mean frequency
Pc	The particle momentum
N_e	the density of electrons
ω	orbital frequency
W_R	The radiation weighting factor
D	Absorbed dose
ICRP	International commission on radiological protection
W_T	Tissue weighting factor
n	The number of electrons per unit volume in the material
m_0	Rest mass of electron
v	The speed of the particle
e	Electron charge
I	Mean excitation energy of the target
c	Velocity of light
E	Energy of particle
M	Mass of particle
Q_{max}	The maximum energy transfer
h	Plank constant
b_{max} and b_{min}	The maximum and minimum impact parameters.
$\delta/2$	The density effect correction
C/Z	The shell correction term

ΔE	An energy transfer
w_i	The weight fraction of i th kind of atom in a compound:
$Z_{effetive}$	an effective atomic number
A_i	Atomic weight of i the element
Z_i	Atomic number of i the element
$N_i Z_i$	The electron densities
n_a	Concentrate of atoms in the material.
N_A	The Avogadro number
A	The atomic mass of the material (in g/mol)
E_0	The initial energy for heavy ion
E_1	The smaller energy for heavy ion
R	The range of heavy ion into target
CSDA	the continuous slowing down approximation
Rmax	the Maximum for Penetration
T	Thickness of target
t	Stopping time
Gy, mGy	Gray) Absorption dose measurement units(
Sv , rem	Sievert) Equivalent and effective dose measurement units(
H_T	The equivalent dose
Q	The quality factor
H_E	The effective dose equivalent
CAB	the Core and Bond
ω	orbital frequency
z	particle atomic number
Z	target atomic number

Chapter One

Introduction

Introduction

(1.1) Preface

Knowledge of the stopping power, energy loss, range, straggling and equivalent dose rate of ions in air, tissue and polymers are very important in many research and application fields, such as radiation dosimetry, radiation biology (such as cell lethality, cytogenesis changes, mutagenesis and DNA recombination), radiation chemistry, radiotherapy and nuclear physics[1].

Heavy charged particles traversing matter lose energy primarily through the ionization and excitation of atoms [2], it is well known that the ionization value in tissues is proportional to cells damage. Therefore, the main aims for calculating the mean energy loss per unit path length, the expression of the stopping power and the range of ions that interaction with the material are :

- For evaluate the amount of the total loss of particle energy .
- For assess the Bragg curve and the radiation dose, which is very important in radiotherapy and thus estimate the potential damage to the vicinity of the tissue [3].

(1.2) Classification of Radiation

Radiation is classified into two main categories depending on its ability to ionize matter, as shown in Figure (1-1). The ionization potential of atoms, i.e. the minimum energy required to ionize an atom, ranges from a few electron volts for alkali elements to 24.6 eV for helium which is in the group of noble gases. Ionization potentials for all other atoms are between the two extremes.

1. Non-ionizing radiation cannot ionize matter because its energy is lower than the ionization potential of matter. Include ultraviolet radiation, visible light, infrared photons, microwaves and radio waves.
2. Ionizing radiation can ionize matter either directly or indirectly because its energy exceeds the ionization potential of matter. Include X rays, γ rays, energetic neutrons, electrons, protons and heavier particles. It can be categorized into two types:

a. Directly ionizing radiation (charged particles) electrons, protons, alpha particles, and heavy ions deposit energy in the medium through direct Coulomb interactions between the directly ionizing charged particle and orbital electrons of atoms in the medium.

b. Indirectly ionizing radiation (neutral particles) photons (x rays, gamma rays), and neutrons deposit energy in the medium through a two-step process:

- In the first step a charged particle is released in the medium (photons release electrons or positrons, neutrons release protons or heavier ions) .

- In the second step, the released charged particles deposit energy to the medium through direct Coulomb interactions with orbital electrons of the atoms in the medium.

Both directly and indirectly ionizing radiation can affect human tissue, thereby enabling the use of ionizing radiation in medicine for both imaging and therapeutic procedures [4].
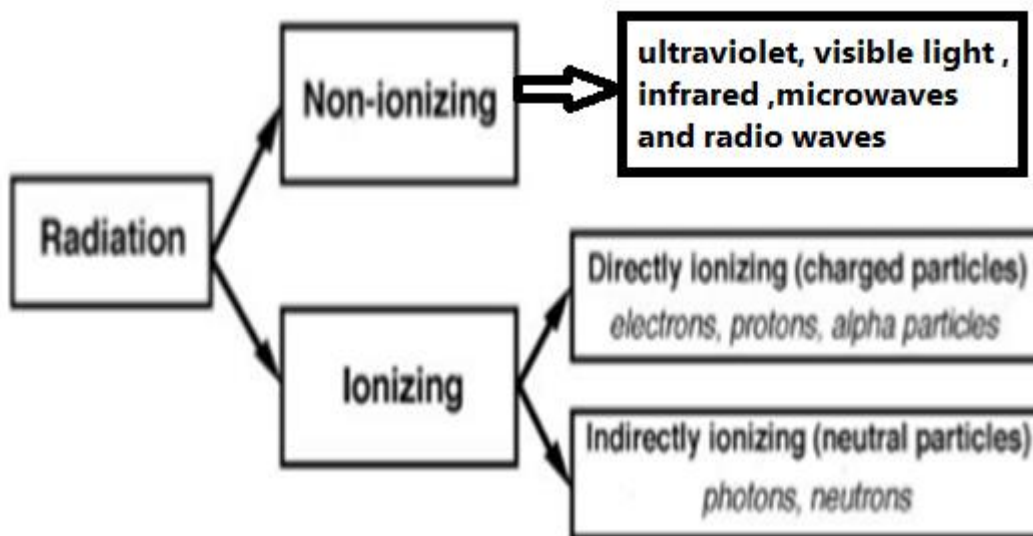
Fig. (1-1) Classification of radiation [4].

(1.3) Passage of Ionizing Particles through Matter

Charged particles passing through matter lose their kinetic energy by dominant electromagnetic interactions which consist of excitation and ionization atoms along their passage. This process usually called collision loss process or collision process. Fast electrons resulting from ionization processes are called δ-rays. If sufficiently energetic, these electrons

will also excite and ionize atoms. Thus, a secondary ionization process will take place. However, the deposited energy per unit path inside the medium is usually lower than the energy lost by collisions, because the fastest δ-rays can be completely absorbed far away from where they were generated or escape from the medium. Furthermore, deflections from the incoming direction are usually small, but become relevant in the final stage of fully absorbing processes [5].

(1.4) Passage of Ionizing Particles through Tissue

When the charged particle ionizes, or excites an atom, it losses energy until no longer has enough energy to interact, the final result of these energy losses is a minute rise in the temperature of the material of which the atom is a part. In this way, all energy stored in biological tissues is dissipated by ionizing radiation that increasing the vibrations of the atomic and molecular structure [6]. Based on the site of interaction this ionization can damage tissues directly by breaking the chemical bonds of important biological molecules (particularly DNA), or indirectly by creating chemical radicals from water molecules in the cells which attack the biological molecules chemically .

To a certain extent, these molecules are repaired by natural biological processes; however, the effectiveness of this repair depends on the extent of the damage. Obviously, if the repair is successful then no effect is observed, however, if the repair is faulty or not made at all, the cell may then suffer three possible :

1. Death of the cell.
2. An impairment in the natural functioning of the cell leading to somatic effects (i.e., physical effects suffered by the irradiated individual only) such as cancer.
3. A permanent alteration of the cell which is transmitted to later generations, i.e., a genetic effect .Figure (1-2) shows the sequence of events occurring in living matter exposed to radiation [7].
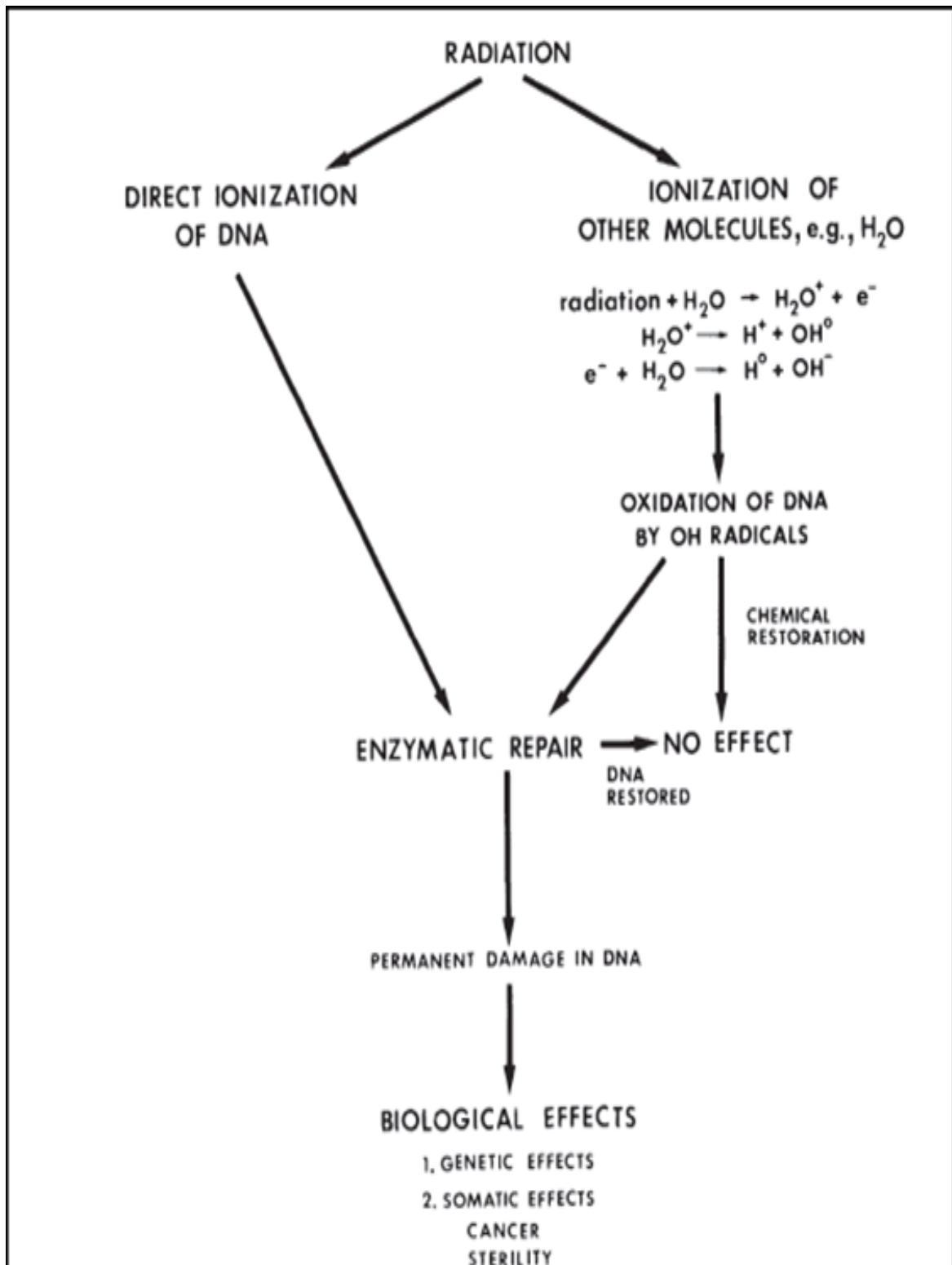
Fig. (1-2) Sequence of events occurring in living matter exposed to radiation [7].

(1.5) Heavy Charged Particles

Heavy charged particles are produced for use in radiotherapy through acceleration of nuclei or ions in cyclotrons, synchrotrons.

Heavy charged particle beams fall into the category of directly ionizing radiation and deposit their energy in tissue through coulomb interactions with orbital electrons of the absorber. As they penetrate into tissue, heavy charged particles lose energy but, in contrast to electrons, do not diverge appreciably from their direction of motion and therefore exhibit a distinct range in tissue. This range depends on the incident particle's kinetic energy and mass. Just before the heavy charged particle expended all of its kinetic energy, its energy loss per unit distance traveled increases drastically and this results in a high dose deposition at that point in tissue. As shown in Figure (1-3d), this high dose region appears close to the particle's range, is very narrow, and defines the maximum dose deposited in tissue. This peak dose is referred to as the Bragg peak and it characterizes all heavy charged particle dose distributions. Because of their large mass compared to the electron mass, heavy charged particles lose their kinetic energy only by interacting with orbital electrons of the absorber; they do not lose any appreciable amount of energy through bremsstrahlung interactions with absorber nuclei [4].
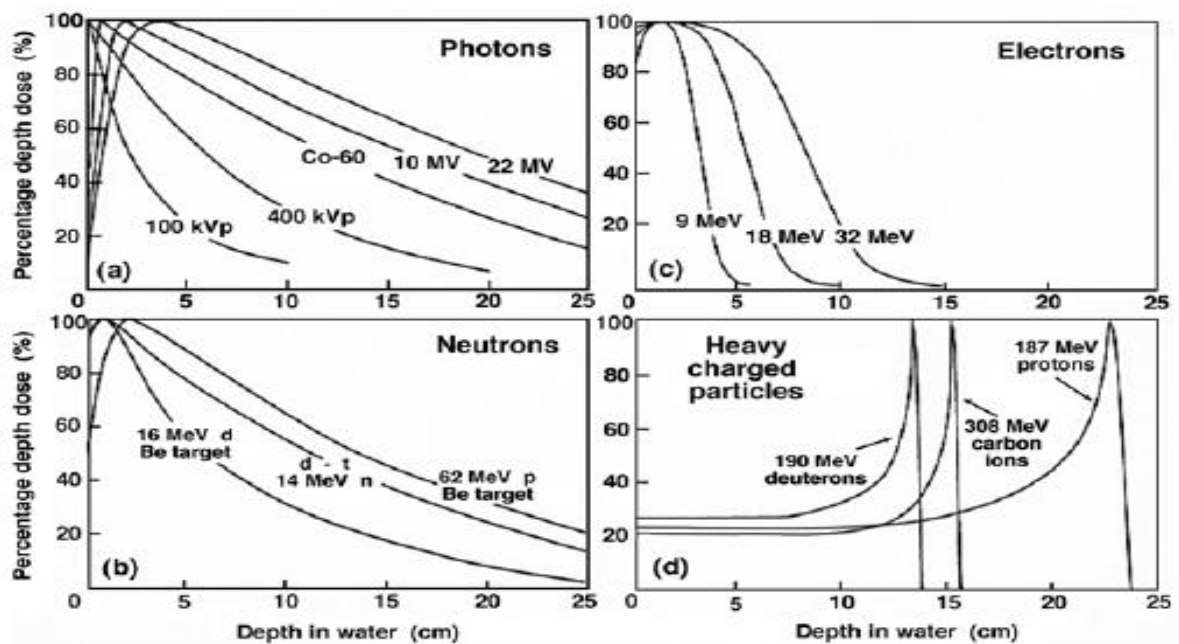
Fig. (1-3) Dose as a function of depth in water for types various from radiation beams and energies. Parts (a, b) are for indirectly ionizing radiation and parts (c, d) are for directly ionizing radiation [4].

(1.6) Heavy Ion Radiotherapy

Nuclear science has contributed significantly to the development of tumor therapy with heavy charged particles [8]. Radiation therapy uses the radiobiological effects of ionizing radiation (charged particles, neutrons, gamma rays or x-rays) to destroy tumor cells. The success of radiotherapy depends on the ability of the therapy system to concentrate the quantity (dose) of radiation on the target region (tumor). Ideally, a lethal while minimizing the irradiation of healthy adjacent tissues [9]. The motivation for the use of heavy particles in radiotherapy where their advantages compared to contemporary photon therapy in relative biological effectiveness (RBE) in tumor cells, compared to normal cells, better dose distributions or both [8], charged particles have a relatively well defined penetration range. The dominant mechanism by which charged particles lose their energies are inelastic interaction with the atomic electrons. They lose most of their energies near the end of their paths, at the so-called Bragg Peak .

In addition, heavy ions exhibit strong increase of the linear energy transfer (LET) in the Bragg peak as compared for photons or Light particles. The radiobiological advantage of high LET radiation in tumor therapy is well known from neutron therapy. Unlike in radiotherapy with neutron beams, in heavy ion radiotherapy the high LET region can also be conformed to the tumor [10].

Between 1977 and 1992, first clinical experiences have been made, especially with helium and neon ions at the Lawrence Berkeley Laboratory and many encouraging results (especially in skull base tumors and par spinal tumors) were achieved (Castro et al. 1994; Castro 1997). Although helium ions are very similar to protons in their biological properties, carbon or neon ions exhibit an increased relative biological effectiveness (RBE) in the Bragg peak as compared with the entrance region. For ions heavier than neon, the RBE in the entrance region is even higher than in the Bragg peak (like for argon). Another disadvantage of very heavy ions for radiotherapy is the increase of nuclear fragmentation processes, which leads to a fragment tail in the depth dose distribution that extends beyond the Bragg peak (see Fig 1-4). Currently the availability of heavy ion radiotherapy is limited, as worldwide only three facilities offer carbon ion radiotherapy: two hospital-based facilities in Japan [Heavy Ion Medical Accelerator (HIMAC), Chiba; Hyogo Ion Beam Medical Center (HIBMC), Hyogo and a physics research facility [10].
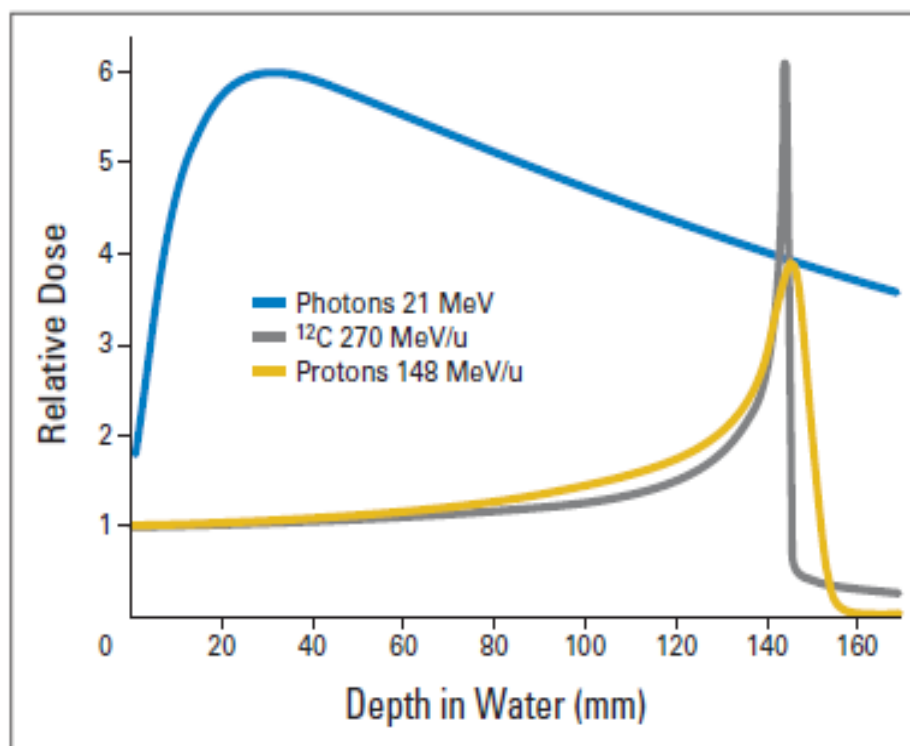
Fig (1-4) Bragg Curve for photons, protons, and carbon ions [11].

(1.7)The Bragg Curve

From the significant properties of the stopping power its reliance on the target thickness demonstrating in the Bragg peak [12]. when the heavy particle passes through an absorbent material, the rate of energy loss (-dE/dx) a significant increase as the particle energy decreases because increase of the target ionization cross section proportionally to the square of the ion velocity $\sim \upsilon^2$, and so, as the heavy particle lose energy, they cause more and more ionizations in their paths until they reach the highest point, known as the Bragg peak. After that point the particles have lost almost all of their energy and are quickly neutralized by attracting electrons from their surroundings. Figure (1-5) shows the Bragg curve [13].

In particular, this behavior is used in radiotherapy when requires delivery a high dose of radiation to deeply embedded malignant tissue with a minimum of damage to tissues surrounding the tumor.

In radiotherapy with heavy ionic radiation, Bragg peaks must be formed sharply to deposit most of the energy in the tumor mass because LET is relatively less before the Bragg peaks and then drops to zero after that; moreover, intensity and the position can be controlled by ion species and energy this physical characteristic of the heavy ion particles provides a much

7

better therapeutic ratio between the tumors and the natural tissues of the photons that do not appear in the Bragg peaks.
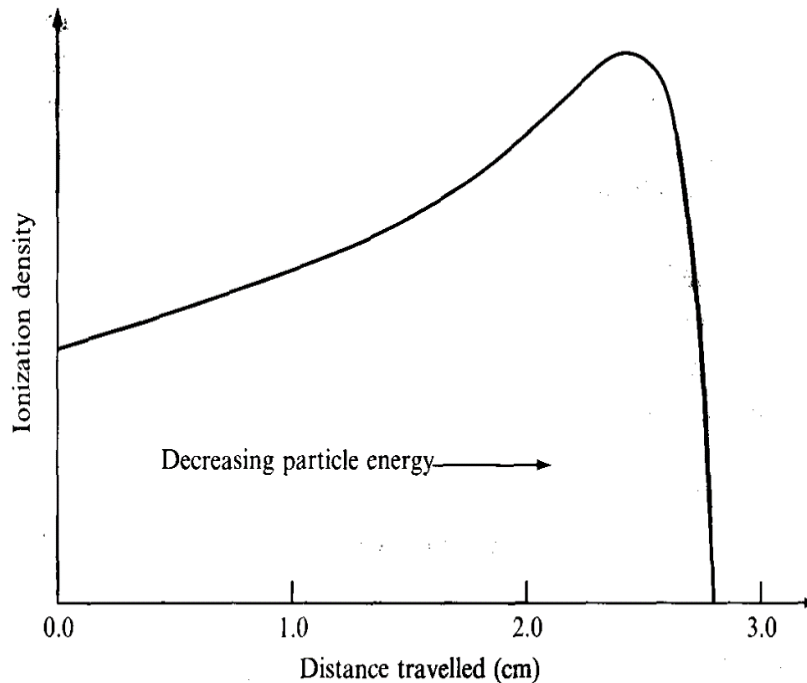
Fig. (1-5) The Bragg curve [13].

(1-8) Specific Ionization

Specific ionization (SI) is the total number of ion pairs produced per unit length of the path of the incident radiation [14] . Empirically, collision energy loss is measured by the number of ion pairs formed along the path of the charged particle path. Suppose that heavy charged particles lose the average amount of energy W in producing a pair of ion, electron and ion. Then the number of ion pairs produced per unit path is [15, 16].

$$i = \frac{1}{W}(-\frac{dE}{dx}) \dots \dots \dots (1-1)$$

The SI values of heavy ions are larger than those of electrons. Specific ionization increases with decreasing energy of the charged particle due to the increased probability of interaction at low energies. Therefore, toward the end of the travel, the charged particle shows a sharp increase in ionization. This peak ionization is called Bragg ionization. This phenomenon is predominant for heavy charged particles and is negligible for electrons [14].

8

(1-9) Characteristics of Heavy Ion

Heavy ion, in nuclear physics, any particle with one or more units of electric charge and a mass. Special types of accelerators are capable of producing fairly intense, high-energy beams of heavy ions, which are used in basic research and in Radiotherapy. Table (1-2) shows characteristics some of heavy ions that were used as projectiles for tissues [17].

Table (1-1) Characteristics some of heavy ions used in medicine.

Name of element	Symbol	Number of protons	Number of neutrons	Atomic weight (amu)	Electrons configuration	Valency	Atomic density atoms/cm³ x10²²
Lithium	Li	3	3	6.01512	$1s^2\ 2s^1$	1	4.633
Carbon	C	6	6	12.000	$[He]2s^22p^2$	4	11.296
Oxygen	O	8	8	15.9949	$[He]2s^22p^4$	2	5.367
Fluorine	F	9	10	18.998403	$[He]\ 2s^2\ 2p^5$	0	3.522

(1-10) *Types of Tissues*

(1-10-1) Adipose tissue

Adipose tissue is composed mostly of adipocytes, its play a key role in energy homeostasis. There are two types of adipose tissue, white adipose tissue (WAT) and brown adipose tissue (BAT), have been identified white fat cells are specialized to store chemical energy, brown adipocytes defend mammals against hypothermia, obesity and diabetes [18]. The chemical compositions of the adipose tissue are (H, C, N, O, Na, S, and Cl) [19].

(1-10-2) *Skin tissue*

The skin is the outer covering of the body, it helps to control and regulate the temperature of our bodies through sweating and expansion of blood vessels to cool the body. Skin layers are a complex combination of tissues that work together to form a basic control system. consists from water (65.3%), lipid (9.4%), protein (24.6%), [20] and some elements (H, C, N, O, Na, P, S, Cl, and K) [19].

(1-10-3) *Blood tissue*

Blood is body fluid in humans and other animals that delivers necessary substances such as nutrients and oxygen to the cells and transports metabolic waste products away from those same cells. the blood composition was taken to be (79 -80.8 %) water, (0.65%) lipid and (18.19%) protein [21] and other elements which are (H, C, N, O, Na, P, S, K, Cl and Fe) [19].

(1-10-4) Muscle tissue

Muscle tissue is soft tissue and leads to the ability of muscles to contract. It is formed during embryonic development through a process known as muscle formation. There are three types of muscle tissue: skeletal, cardiac and smooth muscle [22], In the lean somatic muscle they supposed 75% water, 20% protein, and other elements are (H , C, N , O , Na, P, Cl, K, and S) [19] .

(1-10-5) Lung tissue

The lungs are located in the chest on both sides of the heart in the rib cage. They are conical with a narrow round top at the top, and a large concave base that lies on the convex surface of the diaphragm [23]. The two main biological components of lung are water 79% ,and protein; in addition ,Lung contains lipid 3%,and traces of other elements are (H , C, N , O , Na, P, Cl, K, and S) [19].

(1-10-6) Breast tissue

Breast is a binary device in which females undergo dramatic changes in size, shape, and function in conjunction with the baby's growth, puberty, pregnancy, lactation, and postmenopausal regression [24,25] located on the upper abdominal region of the trunk of the primates. In females, it acts as a mammary gland, which produces and secrete milk and nourishes infants [26]. The chemical compositions of the breast tissue are (H , C, N , O , Na, P, Cl, and S) [19].

(1-10-7) Brain tissue

Brain tissue include: nerve cells (Grey matter) transfer signals of communication, and glial cells (white matter), which Responsible for neurons. [27]. the chemical compositions of the brain tissue are (H, C, N, O, Na, P, Cl, and K) [19]. The brain is supposed include by mass: Grey matter (50.0) %, white matter (50.0) %. [19].

(1-10-8) Cortical bone

There are two types of bone: trabecular (spongy or cancellers) bone and cortical (dense or compact) bone. One of the fundamental differences between cortical and trabecular bone is its apparent porosity. Apparent porosity is the ratio of the mass bone tissue in a specimen to the bulk volume of the specimen. Typical apparent densities for cortical bone and trabecular bone are 1.85 and 0.30 g/cm^3, respectively. Cortical bone accounts for approximately 80% of the skeletal mass [28]. The elements chemical for cortical bone are (H, C, N, O, Na, P, S, Mg, and Ca) [29].

(1-11) Previous Studies

1. Bonderup,(1967) studied the electronic stopping power of heavy particles that are irregularly penetrating the material and based on the ionization rate of the target material and used the quantum penetration theory for shells with energy below 100keV [30].

2. Northcliffe and Schilling. (1970) reported the electronic stopping power and range for representative ions of all atomic numbers $1 \leq Z \leq 103$ in 24 different material media at 38 energies distributed logarithmically throughout the region $0.0125 \leq E/m \leq 12$ MeV/amu. The media include twelve solid elements (Be, C, AI, Ti, Ni,Ge, Zr, Ag, Eu, Ta, Au, and U), nine gaseous elements (H, He, N, O, Ne, Ar, Kr, Xe, and Ra), and three compounds(polyethylene, Mylar, and water) [31].

3. Anthony, et al., (1981) studied the effect of the effective charge in the Beth-Bloke equation in calculating the stopping power of the heavier ions on solid targets within the energy range near the upper limit of the stopping power and explained the dependence of the stopping power on the charge state of the falling particle as well as the amount of charge within the target material [32].

4. Hubert, et al., (1990) Stopping powers and ranges are tabulated for all ions of atomic number $2 < Z < 103$ in the energy region $2.5 < E/A$ d 500 MeV/u for 36 solid materials. The calculations use stopping powers for αparticles and a new parameterization for the heavy-ion effective charge which is deduced from aset of about 600 experimental stopping-power values covering an energy range from 3 to 90 MeV/u for 15 incident heavy ions and 18 solid stopping materials [33].

5. Susuki et. al., (1994) studied the stopping power of the carbon element in which the H_2 ions pass when the hydrogen ions with 9.6MeV / amu and the carbon fiber chip

(1.5-8.5 mg / cm^2) found that the stopping power was (55.8 ± 4.6 (eV). cm^2 / mg). The loss of energy was computed and compared with the amount of energy loss from the Born approximation [34].

6. Takeshi and Bichsel, (1995) stopping power and range functions have been calculated for carbon ions in a number of compounds and tissues and are presented in the form of tables. With a suitable interpolation scheme [35].

7. Randhawa and Virk ,(1996) A comparative study of various stopping power and range formulations has been made by comparing the calculated stopping power and range values with corresponding experimental values for different projectiles, viz. H, He, Li, N, O, Al, Si, Xe, Au, Pb, Bi, U, etc. in different targets, e.g. Be, C, Al, Au, Pb, CR-39, Lexan, Mylar, LR-115, CH, (CH)n, TRIFOL-TN, etc. at various low and high energies. The present study has been undertaken in order to determine the best stopping power and range formulation for calibration of solid state nuclear track detectors [36] .

8. Ziegler ,(1999) calculated the stopping power of the effective light ions (H, He and Li) at energies higher than 1MeV / amu and concluded that the highest stopping power obtained was for the proton at (Au, Al) when energy of the proton is 1MeV . He explained the relationship between the projectile energy and the stopping power [37].

9. Helmut and Andreas , (2003) proposed empirical stopping power tables for ions from $_3$Li to $_{18}$Ar and from 0.001 to 1000 MeV/nucleon in solids and gases , based on large collection of experimental stopping powers taken from the literature and proposed their program MSTAR [38].

10. Bimbot , et al., (2005) in this report presented a critical survey on measurements and calculations of quantities governing the penetration of heavy ions through condensed and gaseous matter over an energy range from 1 keV/u upward. The focus is on the electronic stopping force (or stopping power) for ions from lithium to argon (Z1 = 3 –18), but attention is also given to energy-loss straggling and, to a lesser degree, multiple scattering and ranges. Stopping tables are given for 17 ions on 25 elemental and 34 compound materials covering energies from 0.025 – 1000 MeV/u [39].

11. Sun, et al. ,(2007) energy loss and energy loss straggling in a thin silicon nitride foil were measured for Li, B, C, O, S and Fe ions with energies between 0.4 and 4.0 MeV. The energy distribution of ions after passage of a 34 nm thick foil was measured by

an electrostatic deflector with 0.2% energy resolution. Energy loss values are in good agreement with SRIM calculations [40].

12. Nakamura, (2010) studied the electronic energy loss of heavy particles and explained that the electronic reactions of the charged particles in single collisions caused atomic ionization or mass excitation. He concluded that the peak energy loss for 90% of all collisions was less than 100eV [41].

13. Abuirqeba , (2011) a theoretical study of the calculation of electronic stopping power and range depending on the effective charge of heavy charged particles such as protons and oxygen ions falling on atomic targets such as uranium, lead [42].

14. Zainab,(2012) studied the effect of proton, helium or carbon irradiation on free radicals. TRIM-SRIM software version (1998 and 2003) used to compute the Bragg peak and calculate the effect of proton, helium and carbon ions against free radicals related to oxygen, nitrogen and halogen species [43].

15. Jin, et al., (2014) , electronic stopping powers for (Cl, Br, I, and Au) ions are determined experimentally in two important functional materials, SiC and SiO_2, based on a single ion technique, and new electronic stopping power values are derived over the energy regime from (0 to 15)MeV [44].

16. Msimanga, et al., (2015) stopping force measurement of Ti for ^{12}C, ^{16}O, ^{24}Mg, ^{27}Al and ^{63}Cu ions were carried out by heavy ion Time-of-Flight Elastic Recoil Detection (ToF-ERD) spectrometry and the results are compared with semi-empirical calculations by Ziegler's Stopping and Range of Ions in Matter (SRIM-2010) code , and calculations by Grande and Schiewietz's Convolution approximation for swift Particles (CasP 5.2) code [45].

17. Sig.mund, and Schinner, (2016) reported some highlights of heavy-ion stopping in the energy range where Bethe stopping theory breaks down. The main tools are binary stopping theory (PASS code), the reciprocity principle, and Paul's data base. Comparisons are made between PASS and three alternative theoretical schemes (CasP, HISTOP and SLPA) [46].

18. Metin and Mustafa ,(2017) present the consequences for the stopping power and range values of some human tissues at energies ranging from (1 MeV to 1 GeV) . The considered human tissues are lung, intestine, skin, larynx, breast, bladder, prostate and ovary. stopping power is calculated by considering the number of velocity-dependent effective charge and effective mean excitation energies of the target material. In this study used the Hartree-Fock-Roothaan (HFR) atomic wave function

to determine the charge density and the continuous slowing down approximation (CSDA) method for the calculation of the proton range. Electronic stopping power values of tissues results have been compared with the ICRU 44, 46 reports, SRIM, Janni and CasP data over the percent error rate [47] .

19. Osama, et al., (2017), studied Carbon Ion Radiotherapy: A Review of Clinical Experiences and Preclinical Research, with an Emphasis on DNA Damage/Repair [48]

20. Saad Nafea Yaqoob, (2018) studied the interaction of heavy ions (^{14}N, ^{20}Ne, ^{40}Ar, ^{84}Kr, ^{132}Xe, ^{235}U, ^{252}Cf) with human tissues (skin, trachea, ovary and prostate) in the range of energies (1-1000) MeV. The mass stopping power and the range of these ions were calculated using SRIM2013, CaSP2013 version5.2, SRIM Dictionary and Bethe Formula [49].

(1-12) Aim of the Study

1. Calculating total stopping power and the range for heavy ions (^{7}Li,^{12}C,^{16}O, and ^{19}F) in the elements of human (Adipose, Blood, Breast, Brain, Lung, muscle, Bone, Skin) tissues with energy (0.025- 1000) MeV using several methods for determine the best value stopping power in each tissue.

2. Comparison between the different methods which used in this study to determine the best method.

3. Finding a new formation of a semi- empirical equation representing the total stopping power distribution in terms of energy for each treated element .

4. Calculation the time required to stop a charged particle in an absorber tissue.

5. Determination the depth penetrated by the ions for the purpose to eliminate the tumor accurately and not to harm the healthy tissues adjacent to the tumor.

6. Determination the Bragg peak for each ion in each tissue in order to the sharp peak.

7. Determination the maximum value for the amount (LET), the absorbed dose, the equivalent dose and the effective dose. Provide the information for these quantities in order to achieve the best treatment and less harm to the patient.

Chapter Two

Theory

Theory

(2.1) Mechanisms of Charged – Particle Energy Loss

Mechanisms of energy loss for charged particles can be classified roughly into five categories:

1. Excitation and ionization of the absorbent target,
2. Excitation and ionization of the Projectile,
3. Electron capture,
4. Nuclear stopping ("Recoil loss"),
5. Emission of Electromagnetic radiation.

- For electrons, only processes (1, 4, and 5) are of important.

- For light ions, process (excitation and ionization of the absorbent target) dominates except at the low-speed end, as for electromagnetic radiation is negligible to very high energies.

- For heavier ions, processes (2 and 3) cannot be neglected in general and as well, nuclear stopping becomes relatively more interest at low and moderate velocities [39].

(2.2) Types of Charged-Particle Coulomb-Force Interactions

As a charged particle passes through a matter, It interacts (Coulomb interactions) with the nuclei and orbital electrons of the matter atoms. These interactions may be divided into three groups are shown schematically in Figure (2-1), depending on the classical atomic radius (a) of the absorber atom compared to the size of the classical impact parameter (b) of the charged particle trajectory:

1. b « a , Coulomb interaction of the charged particle with the external nuclear field of the absorber atom ("bremsstrahlung production")
2. b ≈ a , Coulomb interaction of the charged particle with orbital electron of the absorber atom ("hard collision")
3. b » a, Coulomb interaction of the charged particle with the whole absorber atom ("soft collision") [4].
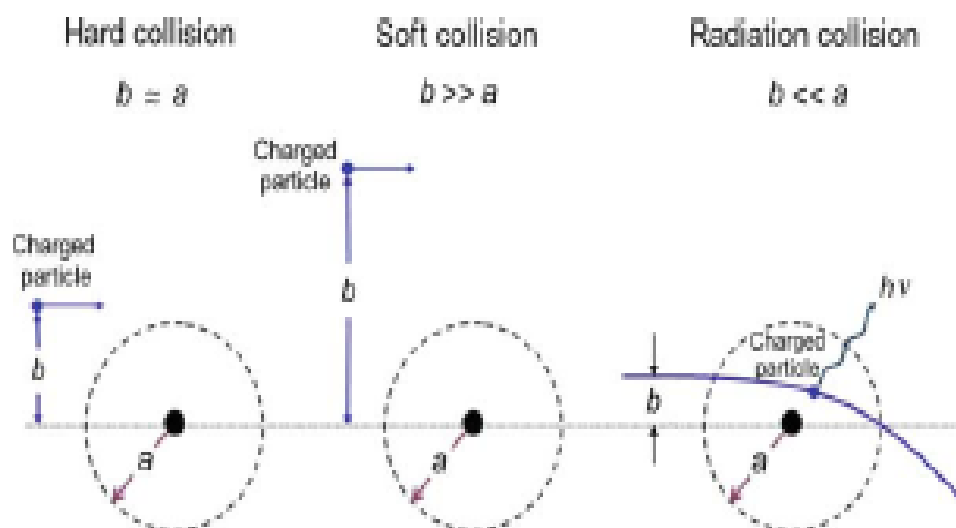
Fig. (2-1) Types of charged-particle coulomb-force interactions [4].

(2.2.1) Coulomb Interaction for Charged Particle with the Nucleus Field ("Radiation Collision")

The charged particle interacts mainly with the nucleus and undergoes either elastic or inelastic scattering possibly accompanied with a change in direction of motion. The vast majority of these interactions are elastic so that the particle is scattered by the nucleus but loses only an insignificant amount of its kinetic energy to satisfy the conservation of momentum requirement. However, a small percentage of the scattering interactions are inelastic and may result in significant energy loss for the charged particle accompanied by emission of x-ray photons. This type of interaction is called bremsstrahlung collision. At given particle acceleration, the probability for this type of interaction is inversely proportional to the square of the mass of the charged particle, making the bremsstrahlung production for charged particles other than electrons and positrons essentially negligible [4].

(2.2.2) Hard Collision

The charged particle may have a direct Coulomb impact interaction with a single atomic orbital electron and transfer to it a significant amount of energy. The interaction is referred to as hard or close collision. The orbital electron leaves the atom as a δ ray, and is energetic enough to undergo its own Coulomb interactions with absorber atoms. The number of hard collisions experienced by a charged particle moving in an absorber is generally small;

however, the energy transfers associated with hard collisions are relatively large, so that the particle loses roughly 50 % of its kinetic energy through hard collisions. The theories that govern hard collisions depend strongly on the characteristics of charged particles and generally assume that the orbital electron (δ ray) released through a hard collision is free before and after the interaction, since the kinetic energy transferred to it from the charged particle is much larger than its atomic binding energy [4] .

(2.2.3) Soft (Distant) Collision

The charged particle interacts with the whole atom and the whole atomic complement of bound electrons. The interaction is called a soft or distant collision. The energy transfer from the charged particle to a given bound electron is very small; however, the number of these interactions is large, so that approximately50% of energy loss by a charged particle occurs through these small-energy-transfer interactions that may cause atomic polarization, excitation or ionization through removal of a valence electron. In the energy region of soft collisions the expressions derived with a given theory are valid for all types of charged particles including electrons and positrons. [4].

(2.3) Stopping Power of Charged Particles

As a charged particle passes through an absorbing matter, it experiences a large number of interactions before its kinetic energy is spent, through of these interactions, the path of charged particle may alter (elastic or inelastic scattering), or it may lose some of its kinetic energy that will be transferred to a medium (collision loss) or to photons (radiation loss). The possible interactions between the charged particle and orbital electrons or the nucleus of the matter atoms is characterized by a specific cross section (probability) σ for the interaction [4].

The energy- loss of the charged particles pass through an absorbent medium depends on the characteristics of the particle and the medium.

The rate of energy loss per unit of path length by a charged particle in an absorbent medium is called the linear stopping power (−dE/dx), it's given in units of MeV/cm. Dividing the linear stopping power by the density ρ of the absorbent medium is the mass stopping power, it's given in units of MeV•cm^2 •g^{-1} .

The mass stopping power is a useful quantity because it expresses the rate of energy loss of charged particle g/cm^2 of the medium traversed. Mass stopping power isnot very different in materials with similar atomic composition.

With regard to charged particle interaction, two types of stopping power are known :

1. nuclear stopping power (Radiation stopping power) resulting from charged particle interaction with a nucleus of the absorbing matter. usually, light charged particles (electrons and positrons) loss of energy through these interactions that are referred to as bremsstrahlung interactions. While the heavy charged particles (protons, α particles, etc.) do not lose any energy during bremsstrahlung.

2. Electronic stopping power resulting from charged particle interaction with orbital electrons of the absorbing medium. Both heavy and light charged particles loss of energy through these interactions, that lead to energy transfer from the charged particle to orbital electrons through excitation and ionization processes for absorber atoms [4].

General, the total stopping power for a charged particle is the sum of the nuclear (radiation) stopping power and electronic stopping power [4].

(2.4) Relationship between total Stopping Power and the Ion Energy

Relationship between the total stopping power and the projectile energy is shown in Figure. (2-2), as well indicating the main atomic processes responsible for the stopping power in Absorbed medium.

- At ($E < 10^{-6}$ MeV/u), the mass stopping power is resulting from elastic collisions of the falling ion with the nuclei of target.

- At ($E > 10^{-5}$ MeV/u), slowdown of ions because of atomic processes involving both projectile and target electrons.

- At ($E > 0.025$ MeV/u), (ion velocities $\upsilon < \upsilon$ e), where υe is the average electron velocity of the target atom, mass sopping power increases as $\sim \upsilon$ because of inelastic collisions (electron capture and electron loss) according of the Lindhard-Sørensen theory, reaches its maximum at ($v \sim v e$) and minimum value at ($\sim v^{-2}$), given by the Bethe-Bloch formula.

- At (E ≈10–10^{3}MeV/u), the energy losses are linked with ionization of the target electrons, and the ∼υ−2 law corresponds with the asymptotic behavior of the ionization cross sections.

- At (E ≥ 5GeV/u), logarithmically, mass stopping power is increase (∼lnγ) with energy of ion that showing the so-called relativistic rise described by the second log term in the Bethe-Bloch formula.

- In the range of super high energies E > 106MeV/u (βγ ≥100), the relativistic rise of stopping power is can celled due to the density correction and stopping power reaches the Fermi plateau. at this range of energies where stopping power no longer increases with increasing ion energy and stays nearly constant [12].
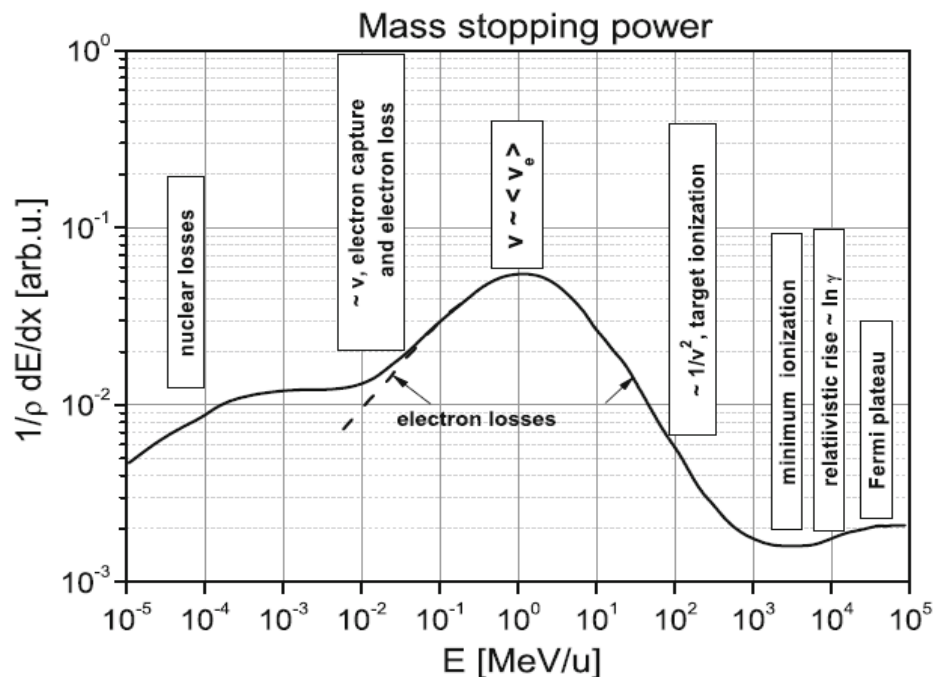
Fig. (2-2) showing contributions of atomic processes of the mass stopping power as a function of the projectile energy for different energies[12] .

(2.5) Theories studied the stopping power

Two different hypotheses were developed to describe the energy loss of a heavy particle interaction with orbital electrons of absorber atoms:

- Bohr's approach (1913) is in the realm of classical physics and is based on the concept of impact parameter between the particle's trajectory and the absorber nucleus.

19

- Bethe's approach (1931) is in the realm of quantum mechanics and relativistic physics, and assumes that the momentum transfer related to the particle's energy loss is quantized.

This basic hypothesis dealing with the energy loss of charged particles in the absorbent medium make the following assumptions :

1. The heavy ion is moving through the absorbent medium much faster than the orbital electrons for atoms of absorber

2. The charged particle loses energy through interactions with orbital electrons of the absorbent medium, while interactions with the nuclei of absorbent medium are negligible [4] .

(2.5.1) Bohr's Theory - The Classical Case

The Bohr Theory uses classical mechanics to calculate the energy transfer due to soft collisions with the atomic electron orbital.

Consider a heavy particle with a charge ze, mass M and velocity v passing through some material medium and suppose that there is an atomic electron at some distance b from the particle trajectory (see Figure. 2-3). Assume that the electron is free and initially at rest, and furthermore, that only moves very slightly during the interaction with the heavy particle so that the electric field acting on the electron may be taken at its initial position. Moreover, after the collision, we assume the incident particle to be essentially deviated from its original path because of its much larger mass M » m_e. This is one reason for separating electrons from heavy particles [50].
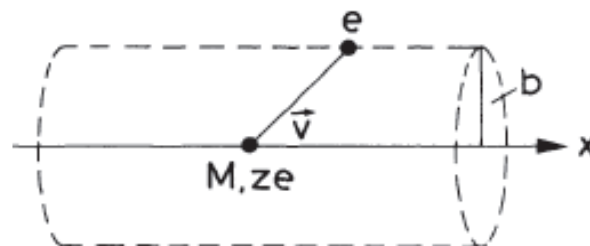
Fig. (2-3) Collision between a charged particle and an atomic electron [50]

Through finding the momentum impulse the electron acquires from colliding with the heavy ion, can be calculation the energy acquired for the electron.

20

$$I = \int F \, dt = e \int E_\perp \, dt = e \int E_\perp \frac{dt}{dx} \, dx = e \int E_\perp \frac{dx}{v} \quad \dots\dots\dots\dots\dots\dots (2-1)$$

Where only the electric field ($E_\perp$) perpendicular to the particle trajectory enters because of symmetry. To calculate the integral ($E_\perp$ dx), we apply Gauss' Law ($\int E.ds = q/\epsilon_o$) where $ds = 2\pi b dx$, $q = ze$ and $\epsilon_0 = 4\pi$ over an infinitely long cylinder centered on the particle trajectory and passing through the position of the electron. Then

$$\int E_\perp \, 2\pi b dx = 4\pi ze \, , \quad \int E_\perp \, dx = \frac{2ze}{b} \, , \quad \dots\dots\dots\dots\dots . (2-2)$$

so that

$$I = \frac{2ze^2}{bv} \quad \dots\dots\dots\dots\dots\dots . (2-3)$$

and the energy acquired for an electron is

$$\Delta E(b) = \frac{I^2}{2m_e} = \frac{2z^2 e^4}{m_e \, v^2 b^2} \quad \dots\dots\dots\dots\dots\dots\dots . (2-4)$$

If we consider (N_e) is the density of electrons , then the energy loss for all the electrons existing at a distance between b and b + db in a thickness dx is

$$-dE(b) = \Delta E(b) N_e dV = \frac{4\pi z^2 e^4}{m_e v^2} \, N_e \frac{db}{b} \, dx \quad \dots\dots\dots\dots . (2-5)$$

Where, the volume of element (dV = 2πb db dx) . the total energy loss can be obtained from integrate eq. (2-5) from b = 0 to ∞; nevertheless, this is contrary to our original presumptions. For example, collisions at very large b would not take place over a short period of time, so the calculation of impulse would not be true. Also, for b = 0, we see that eq. (2-5) gives an infinite energy transfer, so eq. (2-5) is not valid at (b) small. Therefore, the integration must be made over some limits b_{min} and b_{max} between which eq. (2-5) holds.

So ,

$$-\frac{dE}{dx} = \frac{4\pi z^2 e^4}{m_e v^2} \, N_e ln \frac{b_{max}}{b_{min}} \quad \dots\dots\dots\dots\dots . (2-6)$$

To estimate values for b_{min} and b_{max}, we must make some physical arguments. Classically, the maximum energy transferable is in a head-on collision where the electron

obtains an energy of $\frac{1}{2}m_e(2v)^2$. If we take relativity into account, this becomes $2\gamma^2 m_e v^2$, where $\gamma = (1 - \beta^2)^{-1/2}$ and $\beta = {v}/{c}$.

Using (2-4) then, we find

$$\frac{2z^2e^4}{m_e v^2 b_{min}^2} = 2\gamma^2 mv^2, \qquad b_{min} = \frac{ze^2}{\gamma m_e v^2} \ldots \ldots \ldots \ldots \ldots . (2-7)$$

For b_{max}, the electrons are bound to atoms with some orbital frequency v but they are not free. In order for the electron to absorb energy must be the perturbation caused by the passing particle take place in a time short compared to the period $\tau = 1/v$ of the bound electron, otherwise, the perturbation is adiabatic and no energy is transferred. This is the principle of adiabatic invariance. For collisions, the typical interaction time is $t = b/v$, which relativistic ally becomes $t \to t/\gamma = b/(\gamma v)$ so that

$$\frac{b}{\gamma v} \leq \tau = \frac{1}{v} \ldots \ldots \ldots \ldots \ldots . . (2-8)$$

Since there are several bound electron states with different frequencies v, we have used here a mean frequency, $\bar{v}$ averaged over all bound states. An upper limit for b, then, is

$$b_{max} = \frac{\gamma v}{\bar{v}} \ldots \ldots \ldots \ldots \ldots . . (2-9)$$

Replacing into (2-6), we find

$$-\frac{dE}{dx} = \frac{4\pi z^2}{m_e v^2} N_e \ln \frac{\gamma^2 mv^3}{ze^2 \bar{v}} \ldots \ldots \ldots \ldots \ldots . (2-10)$$

This is Bohr's classical equation [50].

(2.5.2) Bethe's Theory - The Quantum Case

Using quantum mechanics and relativistic physics, Bethe (1930) derived the equation of mass stopping power for a charged particle. In calculation, the energy transfer is determined in terms of the transfer momentum rather than the impact parameter, since the momentum transfer is a measurable quantity while the impact parameter is not measurable. Using the eq.(2-6)

where b_{max} and b_{min} are the maximum and minimum impact parameters.

In reality the atomic electrons are of course not free electrons, so the charged particle must transfer at least an amount of energy equal to the first excited state of the atom. If they take the time interval of energy transfer to be $\Delta t \approx b / v$, then $(\Delta t)_{max} \approx b/v$, where $hv \approx \bar{I}$ is the mean ionization potential. Then [15].

$$b_{max} \approx \frac{hv}{\bar{I}} \dots \dots \dots \dots (2-11)$$

Using the uncertainty principle, can estimate b_{min} in the relative coordinate system of the electron and the charged particle. Since electron momentum in the relative coordinate system is $(m_e v)$, so :

$$b_{min} \approx \frac{h}{m_e v} \dots \dots \dots (2-12)$$

Combining these two terms they obtain

$$-dE/dx = \frac{4\pi z^2 e^4 nZ}{m_e v^2} \ln(\frac{2m_e v^2}{\bar{I}}) \dots \dots \dots \dots (2-13)$$

Eq. (2-13) characterizes the energy loss result to particle collisions in the non- relativistic regime, can contain relativistic effects by replacing the logarithm by

$$\ln(\frac{2m_e v^2}{I}) - \ln\left[1 - \frac{v^2}{c^2}\right] - \frac{v^2}{c^2} \dots \dots \dots \dots \dots (2-14)$$

Eq. (2-13) is called as the Bethe mass stopping power equation and it valid for heavy charged particles (protons, α particles, and heavy ions), accounts for quantum mechanical as well as relativistic effects [16, 51].

Fig(2-4) shows, schematic of the shape of the mass stopping power as a function of the charged particle kinetic energy E_K. We note there are three distinguished regions as the kinetic energy increases from zero:

I.   at low energy region: the stopping power rises almost linearly and reaches a maximum at about 250 I , where I is the mean ionization/excitation potential

II.   at intermediate energy region: the stopping power decreases as $1/v^2$ or $1/E_K$ where υ is the velocity of the charged particle to reach a broad minimum at ~2.5 $m_o c^2$ where $m_o c^2$ is the rest energy of the charged particle.

23

III.   relativistic energy region: the stopping power rises slowly with increasing EK because of relativistic effects [4] .
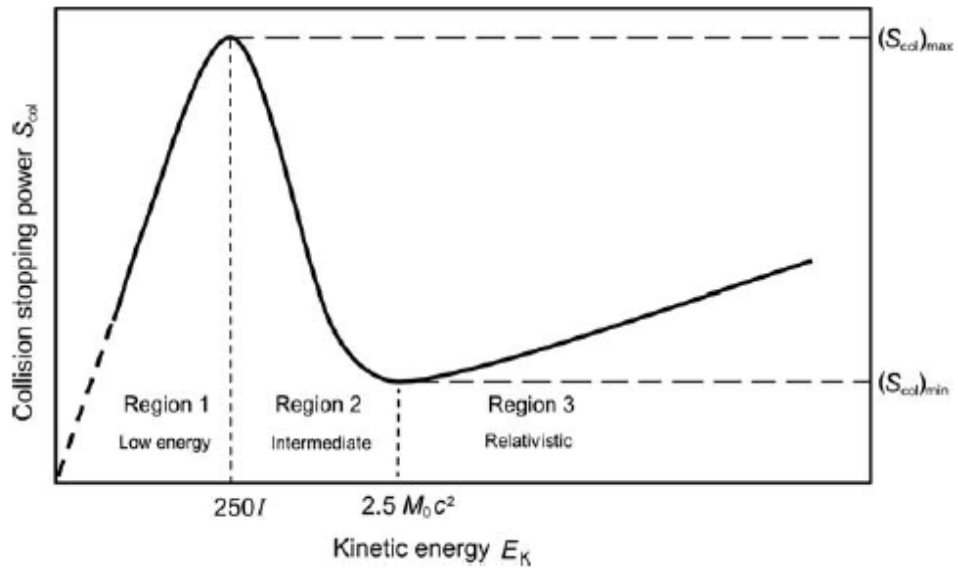
Fig. (2-4) Schematic of the shape of the total energy loss as a function of the charged particle kinetic energy EK [4].

(2.5.3) The Bethe –Bloch formula:

Eq. (2-13) is generally known as the Bethe formula. It is a quantum mechanical result derived on the basis of the Born approximation which is essentially an assumption of weak scattering. The result is valid provided that [16, 51].

$$\frac{ze^2}{\hbar v} = \left(\frac{e^2}{\hbar c}\right)\frac{z}{\left(\frac{v}{c}\right)} = \frac{z}{137\left(\frac{v}{c}\right)} << 1 \quad .... \ (2-15)$$

On the other hand, Bohr has used classical theory to derive a somewhat similar expression for the stopping power: -

$$-\left(\frac{dE}{dx}\right)_{class} = \frac{4\pi z^2 e^4 nZ}{m_e v^2} \ ln[\frac{M\hbar v}{2ze^2(m_e + M)}\frac{2m_e v^2}{\bar{I}}] \quad .... \ (2-16)$$

This holds if

$$\frac{ze^2}{\hbar v} \gg 1 \ .... \ (2-17)$$

24

The Bethe formula, (2-13), is appropriate for heavy charged particles. For fast electrons (relativistic) [16, 51].

$$-\frac{dE}{dx} = \frac{2\pi e^4 nZ}{m_e v^2}\left[ln\left(\frac{m_e v^2 E}{I^2(1-\beta^2)}\right)-\beta^2\right] \ldots\ldots\ldots\ldots (2-18)$$

By considering the minimum and the maximum values of the impact parameter b as $b_{min}\sim ze^2/mv^2$ and $b_{max}\sim v/\omega$.

Inserting these values for b_{min} and b_{max} the energy loss becomes:

$$-\frac{dE}{dx} = 4\pi Z \frac{z^2 ne^4}{mv^2} ln\left[\frac{mv^3}{ze^2\omega}\right] \ldots\ldots\ldots\ldots. (2-19)$$

The relativistic form of this equation is made by equating the particle energy, $E = \gamma M\ c^2$, where z = particle atomic number, $M =$ particle mass(u) , Z = target atomic number [37].

$$-\frac{dE}{dx} = \frac{4\pi Ze^4}{mv^2}z^2\ ln[\frac{\gamma^2 mv^3}{ze^2\omega}] \ldots\ldots\ldots\ldots\ldots (2-20)$$

where $\omega=$ orbital frequency

Bohr used this expression to form the basis of his evaluation of the energy loss of a heavy particle to a medium of harmonically bound electrons.

Bloch evaluated the differences between the classical (Bohr) and quantum mechanical (Bethe) approaches for particle with velocities much larger than the target electrons. The original Bethe-Block relativistic stopping formulae, $-dE/dx$ may be stated as: [37]

$$-\frac{dE}{dx} = \frac{4\pi e^4 Z}{m_e v^2}z^2\left[ln\frac{2mv^2}{\langle I\rangle} - ln(1-\beta^2)-\beta^2+\psi(Z_1)\right] \ldots\ldots\ldots. (2-21)$$

where I is the averaged excitation potential.

The final term, $\psi(Z_1)$ in Eq. (2-21), is Bloch's error and is a small term so that the Block result does not reduce to the Bethe result for the limit $Z_1\alpha/\beta \to 0$, where $\alpha =$ the fine structure constant, $e^2/\hbar c=1/137$ [37].

The Bethe –Bloch model becomes invalid at low energies:

1. When the velocity of the heavy particle is comparable with K shell electron
2. Charge exchange the ion picks up electrons from the medium reducing its charge
3. Nuclear interactions dominate below 0.01 MeV [51].

(2.6) Fano Corrections for mass Stopping Power Equation

Fano published (1960) various extensions of Bethe's and Bloch's work and described two additional corrective terms, the shell correction term (C/Z) and the density effect correction (δ/2). Both of these corrections (shell-correction term at very low energies (E ≤10 MeV/amu) and the density-effect correction at very high energies (E ≥2 GeV/amu) depend on the nature of the absorbing material and the projectile velocity but are presumably independent of the projectile charge [37].

Fano's approach was to consider the momentum (p) transferred to a bound electron with a transfer energy (ΔE) .Assume three regions for transfer of the energy to an atomic electron at a distance (x) from the particle:

1. For small ΔE , one assumes that $\Delta p . \Delta x \ll \hbar$, so that the interaction between the particle and electron reduces to dipole matrix elements .
2. For intermediate ΔE , one assumes that only the longitudinal electromagnetic terms of the interaction contribute to the momentum transfer.[37]
3. For large ΔE, one assumes that the electrons of target may be considered to be unbound, and the transfer can be reduced to standard two-particle relativistic interactions.

The shell correction term (C/Z) introduced to account for the overestimate in I, various theories have been developed for its determination. Since the K shell electrons are the fastest of all orbital electrons, they are the first to be affected by low particle velocity with decreasing particle velocity. The shell correction is often classed as the K shell correction, labeled CK/Z and all possible higher shell corrections are ignored. The correction term C/Z is a function of the absorbing medium and charged particle velocity so that, for the same medium and particle velocity, it is the same for all particles including electrons and positrons [50].

The density effect emergences from the fact that the electric field of the charged particle polarize the atoms along its path. due to polarization, electrons far from the path of the particle will be shielded from the full electric field intensity. Because Collisions with these

outer lying electrons will contribute less to the loss of energy than predicted by the Bethe Bloch equation. This effect increasing importance with increase the ion energy. Furthermore, this effect depends on the density of the material (hence the term "density" effect), because the induced polarization will be greater in condensed materials than in lighter materials such as gases. In Fig. (2-5), A comparison of the Bethe - Bloch formula with and without corrections [50].
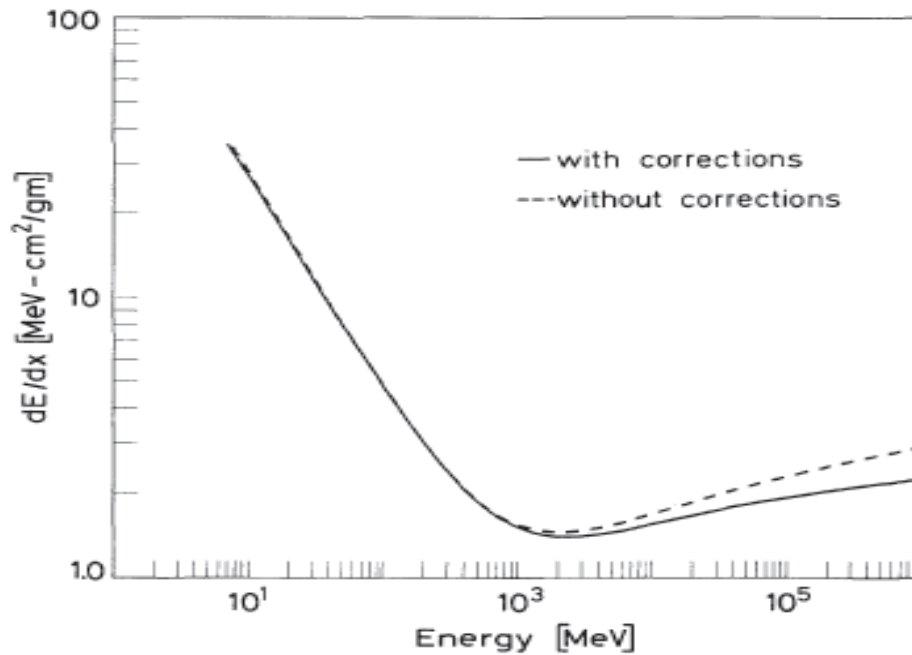
Fig. (2-5) Comparison of the Bethe-Bloch equation for copper with and without the shell and density corrections [50].

Presumption these approximations, Fano proposed a relativistic version of the Bethe-Bloch stopping power equation where two additional corrective terms are comprised (the Shell Correction ,(C/Z), and the Density Effect correction ,(δ/2)). [37]

$$-\frac{dE}{dx} = \frac{4\pi e^4 Z_2}{m_e v^2} Z_1^2 [ln \frac{2mv^2}{\langle I \rangle} - ln(1 - \beta^2) - \beta^2 - \frac{C}{Z} - \frac{\delta}{2}] \dots \dots \dots (2 - 22)$$

Which is usually simplified using the definitions [37]:-

$$r_0 = \frac{e^2}{m_e c^2} \quad \text{(the Bohr electron radius)}$$

$$f(\beta) = \ln[2mc^2 \beta^2/(1 - \beta^2)] - \beta^2 \dots \dots (2 - 23) \text{ (Combining the relativistic terms)}$$

27

$$-\frac{dE}{dx} = \frac{4\pi r_0^2 m_e c^2 Z_2}{\beta^2} Z_1^2 [f(\beta) - ln\langle I \rangle - \frac{C}{Z} - \frac{\delta}{2}] \ldots\ldots\ldots\ldots. (2-24)$$

There have been many corrections proposed to improve on Fano's theoretical approximations. Traditionally, this is done by expanding this equation in powers of $Z1$, which can be used to add additional corrections to the ion and target interaction.

The Bethe-Bloch energy loss formula can be expressed as:

$$-\frac{dE}{dx} = \frac{kZ_2}{\beta^2} Z_1^2 [L_0(\beta) + Z_1 L_1(\beta) + Z_2^2 L_2(\beta) \ldots] \ldots\ldots.. (2-25)$$

where $k = 4\pi r_0^2 m_e c^2$, the term ,L_0 contains all the correction factors of the Fano formulation, Eq. (2-24) and extra higher order terms are added, $L_1, L_2, \ldots\ldots$.

The term $L(\beta)$, in Eq. (2-25) ,is called as the Stopping Number ,and is contain all the corrections to the energy loss process for heavy charged particles [37].

$$L(\beta) \equiv [L_0(\beta) + z L_1(\beta) + z^2 L_2(\beta)] \ldots\ldots\ldots.. (2-26)$$

$$-\frac{dE}{dx} = \frac{kZ_2}{\beta^2} z^2 L(\beta) \ldots\ldots\ldots. (2-27)$$

The second term of the stopping number expansion,L_1, is usually called the Barkas correction or the z^3 correction, and the third term, L_2, is called the Bloch correction or the z^4 correction. Note that only the stopping number term L_1 contains an odd power of z , and hence would be sensitive to the sign of the particle's charge (positive or negative). Barkas correction should apply to the sum of all odd-power terms of z in Eq. (2-26) because it is based in part on the stopping differences between particles with opposite charge signs $(+ \ or \ -)$ [37].

(2.7) Stopping Power in Compounds

If the particle travels in a compound or a mixture of several elements, the stopping power can give through the assumption of Bragg's Rule. It states that atoms contribute nearly independently to the stopping power, and hence their effects are additive

$$\frac{1}{\rho}\frac{dE}{dx} = \frac{w_1}{\rho_1} (\frac{dE}{dx})_1 + \frac{w_2}{\rho_2} (\frac{dE}{dx})_2 + \cdots, \quad \ldots\ldots\ldots.. (2-28)$$

where w_1, w_2, etc. are the fractions by weight of elements 1,2,… in the compound.

generally, if a_i is the number of atoms of the ith element in the molecule M, then [50]

$$w_i = \frac{a_i A_i}{A_m} \quad \dots\dots\dots\dots\dots (2-29)$$

Where Ai is the atomic weight of ith element $A_m = \sum a_i A_i$

If the particle moves in a compound or a mixture instead of a pure element, an effective atomic number $Z_{effetive}$ is [52]:-

$$Z_{effective} = \frac{\sum_{i=1}^{L}(\frac{W_i}{A_i})Z_i^2}{\sum_{i=1}^{L}(\frac{W_i}{A_i})Z_i} \quad \dots\dots\dots\dots\dots.. (2-30)$$

where L=number of elements in the compound or mixture

A_i = Atomic weight of i the element

W_i =Wight fraction of i the element

$Z_{i=}$ Atomic number of i the element

The accuracy of Bragg's rule is limited because the energy loss to the electrons in any material depends on the detailed orbital and excitation structure of the matter. Bragg's rule of stopping power additively can be expressed in terms of stopping cross sections as

$$\varepsilon(compound) = \sum_i n_i \varepsilon(i) \quad \dots\dots\dots\dots\dots (2-31)$$

where n_i is the number of atoms of element i in the molecule [53].

(2.8) Mean Excitation Energies

Using the following approximate empirical formulas can estimate the I value in eV for an element with atomic number Z: [54]

$$I \cong \begin{cases} 19.0 \ eV \ , Z_2 = 1 \ (Hydrogen) \\ 11.2 + 11.7Z_2 \ eV, 2 \leq Z_2 \leq 13 \\ 52.8 + 8.71 \ Z_2 \ eV, Z_2 > 13 \end{cases} \dots\dots\dots(2\text{-}32)$$

For most applications, values obtained using these equations are accurate because of only the logarithm of I enters in the stopping power equation. The value of I for any element depends only on the chemical composition of element and on the state of the material (solid, liquid, or gas) but does not depend on the type of charged particle interacting. For according to Bragg's rule, when the material is a compound or mixture, We can write the formula (2-32) as the following

$$n \ln I = \sum_i N_i Z_i \ln I_i \quad \dots\dots\dots\dots. (2-33)$$

where n is the total number of electrons cm^{-3} in the material (n=N_i Z_i)[54].

In the ICRU Report 37, typical values of the mean excitation energies (I) are listed in Table (2-1) for several elements and compounds of interest in medical physics and dosimetry[4].

Table (2-1) Average excitation potential (I) for several elements and compounds (from the ICRU Report 37) [4].

Element	H	C	Al	Cu	Ag	W	Pb	Ra	U	Cf
I(eV)	19.2	78	167	322	470	772	823	862	890	966
Compound	I(eV)				Compound			I(eV)		
Air	85.7				Lithium fluoride			94		
Water (liquid)	75				Photographic emulsion			331		
Water (vapor)	71.6				Sodium iodide			452		
Muscle (skeletal)	75.3				polystyrene			68.7		
Bone (compact)	91.9				A-150 plastic			65.1		

(2.9) Range

(2.9.1) Range of Charged Particles

Range is an experimental concept of the charged particle that expresses the thickness of the absorption material that the charged particle can penetrate. It depends on:

- Kinetic energy of the particle
- Mass and charge of the particle
- Configure the absorbent medium.

In a particular absorption medium, the charged particles lose their energy in ionizing and radiation collisions, which result in a large number of effects in the charged particle path due to elastic scattering [4] .

For light charged particles (electrons and positrons), the scattering effects are much more clear in comparison to heavy charged particles for the following reasons: -

1. The path of heavy charged particles is in a straight line as it passes through an absorbent medium, as shown in Figure (2-6) because they do not suffer from radiation loss, transfer only small amounts of energy into individual ionizing collisions, and suffer mainly from small angle distortions in elastic scattering.

2. The path of light charged particles (electrons and positrons) is a zigzag path when it passes through an absorbing medium, as shown in Figure (2-6), because of with kinetic energy E_K can lose energy up to $(1/ 2E_K)$ in individual ionizing collisions and energy up to E_K in individual radiation collisions , Since they can also be scattered with very large scattering angles[4].
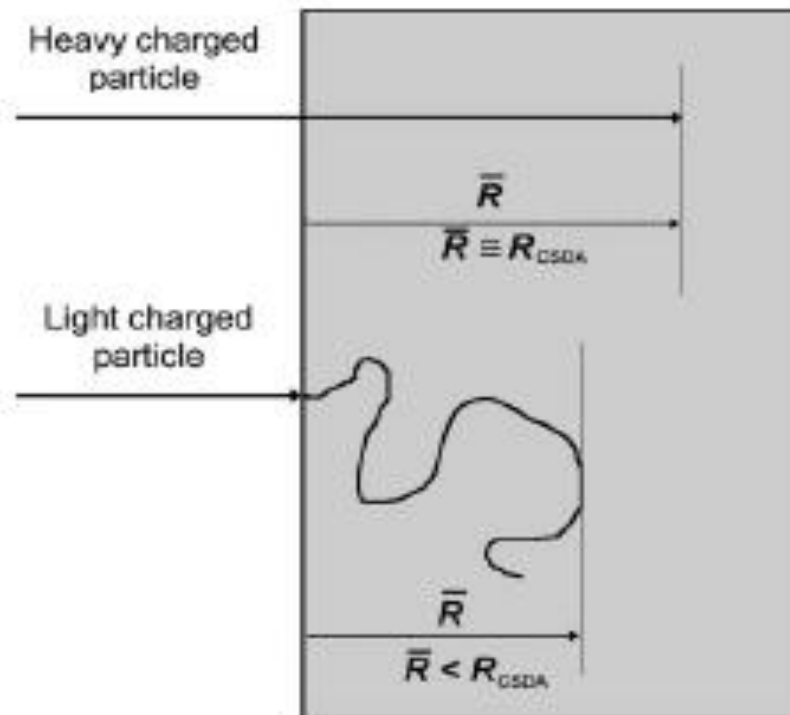
Fig. (2-6) penetration of charged particle into the medium of absorbing[4].

The range is expressed by following equation (2-34):

$$R = \int_{0}^{E} -\left[\frac{dE}{dx}\right]^{-1} dE \dots\dots\dots\dots (2-34)$$

The range is actually an average value because scattering is a statistical process and there will, therefore, be a spread of values for individual particles. The spread will be greater for light particles and smaller for heavier particles. These properties have implications for the use of radiation in therapeutic situations, where it may be necessary to deposit energy within a small region at a specific depth of tissue, for example to precisely target a cancer.

Practically, not all charged particles that start with the same energy will have the same range. Figure. (2-7) display Range-energy curves calculated for different charged particles in silicon.[55]

Using the Bragg Kleeman rule, can calculate the range for the same particle in different materials [50]

$$\frac{R_1}{R_2} = \frac{\rho_2}{\rho_1}\frac{\sqrt{A_1}}{\sqrt{A_2}} \quad \dots\dots\dots\dots\dots. (2-35)$$

where ρ is the densities and A is the atomic numbers of the materials.

For compounds, can calculate the range approximately from the formula:

$$R_{compound} = \frac{A_{compound}}{\sum \frac{a_i A_i}{R_i}} \quad \dots\dots\dots\dots. \quad (2-36)$$

where A_i and R_i are the atomic weight and range of the ith constituent element, As well a_i is the number of atoms of the i_{th} element in the compound molecule [50].
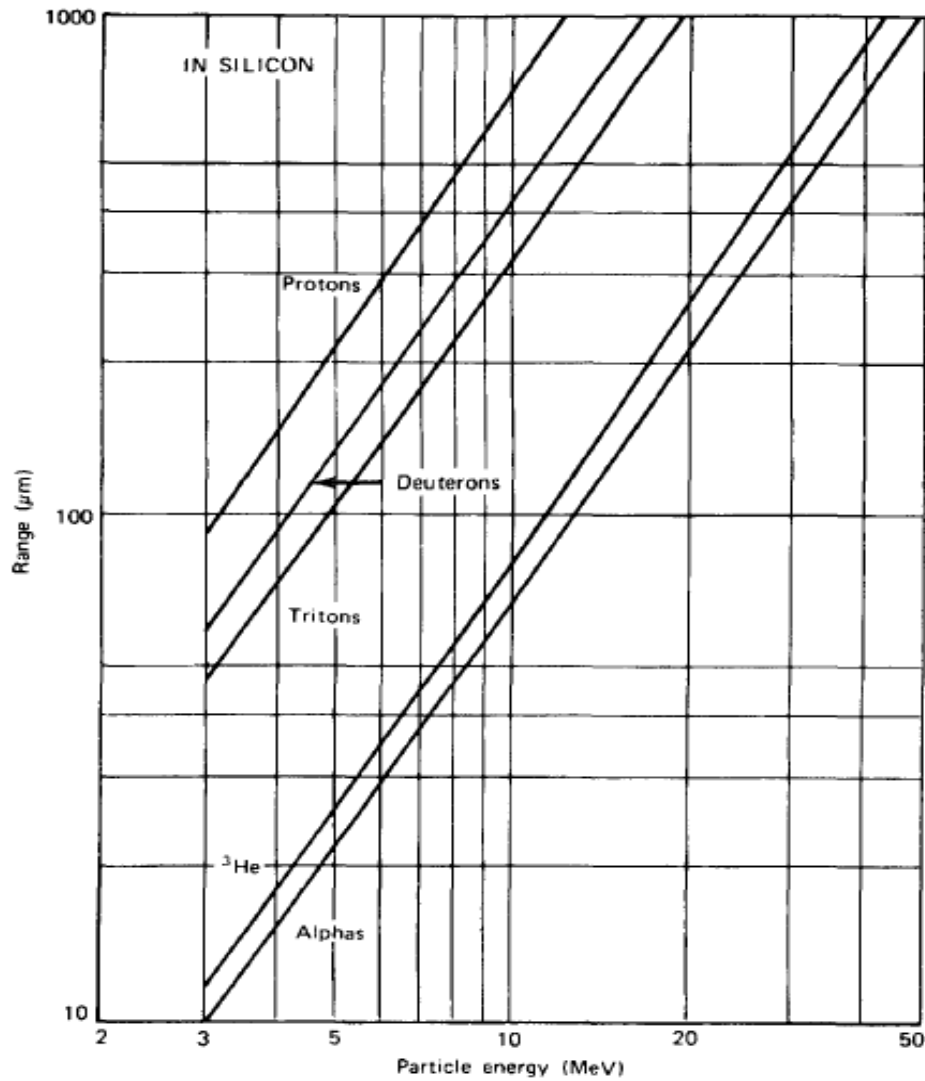
Figure (2-7) Range-energy curves calculated for different charged particles in silicon [55].

(2.9.2) Continuous Slowing Down Approximation (CSDA) Range

Generally, the concepts of range R must be distinguished from the concept of the path-length of a charged particle. This path-length simply provides the total path-length of the charged particle in the absorber and can be calculated, as suggested by Martin Berger and Stephen Seltzer in 1983, using the continuous slowing down approximation (CSDA) as follows:

$$R_{CSDA} = \int_0^{(E_K)_0} \frac{dE}{S_{tot}(E)} \;\dots\dots\dots\dots\dots\dots\dots\; (2-37)$$

R_{CSDA} is the mean path length of the heavy charged particles in the absorbing medium

33

E_K is the initial energy of the charged particle

S_{tot} (E) is the total stopping power of the heavy charged particle

- RCSDA for heavy charged particles is a very good approximation to the average range of the charged particle in the absorption medium, due to the essentially rectilinear path of the charged particle (see Figure. 2-6) in the absorption medium.
- RCSDA for light charged particles is reach to twice the range of charged particles in the absorption medium, due to the very zigzag path that the light charged particles experience in the absorption medium. (see Figure. 2-6) [4].

(2.9.3) The Maximum for penetration

The maximum penetration depth R_{max} is defined as the depth in the absorbing medium beyond which no particles are observed to penetrate. For heavy charged particles $R_{max} \approx R_{CSDA}$ for all absorbing media, while for light charged particles $R_{max}/R_{CSDA} \approx 1$ for low Z absorbers and decreases with increasing Z to reach $R_{max}/R_{CSDA} \approx 0.5$ for high Z absorbers [4].

(2.9.4) Range Straggling

The range straggling is defined as the fluctuation in path length for individual particles of the same initial energy. The same stochastic factors that lead to energy straggling at a given penetration distance also result in somewhat different total path lengths for each particle. For heavy charged particles (proton or α -particle , heavy ions) , the straggling values to a few percent for the mean range [55].

(2.10) Stopping time

Stopping time is the time wanted to stop a charged particle in a material, can be concluded from its range and average velocity. For non-relativistic particles of mass m and kinetic energy E, the velocity

$$v = \sqrt{\frac{2E}{m}} = c\sqrt{\frac{2E}{mc^2}} = (3.00 \times 10^8)\sqrt{\frac{2E}{(931 MeV/amu)m_A}} \dots \dots \dots \dots \dots (2-38)$$

Where m_A is the mass of particle in (amu) and E is the energy of particle in MeV. If we assume that the average velocity of particle as it slows down is (v) = Kv , then the stopping time t is calculated from the range R as

$$t = \frac{R}{\langle v \rangle} = \frac{R}{Kc}\sqrt{\frac{mc^2}{2E}} = \frac{R}{K(3.00 \times 10^8 \ m/s}\sqrt{\frac{931 \ MeV/amu}{2}}\sqrt{\frac{m_A}{E}} \quad .... \quad (2-39)$$

If the particle were uniformly decelerated, then (v) would be given by v/2 and K would be 0.5. However, charged particles generally lose energy at a greater rate near the end of their range, and K should be a somewhat higher fraction. By assuming K = 0.60, the stopping time can be estimated as

$$t \cong 1.2 \times 10^{-7} R \sqrt{\frac{m_A}{E}} \quad .... (2-40)$$

Where (t) measured in the unit of seconds, R in the unit of meters, mA in amu, and E in MeV. This approximation is true for heavy particles (proton, alpha particles, etc.) , while It is not true for relativistic particles such as fast electrons [55].

(2.11) Linear Energy Transfer

LET is the amount of energy deposited per unit length of the path by the radiation. Also, LET is the stopping power equivalent.

$$LET = -\frac{dE}{dX} \times \rho \ .... (2-41)$$

LET depends on the velocity, charge and mass of the particle. The LET units is (keV/mm) and is very beneficial in concepts of radiation protection. Electromagnetic radiations and electrons, have low LET, because they interact with matter and lose only little energy per interaction, while heavy particles (a-particles, neutrons, and protons) have high LET, because lose energy very rapidly, producing many ionizations in a short distance. The dose delivered by high-LET particles increases with depth and reaches its maximum at the end of the particle track, the Bragg peak, with a sharp edge and with little scatter. Such dense ionizations can cause complex DNA damage [56] in Table (2-3) listed some approximate LET values in tissue [14].

Table (2-3) LET values of some radiations in tissue [14].

Radiation	LET(KeV/μm)
X-ray (3MV)	0.5
X-ray(250KV)	3.0
Alpha particles (5MeV)	100.0
Electrons (1MeV)	0.25
Neutrons (14MeV)	20.0

(2.12) Thickness of Target

For absorbers that are penetrated by a given charged particle, the thickness can be calculated from [57]:

$$T = R/\rho \quad .... (2-42)$$

(2.13) Radiation Dosimetry

(2.13.1) Introduction

Radiation dosimetry is the branch of science that attempts to correlate the amount of measurements specified in the radiation field to physical, chemical, and biological changes that the radiation would produce in a medium. The concepts of radiation exposure and dose play prominent roles in radiation measurements, due their importance in personnel protection at radiation facilities and in the medical of radiation [58].

When radiation interacts with a target it produces excited and ionized atoms and molecules as well as large numbers of secondary electrons. The secondary electrons can produce additional ionizations and excitations until, finally, the energies of all electrons fall below the threshold necessary for exciting the medium. The initial electronic transitions, which produce chemically active species, are completed in very short times ($\leq 10^{-15}$ s) in local regions with in the path traversed by a charged particle. These changes, which require the direct absorption of energy from the incident radiation by the target, represent the initial physical perturbations from which subsequent radiation effects evolve. It is natural

therefore to consider measurements of ionization and energy absorption as the basis for radiation dosimetry [58].

The term radiation dose is defined through two main concepts:

1. The absorbed dose is the energy deposited per gram in an absorbing medium (mainly tissue).
2. The effective dose equivalent is characterized the damaging effect of the radiation type, which is characterized by the term effective dose equivalent.

The term radiation exposure, which applies to air only and is a measure of the amount of ionization produced by x-rays and gamma radiation in air [59].

(2.13.2) Absorbed dose

It is the concentration of energy deposited in tissue due to exposure to ionizing radiation [60]. It represents the energy deposited by charged particles per gram of material. the conventional unit for absorbed dose is the rad (radiation absorbed dose), and is equal to the absorption of 100 erg of energy in 1 g of absorbing medium, typically tissue:

$1\,rad = 100\,erg/g$

The SI unit of absorbed dose is the gray (Gy) and is defined as the absorption of 1 Joule of energy per kilogram of medium: [59]

1Gy= 1 J/kg

The absorbed dose is relevant to all types of ionizing radiation fields, whether directly or indirectly ionizing, as well as to any ionizing. The absorbed dose is used to estimate the potential of biochemical changes in many tissues. The absorbed dose reflects the intensity of the energy deposited in any small amount of tissue found anywhere in body of organism [60].

$$\text{Absorbed dose(rad)} = \frac{E}{1g}\frac{1.6\times10^{-13}J}{1MeV}\frac{10^7 erg}{1J}\frac{1\,rad}{\frac{100erg}{g}} \dots \dots \dots (2-43)$$

(2.13.3) Equivalent dose

The most important difference between the absorbed dose in tissue and the equivalent dose is that the absorbed dose represents the amount of energy stored in a small volume of tissue. So, the equivalent dose is the amount of the effect of a particular type of radiation on the tissue.

The definition of equivalent dose is important because radiations of different produce different amounts of biological damage even though the deposited energy is the same. The

radiation absorbed dose is a suitable measure of biological injury so as the biological effects of radiation were directly proportional to the energy deposited by radiation in an organism. For the same absorbed dose, Radiation damage increases with the linear energy transfer (LET) of the radiation; therefore, the biological damage from high-LET radiation (heavy charged particles) is much greater than from low-LET radiation (light charged particles) [61].

The dose equivalent (H_T) is defined as the product of the absorbed dose and a factor Q (the quality factor) , that describes the damage linked with each type of radiation:

$$H_T = D \times Q \ldots\ldots\ldots\ldots. (2-44)$$

The quality factor Q (without dimensions) is dependent on type of particle and its energy. The average values of the quality factor for radiations of interest are given in Table (2-4)

In the conventional system of units , the unit of dose equivalent is the rem which is calculated from the absorbed dose as

rem= rad $\times$Q

The SI unit of dose equivalent is the Sievert (Sv) or

Sieverts= Gy $\times$Q

The Sievert , as is the gray, is a very large unit, corresponding to 100 rem in conventional units [50].

Table (2-4) weighting factors of Radiation [50]

Type	Energy range	Radiation weighting factor
Photons and Electrons	all energy	1
Neutrons	$< 10 KeV$	5
	$10 keV$ - 100keV	10
	$> 100 keV - 2MeV$	20
	$> 2MeV - 20MeV$	10
	$> 20MeV$	5
Protons	$> 2MeV$	5
$\alpha - particle, heavy\ nuclei$	all energy	20

(2.13.4) Effective dose

It is, of course, more serious if the entire body receives a given exposure than if only a single organ receives that exposure. Thus, when a dose equivalent is specified, it is important to know whether the reference is to a limited region of the body or the whole body. If only a small part of the body is irradiated, it is possible to translate an organ dose into the whole-body dose that would produce the same overall risk of a fatal cancer, with the use of appropriate weighting factors. This translated dose is called the effective dose equivalent H_E or often just the effective dose E.

The effective dose equivalent HE is related to the individual tissue doses H_T and D_T by tissue weighting factors W_T and a summation over tissues:

$$H_E = \sum W_T \times H_T \dots \dots \dots \dots \dots (2-45)$$

Table (2-5) Weighting factors for (Organ or tissue)   [62]

Organ or tissue	W_T (weighting factors)
Bone marrow , lung, stomach, breast, remainder	0.12
Gonads	0.08
Bladder, liver, esophagus, thyroid	0.04
Bone surface, skin, brain	0.01

The effective dose is associated with two different weight factors:

• First, the radiation weight factor W_R and

• Second, the tissue weight factorW_T.

Effective dose is a calculated value. There are three factors that have been taken into account when calculating:

1. The absorbed dose for all organs the body.
2. The level of relative damage to radiation.
3. The sensitivities values of each organ to radiation [63].
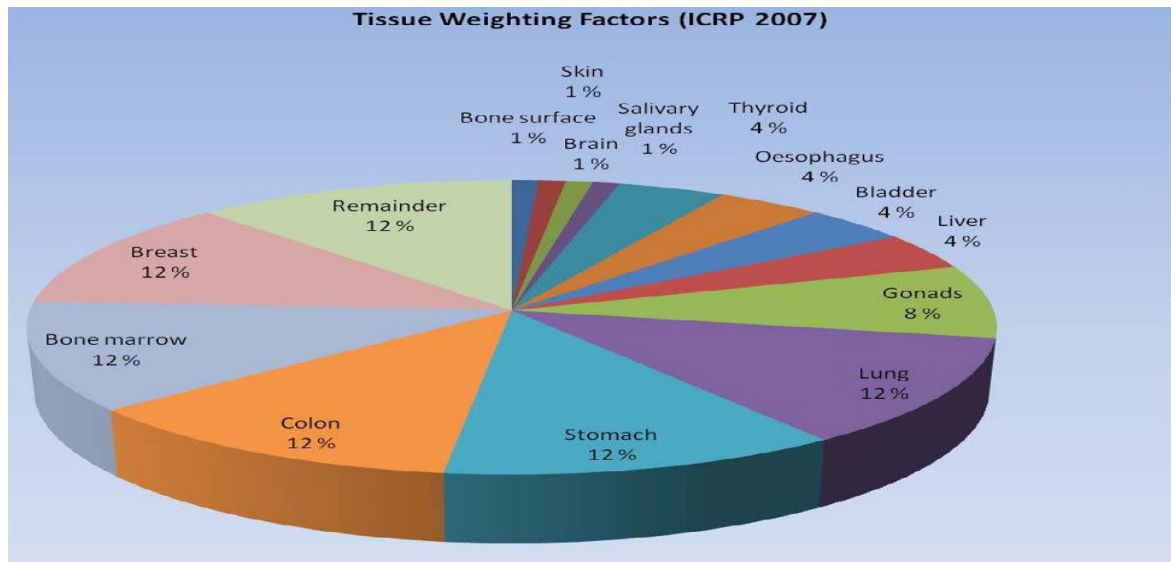
Fig.(2-8) Tissue weighting factors (ICRP 2007)[63].

(2.14) Computer Codes for Calculating the Stopping Power of Heavy Ions

There are many models which have been developed to predict energy loss properties. These particularly focus on stopping power although some are capable of predicting other properties.

The first attempts to describe stopping power in the early 20th Century were classical treatments of incident particles by Bohr [64] . This classical theory is accurate at higher energies; however, it becomes less accurate as incident ion energy decreases. This approach is widely used since it gives a reasonable description of the interaction of target electrons with projectiles [65 ‹66] .

In the 1920, Bethe suggested a different approach to the purely classical treatment. This theory treats the Coulomb interaction between the projectile and target electrons by quantal scattering theory in the first-Born approximation [67]. As classical Bohr theory, there is a simple Z^2 relationship of stopping power to the incoming ion charge.

At low energies both theories require correction due to the motion of target electrons in the medium. This correction takes the form of the Bloch correction. This can be described as

$$\Delta L_{Bloch} = \varphi(1) - R_e \varphi \left(1 + i \frac{zv_0}{v} \right) \dots \dots \dots \dots . (2\text{-}46)$$

With $\varphi(x) = \frac{d \ln[\Gamma(x)]}{dx}$ the Bloch correction is added to first order quantal perturbation theory and is proportional to Z^4 at low speeds, becoming negligible at higher speeds.

Another effect requiring a correction to theory due to a difference in stopping between a particle and antiparticle was discovered by Barkas et al. [68] and confirmed by

measurements of Anderson et al. [69]. This higher order correction to the Z^2 quantum theory is proportional to Z^3 and is also more prominent at low energies. It was described by Ashley et al. [70] as the addition to Bethe theory

$$\Delta L_{Barkas-Anderson} = \frac{Ze^4 w_i}{mv^3} \dots\dots\dots (2-47)$$

Whilst many different developments for predictions of stopping power exist, an extended list of published tables and computer programs for stopping power has been recently published in can consider mainly the four programs mentioned which are all recent, easily available and capable of treating many ions and targets over a wide energy range. Figure (2-9) shows a typical comparison of four computer programs for C ions in amorphous carbon [71].
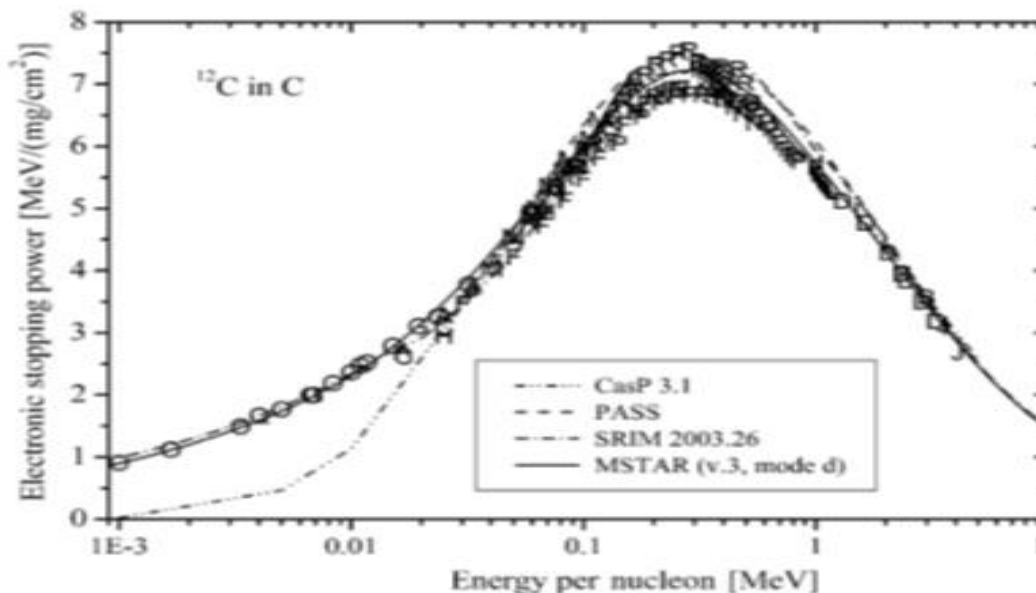
Fig. (2-9) Mass stopping power for C ions interaction with amorphous carbon calculated using (SRIM, PASS, CasP) programs [71].

(2.14.1) SRIM Code

SRIM is an acronym for Stopping and Range of Ion in Matter. Ziegler et al.'s SRIM software is probably the most widely used computer program to predict stopping powers of ions in matter. This software also includes a Monte Carlo program to predict other macroscopic and microscopic energy loss properties. Monte-carlo simulation provides a very good method of estimating ion implantation parameters. The moving atom is convention considered an ion (whether it is charged or neutral) and the target is an atom. The software simulates the slowing down and scattering of an energetic ion through interactions with the target atoms. The collision cascade simulation is achieved by

41

following the ions, which after penetration into the target suffer multiple nuclear and electronic collisions. The program follows one ion at a time until the associated stopping power slows the ion to some per-determined velocity [72].

The SRIM code simulates the transport of heavy ions more than 2GeV/ amu in matter. The models are based on quantum mechanical treatments and, thus statistical, in the sense that the ions makes macroscopic movements during their collision, thus the collision results are averaged [73].

The statistical improvements in SRIM's stopping power accuracy when comparing to the experimental data, In addition to the SRIM-1998 and the percentage of data points within 5% and 10% of the SIRIM calculation. . The experimental stopping power of heavy ions has more scatter than light ions, so there are bigger errors for heavy ions. The accuracy of the SRIM-2010 of individual ions or targets can be determined by displaying shapes that compare experimental values with equivalent SRIM calculations.

The measurement of the stopping power of ions in compound deviates by less than 20% from those predicted by the Bragg's rule. The rule of Bragg becomes inaccurate if there are any differences between the bonding in the base material and the compounds.

SRIM used the CAB approach in order to generate corrections between the Bragg's base and compounds containing common elements H, C, N, O, F, S and Cl. These light atoms have a greater correlation effect on the stopping powers. Heavier atoms are assumed not to contribute anomalously to stopping because of their bonds. When using SRIM, we have the option to use compound dictionary that contains chemical bonding information for about 150 compounds. When a particular compound is selected, the chemical bond diagram will be shown and calculate the best correction of the stopping power[73] .

(2.14.2) CasP Code

CasP is an acronym for Convolution approximation for swift Particles. Unitary convolution approximation provides an impact parameter dependent version of quintal perturbation theory. The impact parameter in a collision denotes the perpendicular distance between the incoming projectile trajectory and the target nucleus (initially at rest) [5]. Close and distant interactions are treated differently in this approach with distant interactions determined using a 'traditional' perturbation approach and close interactions determined by a Coulomb interaction with respect to an impact parameter [39]. This covers energies in the transition from the classical to the perturbation regime. The theory does not currently account for Barkas-Anderson corrections. This theory developed by Grande and Schiwietz

[74] is used in the CasP program. Input data avoids the need for effective charge considerations but uses the mean ionization value of the target material .

(2.14.3) PASS Code

PASS is an acronym for Peter-Andreas-Sigmund-Schinner .The code is one of the most developed, widest range models. PASS allows to compute stopping forces for all ions in all elemental materials and compounds which was used in the ICRU data tables for the 'Stopping of ions heavier than helium' [39]. The PASS implements binary stopping theory developed by Sigmund and Schinner [75]. it similar to that of classical Bohr Theory however it avoids Bethe and Bloch's perturbation theory, as well as the necessity for discerning between close and distant collisions as is the case with classical theory. This simplification is achieved by considering binary scattering of the projectile and the target electrons [76]. The projectile electrons are treated as a screening of the interaction [39]. However, the accuracy of the predictions depends on available information on atomic or molecular oscillator strengths.   This model includes corrections for relativistic effects and shell effects with the program inherently inclusive of the Barkas-Anderson effect [39].

(2.14.4) MSTAR Code

MSTAR is an acronym for MoreSTAR (going beyond PSTAR code and ASTAR code). MSTAR is a program that calculates total energy loss for heavy ions (Lithium to Argon) at specific energies from 0.001 to 1000 MeV/nucleon and for any element, mixture or compound contained in ICRU Report 49. The MSTAR code of Paul and Schinner. The code has been updated repeatedly and is available on the Internet [38].

(2001),The basic description of its first version has been published [38]. also, the fitting functions and various details have been improved in version 2.00 [77]. For version 3.00 (2002), data from recent publications (2002), and data for nickel targets have been included in the data base. All the fits for solid data have been redone. Version 3.11 (2003) will also calculate B, Zr, Gd and Ta targets . A table based on this version has been published [78]. The present version 3.12 (2004) is mathematically identical to version 3.11, except for an improved error function subroutine.

Mainly, MSTAR is based upon the alpha stopping power included in ICRU Report 49 [79]. MSTAR can as well produce the alpha stopping power that serve as input; except for (B, Ni, Zr, Gd, and Ta) , these are identical to those included in ICRU Report 49 [79].

(2.15) Chemical Compositions of the Human Tissues

The chemical composition of human tissues is of great interest to study micro-distributions of human radiation treatment. At high energies, initial interactions are almost independent on chemical composition, whereas secondary reactions primarily responsible for biological effects depend on chemical composition. The chemical composition of human tissues generally depends on strain, diet, age, sex, health, etc., and may vary significantly (5-10%) among individuals[80] .

The chemical composition of human tissues is usually given in terms of biological molecules (e.g., protein, fat, vitamins, etc.), and they are not readily adaptable to dosimetry calculations. In the usual energies of machine therapy, the effects of molecular association are negligible, and one can represent human tissue through its atomic structures (% by weight of elements). The average atomic structures of various biological molecules are readily available, and the average atomic structures of human tissues can be calculated from these data [80].

Each tissue consists of basic elements are H, C, O, N, and some other elements such as P, S, K, etc. Therefore, the knowledge of the ratios of these elements is important to calculate the mass stopping power for heavy ion in the tissues as well as the density of the tissue.

Table (2-6) The chemical composition of various human tissues studied and the fractional weight of the elements in the tissues [19,29]

Human Tissue	Density g/cm^3	Composition (element: fraction) by weight											
		H	C	N	O	Na	P	S	Cl	K	Fe	Mg	Ca
Adipose tissue	0.930	0.116	0.681	0.002	0.198	0.001	----	0.001	0.001	----	-----	----	----
Blood	1.060	0.102	0.11	0.033	0.745	0.001	0.002	0.002	0.003	0.002	0.01	-----	-----
Brain	1.040	0.107	0.145	0.022	0.712	0.002	0.004	0.002	0.003	0.003	-----	----	------
Breast	1.020	0.106	0.332	0.030	0.527	0.001	0.001	0.002	0.001	-----	------	----	-------
Lung	1.050	0.103	0.105	0.031	0.749	0.002	0.002	0.003	0.003	0.002	----	-----	-----
Skin	1.090	0.1	0.204	0.042	0.645	0.002	0.001	0.002	0.003	0.001	-----	-----	-----
Bone	1.092	0.034	0.155	0.042	0.435	0.001	0.103	0.003	-----	----	-----	0.02	0.225
Muscle	1.0599	0.103	0.099	0.032	0.757	0.001	0.002	0.003	0.001	0.003	-----	-----	-----

Chapter Three

Calculations, results and discussion

Chapter Three: Calculations, results and discussion

Calculations, results and discussion

(3.1) calculation of $Z_{effective}$

The effective atomic number for (adipose, blood, breast, brain, lung , muscle, bone, skin) tissues were calculated according to eq.(2-30) .The results tabulated in table (3-1) .

Table (3-1) The effective atomic number for (adipose, blood, breast, brain, lung, muscle, bone, skin) tissues.

Tissue	$Z_{effective}$
Adipose tissue	5.8440
Breast	6.5990
Skin	6.9170
Brain	7.0490
Muscle	7.060
Blood	7.1260
Lung	7.1310
Bone	10.8159

(3.2) Mass Stopping Power for Heavy Ions in Elements Component for the Studied Tissues

(3.2.1) SRIM program

Using SRIM program ,the mass stopping power for (Li ,C,O, and F) ions which interacts with elements (H,C,O,N,P,K,O, S, Na ,Fe ,Mg , and Ca) which represent the chemical composition of (adipose , blood, breast, brain ,lung , muscle, bone, skin) tissues for the energy range (0.025 -1000) MeV , are plotted by using the Matlab2015 program in figure (3.1.a) for Lithium, figure (3.1.b) for Carbon , figure(3.1.c) for Oxygen and figure (3.1.d) for Fluorine.

(3.2.2) PASS program

Using PASS program ,the mass stopping power for (Li ,C,O,F) ions which interact with elements (H,C,O,N,P,K,O, S, Na ,Fe ,Mg ,Ca) which represent the chemical composition of (adipose, blood, breast, brain ,lung , muscle, bone, skin) tissues for the energy range (0.025 -1000) MeV , are plotted by using the Matlab2015 program in figure (3.2.a) for Lithium, figure (3.2.b) for Carbon , figure (3.2.c) for Oxygen and figure (3.2.d) for Fluorine.

Chapter Three: Calculations, results and discussion

(3.2.3) CasP program

Using CasP program ,the mass stopping power for (Li ,C,O,F) ions which interact with elements (H,C,O,N,P,K,O, S, Na ,Fe ,Mg ,Ca) which represent the chemical composition of (adipose, blood, breast, brain ,lung , muscle, bone, skin) tissues for the energy range (0.025 - 1000) MeV , are plotted by using the Matlab2015 program in figure (3.3.a) for Lithium, figure (3.3.b) for Carbon , figure (3.3.c) for Oxygen and figure (3.3.d) for Fluorine.

(3.2.4) Bethe formulae

The mass stopping power for (Li ,C,O,F) ions which interact with elements (H,C,O,N,P,K,O, S, Na ,Fe ,Mg ,Ca) which represent the chemical composition of (adipose, blood, breast, brain ,lung , muscle, bone, skin) tissues, were calculated according to eq.(2-9) of energy range of (0.025 -1000) MeV and are plotted in figure (3.4.a) for Lithium, figure (3.4.b) for Carbon , figure (3.4.c) for oxygen and figure (3.4.d) for Fluorine.

Figure (3.1.a): Total energy loss for Lithium ion in the components of tissues studied using the SRIM program
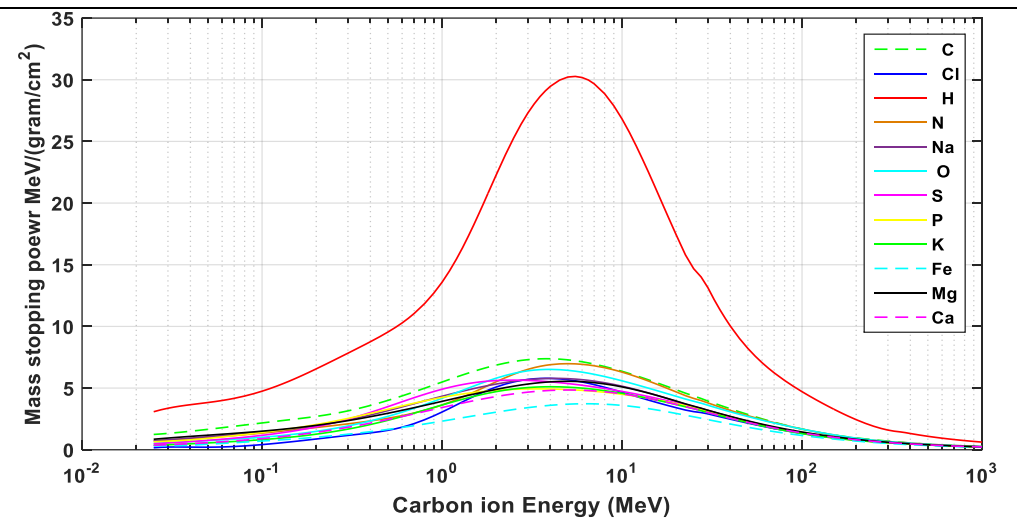
Figure (3.1.b): Total energy loss for Carbon ion in the components of tissues studied using the SRIM program
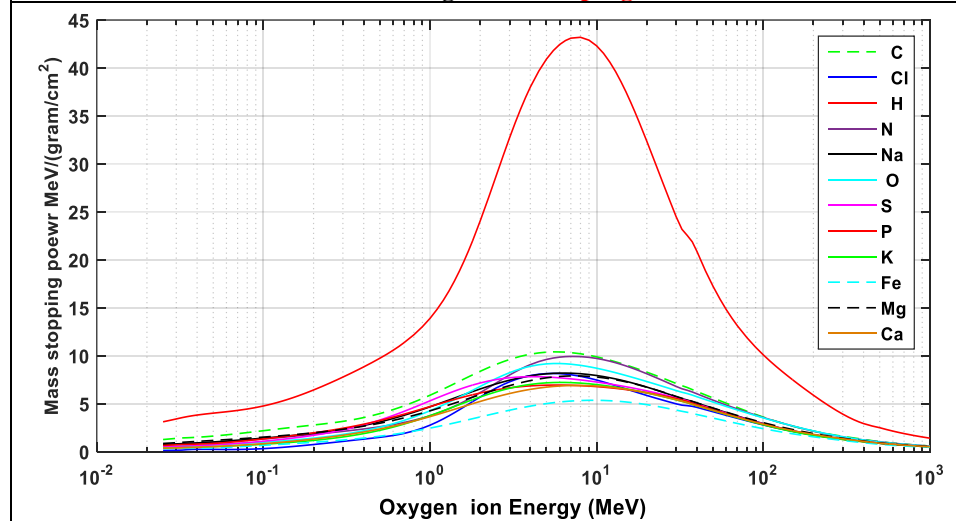
Figure (3.1.c): Total energy loss for Oxygen ion in the components of tissues studied using the SRIM program
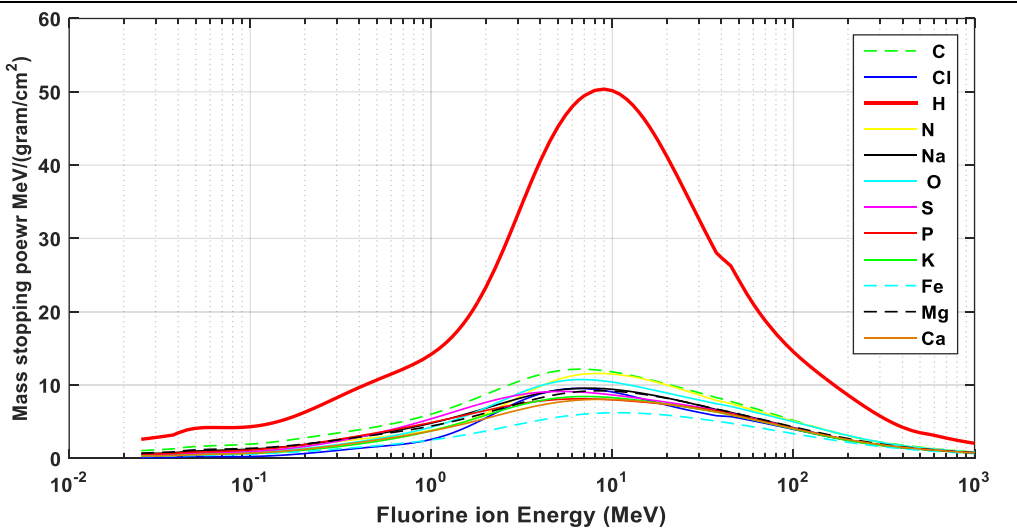
Figure (3.1.d): Total energy loss for Fluorine ion in the components of tissues studied using the SRIM program

Figure 3.1: Total energy loss for heavy ions in the components of tissues studied using the SRIM program
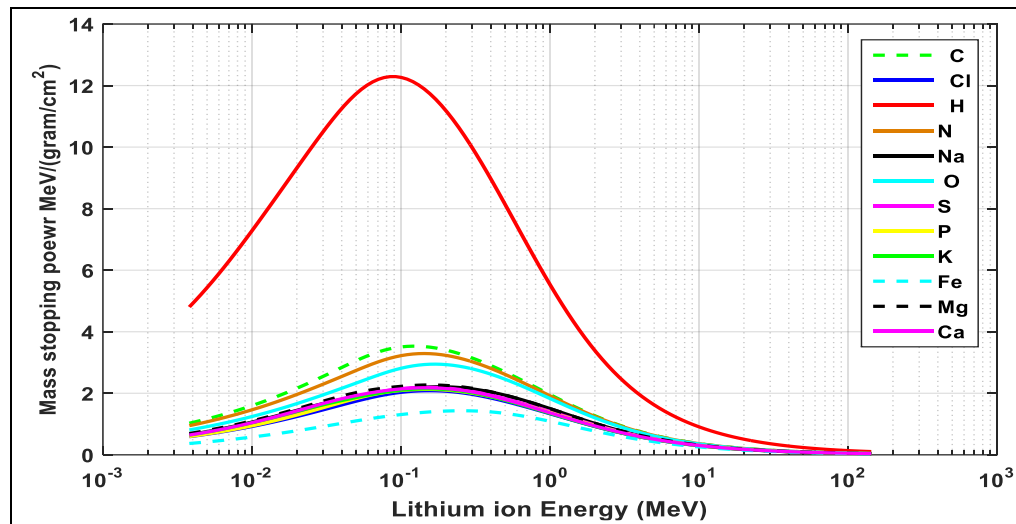
Figure (3.2.a): Total energy loss for Lithium ion in the components of tissues studied using the PASS program
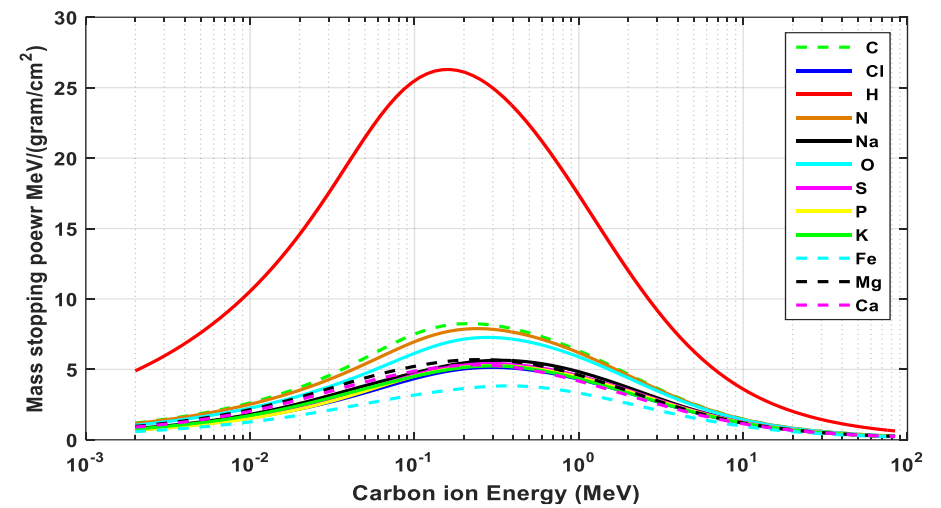
Figure (3.2.b): Total energy loss for Carbon ion in the components of tissues studied using the PASS program
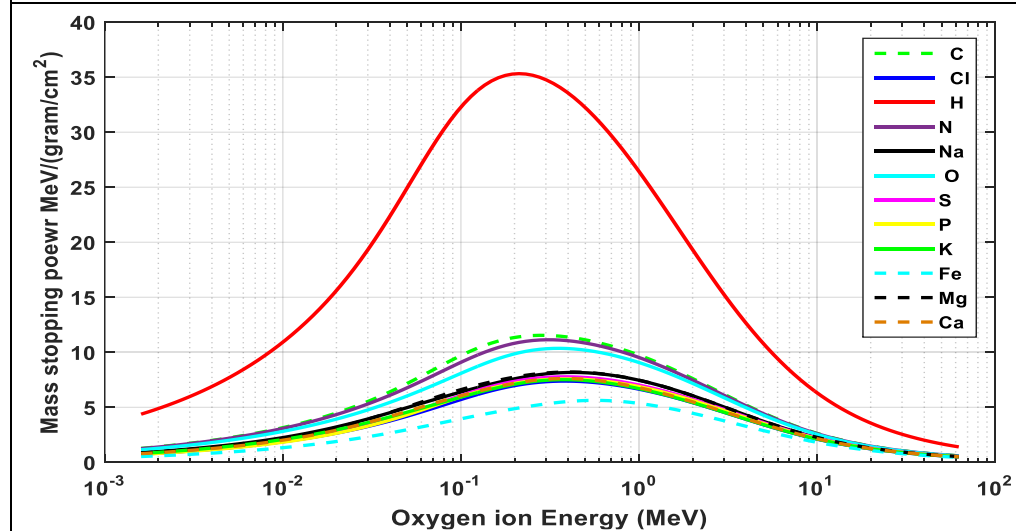
Figure (3.2.c): Total energy loss for Oxygen ion in the components of tissues studied using the PASS program
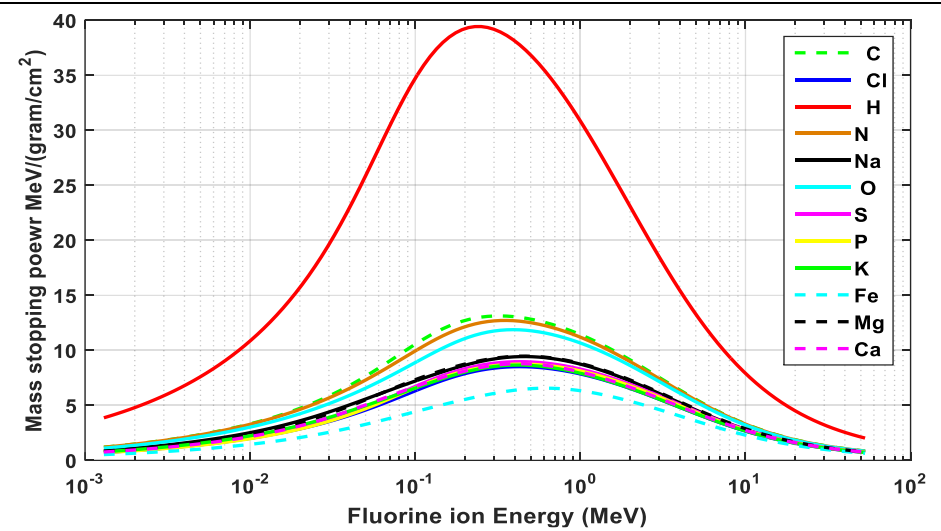
Figure (3.2.d): Total energy loss for Fluorine ion in the components of tissues studied using the PASS program

Figure 3.2: Total energy loss for heavy ions in the components of tissues studied using the PASS program
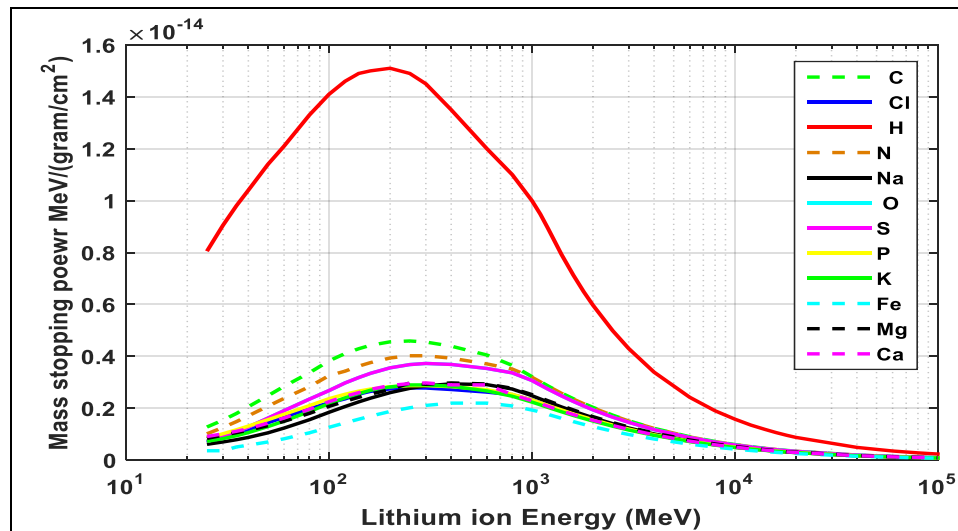
Figure (3.3.a): Total energy loss for Lithium ion in the components of tissues studied using the CasP program
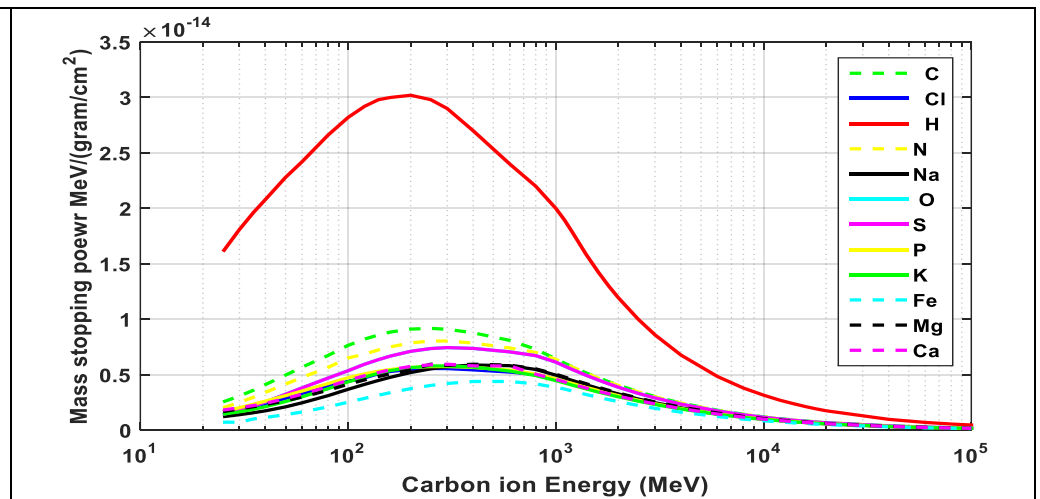
Figure (3.3.b): Total energy loss for Carbon ion in the components of tissues studied using the CasP program
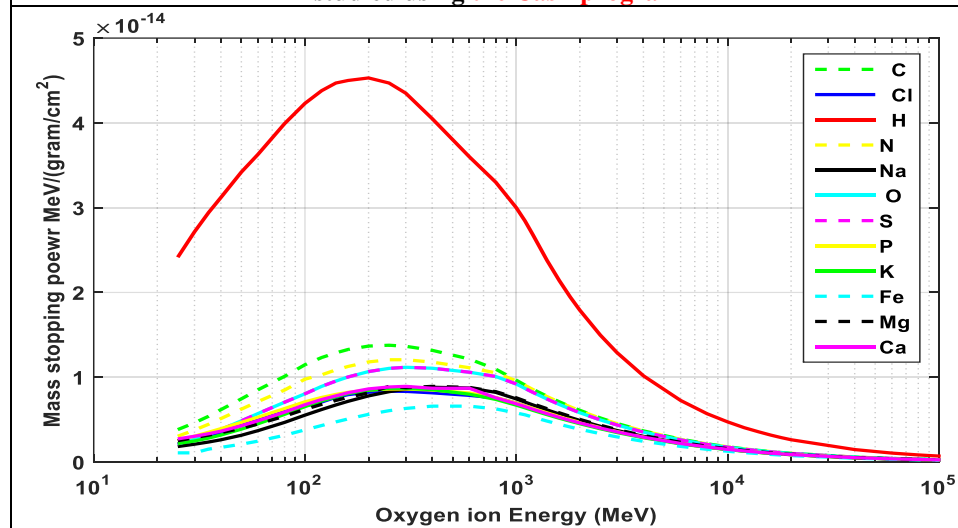
Figure (3.3.c): Total energy loss for Oxygen ion in the components of tissues studied using the CasP program
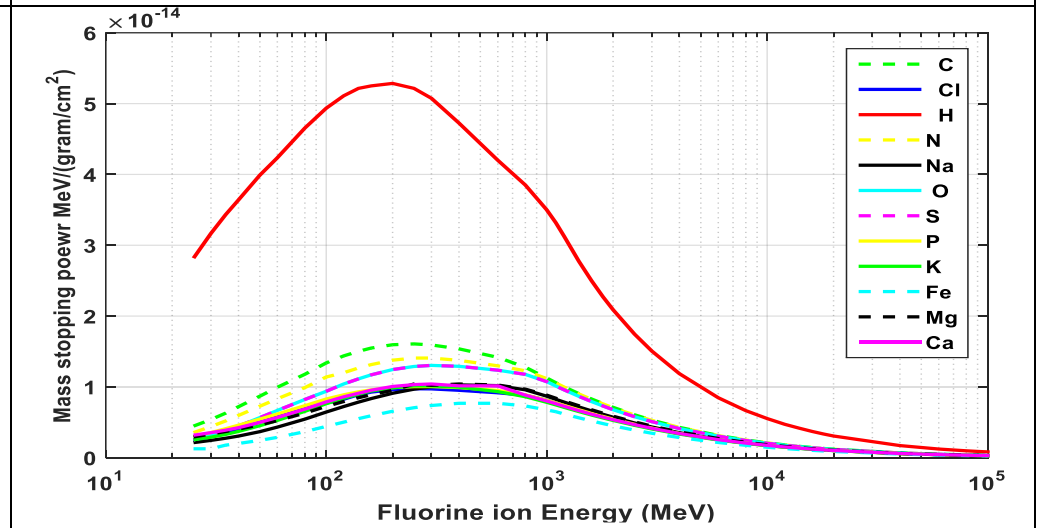
Figure (3.3.d): Total energy loss for Fluorine ion in the components of tissues studied using the CasP program

Figure (3.3): Total energy loss for heavy ion in the components of tissues studied using the CasP program
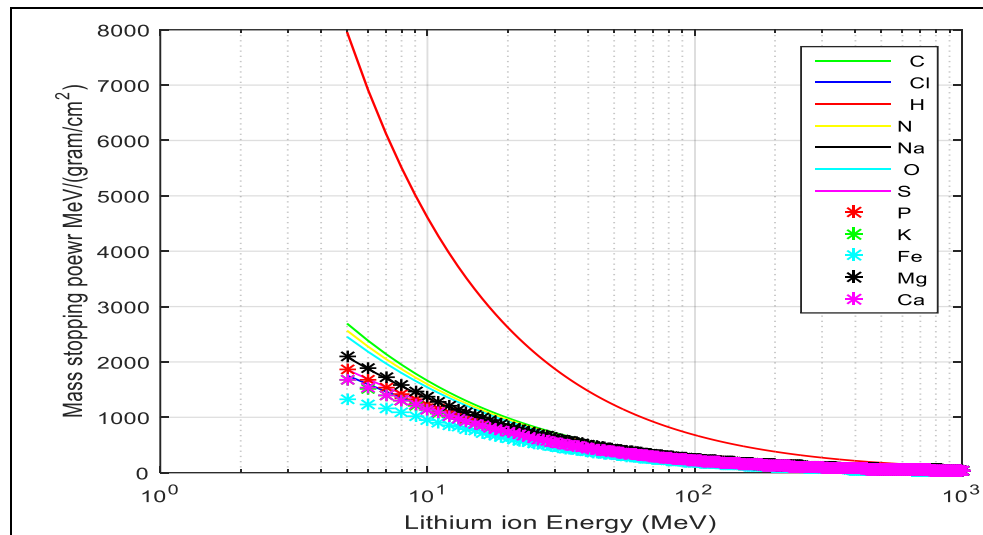
Figure (3.4.a): Total energy loss for Lithium ion in the components of tissues studied using Bethe formulae
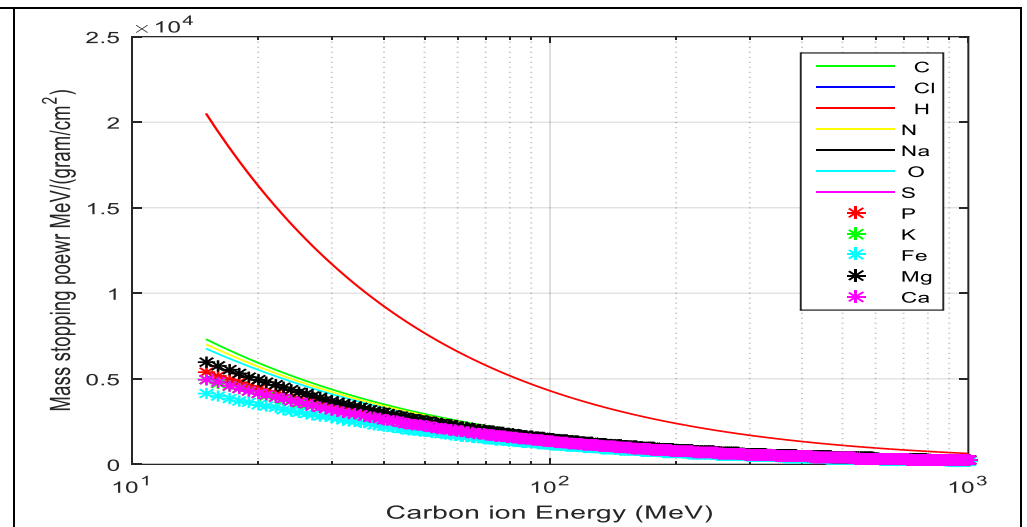
Figure (3.4.b): Total energy loss for Carbon ion in the components of tissues studied using Bethe formulae
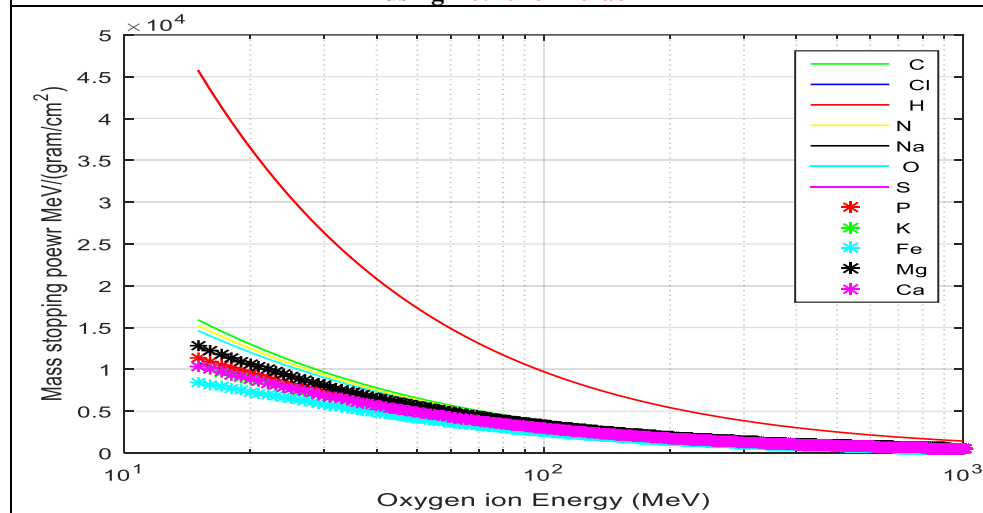
Figure (3.4.c): Total energy loss for Oxygen ion in the components of tissues studied using Bethe formulae
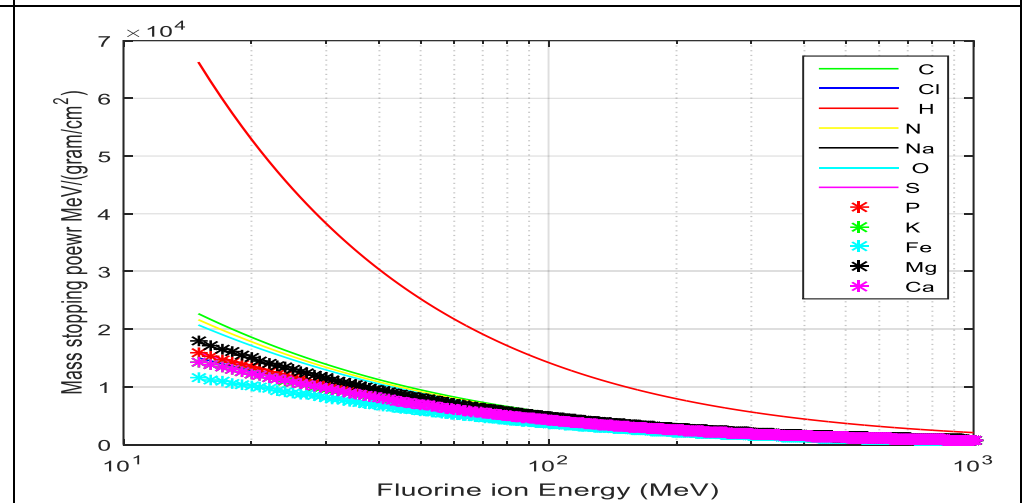
Figure (3.4.d): Total energy loss for Fluorine ion in the components of tissues studied using Bethe formulae

Figure (3.4.): Total energy loss for heavy ion in the components of tissues studied using Bethe formulae

Chapter Three: Calculations, results and discussion

From the above figures (3-1) to (3-4) , the following notes are observed

1. The maximum value of the energy loss for heavy ion is found in the hydrogen element, at same energy value because hydrogen has molecules in the traversing path of the ions and hence the more probability of interaction and more energy lost. [81] Therefore, hydrogen atoms are responsible for losing the greatest energy in human tissue.

2. At low energies, the mass stopping power increases with the increase the energy of the particles which has low speed so it will stay longer in the target, so the probability of electronic transmission will increase, causing increase of loss of their energies.

3. At high energies, the mass stopping power decreases with the increase the energy of the particles which has high speed so it will stay shorter in the target, so the probability of electronic transmission will decrease, causing decrease of loss of their energies.

4. the increasing of value of stopping power is linear with the increase of atomic number Z for the falling particle, this is due to the mass stopping power is proportional to z^2 of the falling particle.

5. We can observe same behavior in all methods except Bethe formula in low energies were deleted because of their failure and give negative values for mass stopping power.

(3.3) Mass stopping power for heavy ions with tissues

(3.3.1) Bragg's Rule

The mass stopping power for (**Li ,C,O, and F**) ions which interact with chemical composition of tissues (adipose, blood, breast, brain ,lung , muscle, bone, and skin) were calculated by considering the percentage values of each element presented in these tissues, using eq. (2- 28) for mixture or compounds of above tissues and (Bethe formulae , SRIM ,CasP , PASS) programs. The results were tabulated in the appendix (A).

(3.3.2) SRIM Dictionary

The mass stopping power for each element in (adipose, blood, breast, brain ,lung , muscle, bone, and skin) tissues, were calculated by SRIM Dictionary program for (**Li ,C,O, and F**) ions with energy range (0.025-1000) MeV . The results were tabulated in the appendix (A).

The mass stopping power for each element in (adipose, blood, breast, brain ,lung , muscle, bone, and skin) tissues, were calculated by MSTAR program for (**Li ,C,O, and F**) ions with energy range (0.025-1000) MeV. The results were tabulated in the appendix (A).

(4.2.3) MSTAR

The mass stopping power for each element in (adipose, blood, breast, brain ,lung , muscle, bone, and skin) tissues, were calculated by MSTAR program for (**Li ,C,O, and F**) ions with energy range (0.025-1000) MeV. The results were tabulated in the appendix (A).

Chapter Three: Calculations, results and discussion

.(3.4) Comparison between methods to calculate mass stopping power

The mass stopping power for (Li, C, O, and F) ions interaction with the tissues (adipose, blood, breast, brain , lung , muscle, bone, and skin) by SRIM ,SRIM Dictionary, CasP program, PASS program ,MSATR program, Bethe formula and average their values are tabulated in the appendix (A) and plotted in figures (3-5)- (3-36).

From these figures, the following notes are observed:

1. At low energies, the mass stopping power increases with the increase of energy of the falling particle, as the positive charged particle moving through a material interacts through Coulomb forces with the negative electrons and the positive nuclei that constitute the atoms of that material. Thus, the particle with low energy (low velocity) have enough time to interact (inelastic collisions) with electrons and nuclei, this may result in the transfer a lot of energy from the moving charged particle to the bound electron, via the ionization or excitation. this mean (high stopping power in low energy), but if a particle has high energy it doesn't have enough time to interact with atomic electrons and nuclei so the loss of energy going low.

2. The curves diverge from each other at low energy are due to many reasons:

   - The I value and shell correction has an influence on the stopping power especially for targets having high atomic number, some elements have different stopping power values according to their physical and chemical structure (gas or liquid or solid) .

   - These differences result too from the utilization of different theories in the calculation of the stopping power, e.g. the program SRIM use BK +LSS theory and take into account the degree of ion stripping [73], while MSTAR code use three corrections: shell corrections, Barkas correction and Bloch correction. PASS code includes corrections for relativistic effects and shell effects with the program inherently inclusive of the Barkas-Anderson effect. Also, the CasP program input data avoids the need for effective charge considerations but uses the mean ionization value of the target material [39].

3. In calculating the average of mass stopping power, value calculated by the Bethe formula for energies from (0.025 – 40) were deleted because the Bethe formula is not valid at low energy, because in this region the charged particle captures and loses electrons as it moves, thus reducing its net charge and stopping power. More over the term $\ln \frac{2mv^2}{I}$ eventually becomes negative giving a negative value for the stopping power [82].
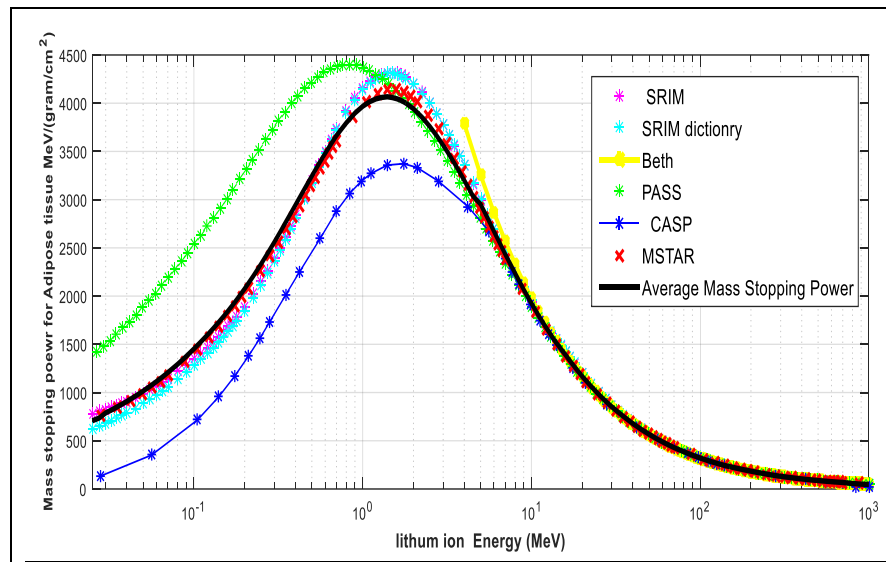
Fig. (3-5) Mass stopping power for Lithium in Adipose tissue
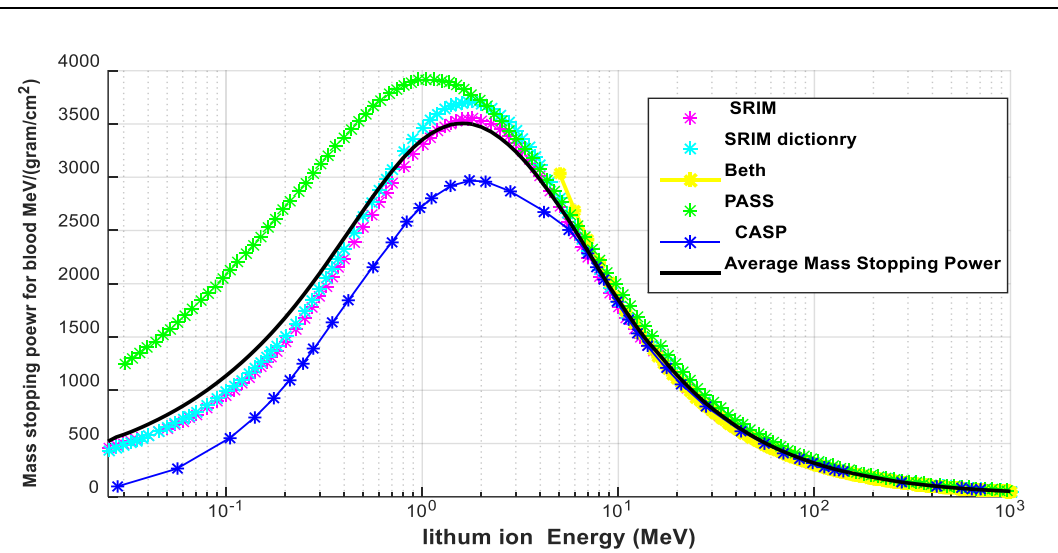
Fig. (3-6) Mass stopping power for Lithium in blood tissue
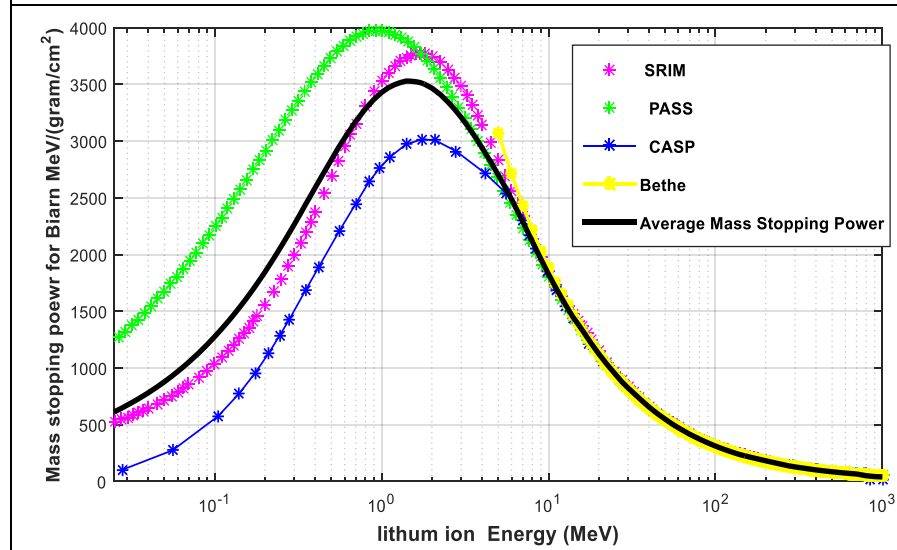
Fig. (3-7) Mass stopping power for Lithium in Brain tissue
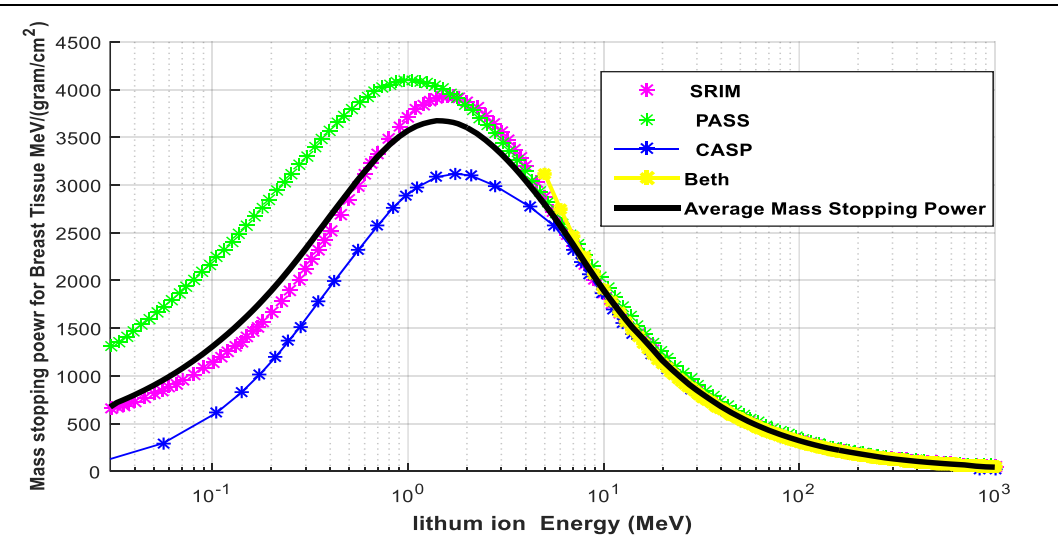
Fig. (3-8) Mass stopping power for Lithium in Breast tissue
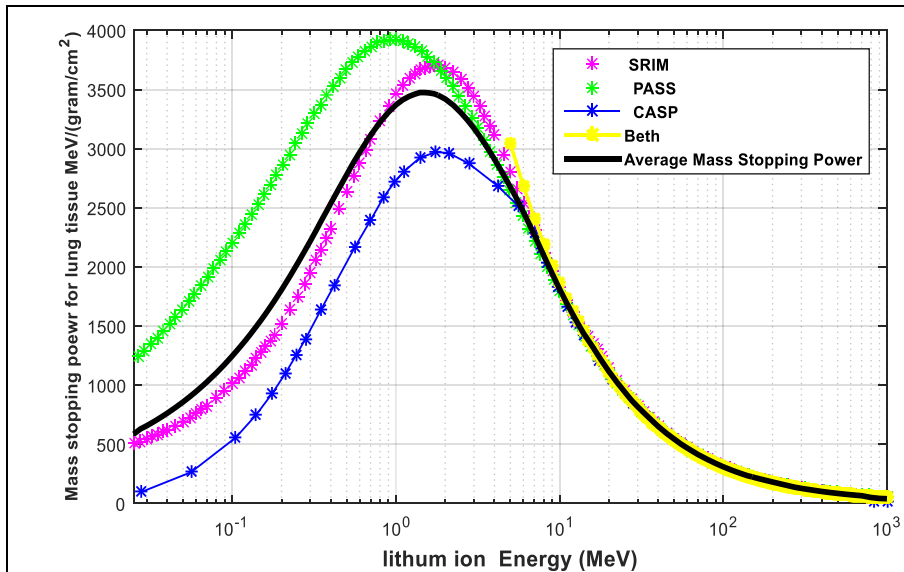
Fig. (3-9) Mass stopping power for Lithium in Lung
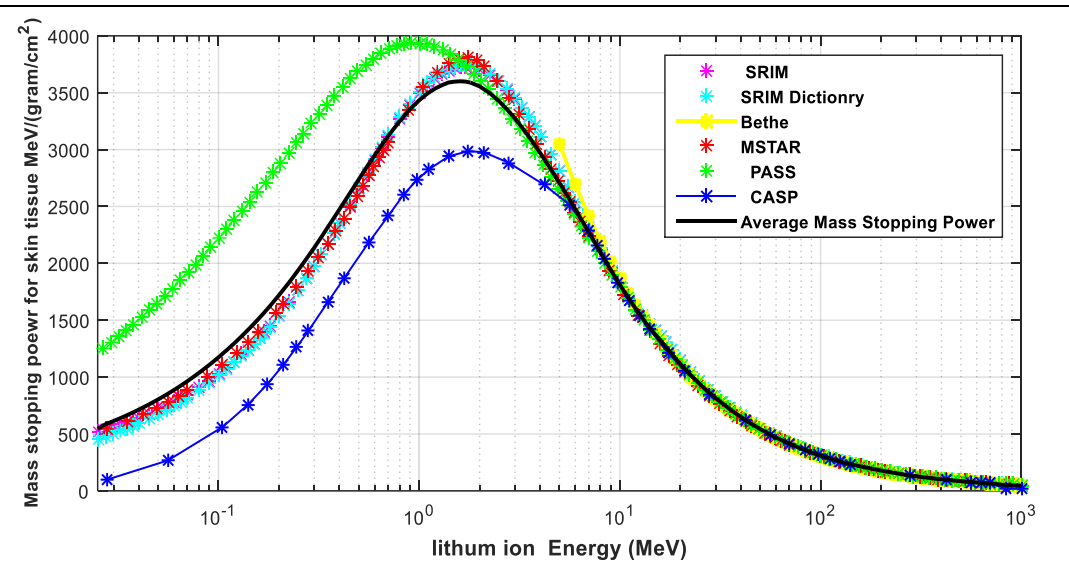
Fig. (3-10) Mass stopping power for Lithium in Muscle
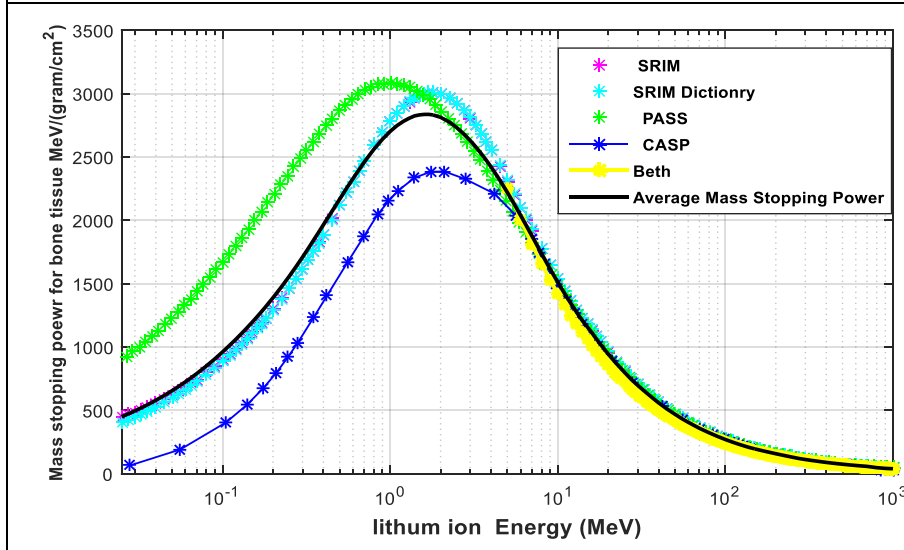
Fig. (3-11) Mass stopping power for Lithium in Bone
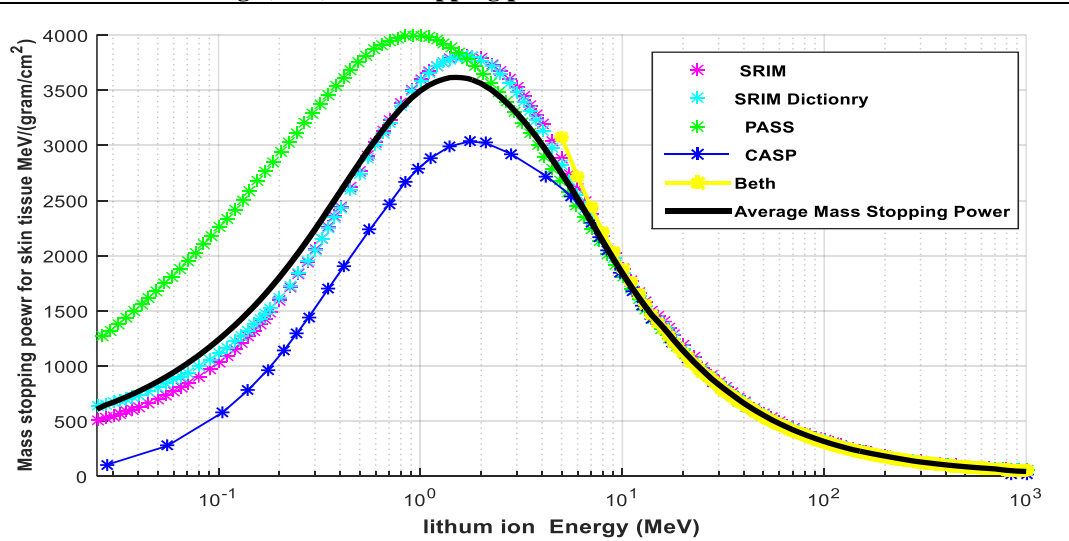
Fig. (3-12) Mass stopping power for Lithium in Skin
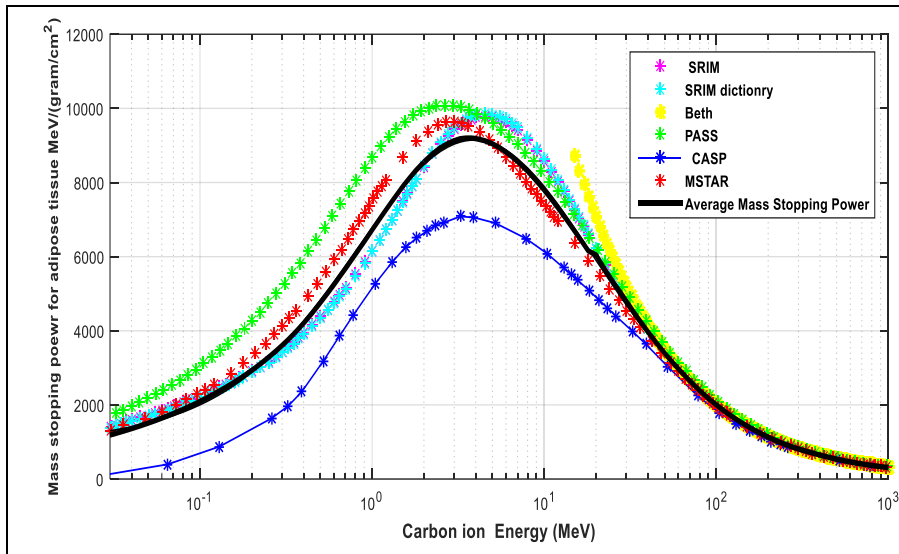
Fig. (3-13) Mass stopping power for Carbon in Adipose tissue
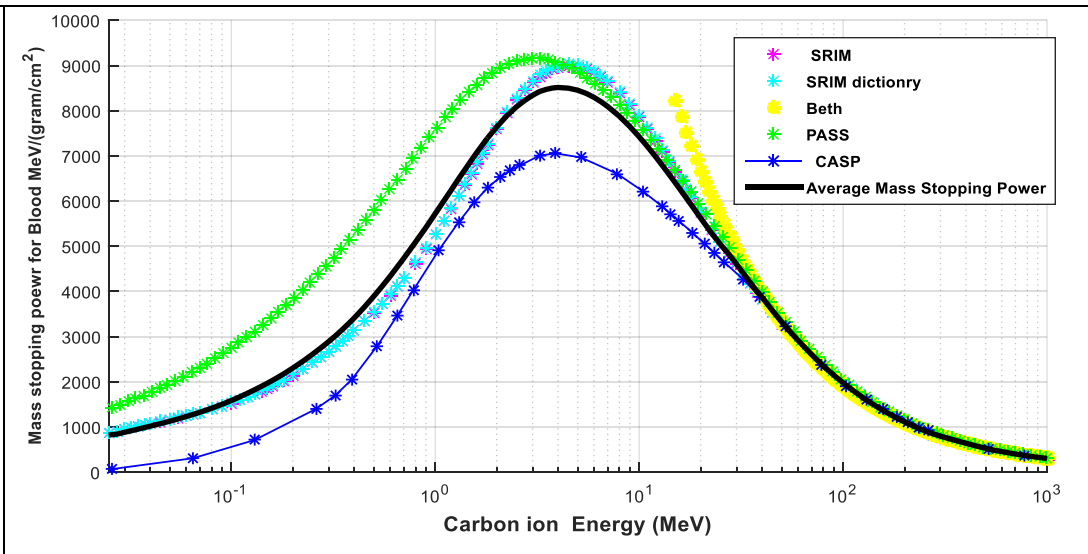
Fig. (3-14) Mass stopping power for Carbon in Blood
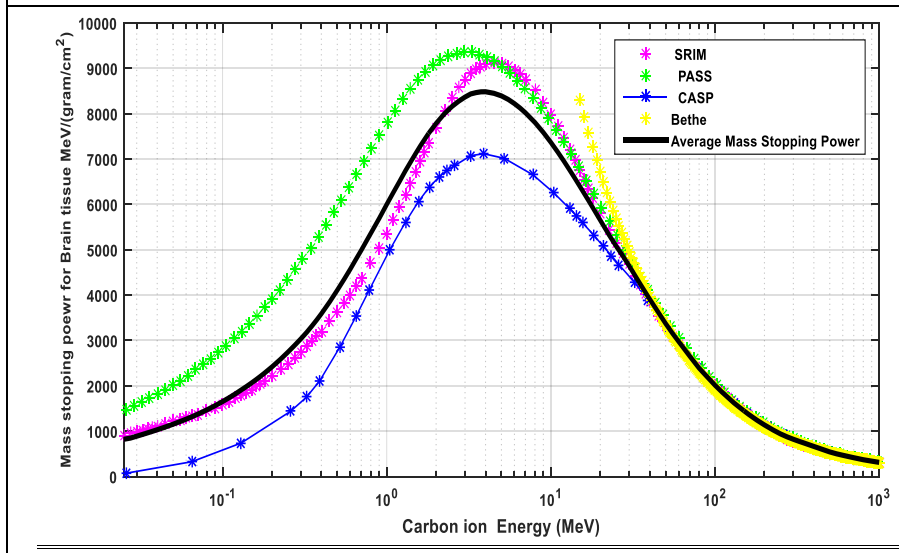
Fig. (3-15) Mass stopping power for Carbon in Brian
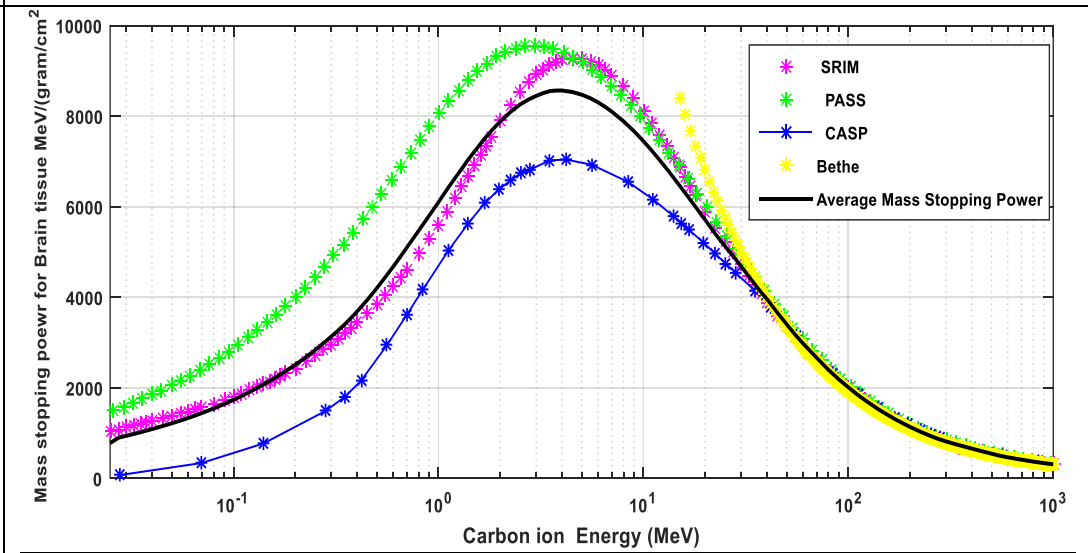
Fig. (3-16) Mass stopping power for Carbon in Breast
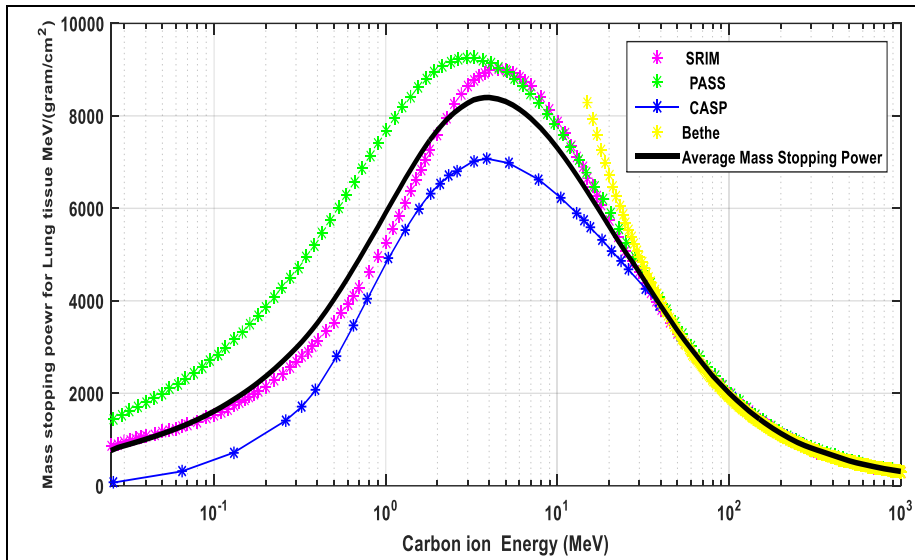
Fig. (3-17) Mass stopping power for carbon in Lung
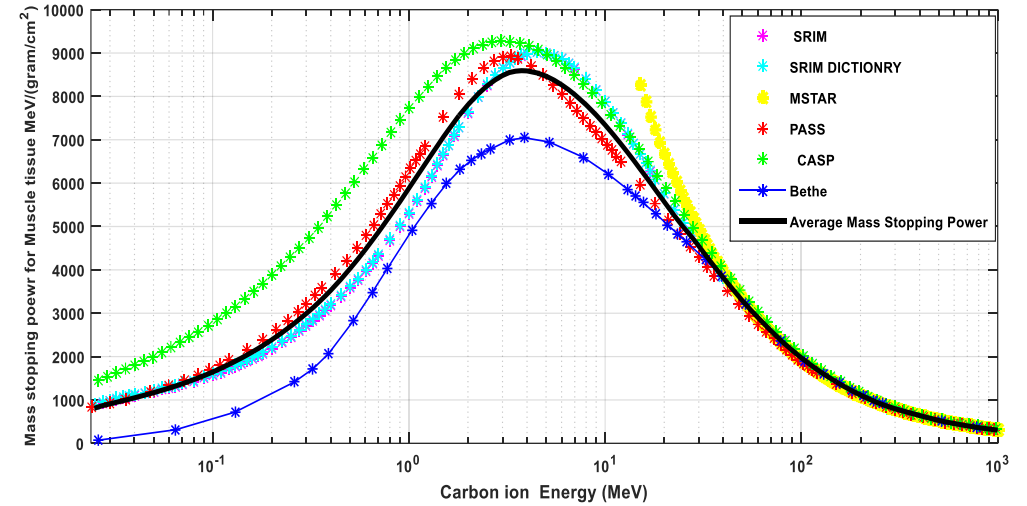
Fig. (3-18) Mass stopping power for Carbon in Muscle
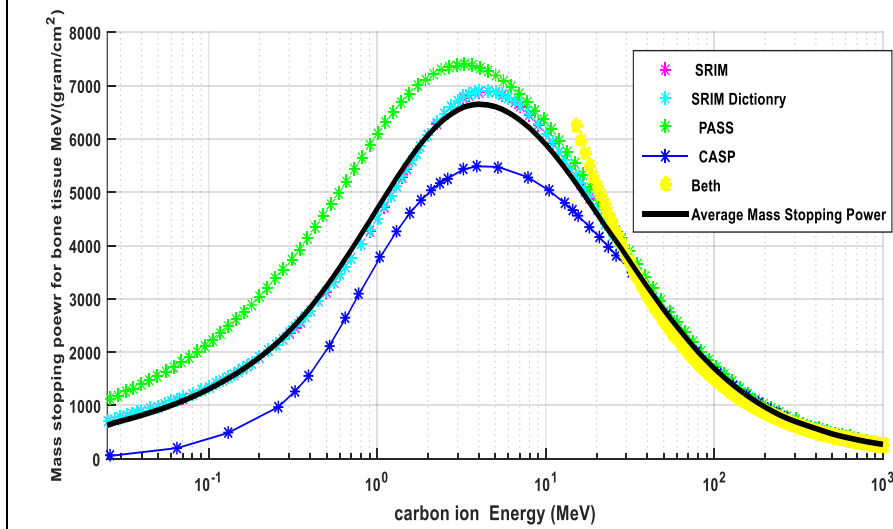
Fig. (3-19) Mass stopping power for carbon in Bone
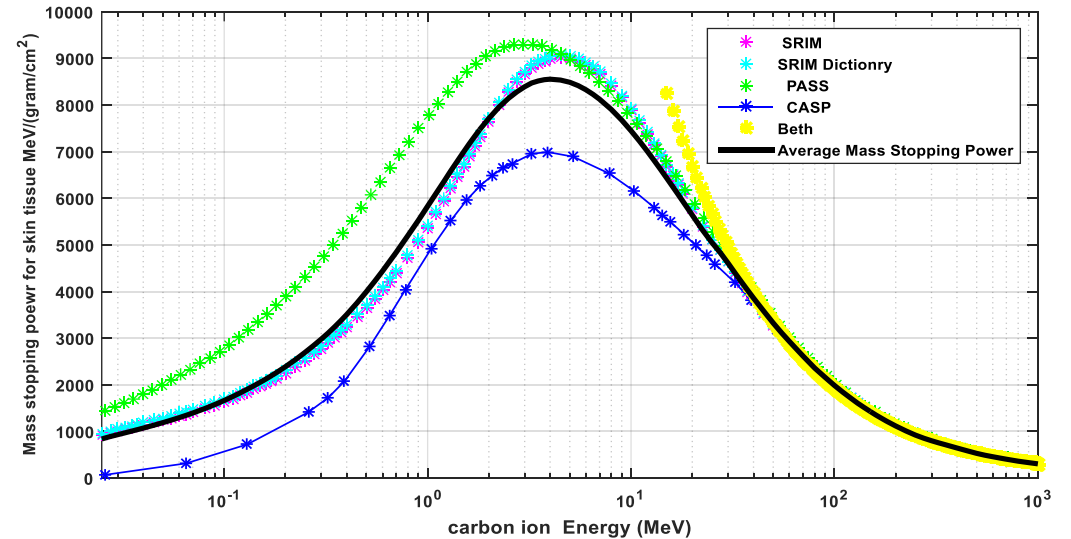
Fig. (3-20) Mass stopping power for carbon in Skin
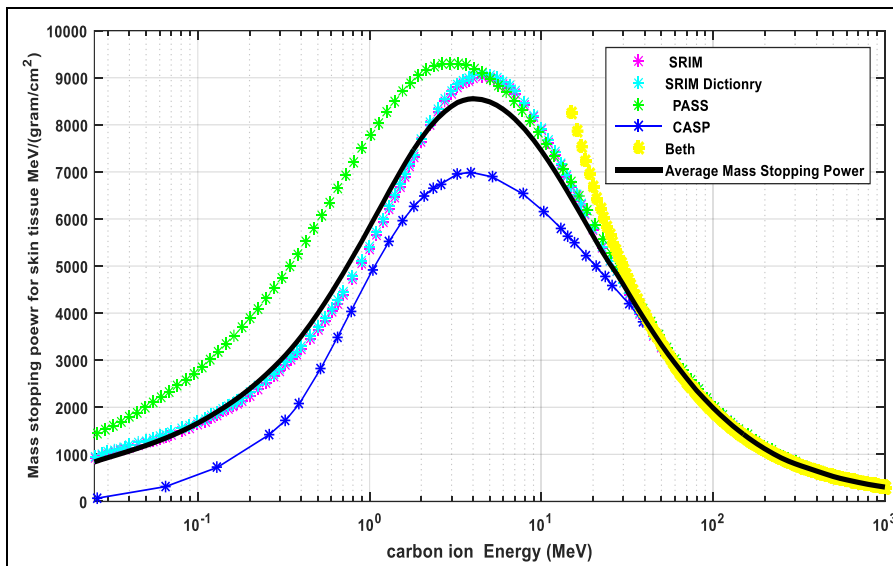
Fig. (3-21) Mass stopping power for Oxygen in Adipose tissue
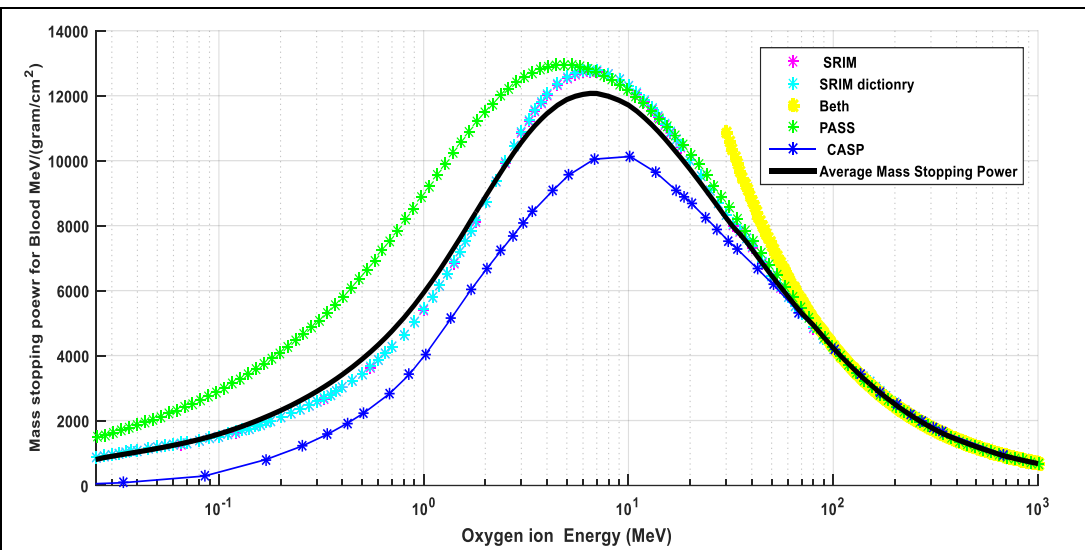
Fig. (3-22) Mass stopping power for Oxygen in Blood
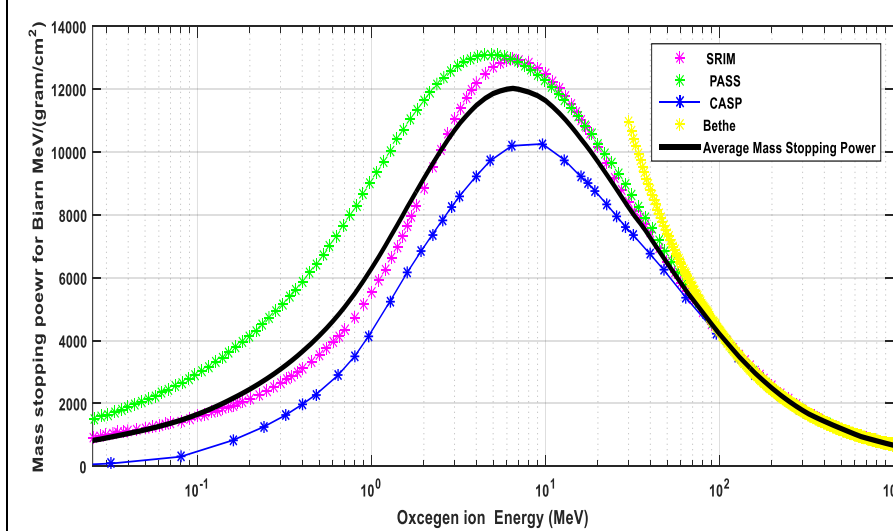
Fig. (3-23) Mass stopping power for Oxygen in Brian
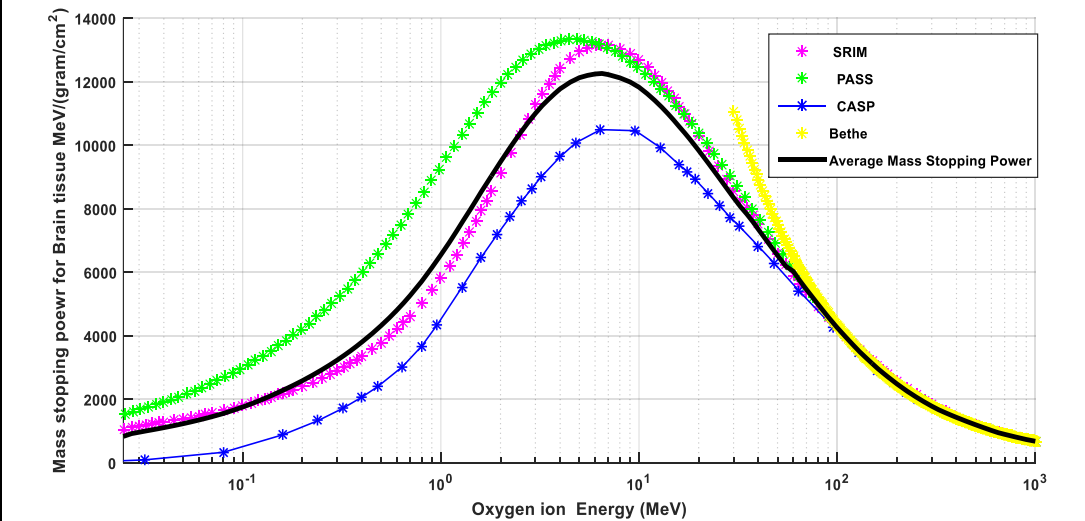
Fig. (3-24) Mass stopping power for Oxygen in Breast
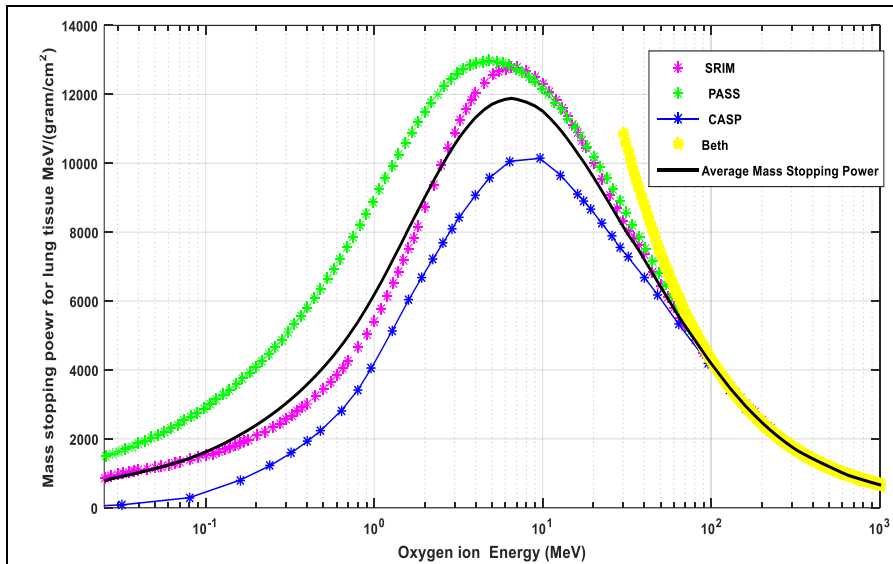
Fig. (3-25) Mass stopping power for Oxygen in Lung
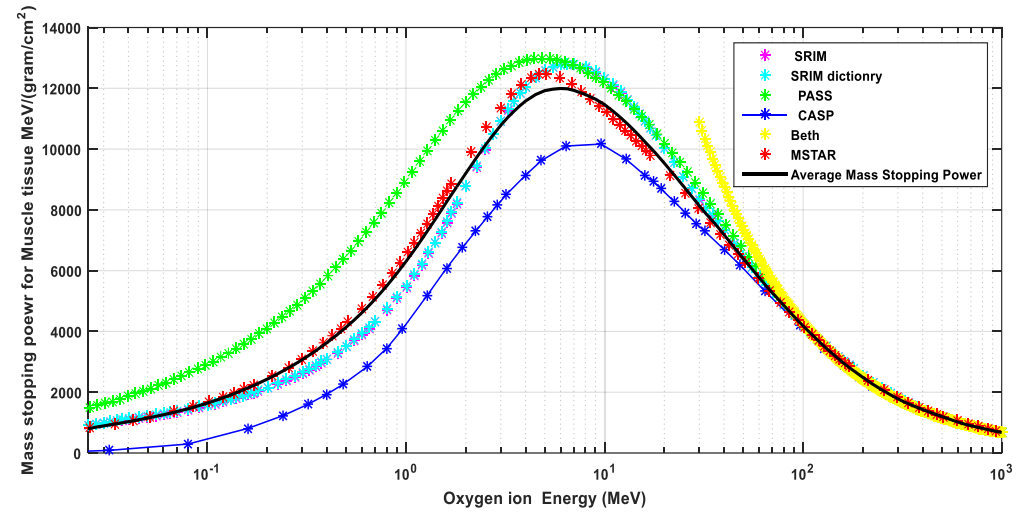
Fig. (3-26) Mass stopping power for Oxygen in Muscle
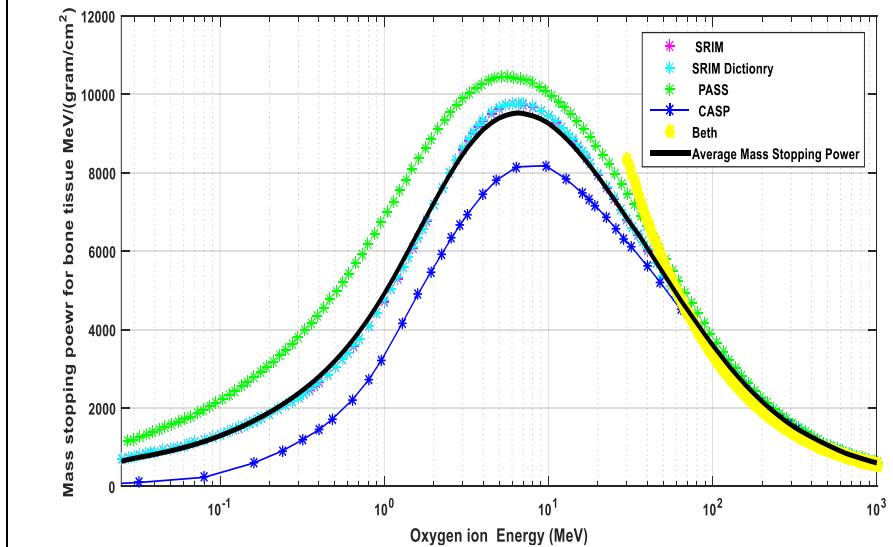
Fig. (3-27) Mass stopping power for Oxygen in Bone
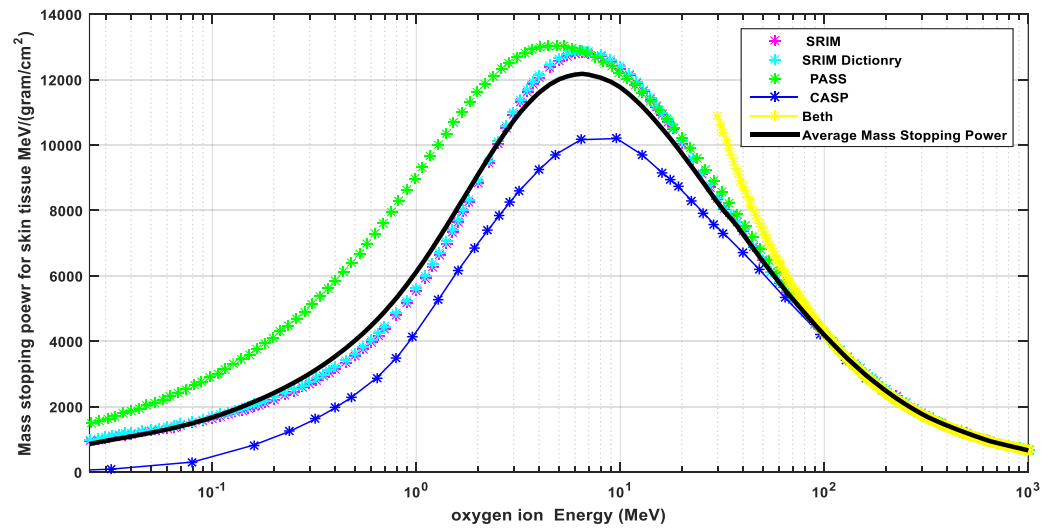
Fig. (3-28) Mass stopping power for oxygen in Skin
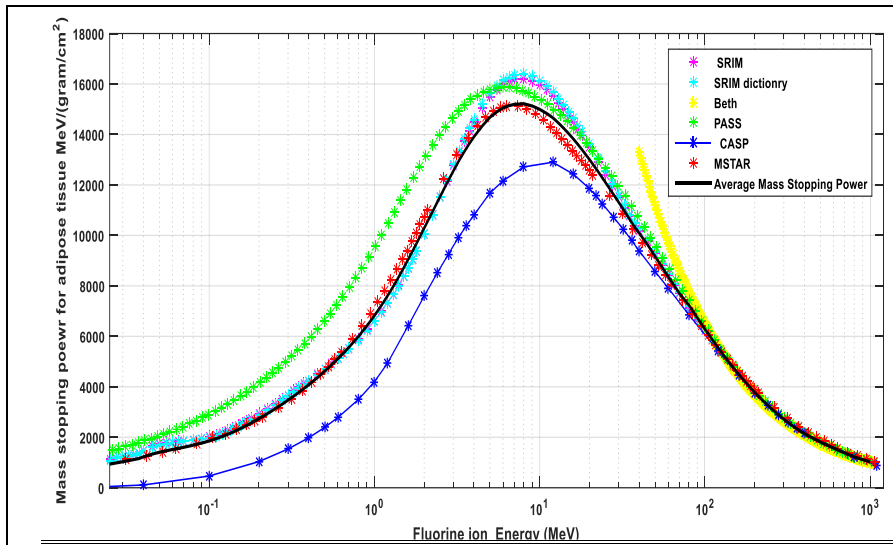
Fig. (3-29) Mass stopping power for Fluorine in Adipose tissue
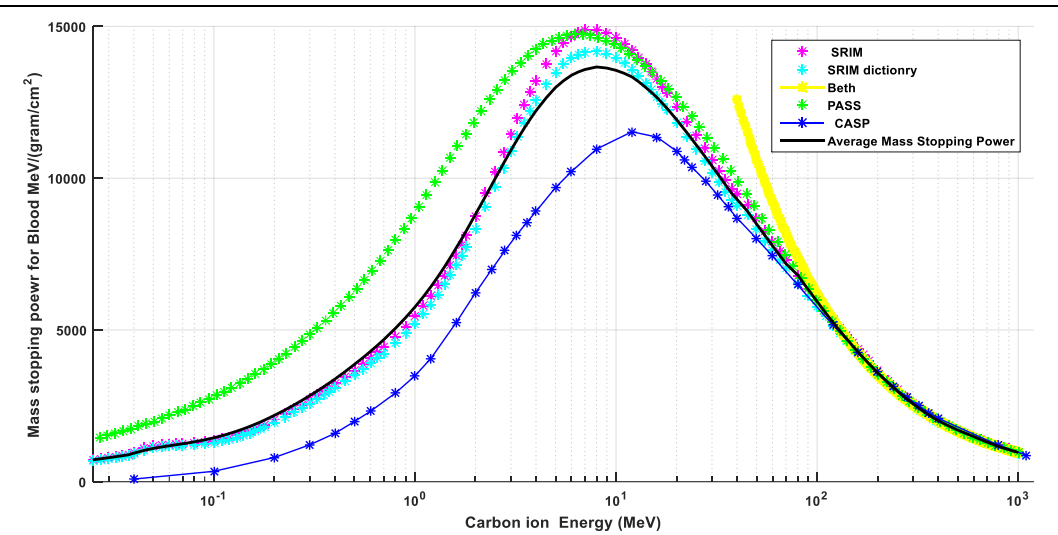
Fig. (3-30) Mass stopping power for Fluorine in Blood
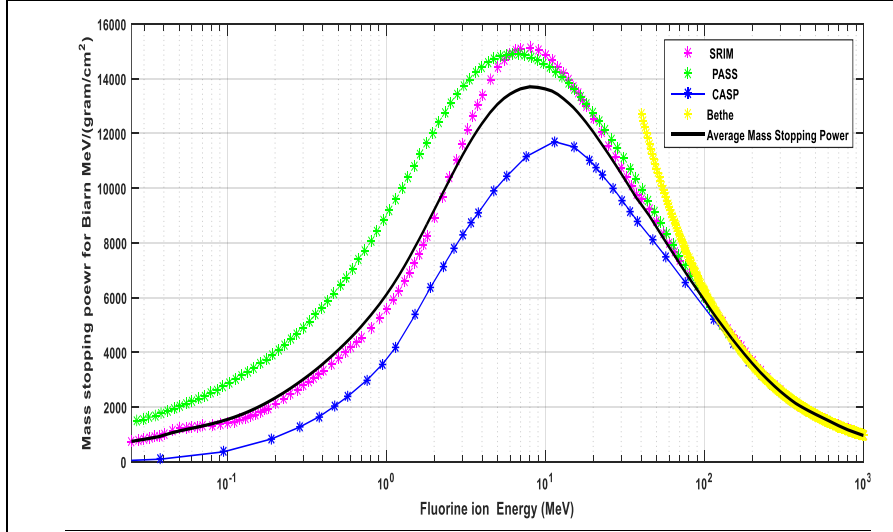
Fig. (3-31) Mass stopping power for Fluorine in Brain
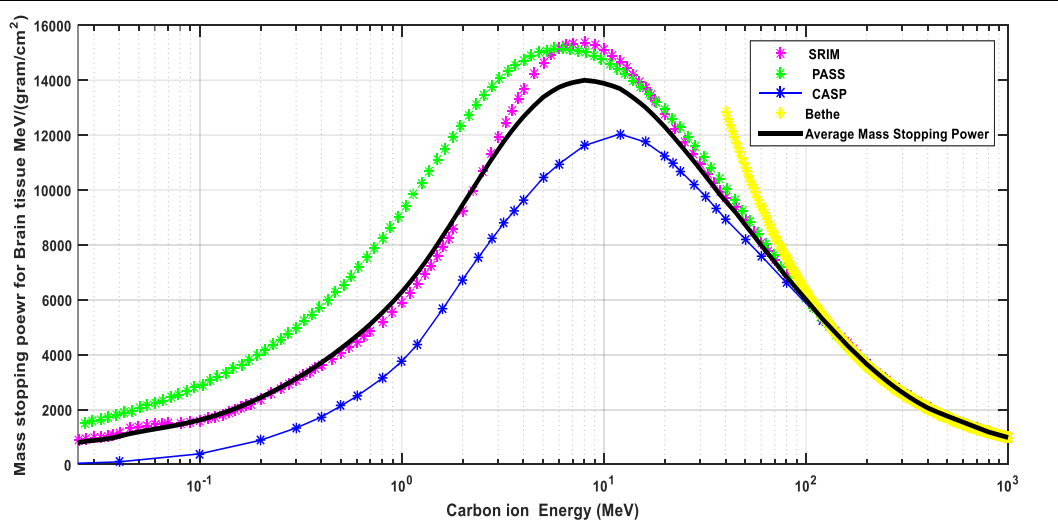
Fig. (3-32) Mass stopping power for Fluorine in Breast
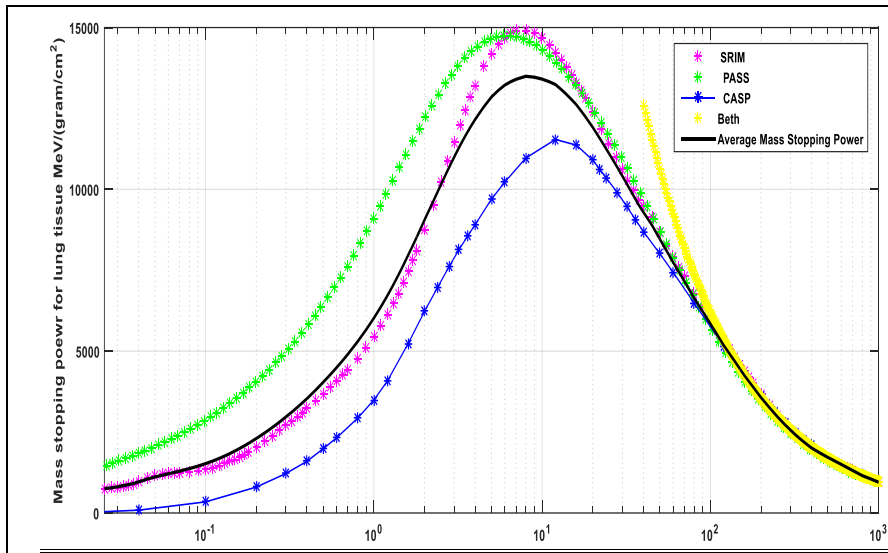
Fig. (3-33) Mass stopping power for Fluorine in Lung
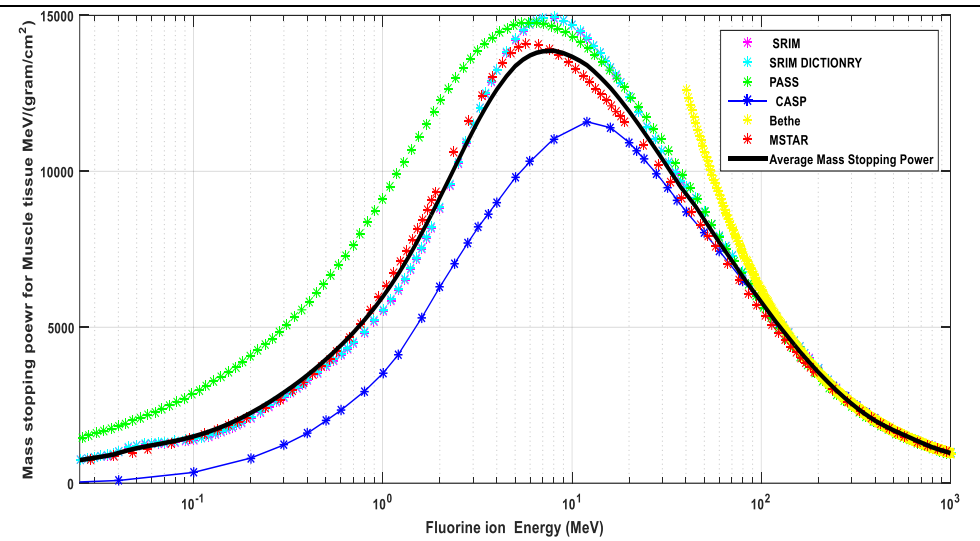
Fig. (3-34) Mass stopping power for Fluorine in Muscle
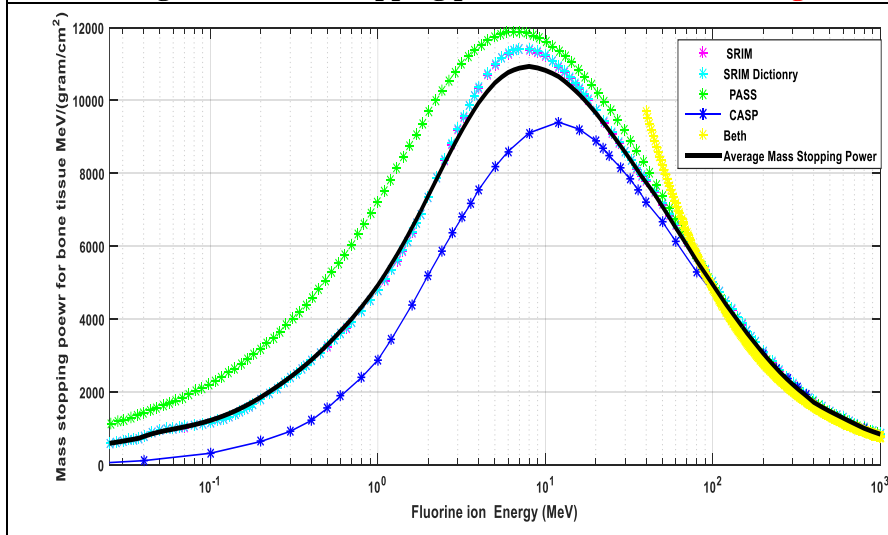
Fig. (3-35) Mass stopping power for Fluorine in Bone
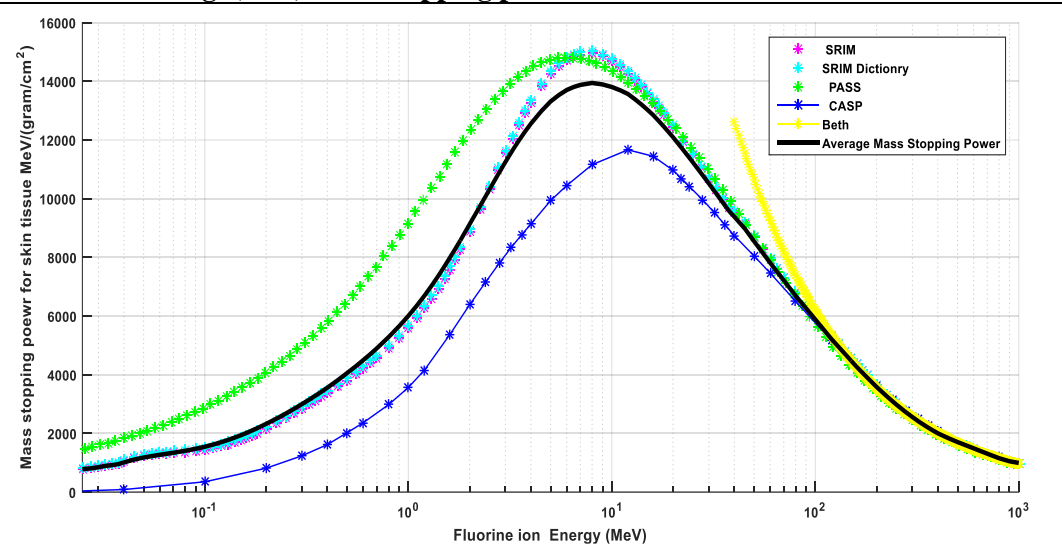
Fig. (3-36) Mass stopping power for Fluorine in Skin

Chapter Three: Calculations, results and discussion

Also from above figures. (3-5)- (3-36), it can be determine the maximum value of energy loss of (**Li, C,O, and F**) ions along their path in the targets tissues (adipose, blood, breast, brain ,lung , muscle, bone, and skin) and the range which corresponding this values and time needed to stop the ion in tissue . The results are tabulated in table (3-2).

From Table (3-2) the following notes are absorbed

1. At each ion , the largest amount of energy lost is in the adipose tissue because it's less dense than density of studied tissues. While the values of the mass stopping power in (blood , brain, breast, lung, muscle) tissues are converged , because mass stopping power does not differ greatly for materials with similar atomic composition , also the effective atomic numbers for these tissues are almost equals.

2. The increasing of value of stopping power is linear with the increase atomic number Z for the falling particle, this is due to the mass stopping power is proportional to z^2 of the falling particle.

3. The maximum value of range for ions (**Li ,C,O, and F**) that can lose along their path in (adipose, blood, breast, brain ,lung , muscle, bone, skin) tissues and from table (3-1) we Note the following-:

   a. The range of heavy ion depends on its energy .

   b. At low energies, the particles have a low speed, so they will stay longer in the target, so the probability of electronic transmission will increase, causing increase of loss of their energies. The slower particle spends a longer time in an atom; therefore, its range will be short.

   c. At high energies, particles have a high speed so their stay time in the target will be small therefore its range will be longer.

   d. The values of the range for each ion in all tissues are converged, because the effective atomic numbers of the tissues are almost equals.

   e. The magnitude of the range of heavy ion depends on the effective atomic number of the target material and its nature.

4. The stopping time of heavy ion depends on the energy and the ion mass. In addition, dependence on the range of heavy ion inside the material.

Chapter Three: Calculations, results and discussion

Table (3-2) Maximum mass stopping power calculated by present work lost along (Li ,C,O,F) ion's path for (Adipose tissue, Blood, Breast, Brain ,Lung , muscle, Bone, Skin)   in (MeV.cm²/g) and Maximum Range and Maximum Stopping time

Ions	Tissues	Energy (MeV)	Maximum mass stopping power lost along ion's path in target (MeV.cm²/gm)	Maximum Range for Ions ($gram/cm^2$)	Maximum Stopping time (nsec)
Lithium	Adipose	1.5	4042.086	0.02815	0.079
	Blood	1.5	3505.317	0.036	0.088
	Brain	1.5	3529.163	0.0322	0.080
	Breast	1.5	3665.277	0.0315	0.0797
	Lung	1.5	3474.038	0.03291	0.0809
	Muscle	1.5	3583.974	0.0348	0.0856
	Bone	1.6	2829.235	0.0448	0.0583
	Skin	1.5	3614.352	0.03273	0.0440
Carbon	Adipose	4.5	9145.656	0.02074	0.0442
	Blood	4.5	8498.728	0.0267	0.04943
	Brain	4	8455.021	0.02540	0.0508
	Breast	4.5	8549.943	0.02454	0.0481
	Lung	4.5	8373.308	0.0257	0.0379
	Muscle	4.5	8564.232	0.02596	0.0485
	Bone	4.5	6641.341	0.03303	0.0337
	Skin	4.5	8524.017	0.02567	0.0303
Oxygen	Adipose	7	13209.053	0.02095	0.0413
	Blood	7	12061.616	0.0266	0.0455
	Brain	7	11992.885	0.02539	0.04429
	Breast	6.5	12230.976	0.02437	0.0450
	Lung	6.5	11853.673	0.02626	0.0471
	Muscle	6.5	11948.799	0.0259	0.0464
	Bone	7	9520.851	0.0329	0.0448
	Skin	7	12161.869	0.0254	0.0240
Fluorine	Adipose	9	15212.064	0.022630	0.0429
	Blood	9	13628.535	0.02263	0.0372
	Brain	9	13700.48	0.02704	0.04533
	Breast	9	14021.603	0.02595	0.0444
	Lung	9	13520.546	0.02753	0.0457
	Muscle	9	13899.454	0.02768	0.0460
	Bone	9	10908.018	0.03414	0.03101
	Skin	9	13866.269	0.02676	0.0243

(3.5) Semi-empirical equation for calculating mass stopping power for heavy ions

The semi-empirical formula for mass stopping power by calculation of weighted average for mass stopping power were calculated by using Matlab-2015 software, compared with six methods in (adipose, muscle) tissues, and compared with five methods in (blood, skin, bone) tissues, and compared with four methods in (breast, brain, lung) tissues.

$$S.P. in (P.W) = (P_1E^5 + P_2E^4 + P_3E^3 + P_4E^2 + P_5E + P_6)/(E^3 + q_1E^2 + q_2E + q_3 .... (3-1)$$

where E is the energy of the ion, $(P_1, P_2, P_3, P_4, P_5, P_6, q_1, q_2, q_3)$ are the parameters their values for each tissue shown in Table (3-3).

Table (3-3) Semi-empirical formula and parameters for mass stopping power for (⁷Li, ¹²C,¹⁶O, and ¹⁹F) ions interaction with in (Adipose tissue, Blood, Breast, Brain ,Lung , muscle, Bone, Skin) tissues

$S.P. in (P.W) = (P_1E^5 + P_2E^4 + P_3E^3 + P_4E^2 + P_5E + P_6)/(E^3 + q_1E^2 + q_2E + q_3)$			
	Lithium	**Carbon**	**Oxygen**	**Fluorine**
Adipose Tissue	p1 = -0.0858 p2 = 84.03 p3 = 2.567e+04 p4 = -7157 p5 = -374.9 p6= -3.569e+04 q1 = 3.253 q2 = 1.103 q3 = -0.7314 **R-square:0.9998**	p1 = 0.0007103 p2 = -0.9813 p3 = 442.3 p4 = 1.959e+05 p5 = -3.531e+04 p6 = -4172 q1 = 13.7 q2 = 12.72 q3 = -4.277 **R-square:0.9995**	p1 =0.00278 p2 = -4.015 p3 = 1816 p4 = 3.698e+05 p5 = -1.696e+06 p6 = -2.062e+05 q1 = 12.66 q2 = -38.87 q3 = -187.0 **R-square: 0.9993**	p1 =0.005214 p2 = -7.691 p3 = 3379 p4 = 4.574e+05 p5 = 8.768e+04 p6 = -694.5 q1 = 17.03 q2 = 59.99 q3 = 0.2615 **R-square: 0.9999**
	Lithium	**Carbon**	**Oxygen**	**Fluorine**
Blood Tissue	p1 = 6.678e-05 p2 = -0.1131 p3 = 73.88 p4 = 2.647e+04 p5 = -4616 p6 = - 213.8 q1 = 4.185 q2 = 1.901 q3 = -0.6015 **R-square:0.9999**	p1 = 0.001066 p2 = -1.47 p3 = 614.4 p4 = 1.777e+05 p5 = 1.388e+04 p6 = -253.4 q1 = 12.7 q2 = 19.82 q3 = -0.246 **R-square: 0.9997**	p1 = 0.002848 p2 = -4.177 p3 = 1843 p4 = 3.42e+05 p5 = -3.034e+05 p6 = -3.678e+04 q1 = 15.54 q2 = 28.88 q3 = -44.8 R-square: 0.9998	p1 = -0.005355 p2 = 10.52 p3 = -6631 p4 = 2.644e+06 p5 = 1.204e+08 p6 = 1.568e+07 q1 = 408.9 q2 = 4855 q3 = 1.848e+04 **R-square: 0.9993**
	Lithium	**Carbon**	**Oxygen**	**Fluorine**
Brain Tissue	p1 = 5.208e-05 p2 = -0.111 p3 = 75.2 p4 = 2.619e+04 p5 = 1322 p6 = -10.88 q1 = 4.466 q2 = 2.606 q3 = -0.004634 **R-square: 1**	p1 = 0.000951 p2 = -1.322 p3 = 568.9 p4 = 1.881e+05 p5 = -1.842e+05 p6 = -1.237e+04 q1 = 13.42 q2 = 2.881 q3 = -18.63 **R-square: 0.9996**	p1 = -0.001423 p2 = 2.542 p3 = -1321 p4 = 9.11e+05 p5 = 3.967e+07 p6 = 4.065e+06 q1 = 164 q2 = 2001 q3 = 4809 **R-square: 0.9997**	p1 = 0.003439 p2 = -5.229 p3 = 2444 p4 = 5.226e+05 p5 = -1.295e+05 p6 = -1.921e+04 q1 = 23.30 q2 = 59.83 q3 = -23.97 **R-square: 0.9993**

	Lithium	Carbon	Oxygen	Fluorine
Breast Tissue	p1 = 4.805e-05 p2 = -0.1018 p3 = 72.81 p4 = 2.692e+04 p5 = -1.624e+05 p6 = -6163 q1 = -1.447 q2 = -24.58 q3 = -14.8 **R-square: 0.9999**	p1 =0.0009356 p2 = -1.286 p3 = 548 p4 = 1.909e+05 p5 = 1.099e+04 p6 = -308.9 q1 = 14.43 q2 = 17.97 q3 = -0.3488 **R-square: 0.9996**	p1 = 0.002454 p2 = -3.565 p3 = 1571 p4 = 3.813e+05 p5 = -2.915e+04 p6 = -6086 q1 = 19.33 q2 = 38.73 q3 = -7.154 R-square: 0.9994	p1 = 0.003971 p2 = -5.972 p3 = 2732 p4 = 5.019e+05 p5 = 8.834e+04 p6 = -404.9 q1 = 21.6 q2 = 68.41 q3 = 1.022 **R-square: 0.9995**
	Lithium	Carbon	Oxygen	Fluorine
Lung Tissue	p1 = 1.311e-05 p2 = -0.06409 p3 = 62.29 p4 = 2.623e+04 p5 = - 1.44e+05 p6 = - 5830 q1 = - 0.777 q2 = - 23.07 q3 = - 13.87 **R-square: 0.9999**	p1 = 0.0009532 p2 = -1.321 p3 = 577.9 p4 = 1.853e+05 p5 = -7.818e+05 p6 = -4.643e+04 q1 = 10.29 q2 = -43.09 q3 = -76.94 **R-square: 0.9996**	p1 = -0.001488 p2 = 2.658 p3 = -1381 p4 = 9.203e+05 p5 = 4.148e+07 p6 = 4.22e+06 q1 = 171.2 q2 = 2117 q3 = 5082 **R-square: 0.9996**	p1 = 0.003826 p2 = -5.781 p3 = 2661 p4 = 4.892e+05 p5 = 8.913e+04 p6 = -207.1 q1 = 21.84 q2 = 70.14 q3 = 1.441 **R-square: 0.9995**
	Lithium	Carbon	Oxygen	Fluorine
Muscle Tissue	p1 = 0.0001178 p2 = -0.1859 p3 = 95.74 p4 = 2.453e+04 p5 = -3.287e+04 p6 = -1495 q1 = 2.44 q2 = -2.544 q3 = -3.735 **R-square: 0.9999**	p1 = -0.0005363 p2 = 0.8344 p3 = -298 p4 = 2.958e+05 p5 = 6.155e+06 p6 = 5.22e+05 q1 = 64.32 q2 = 429.1 q3 = 676.6 **R-square: 0.9995**	p1 = 0.002893 p2 = -4.238 p3 = 1867 p4 = 3.394e+05 p5 = -3.085e+05 p6 = -3.063e+04 q1 = 16.39 q2 = 22.17 q3 = -39.22 **R-square: 0.9992**	p1 = 0.005139 p2 = -7.61 p3 = 3351 p4 = 4.017e+05 p5 = 6.326e+04 p6 = -600.3 q1 = 15.97 q2 = 59.11 q3 = 0.2404 **R-square: 0.9995**
	Lithium	Carbon	Oxygen	Fluorine
Bone Tissue	p1 = 6.191e-05 p2 = -0.1155 p3 = 73.54 p4 = 2.185e+04 p5 = -1.739e+04 p6 = -804 q1 = 3.738 q2 = -0.915 q3 = -2.443 **R-square: 0.9998**	p1 = -0.0003501 p2 = 0.5143 p3 = -135.1 p4 = 2.352e+05 p5 = 3.681e+06 p6 = 2.576e+05 q1 = 50.86 q2 = 370.2 q3 = 462.6 **R-square: 0.9998**	p1 = 0.002119 p2 = -3.155 p3 = 1453 p4 = 3.16e+05 p5 = -6.567e+05 p6 = -6.097e+04 q1 = 19.16 q2 = 1.073 q3 = -100.7 **R-square: 0.9993**	p1 = 0.003489 p2 = -5.082 p3 = 2320 p4 = 4.243e+05 p5 = 3.008e+04 p6 = -1138 q1 = 24.77 q2 = 65.99 q3 = -1.817 **R-square: 0.9998**
	Lithium	Carbon	Oxygen	Fluorine
Skin Tissue	p1 = 9.298e-05 p2 = -0.1576 p3 = 88.54 p4 = 2.51e+04 p5 = -1.915e+05 p6 = -8213 q1 = -3.342 q2 = -28.33 q3 = -19.4 **R-square: 0.9999**	p1 = 0.0009162 p2 = -1.28 p3 = 556.6 p4 = 1.829e+05 p5 = -5.237e+04 p6 = -5356 q1 = 13 q2 = 14.4 q3 = -7.057 **R-square: 0.9996**	p1 = 0.002683 p2 = -3.965 p3 = 1789 p4 = 3.449e+05 p5 = -2099 p6 = -4489 q1 = 16.45 q2 = 41.97 q3 = -5.144 **R-square: 0.9994**	p1 = 0.004180 p2 = -6.408 p3 = 2991 p4 = 4.601e+05 p5 = -3.423e+05 p6 = -4.717e+04 q1 = 18.73 q2 = 47.24 q3 = -54.95 **R-square: 0.999**

(3.6) Comparison between the present work and theoretical calculation mass stopping power

The total energy loss for (Li ,C,O, and F) ions interaction with human tissues were calculated by six methods in (adipose ,muscle) tissues , and five methods in (blood ,skin , bone) tissues, and four methods in (breast, brain ,lung) tissues, then, by using MATLAB 2015 a program , the fitting of the average values were calculated and plotted in figures (3-37) - (3-68).
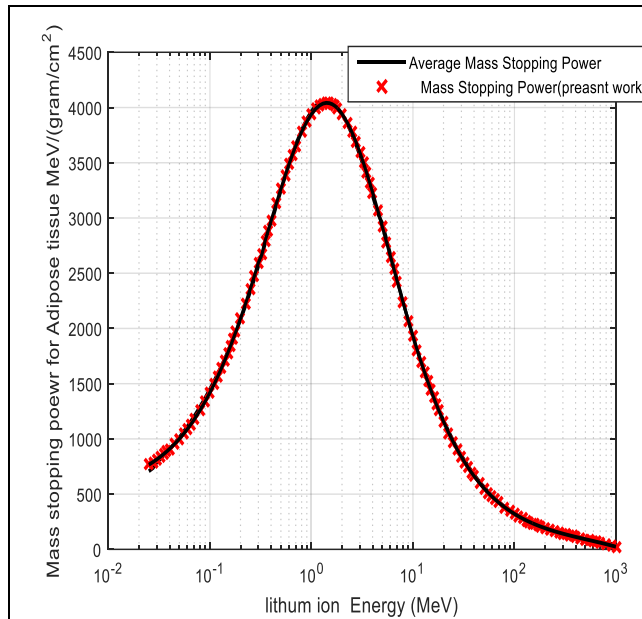
Fig. (3-37) Comparison between mass stopping power for Lithium with Adipose tissue calculated by P.W and average of six methods
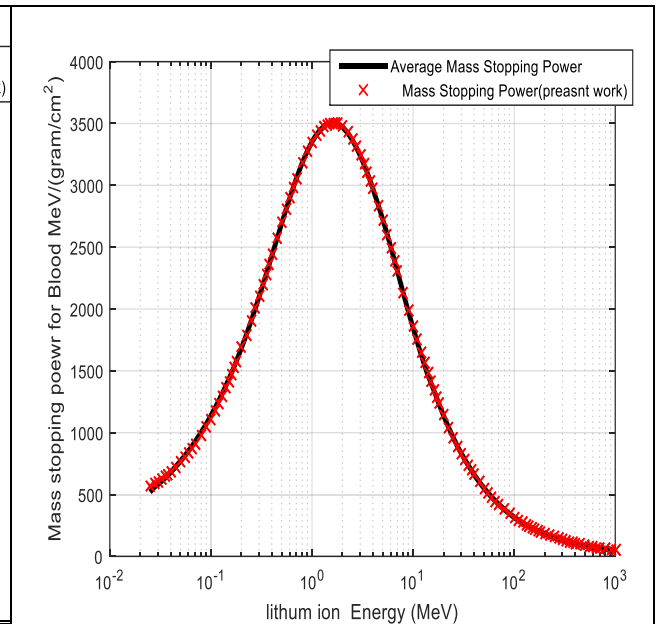
Fig. (3-38) Comparison between mass stopping power for Lithium with Blood tissue calculated by P.W and average of five methods
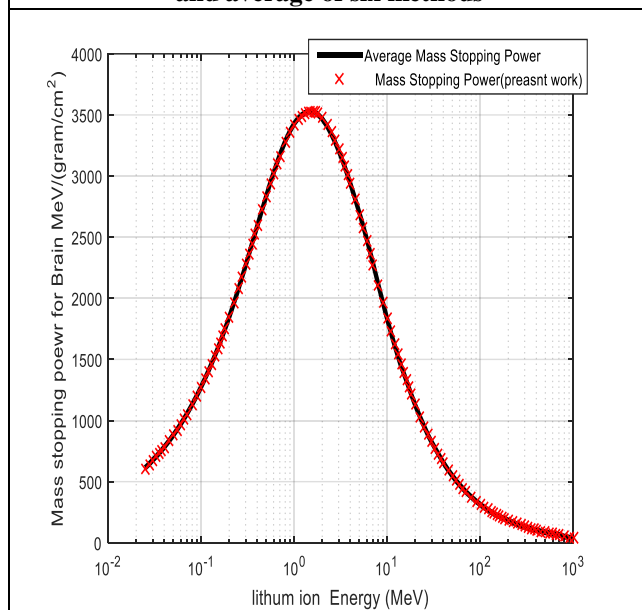
Fig. (3-39) Comparison between mass stopping power for Lithium with Brain tissue calculated by P.W and average of four methods
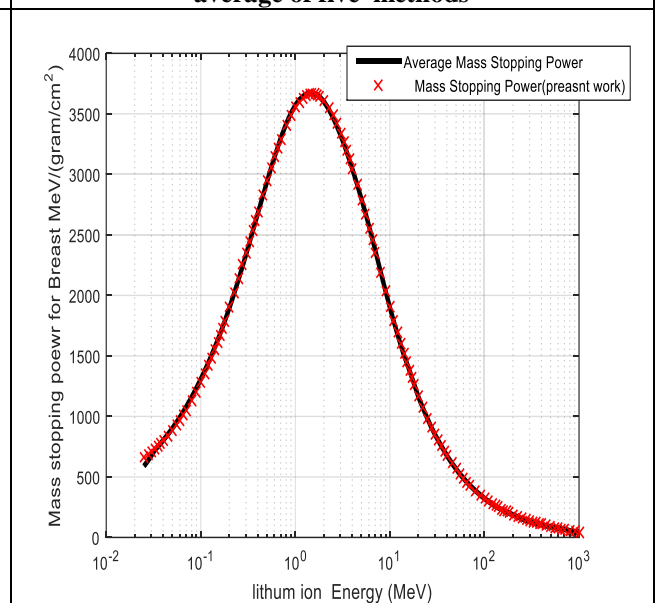
Fig. (3-40) Comparison between mass stopping power for Lithium with Breast tissue calculated by P.W and average of four methods
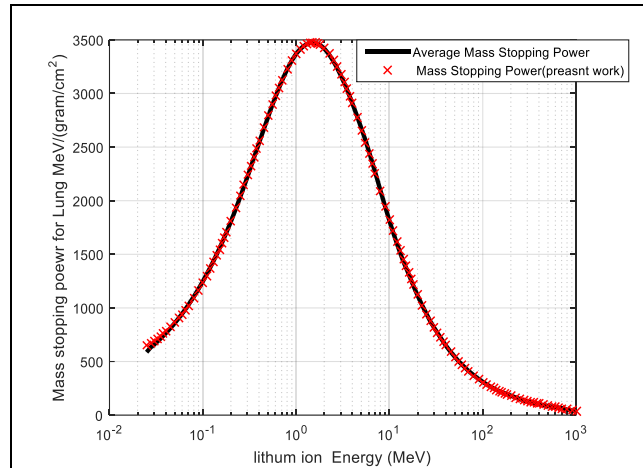
Fig. (3-41) Comparison between mass stopping power for Lithium with Lung tissue calculated by P.W and average of four methods
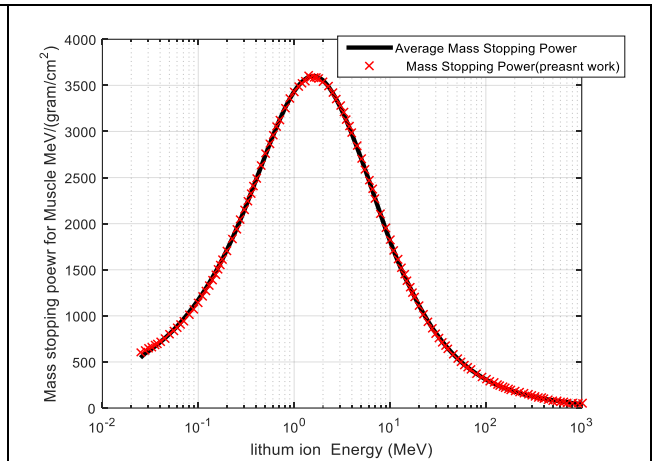
Fig. (3-42) Comparison between mass stopping power for Lithium with Muscle tissue calculated by P.W and average of six methods
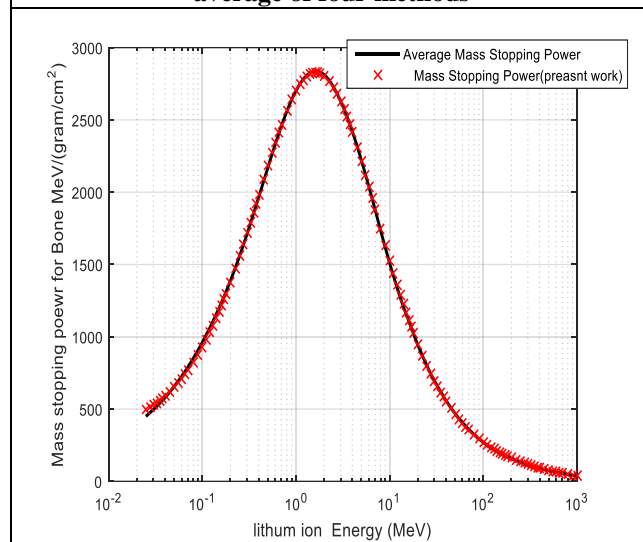
Fig. (3-43) Comparison between mass stopping power for Lithium with Bone tissue calculated by P.W and average of five methods
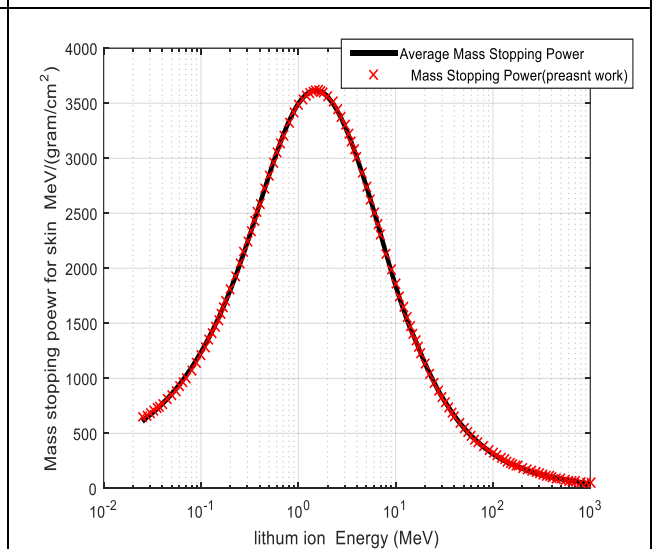
Fig. (3-44) Comparison between mass stopping power for Lithium with Skin tissue calculated by P.W and average of five methods
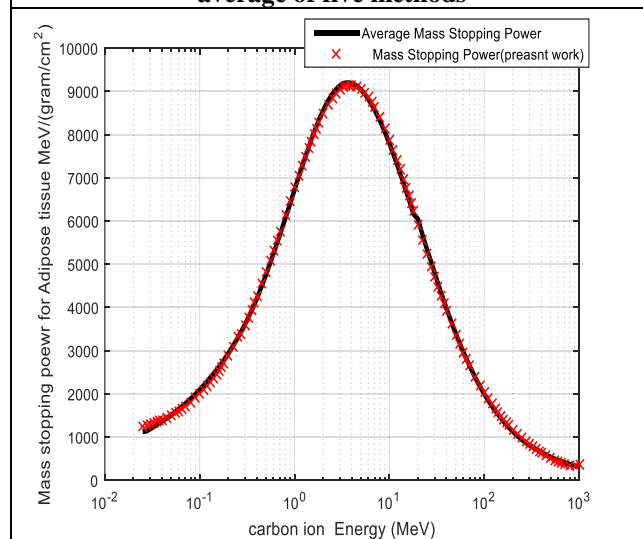
Fig. (3-45) Comparison between mass stopping power for Carbon with adipose tissue calculated by P.W and average of six methods
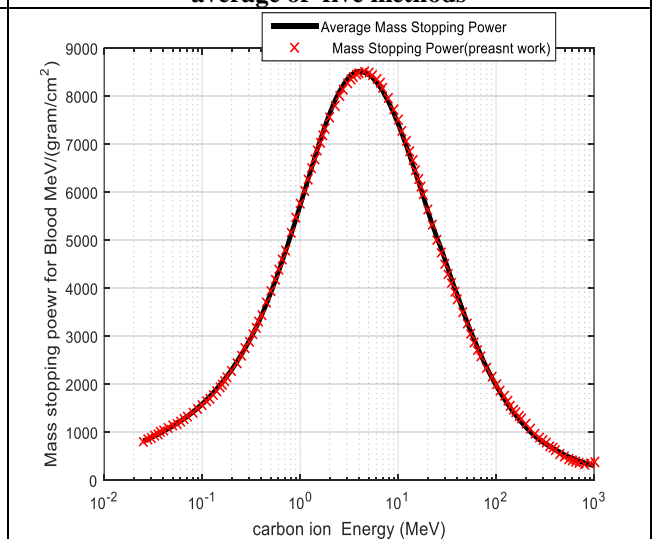
Fig. (3-46) Comparison between mass stopping power for Carbon with Blood tissue calculated by P.W and average of five methods
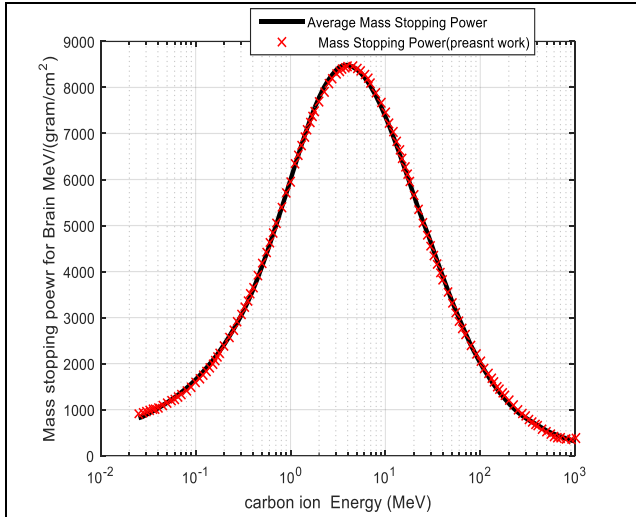
Fig. (3-47) Comparison between mass stopping power for Carbon with Brain tissue calculated by P.W and average of four methods
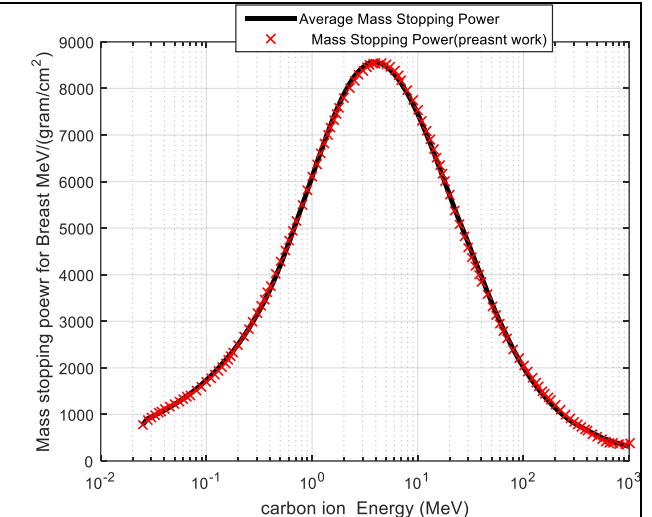
Fig. (3-48) Comparison between mass stopping power for Carbon with Breast tissue calculated by P.W and average of four methods
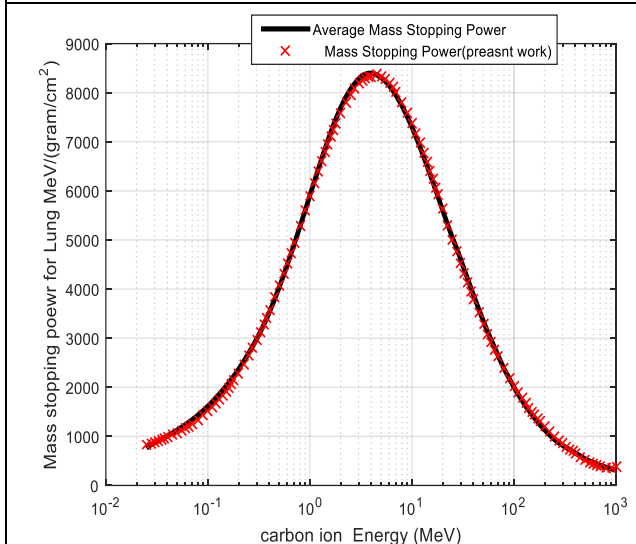
Fig. (3-49) Comparison between mass stopping power for Carbon with lung tissue calculated by P.W and average of four methods
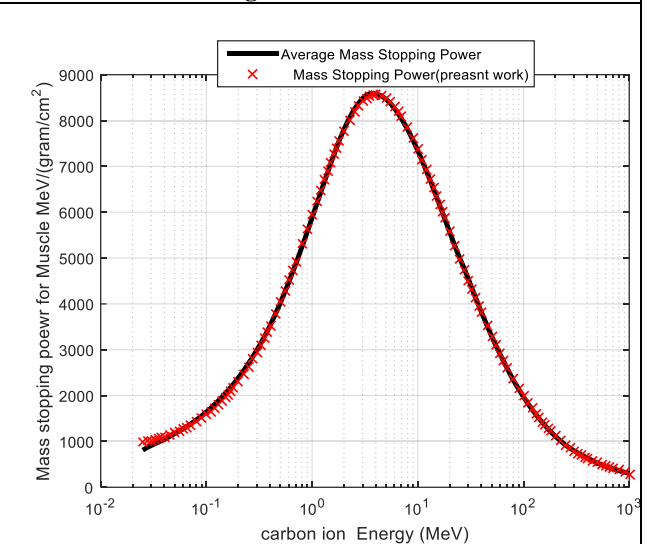
Fig. (3-50) Comparison between mass stopping power for Carbon with muscle tissue calculated by P.W and average of six methods
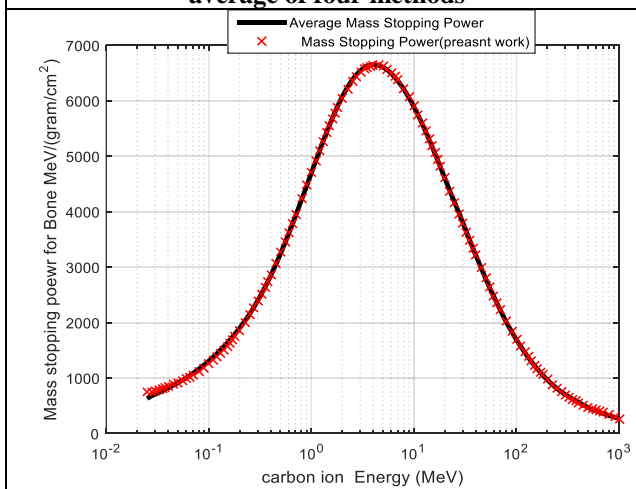
Fig. (3-51) Comparison between mass stopping power for Carbon with bone tissue calculated by P.W and average of five methods
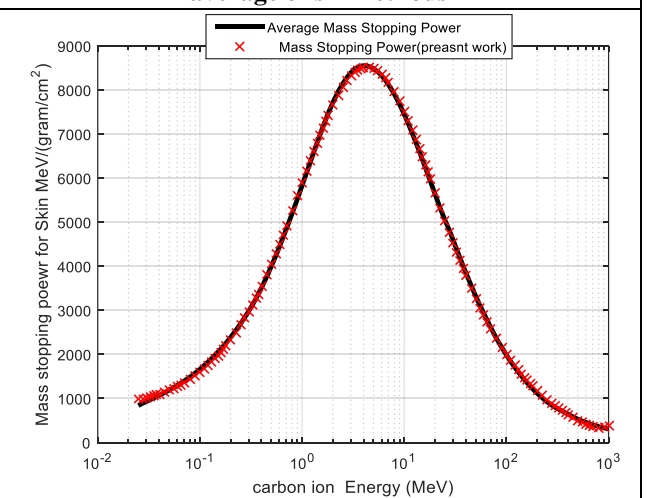
Fig. (3-52) Comparison between mass stopping power for Carbon with skin tissue calculated by P.W and average of five methods
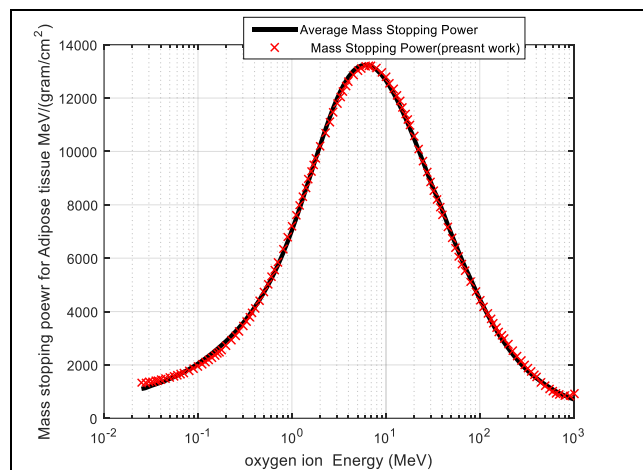
Fig. (3-53) Comparison between mass stopping power for Oxygen with adipose tissue calculated by P.W and average of six methods
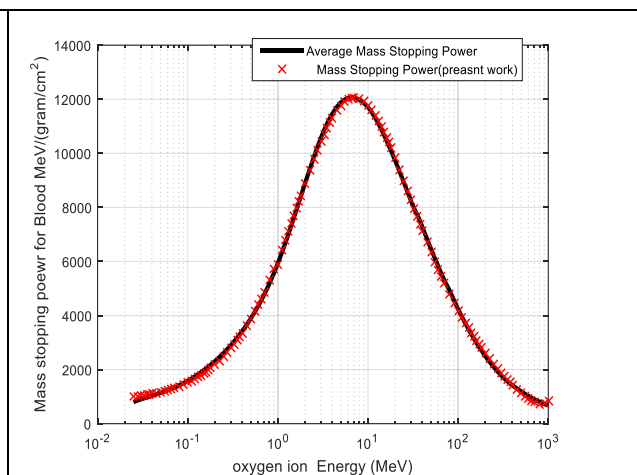
Fig. (3-54) Comparison between mass stopping power for Oxygen with Blood tissue calculated by P.W and average of five methods
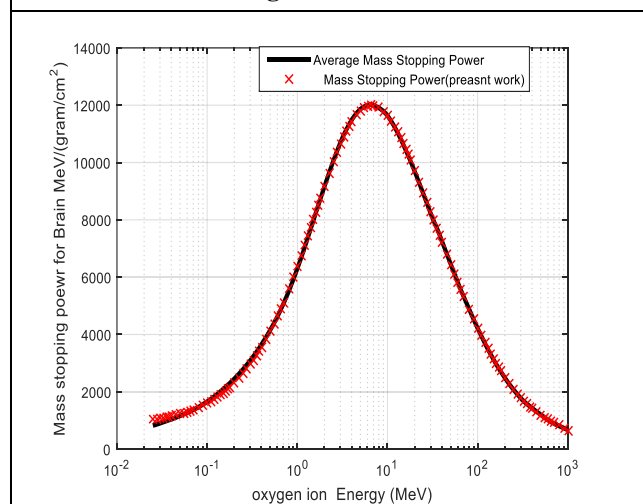
Fig. (3-55) Comparison between mass stopping power for Oxygen with brain tissue calculated by P.W and average of four methods
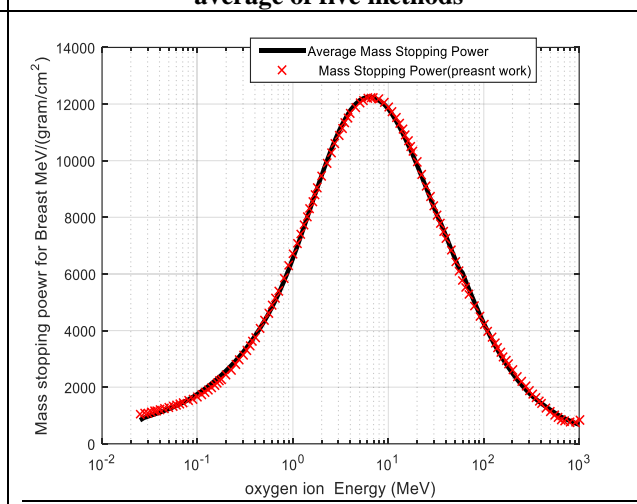
Fig. (3-56) Comparison between mass stopping power for Oxygen with breast tissue calculated by P.W and average of four methods
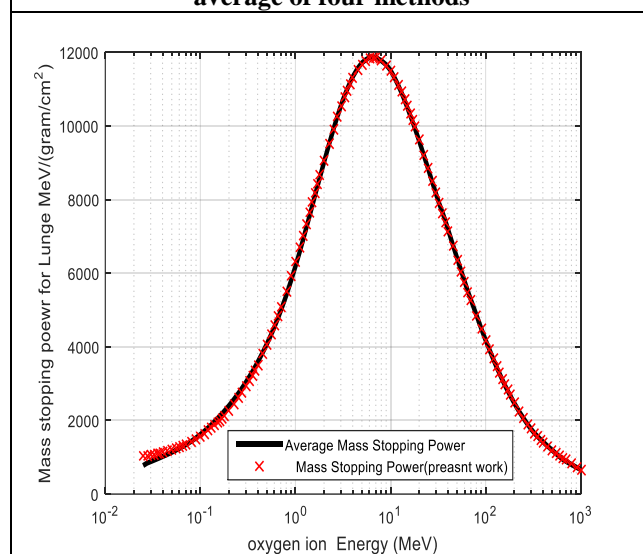
Fig. (3-57) Comparison between mass stopping power for Oxygen with lung tissue calculated by P.W and average of four methods
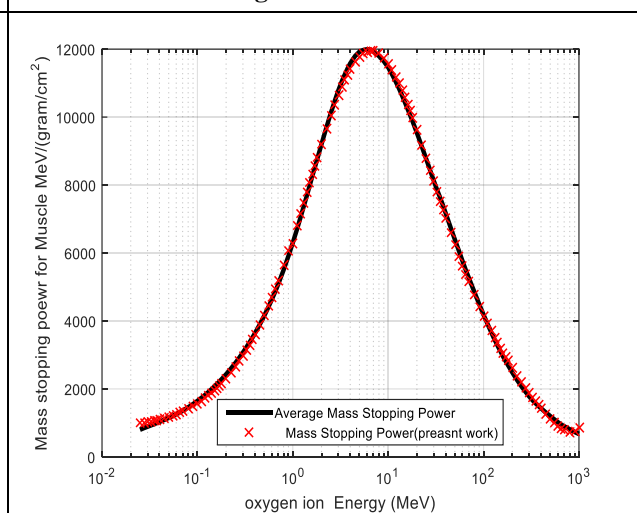
Fig. (3-58) Comparison between mass stopping power for Oxygen with muscle tissue calculated by P.W and average of six methods
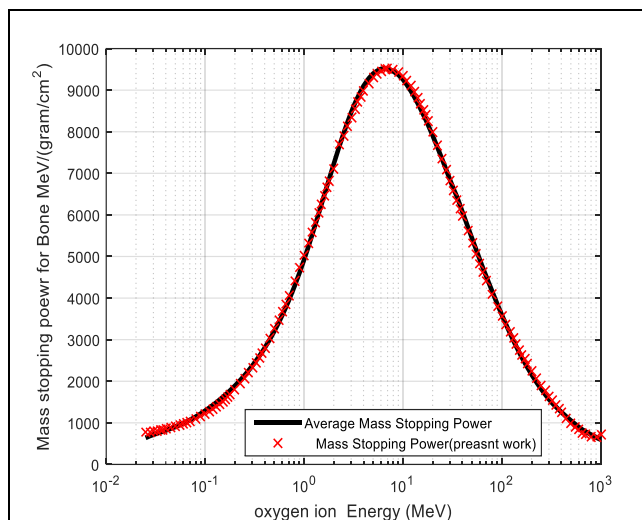
Fig. (3-59) Comparison between mass stopping power for Oxygen with bone tissue calculated by P.W and average of five methods
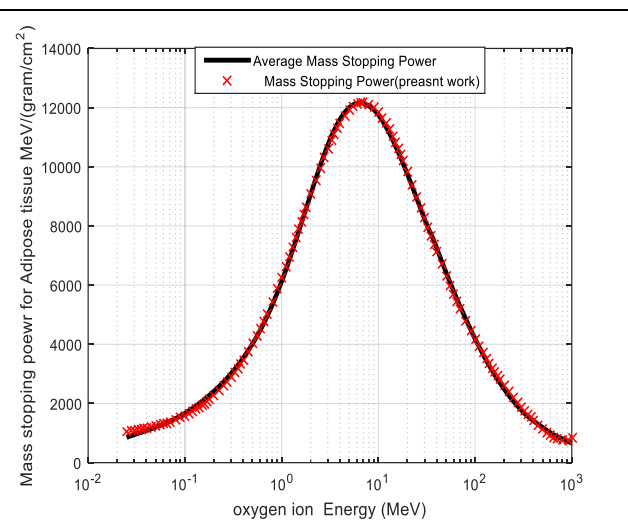
Fig. (3-60) Comparison between mass stopping power for Oxygen with skin tissue calculated by P.W and average of five methods
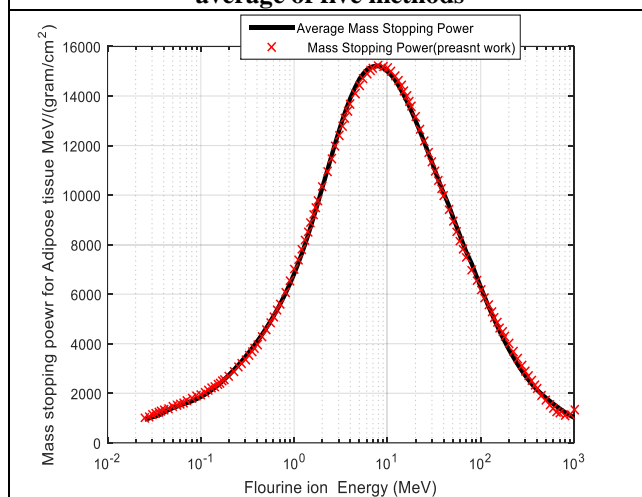
Fig. (3-61) Comparison between mass stopping power for Fluorine with adipose tissue calculated by P.W and average of six methods
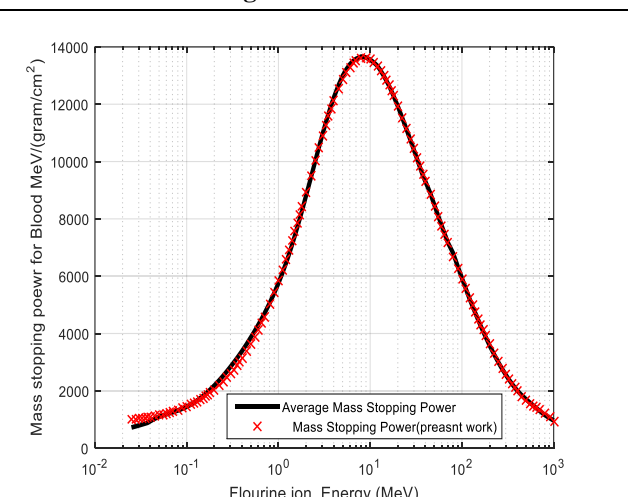
Fig. (3-62) Comparison between mass stopping power for Fluorine with blood tissue calculated by P.W and average of five methods
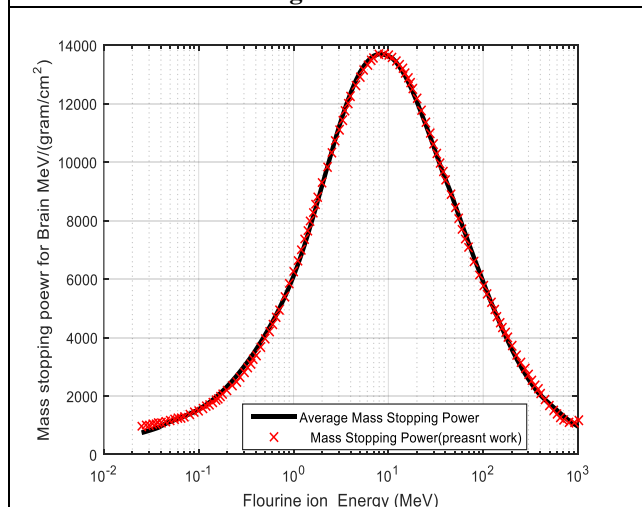
Fig. (3-63) Comparison between mass stopping power for Fluorine with brain tissue calculated by P.W and average of four methods
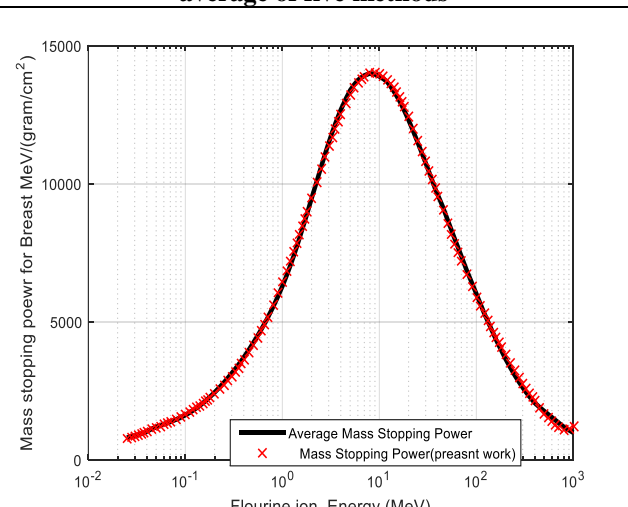
Fig. (3-64) Comparison between mass stopping power for Fluorine with breast tissue calculated by P.W and average of four methods
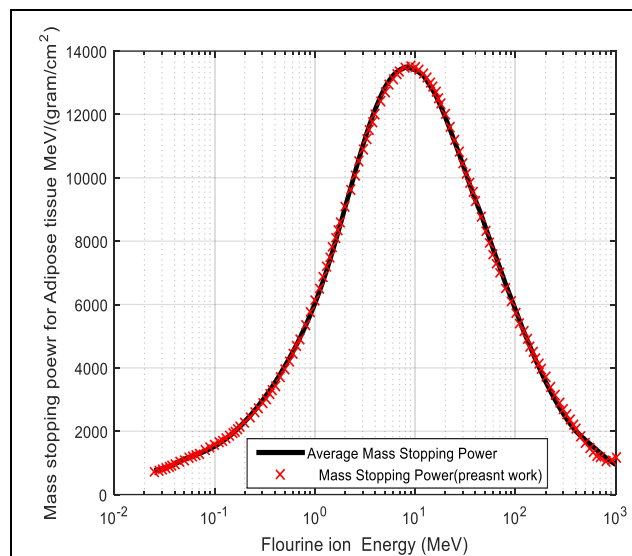
Fig. (3-65) Comparison between mass stopping power for Fluorine with lung tissue calculated by P.W and average of four methods
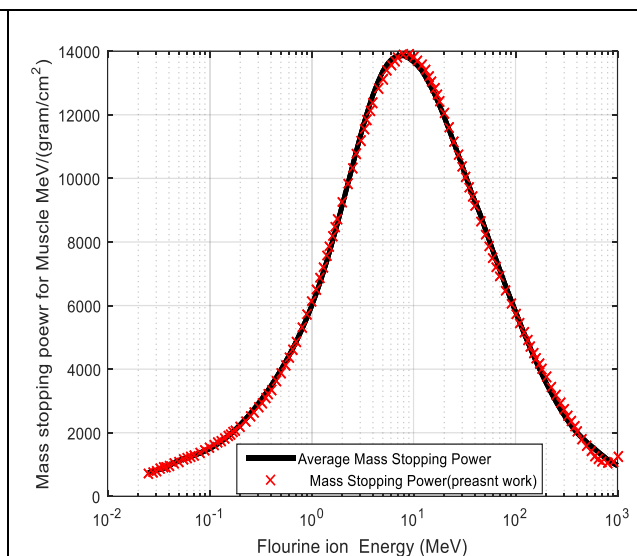
Fig. (3-66) Comparison between mass stopping power for Fluorine with Muscle tissue calculated by P.W and average of six methods
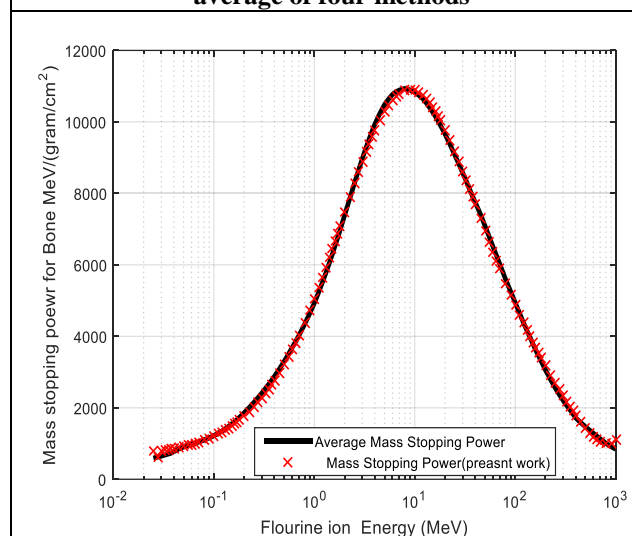
Fig. (3-67) Comparison between mass stopping power for Fluorine with bone tissue calculated by P.W and average of five methods
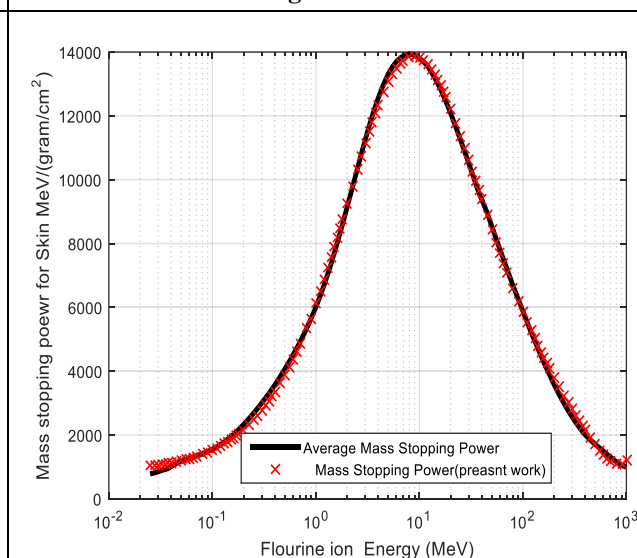
Fig. (3-68) Comparison between mass stopping power for Fluorine with skin tissue calculated by P.W and average of five methods

(3.7) Comparison between values of mass stopping power (P.W.) and ICRU73 [39]

The values of the total energy loss for (Li ,C,O, and F) ions interaction with adipose tissue and bone tissue are largely consistent with those calculated by ICRU 73 [39] and is noted this From figures (3-69) - (3-76).

70
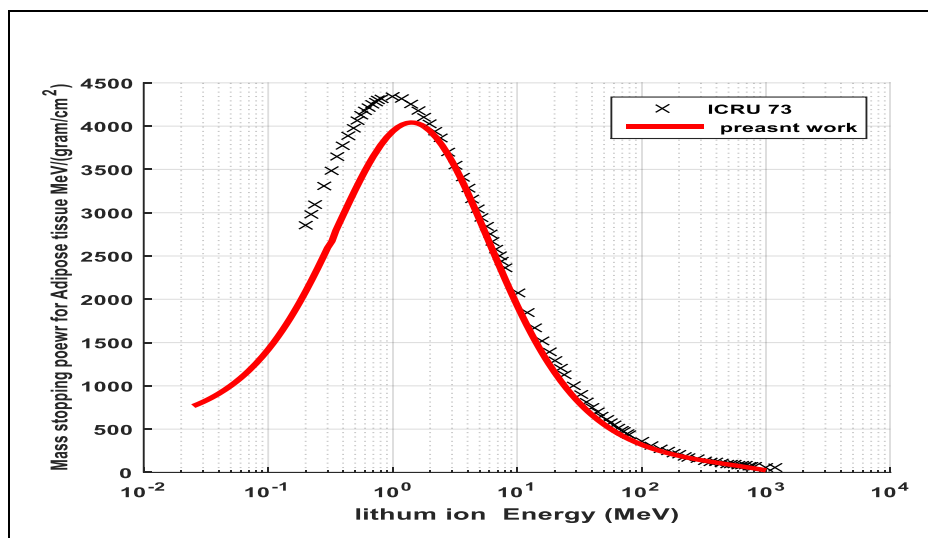
Fig. (3-69) Comparison between values of (P.W.) and ICRU73 for Lithium in Adipose tissue
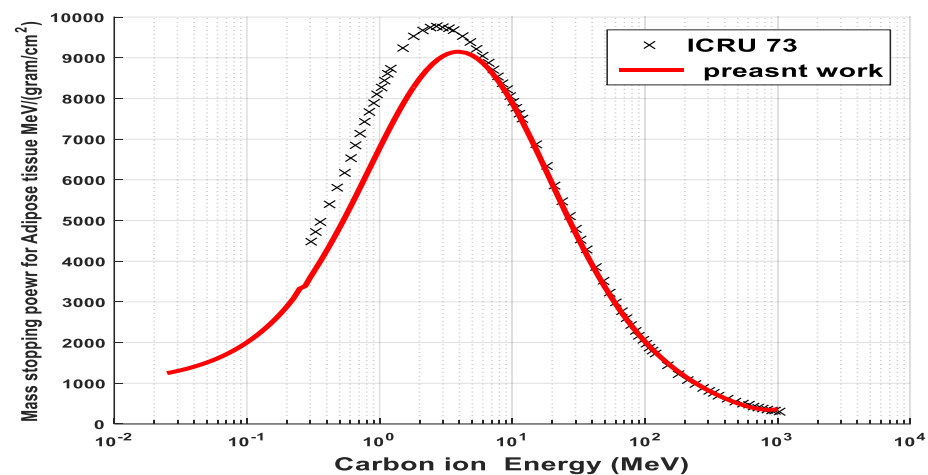
Fig. (3-70) Comparison between values of (P.W.) and ICRU73 for carbon in Adipose tissue
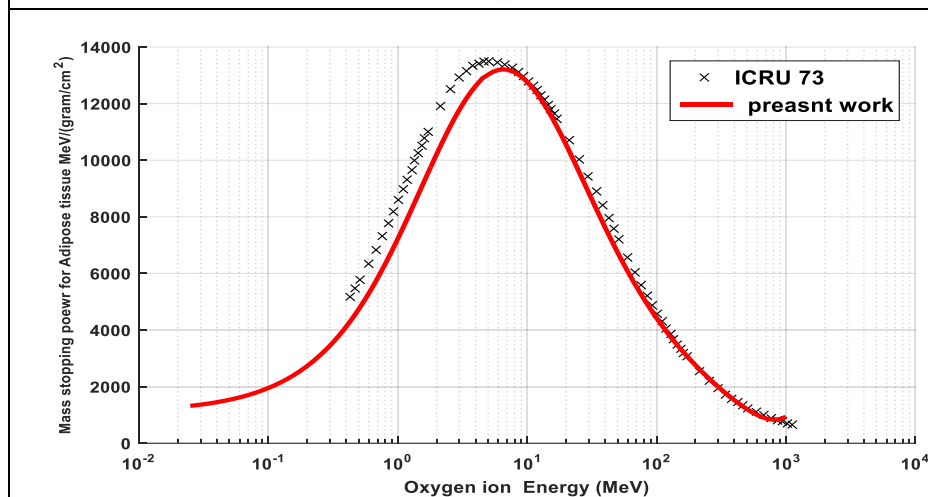
Fig. (3-71) Comparison between values of (P.W.) and ICRU73 for oxygen in Adipose tissue
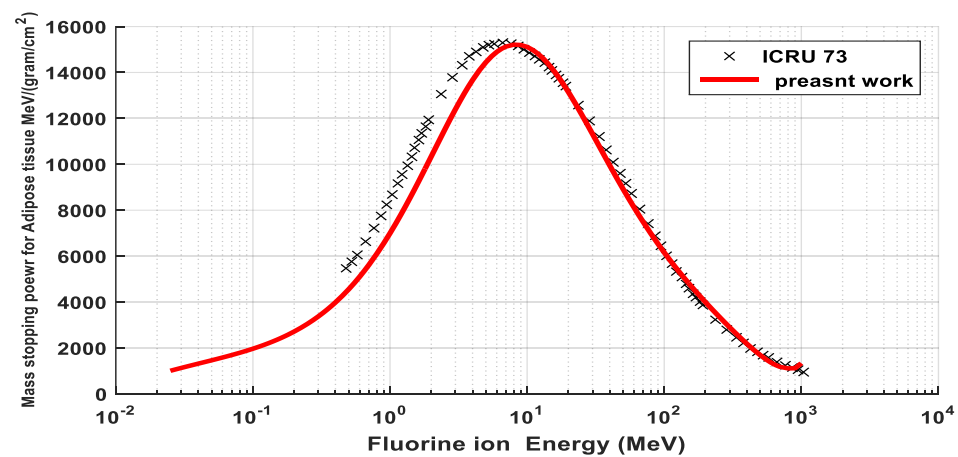
Fig. (3-72) Comparison between values of (P.W.) and ICRU73 for fluorine in Adipose tissue

Fig. (3-73) Comparison between values of (P.W.) and ICRU73 for Lithium in Bone tissue
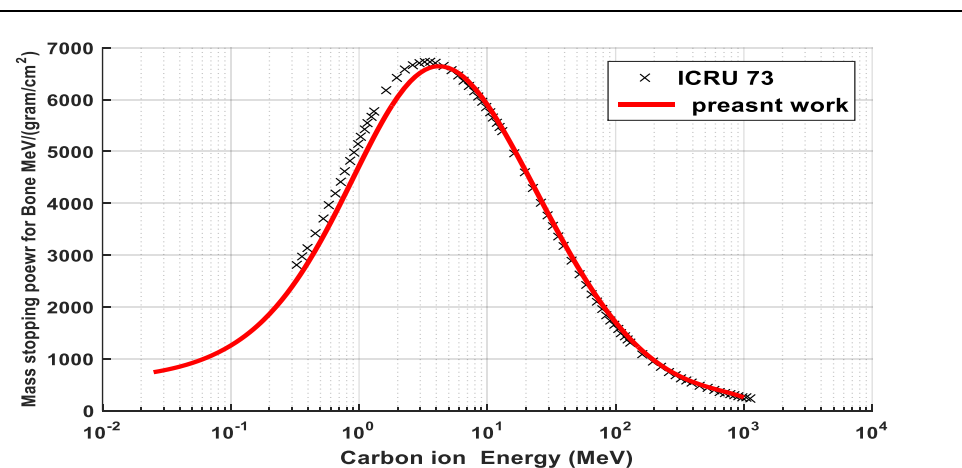
Fig. (3-74) Comparison between values of (P.W.) and ICRU73 for carbon in Bone tissue
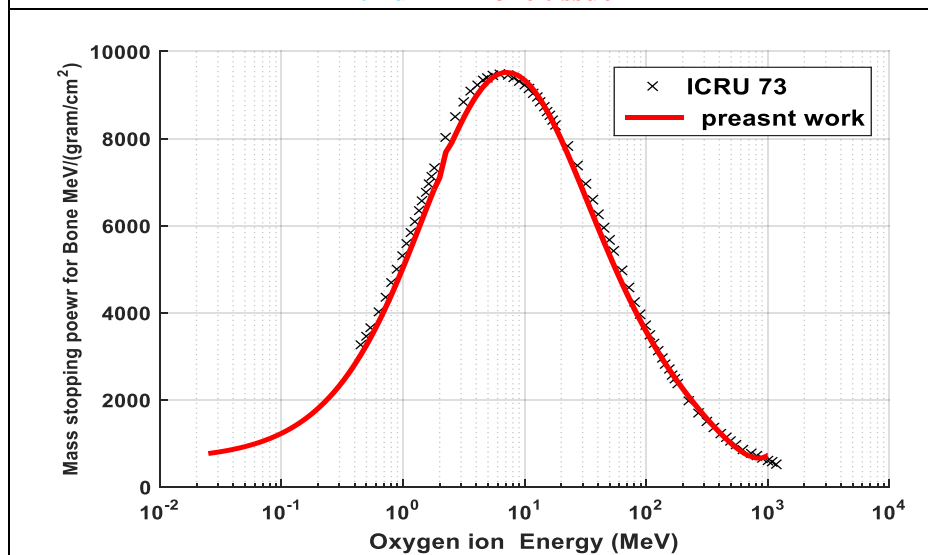
Fig. (3-75) Comparison between values of (P.W.) and ICRU73 for oxygen in Bone tissue
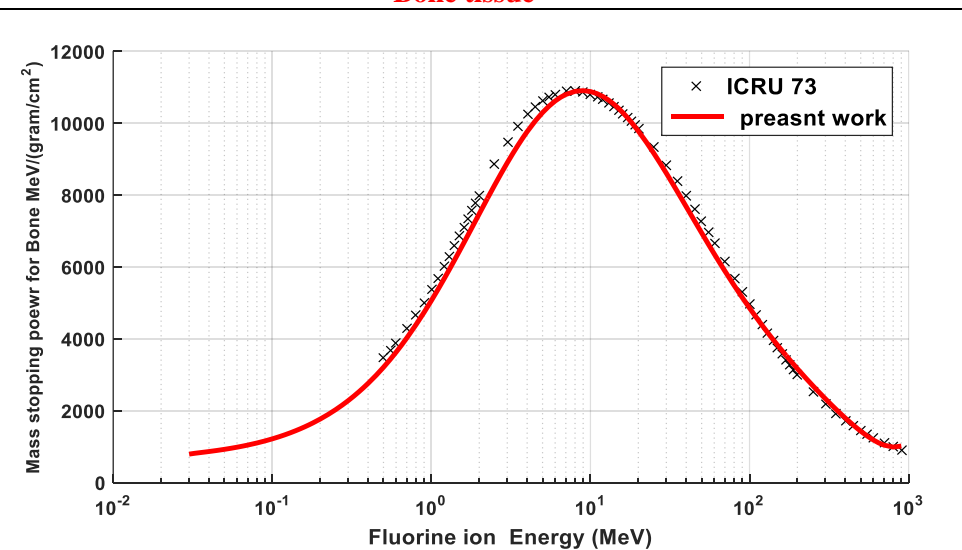
Fig. (3-76) Comparison between values of (P.W.) and ICRU73 for fluorine in Bone tissue

Chapter Three: Calculations, results and discussion

(3.8) Semi-empirical formulas for the Range of ions penetrated the tissues

The Range of (Li, C, O, and F) ions in (adipose, blood, breast, brain, lung , muscle, bone, and skin) tissues were calculated by linear integration of total energy loss to each tissue by using eq. (2-34). And then getting the semi-imperical equation by using Matlab program for the range of (Li, C, O, and F) ions in the tissue for energy interval (0.025 - 1000) MeV are shown in table (3- 4)

Table (3-4) Semi-empirical formulas for Range in (Li ,C,O,F) ions interaction with tissues

tissue	element	Energy (MeV)	$R = aE^b + c$ Constant			
Adipose	**Lithium**	E≤ 1.5	a= - 0.004939	b = - 0.4934	C = 0.03219	R-square: 0.9996
		E> 1.5	a = 0.001495	b = 0.761	C = 0.02535	R-square: 0.999
	Carbon	E≤ 3.5	a = - 0.003518	b = - 0.4845	C = 0.022	R-square: 0.9992
		E> 3.5	a = 0.0002752	b = 0.7431	C= 0.0199	R-square: 0.9999
	Oxygen	E≤ 6	a = - 0.003305	b = - 0.5021	C = 0.02198	R-square: 0.9993
		E> 6	a = 0.0001666	b = 0.6965	C = 0.0203	R-square: 0.9997
	Fluorine	E≤ 7	a = -0.00318	b = -0.5283	C= 0.02346	R-square: 0.9992
		E> 7	a = 0.0001396	b = 0.6714	C= 0.02202	R-square: 0.9997
Blood	**Lithium**	E≤ 1.5	a = -0.005218	b = - 0.5379	C = 0.04023	R-square: 0.999
		E> 1.5	a = 0.001476	b = 0.7633	C = 0.03499	R-square: 0.9996
	Carbon	E≤ 4	a = -0.003876	b = -0.5234	c = 0.02801	R-square: 0.9993
		E> 4	a = 0.0002842	b = 0.7405	C = 0.02586	R-square: 0.9992
	Oxygen	E≤ 6	a = -0.00371	b = - 0.5323	C = 0.02767	R-square: 0.9998
		E> 6	a = 0.0001766	b = 0.6962	C = 0.02589	R-square: 0.9999
	Fluorine	E≤ 8	a = -0.00318	b = - 0.5283	C= 0.02346	R-square: 0.9992
		E> 8	a = 0.0001396	b = 0.6714	C = 0.02202	R-square: 0.9995
Brain	**Lithium**	E≤ 1.5	a = -0.005462	b = -0.501	C= 0.03668	R-square: 0.9997
		E> 1.5	a= 0.001493	b = 0.7667	C = 0.03101	R-square: 0.9996
	Carbon	E≤ 4	a = - 0.003632	b = - 0.5311	C = 0.02714	R-square: 0.9997
		E> 4	a = 0.0002795	b = 0.7394	C = 0.02469	R-square: 0.9992
	Oxygen	E≤ 7	a = - 0.003367	b = - 0.5466	C= 0.02655	R-square: 0.9999
		E> 7	a = 0.0001725	b = 0.6999	C = 0.024900	R-square: 0.9998
	Fluorine	E≤ 8.5	a = - 0.00332	b = -0.5636	C = 0.028	R-square: 1
		E> 8.5	a = 0.0001058	b = 0.6693	C= 0.02658	R-square: 1
Breast	**Lithium**	E≤ 1.5	a = -0.005063	b = -0.5125	C = 0.03561	R-square: 0.999
		E> 1.5	a= 0.00131	b = 0.7798	C = 0.03096	R-square: 0.9992
	Carbon	E≤ 4	a = -0.003607	b = -0.5216	c = 0.02613	R-square: 0.9993
		E> 4	a = 0.0002849	b = 0.7368	C = 0.02417	R-square: 0.9995
	Oxygen	E≤ 6	a = -0.003273	b = -0.5398	c = 0.02523	R-square: 0.9998
		E> 6	a = 0.0001722	b = 0.6994	C = 0.02373	R-square: 0.9991
	Fluorine	E≤ 8	a = -0.003261	b = -0.5558	c = 0.02667	R-square: 0.999
		E> 8	a = 0.0001528	b = 0.6637	C = 0.02529	R-square: 0.999

Lung	**Lithium**	E≤ 1.5	a = -0.005373	b = -0.5099	C = 0.03728	R-square: 0.9993
		E> 1.5	a = 0.001319	b= 0.7846	C = 0.03264	R-square: 0.9996
	Carbon	E≤ 4	a = -0.003624	b = -0.537	C = 0.02772	R-square: 0.9997
		E> 4	a = 0.0002913	b = 0.734	C = 0.0258	R-square: 0.9992
	Oxygen	E≤ 6	a = -0.003403	b = - 0.5492	C = 0.02714	R-square: 0.9997
		E> 6	a= 0.0001816	b= 0.6931	C= 0.0256	R-square: 0.9992
	Fluorine	E≤ 8	a = -0.00337	b = -0.5624	C = 0.02825	R-square: 0.9999
		E> 8	a = 0.0001588	b = 0.6618	C = 0.02685	R-square: 0.9999
Muscle	**Lithium**	E≤ 1.5	a = - 0.005306	b = -0.526	c = 0.03909	R-square: 0.9993
		E> 1.5	a = 0.001398	b = 0.7756	C = 0.03402	R-square: 0.9996
	Carbon	E≤ 4	a = -0.003749	b = -0.5235	C= 0.02718	R-square: 0.9997
		E> 4	a = 0.0002932	b = 0.7362	C= 0.02507	R-square: 0.9992
	Oxygen	E≤ 6	a = -0.003336	b = -0.5507	C = 0.02674	R-square: 0.9991
		E> 6	a= 0.0001899	b =0.6862	C= 0.02518	R-square: 0.9992
	Fluorine	E≤ 8	a = -0.003453	b = -0.5585	C = 0.0285	R-square: 0.9999
		E> 8	a = 0.0001577	b = 0.6634	C = 0.027	R-square: 0.999
Bone	**Lithium**	E≤ 1.5	a = -0.006896	b = -0.5136	C = 0.0486	R-square: 0.9993
		E> 1.5	a = 0.001711	b = 0.7644	C = 0.04235	R-square: 0.999
	Carbon	E≤ 4	a = -0.004584	b = -0.5316	C = 0.03434	R-square: 0.9999
		E> 4	a = 0.000379	b = 0.7186	C = 0.03191	R-square: 0.9992
	Oxygen	E≤ 6	a = -0.004379	b = -0.5436	C = 0.0341	R-square: 0.9997
		E> 6	a = 0.0002397	b = 0.6722	C= 0.03206	R-square: 0.9994
	Fluorine	E≤ 8	a = -0.004112	b = -0.5661	C = 0.035	R-square: 0.9999
		E> 8	a= 0.0002064	b = 0.6468	C = 0.03329	R-square: 0.9993
Skin	**Lithium**	E≤ 1.5	a = -0.005319	b = -0.512	C = 0.03705	R-square: 0.9993
		E> 1.5	a = 0.001342	b = 0.7796	C = 0.03212	R-square: 0.9992
	Carbon	E≤ 4	a = -0.003871	b = - 0.5134	C = 0.027	R-square: 0.9999
		E> 4	a= 0.0002868	b = 0.7386	C = 0.0248	R-square: 0.9992
	Oxygen	E≤ 6	a = -0.003645	b = - 0.5253	C = 0.02648	R-square: 0.9991
		E> 6	a= 0.0001798	b = 0.6946	C = 0.0246	R-square: 0.999
	Fluorine	E≤ 8	a = -0.003479	b = - 0.5481	C = 0.02763	R-square: 0.9999
		E> 8	a = 0.0004577	b = 0.4694	C = 0.0127	R-square: 0.999

(3.9) Comparison of the range of heavy ions

The value of range for (Li, C,O , and F) ions that can lose along its path in (adipose, blood, breast, brain , lung , muscle, bone, skin) tissues were tabulated in the appendix (A) and illustrated in figures (3-77)-(3-84) . from figures ,we Note that the tracks tend to be completely straight because the particles do not deviate greatly by any single encounter, and interactions occur in all directions simultaneously, Except at their very End [55].
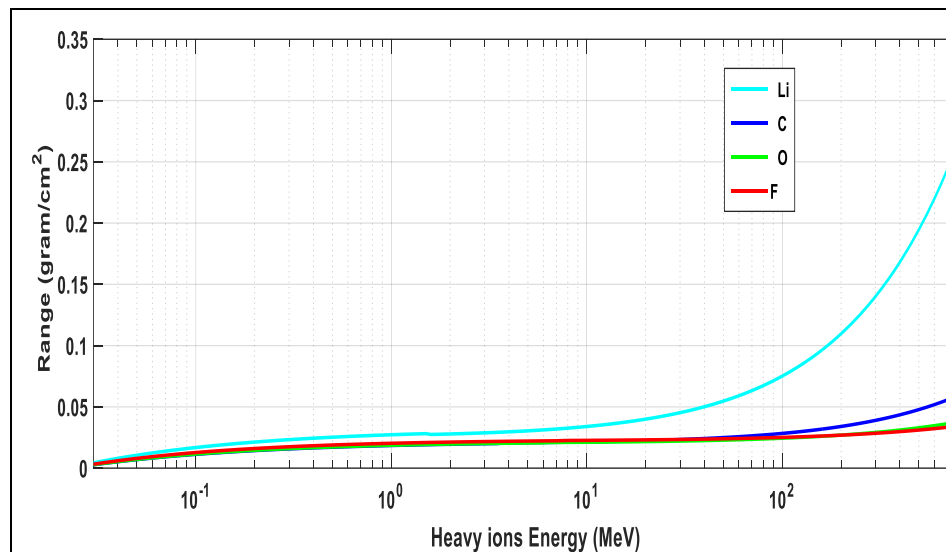
Fig. (3-77) Comparison between the range (Li ,C,O,F) ions in Adipose tissue
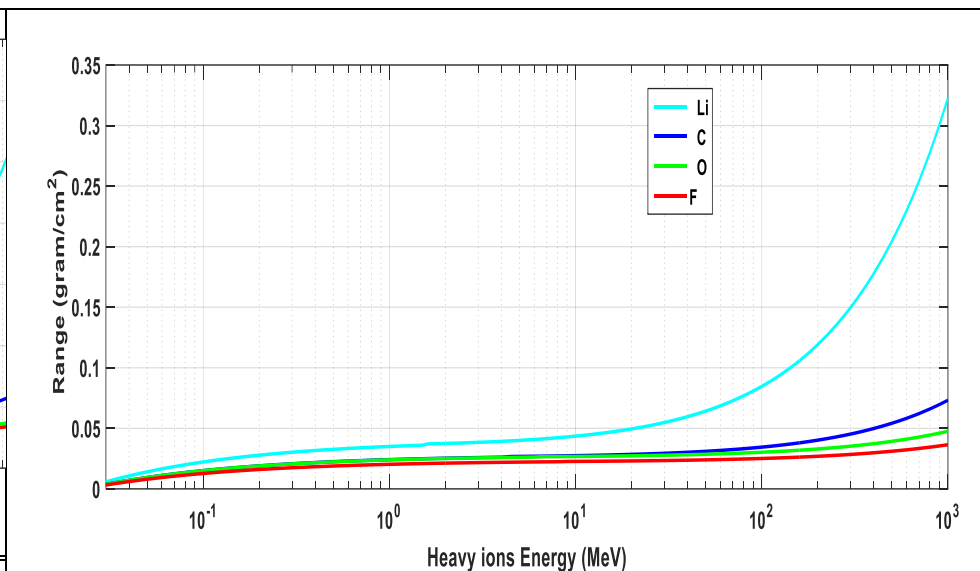
Fig. (3-78) Comparison between the range (Li ,C,O,F) ions in Blood
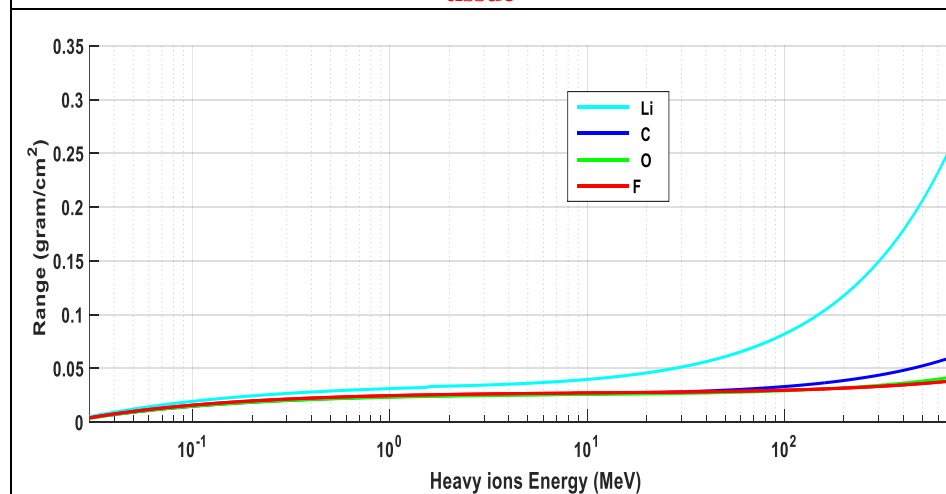
Fig. (3-79) Comparison between the range (Li ,C,O,F) ions in Brain
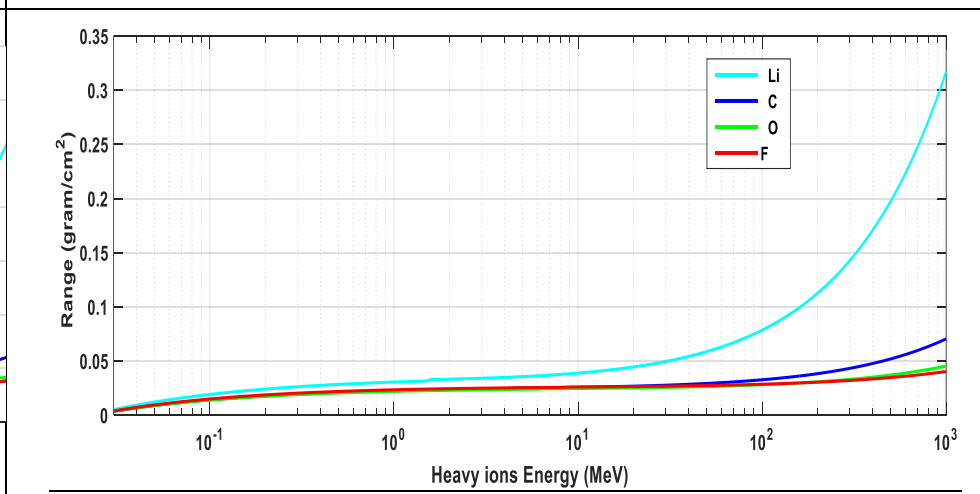
Fig. (3-80) Comparison between the range (Li ,C,O,F) ions in Breast
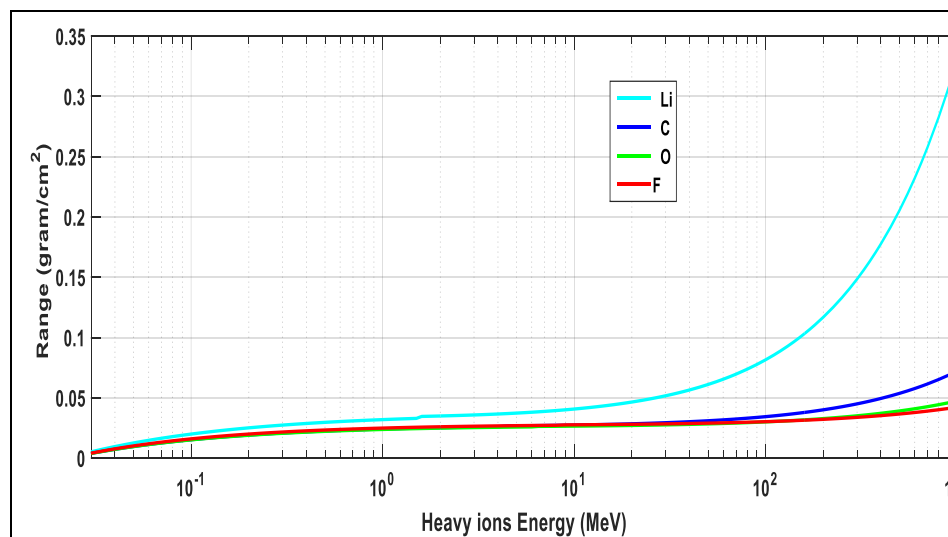
Fig. (3-81) Comparison between the range (Li ,C,O,F) ions in Lung
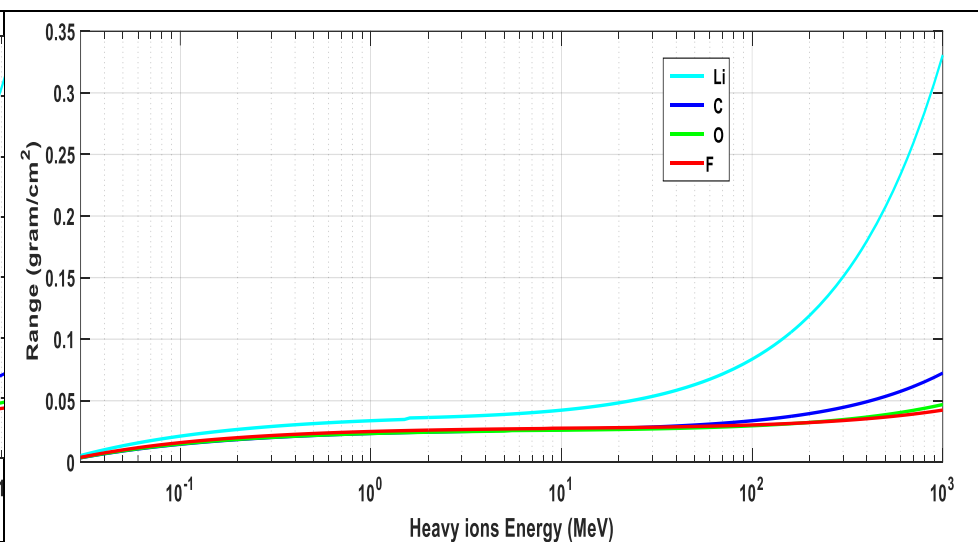
Fig. (3-82) Comparison between the range (Li ,C,O,F) ions in Muscle
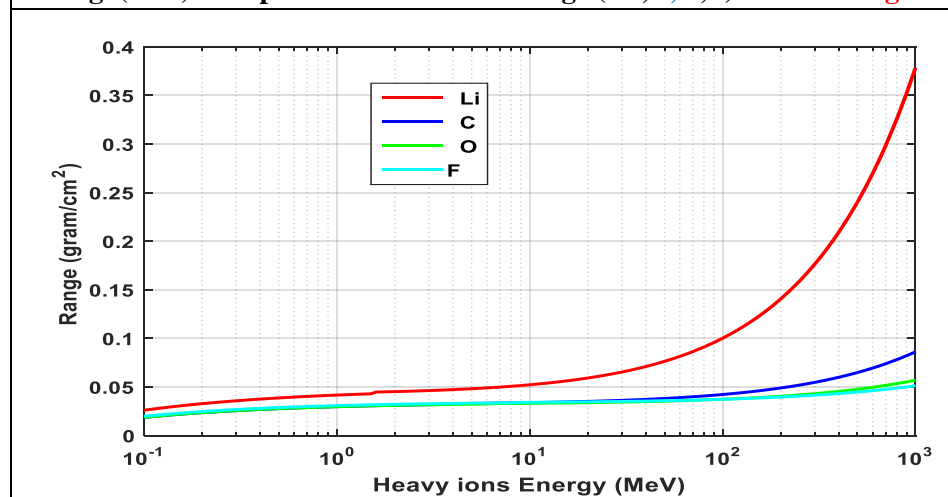
Fig. (3-83) Comparison between the range (Li ,C,O,F) ions in Bone
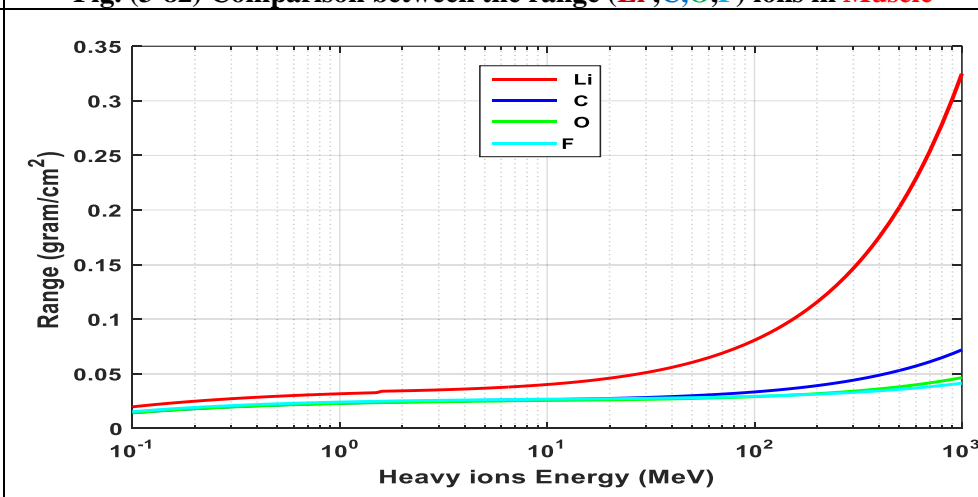
Fig. (3-84) Comparison between the range (Li ,C,O,F) ions in Skin

Chapter Three: Calculations, results and discussion

(3.10) The thickness of the absorbent target

The maximum thickness of the targets (**Li, C, O, and F**) ions that can penetrate and corresponds to the maximum mass stopping power and maximum range for (adipose, blood, breast, brain , lung , muscle, bone, and skin) tissues , were calculated by using eq.(2-42) (where ρ is the density of tissue and its values are listed in the table(2-6)) and were tabulated in table (3-5) and we note the following :-

- The target thickness of the heavy ion can penetrate it at low energy is less than it can penetrate thickness at high energy
- The values the thickness of tissues that the heavy ions can penetrate are converged because the effective atomic numbers of the tissues are almost equals.
- The range of heavy ion is practically equal to the depth the penetration because heavy charged particles travel in straight lines.

(3.11) linear energy transfer

The linear energy transfer (LET) for (**Li, C, O, and F**) ions along its path in (adipose, blood, breast, brain, lung , muscle, bone, skin) tissues were calculated by using eq.(2-41) . Results were tabulated in the appendix (B) and plotted in figures (3-85) - (3-88). From figures can calculation the maximum linear energy transfer (LET) for (**Li, C, O, and F**) ions along its path in (adipose, blood, breast, brain , lung , muscle, bone, and skin) tissues and are tabulated in table (3-5)

The linear energy transfer represents the amount of target resistance against the fallen mass, therefore it is proportional to the density of the target material. From figures, we note the value largest of linear energy transfer (LET) is in the bone tissue because it's larger dense than density of studied tissues

(3.12) Comparison between (LET) for heavy ions

The linear energy transfer (LET) is the amount of energy deposited per unit length of the path by the radiation. The maximum value of (LET) for (**Li, C, O, and F**) ions for every tissue from studied tissue were plotted in the figures (3-89)-(3-96). From figures, we note the following

1. At the same tissue, the value largest of (LET) is in the Fluorine ion because the linear energy transfer depends on the velocity, charge and mass of the falling particle.
2. The heavy ions lose energy very rapidly, producing many ionizations in a short distance, thus have high LET .

Chapter Three: Calculations, results and discussion

 Table (3-5) Maximum Thickness and Maximum LET for (Li ,C,O, and F) ions interaction with tissues

Ions	Tissues	Energy (MeV)	Maximum Liner Energy (MeV/cm)	Maximum thickness of the target (cm)
Lithium	Adipose	1.5	3759.14	0.03059
	Blood	1.5	3715.636	0.034
	Brain	1.5	367033	0.03098
	Breast	1.5	3738.583	0.0309
	Lung	1.5	3647.74	0.03134
	Muscle	1.5	3797.517	0.03315
	Bone	1.6	5432.13	0.0410
	Skin	1.5	3939.643	0.03003
Carbon	Adipose	4.5	8507.659	0.02255
	Blood	4.5	9008.652	0.02078
	Brain	4	8793.222	0.024424
	Breast	4.5	8720.942	0.02454
	Lung	4.5	8791.973	0.02443
	Muscle	4.5	9077.230	0.0684
	Bone	4.5	12751.374	0.0302
	Skin	4.5	9291.179	0.02355
oxygen	Adipose	7	12284.419	0.02277
	Blood	7	12785.313	0.02507
	Brain	7	12472.601	0.024411
	Breast	6.5	12475.595	0.02389
	Lung	6.5	12446.357	0.02501
	Muscle	6.5	12664.532	0.02463
	Bone	7	18280.035	0.0302
	Skin	7	13256.44	0.02328
Fluorine	Adipose	9	14147.220	0.0246
	Blood	9	14446.247	0.02135
	Brain	9	14248.499	0.026
	Breast	9	14302.035	0.02544
	Lung	9	14196.57	0.02622
	Muscle	9	14732.031	0.02636
	Bone	9	20943.394	0.03089
	Skin	9	15114.233	0.02455
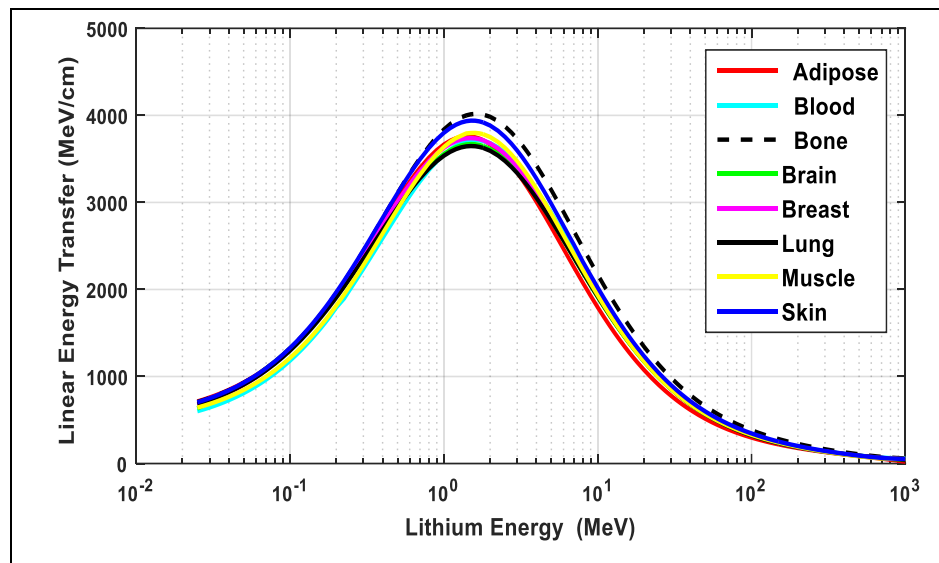
Fig. (3-85) LET for Lithium interact with tissues calculated by P.W
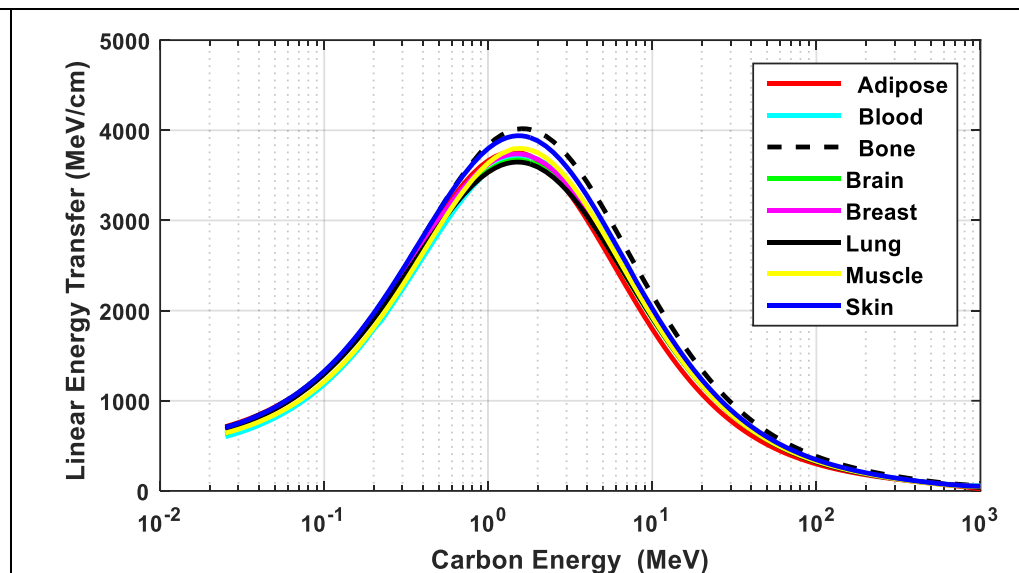
Fig. (3-86) LET for Carbon interact with tissues calculated by P.W
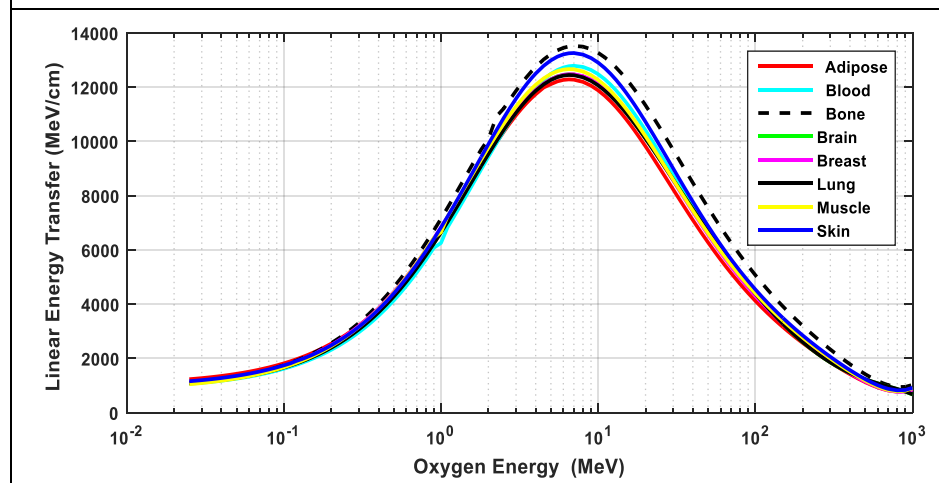
Fig. (3-87) LET for Oxygen interact with tissues calculated by P.W
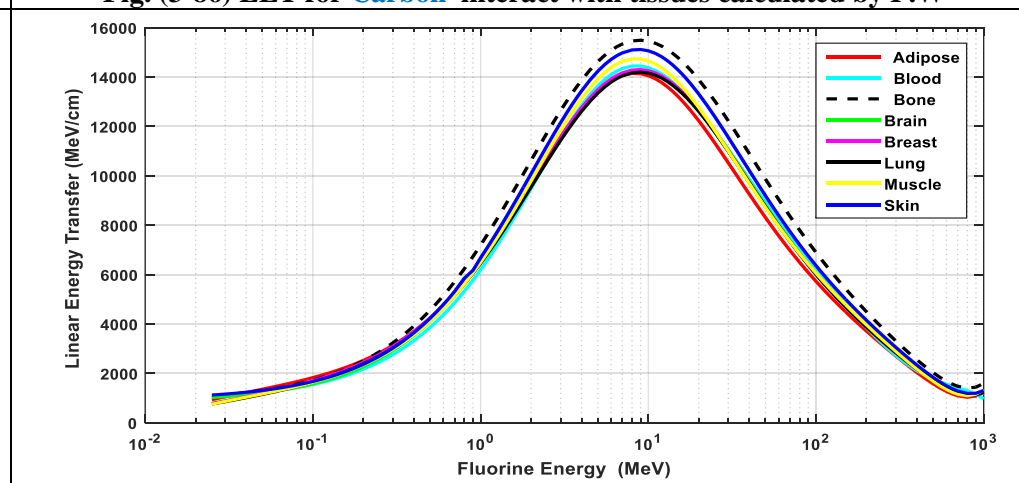
Fig. (3-88) LET for Fluorine interact with tissues calculated by P.W
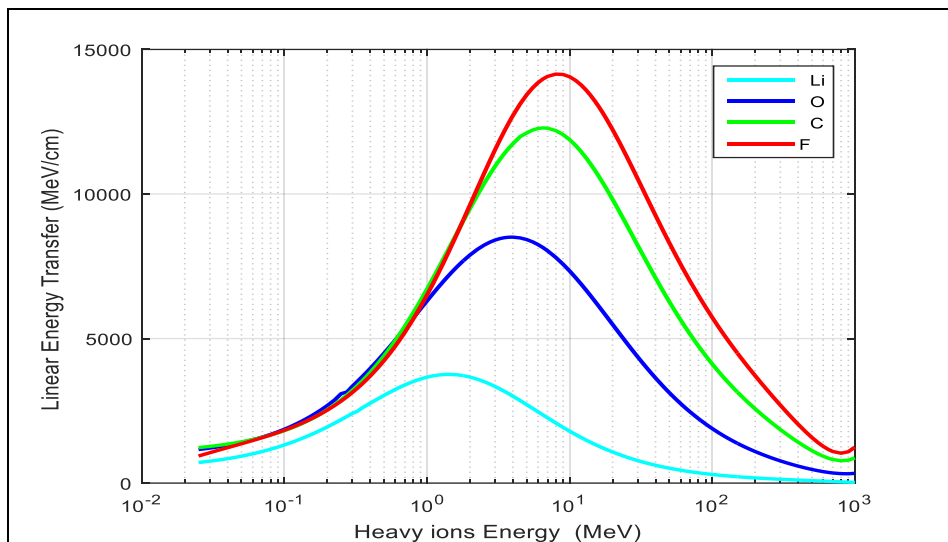
Fig. (3-89) Comparison between LET for (Li ,C,O,F) ions interact with Adipose tissue
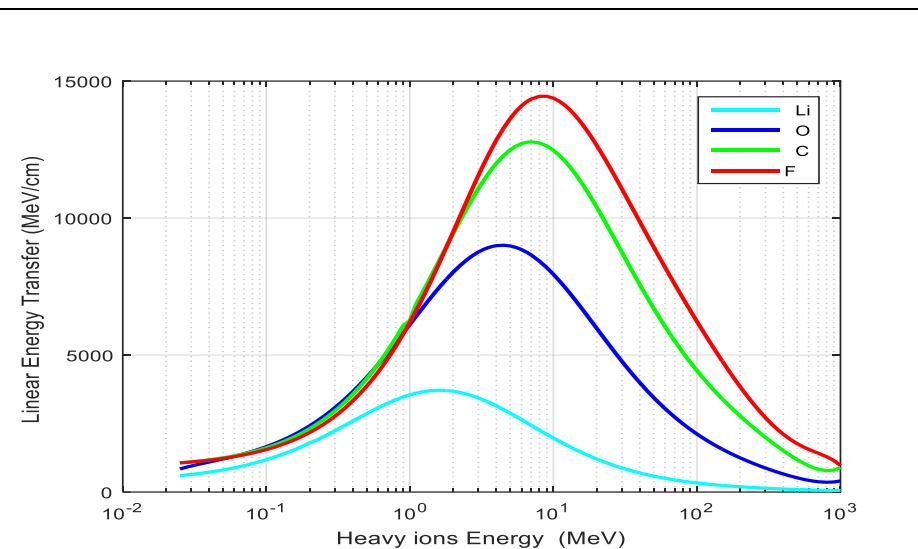
Fig. (3-90) Comparison between LET for (Li ,C,O,F) ions interact with Blood
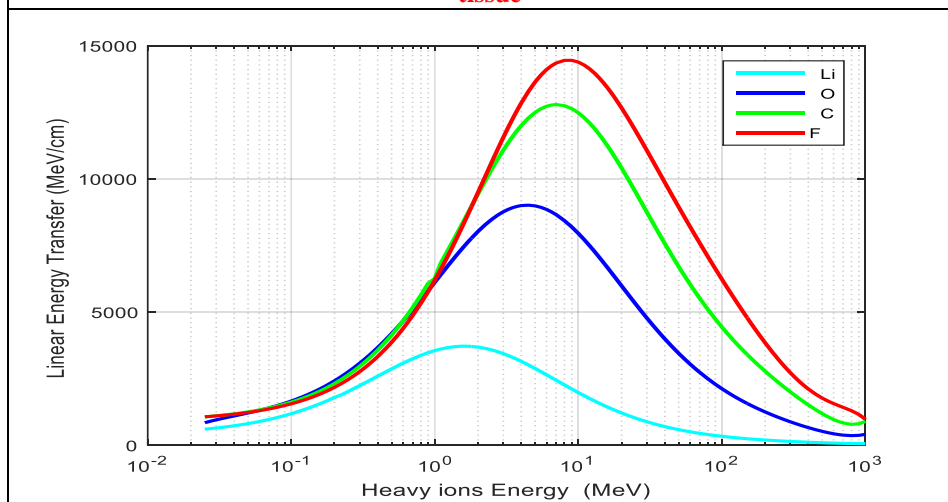
Fig. (3-91) Comparison between LET for (Li ,C,O,F) ions interact with Brain
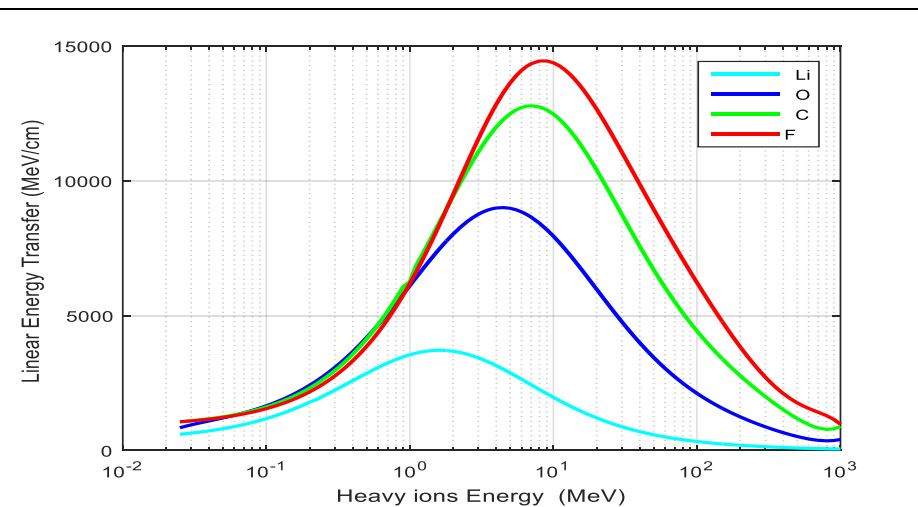
Fig. (3-92) Comparison between LET for (Li ,C,O,F) ions interact with Breast
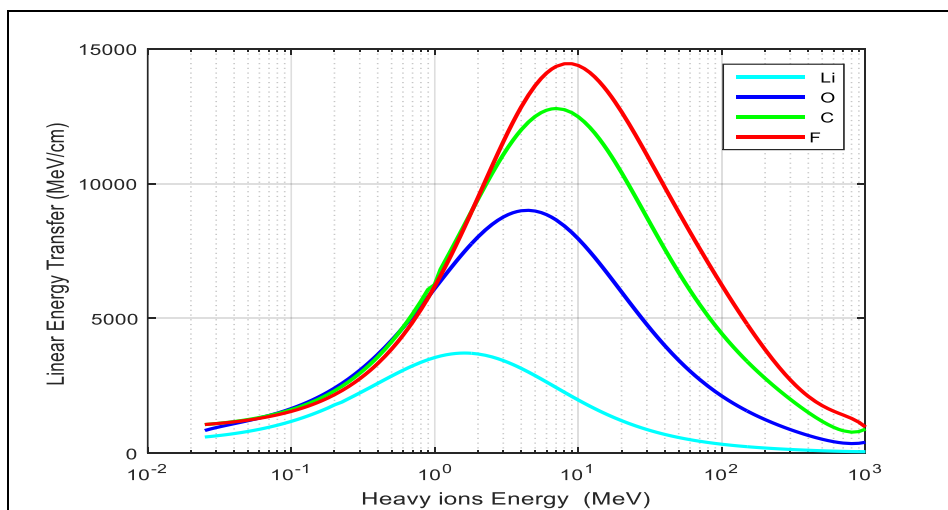
Fig. (3-93) Comparison between LET for (Li ,C,O,F) ions interact with Lung
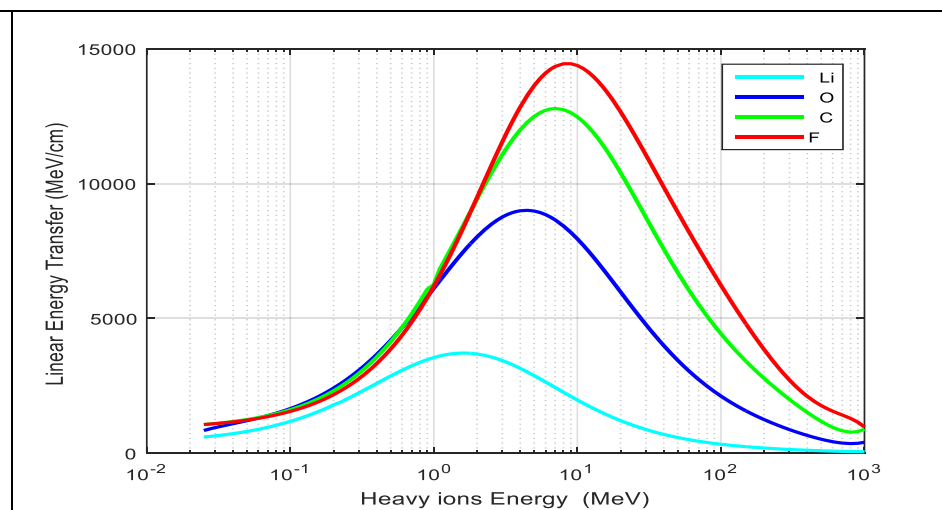
Fig. (3-94) Comparison between LET for (Li ,C,O,F) ions interact with Muscle
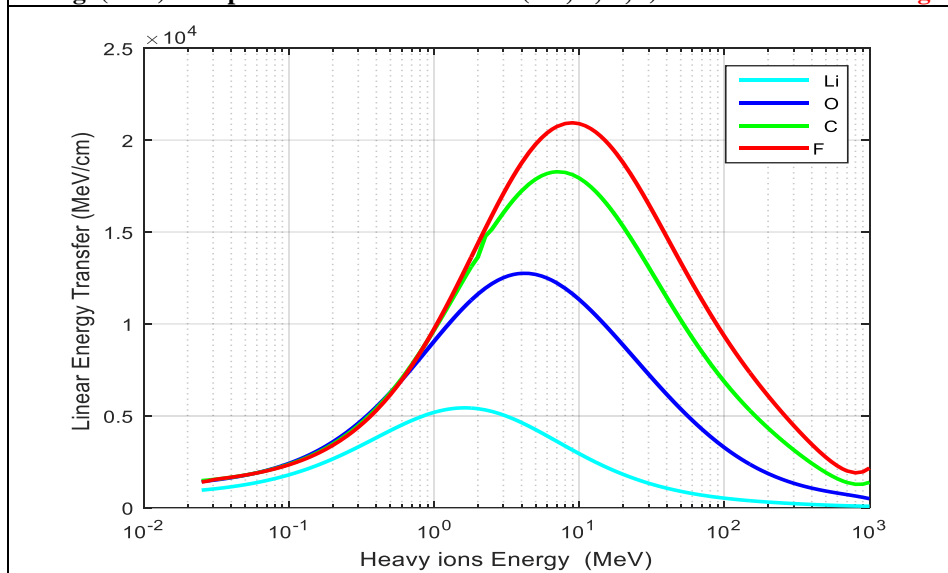
Fig. (3-95) Comparison between LET for (Li ,C,O,F) ions interact with Bone
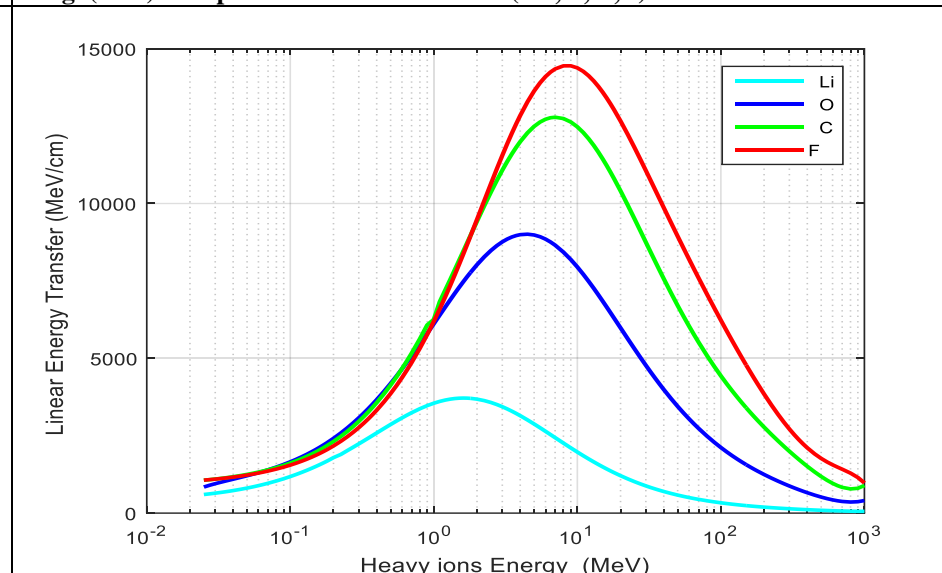
Fig. (3-96) Comparison between LET for (Li ,C,O,F) ions interact with Skin

Chapter Three: Calculations, results and discussion

(3.13) Comparison between Bragg curves for heavy ions

The range as a function of total energy loss for all (Li, C, O, and F) ions in each tissue from tissues (adipose, blood, breast, brain, lung , muscle, bone, skin) were plotted in figures (3-97)-(3-104) , from Figures we note:

1. The number of ions produced per unit distance is small at the beginning of the trajectory, rises to a maximum near the end of the path, and then falls sharply to zero , When the heavy ions become very slow for any further ionization (the end point of the range).

2. When heavy ions are used, the acute Bragg peaks can be formed to deposit most of the energy of heavy ions in the tumor mass; moreover, intensity and the position can be controlled by ion species and energy.

3. The dose delivered by Fluorine ion increases with depth and reaches its maximum at the end of the particle track, the Bragg peak, with a sharp edge and with little scatter.
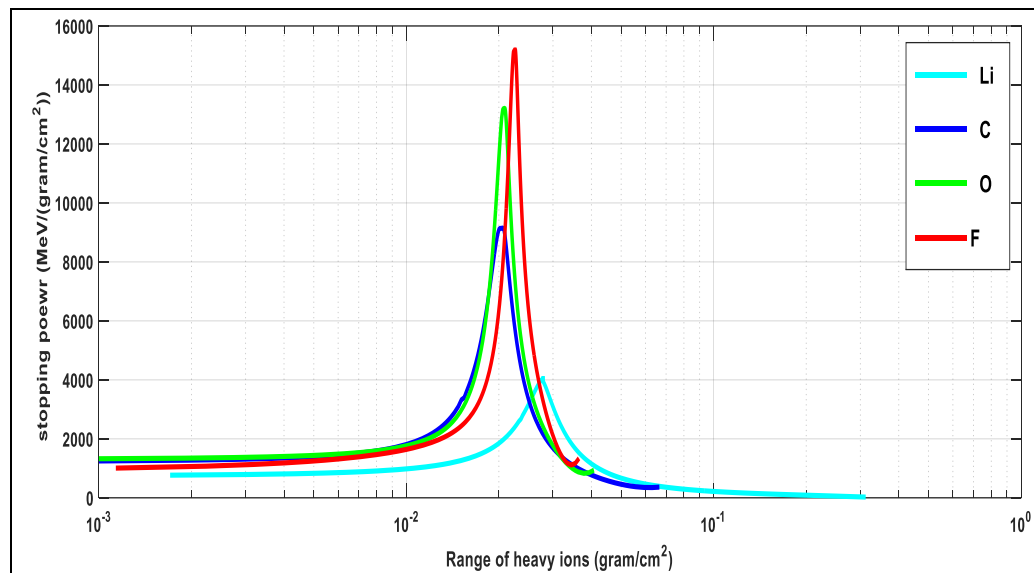
Fig. (3-97) Bragg curves for (Li ,C,O,F) ions in Adipose tissue
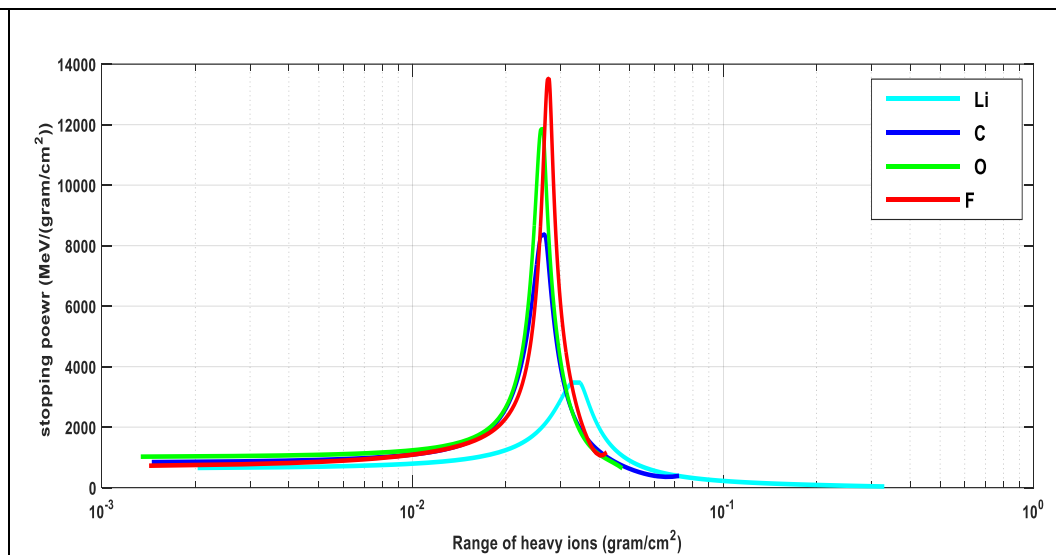
Fig. (3-98) Bragg curves for (Li ,C,O,F) ions in Blood
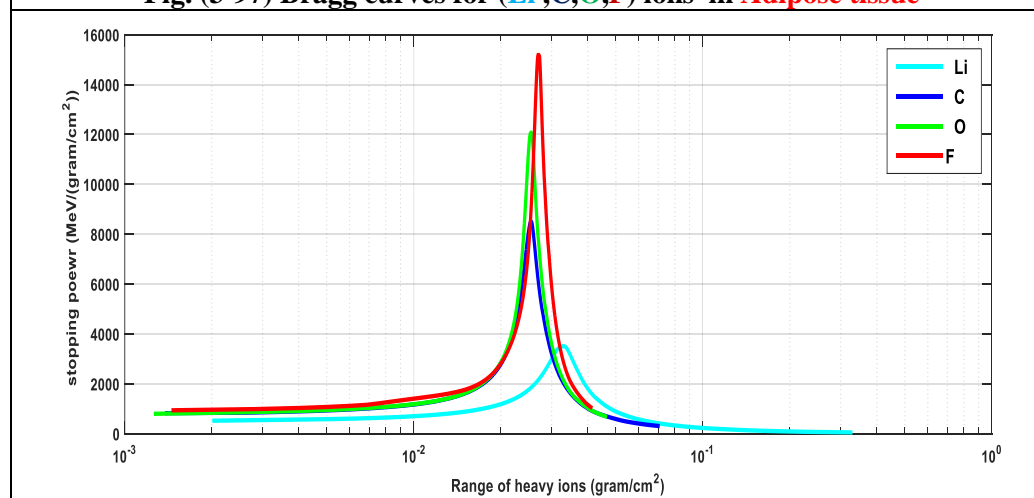
Fig. (3-99) Bragg curves for (Li ,C,O,F) ions in Brain
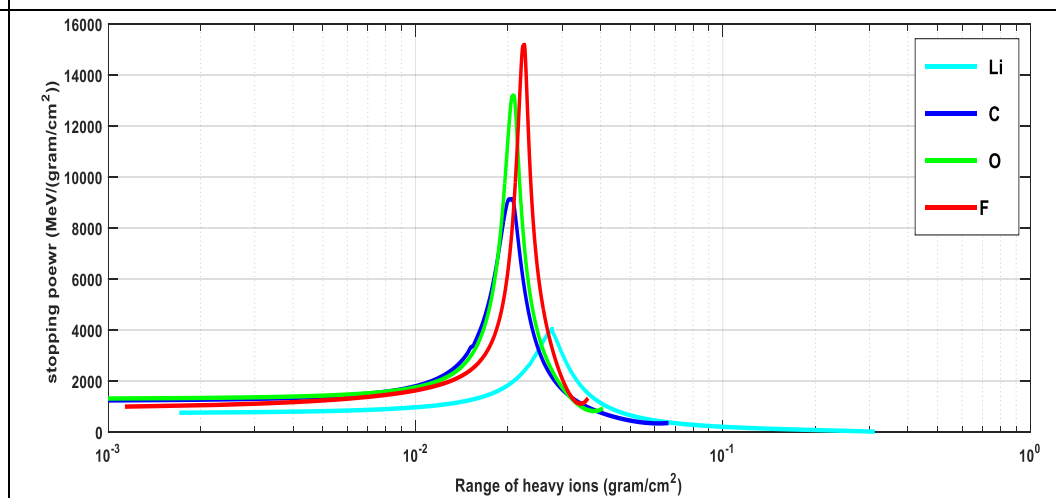
Fig. (3-100) Bragg curves for (Li ,C,O,F) ions in Breast
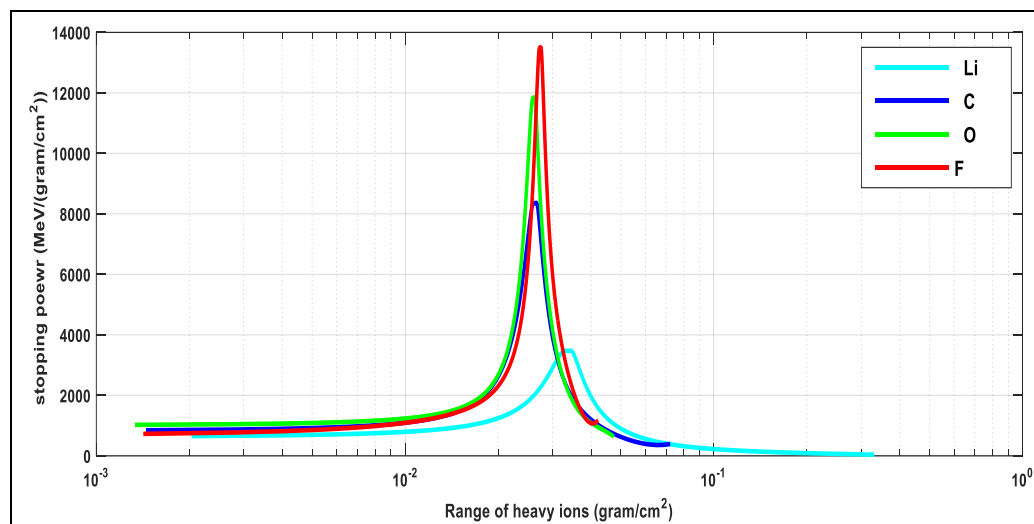
Fig. (3-101) Bragg curves for (Li ,C,O,F) ions in Lung
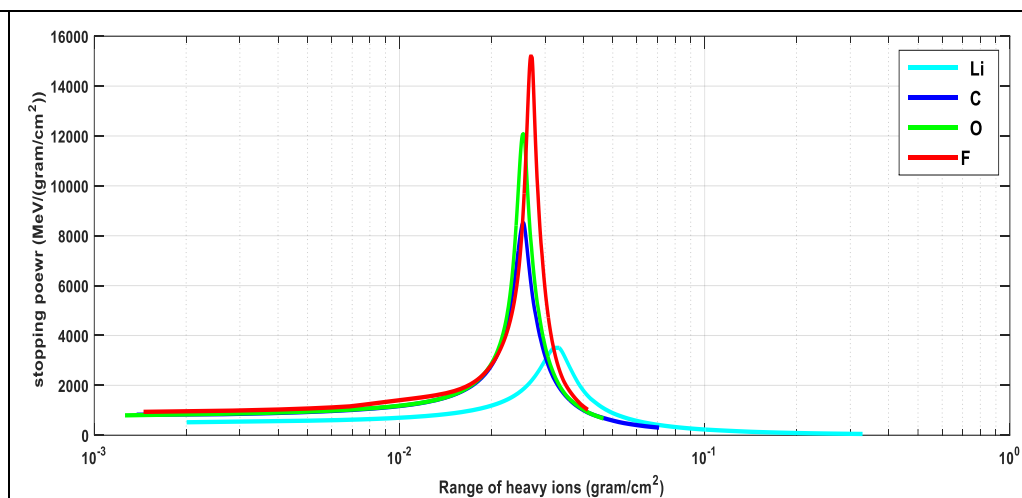
Fig. (3-102) Bragg curves for (Li ,C,O,F) ions in Muscle
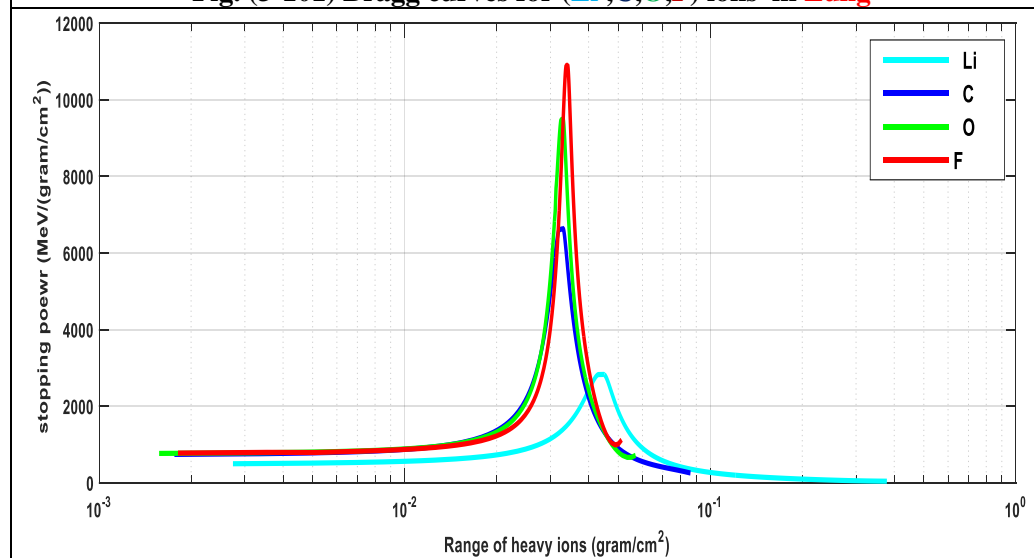
Fig. (3-103) Bragg curves for (Li ,C,O,F) ions in Bone
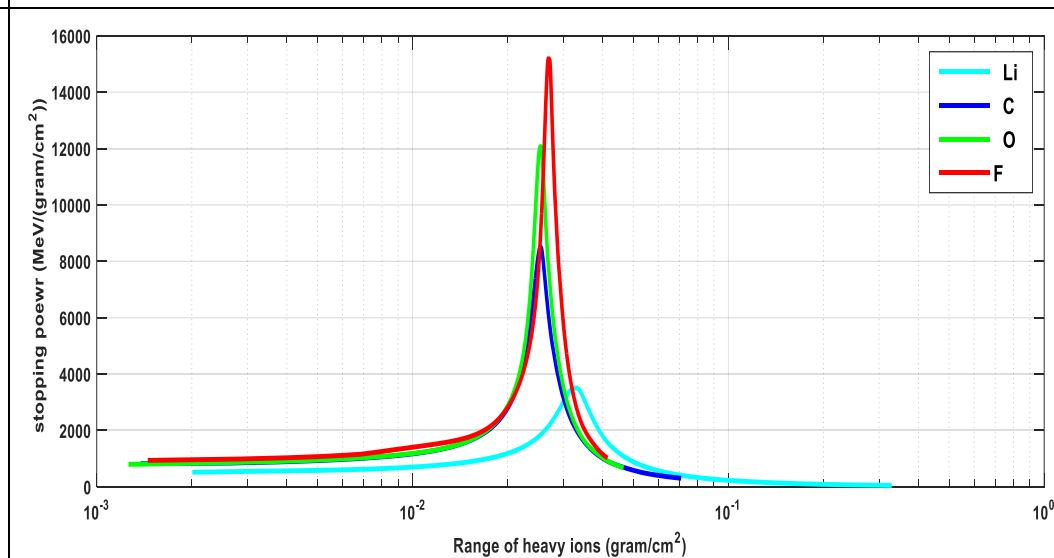
Fig. (3-104) Bragg curves for (Li ,C,O,F) ions in Skin

Chapter Three: Calculations, results and discussion

(3.14) Absorbed doses:

The maximum absorbed dose of (**Li** ,**C**,**O, and F**) ions which interacts with (adipose, blood, breast, brain , lung , muscle, bone, and skin) tissues for the energy range (0.025-1000) MeV were calculated by eq.(2-43) . The results were tabulated in table (3-6).

(3.15) Equivalent dose

The maximum equivalent dose of (**Li** ,**C**,**O, and F**) which interacts with (adipose, blood, breast, brain , lung , muscle, bone, skin) tissues for the energy range (0.025-1000) MeV were calculated by eq.(2-44) . The results were tabulated in table (3-6). (w_R is represents the quality factor of tissue =20 for all heavy ions) .

(3.16) Effective dose

Maximum effective dose of (**Li** ,**C**,**O, and F**) which interacts with (adipose, blood, breast, brain , lung , muscle, bone, skin) tissues for the energy range (0.025-1000) MeV were calculated by eq.(2-45) . The results were tabulated in table (3-6). Where W_T is tissue weighting factor and its values are listed in the table (2-5).

Chapter Three: Calculations, results and discussion

Table (3-6) Maximum absorbed dose, Maximum equivalent dose and Maximum effective dose for (Li ,C,O, and F) ions interaction with tissues

Ions	Tissues	Energy (MeV)	Maximum Absorbed Dose (rad) $\times 10^{-6}$	Maximum Equivalent Dose(rem) $\times 10^{-5}$	Maximum Effective Dose(rem) $\times 10^{-7}$
Lithium	Adipose	1.5	0.0240	0.0480	0.5760
	Blood	1.5	0.0240	0.0480	0.5760
	Brain	1.5	0.0240	0.0480	0.0480
	Breast	1.5	0.0240	0.0480	0.5760
	Lung	1.5	0.0240	0.0480	0.5760
	Muscle	1.5	0.0240	0.0480	0.5760
	Bone	1.6	0.0256	0.0512	0.0512
	Skin	1.5	0.0240	0.0480	0.0480
Carbon	Adipose	4.5	0.0720	0.1440	1.7280
	Blood	4.5	0.0720	0.1440	1.7280
	Brain	4	0.1280	0.1280	0.1280
	Breast	4.5	0.0720	0.1440	0.1440
	Lung	4.5	0.0720	0.1440	1.7280
	Muscle	4.5	0.0720	0.1440	1.7280
	Bone	4.5	0.0720	0.1440	0.1280
	Skin	4.5	0.0720	0.1440	1.7280
oxygen	Adipose	7	0.1120	0.2240	2.6900
	Blood	7	0.1120	0.2240	2.6880
	Brain	7	0.1120	0.2240	0.2240
	Breast	6.5	0.1040	0.2080	0.1040
	Lung	6.5	0.1040	0.2080	2.4960
	Muscle	6.5	0.1040	0.2080	2.4960
	Bone	7	0.1120	0.2240	0.2240
	Skin	7	0.1120	0.2240	0.1120
Fluorine	Adipose	9	0.1440	0.2880	3.45600
	Blood	9	0.1440	0.2880	3.4560
	Brain	9	0.1440	0.2880	0.2880
	Breast	9	0.1440	0.2880	3.4560
	Lung	9	0.1440	0.2880	3.4560
	Muscle	9	0.1440	0.2880	3.4560
	Bone	9	0.1440	0.2880	0.2880
	Skin	9	0.1440	0.2880	3.4560

Chapter Three: Calculations, results and discussion

(3.17) Percentage deviation:

The percentage deviation $[\frac{S_{cal} - S_{exp}}{S_{exp}}] \times 100$ % between the experimental and the calculated mass stopping power values using (SRIM 2013 , SRIM DICTIONRY , PASS ,CasP, MSTAR) programs and Bethe Formula of the tissues (adipose, blood, breast, brain , lung , muscle, bone, skin) for (Li ,C,O, and F) ions have energy range of (0.025 - 1000) MeV . The maximum percentage errors were tabulated in table (3-7).

The maximum percentage errors in (0.025MeV) at Bethe formula and this confirms the Bethe formula is failed in low emerges, also the same conclusion the CaSP program and PASS program but at less value , while the lowest error rate was observed using SRIM , SRIM dictionary and MSTAR .

Table (3-7) Maximum percentage error % of stopping power calculated by six methods

Ions	Tissues	Maximum of percentage deviation % of stopping power											
		SRIM		Dictionary SRIM		MSTAR		PASS		Bethe		CasP	
		E(MeV)	Error ×100%	E(MeV)	Error ×100%	E(MeV)	Error ×100%	E(MeV)	Error ×100%	E(MeV)	Error ×100%	E(MeV)	Error ×100%
Lithium	Adipose	0.03	0.444	0.025	0.043	1000	0.02818	1000	0.9	0.025	43.90	0.025	7.3
	Blood	0.025	0.127	0.025	0.0944	-	-	6	0.82	0.025	52.02	0.025	7.20
	Brain	0.06	0.66	-	-	-	-	9	0.5	0.025	42.34	0.2	4.45
	Breast	0.13	0.890	-	-	-	-	5	0.69	0.025	49.41	0.03	1.15
	Lung	7	0.128	-	-	-	-	10	0.99	0.025	12.9	0.1	2.05
	Muscle	0.3	0.0934	0.3	0.198	60	0.078	7	0.12	0.025	78.6	0.3	1.9
	Bone	1.1	0.367	1000	0.03	-	-	5	0.23	0.025	51.7	0.1	6.98
	Skin	1000	0.223	700	0.06	-	-	2.75	0.34	0.025	41.09	0.6	9.87
Carbon	Adipose	1000	0.2480	1000	0.13	30	0.18	2.25	0.1348	0.025	19.95	0.02	1.584
	Blood	3	0.229	1000	0.12	-	-	4.25	0.9	0.025	32.90	0.8	8.09
	Brain	800	0.29	-	-	-	-	12	0.2	0.025	67.09	1.2	5.9
	Breast	5	0.184	-	-	-	-	4	0.6	0.025	79.123	0.8	3.9
	Lung	1	0.79	-	-	-	-	12	0.9	0.025	36.17	1.4	9.54
	Muscle	40	0.2					2.3	0.1	0.025	43.98	0.1	2.8
	Bone	1.1	0.199	0.025	0.4	-	-	1	0.6	0.03	68.76	0.8	7.09
	Skin	0.8	0.54	800	0.59	-	-	3	0.1780	0.025	76.02	1.1	8.12
oxygen	Adipose	3.5	0.38	1000	0.41	700	0.018	3.75	0.51	0.025	59.8	0.3	10.09
	Blood	0.025	0.239	1000	0.34	-	-	16	0.348	0.025	70.23	0.04	6.001
	Brain	700	0.168	-	-	-	-	14	0.51	0.025	43.98	0.08	2.9
	Breast	0.8	0.193	-	-	-	-	25	0.12	0.025	59.0	0.3	7.065
	Lung	1.5	0.987	-	-	-	-	3.25	0.98	0.025	69.34	0.04	1.98
	Muscle	120	0.29	0.03	0.4	600	0.052	4.2	0.349	0.025	49.09	0.2	3.6
	Bone	1000	0.9	0.025	0.098	-	-	2.25	0.6	0.025	69.34	0.8	9.8
	Skin	1000	0.329	1000	0.23	-	-	5.5	0.198	0.025	56.0	1.8	3.9
Fluorine	Adipose	0.025	0.094	1000	0.189	1.8	0.099	12	0.22	0.025	38.08	1.6	7.9
	Blood	6	0.139	1000	0.0555	-	-	20	0.35	0.025	41.76	6	9.09
	Brain	0.025	0.198	-	-	-	-	5.5	0.29	0.025	50.4	2.5	8.21
	Breast	1000	0.128	-	-	-	-	40	0.19	0.025	21.0	2.5	9.5
	Lung	5	0.40	-	-	-	-	7	0.45	0.025	29.8	5	2.3
	Muscle	60	0.723	1000	0.210	0.6	0.77	10	0.67	0.025	44.09	0.025	8.9
	Bone	500	0.998	1000	0.530	-	-	16	0.21	0.025	20.8	0.04	1.38
	Skin	1000	0.134	0.025	0.168	-	-	9	0.76	0.025	60.98	1.1	2.98

Chapter Three: Calculations, results and discussion

Chapter Four

Conclusions and

future work

(4.1) Conclusions

1. One of the important results obtained in our study is the Bragg Curve which can calculate the maximum value of energy lost at a specified value of particle energy, through which could to tell the physician how much heavy ions energy to use in the treatment and its Range in human tissue, in order to achieve the best treatment and less damage to tissues surrounding the tumor.

2. When heavy ions are used, the acute Bragg peaks can be formed to deposit most of the heavy ion energy in the tumor mass .Moreover, intensity and the position can be controlled by ion species and energy.

3. The dose delivered by Fluorine ion increases with depth and reaches its maximum at the end of the particle track, the Bragg peak, with a sharp edge and with little scatter.

4. Hydrogen atoms are responsible for losing the greatest energy in human tissue.

5. The values of the mass stopping power obtained in the current research in good agreement with ICRU -73 for adipose tissue and Bone.

6. There is a good correlation between semi empirical formulas and theoretical results for both mass stopping power and range of ions.

7. The magnitude of the range of heavy ions depends on the effective atomic number of the target material and its nature.

8. The range of charged particles is practically equal to the depth of their penetration because heavy charged particles travel in straight lines.

9. A slow (low energy) ion loses more energy by ionizing atoms than a fast (high energy) ion , since the slower particle spends a longer time in an atom, and thus there is a greater probability that an electronic transition will occur in the atom.

10. the increasing value of stopping power is linear with the increase of atomic number Z for the falling particle, this is due to the mass stopping power is proportional to z^2 of falling particle.

11. The increase of value of the LET with the increase of atomic number Z for the falling particles on the same material, because the Linear Energy Transfer depends on the velocity, charge and mass of the falling particle.

12. The dose delivered by high-LET particles increases with depth and reaches its maximum at the end of the particle track, the Bragg peak, with a sharp edge and with little scatter.

13. The failure of Bethe equation when calculating the total energy loss of the human tissues at low energies.

14. the differences in stopping power values, at energy range (0.025-1000) MeV , are due to many reasons. The I value and shell correction has an influence on the stopping power especially for targets having high atomic number, some elements have different stopping power values according to their physical and chemical structure (gas or liquid or solid). These differences result from the utilization of different theories in the calculation of the stopping power.

(4.2) Recommendations and future works:

In this study, we provided the physician with accurate data for used ions to achieve the best treatment for the affected area and less damage to the neighboring area. In order to develop this study, the following studies were proposed: -

1. Study of the stopping power and range of other ions in same tissue.
2. Study of stopping power and range of the same particles with other materials and tissues.
3. Comparison between the mass stopping powers of light and heavy ions for the same materials.
4. Calculation of the range of the heavy ions in tissues using new methods

Chapter Four: Conclusions and future work

REFERENCES

Reference

1- Sigmund, Peter. Stopping of heavy ions: a theoretical approach. Vol. 204. Springer Science & Business Media, 2004.

2- El-Ghossain, Maher O. "Calculations of stopping power, and range of electrons interaction with different material and human body parts." INTERNATIONAL JOURNAL OF SCIENTIFIC & TECHNOLOGY RESEARCH VOL. 6, ISSUE 01, JANUARY , 2017.

3- Song, Hong, Srinivasan Senthamizhchelvan, Robert F. Hobbs, and George Sgouros. "Alpha particle emitter radiolabeled antibody for metastatic cancer: what can we learn from heavy ion beam radiobiology?." Antibodies Vol. 1, no. 2, 2012, p. 124-148.

4- Podgoršak, Ervin B. "Radiation physics for medical physicists". Berlin: Springer 2006, p. 141-169 .

5- Pier-giorgio, Rancoita, and Leroy Claude. "Principles Of Radiation Interaction In Matter And Detection". World Scientific, 2015.

6- L'Annunziata, Michael F. "Radioactivity: introduction and history, from the quantum to quarks". Elsevier, 2016.

7- Leo, William R. "Techniques for nuclear and particle physics experiments: a how-to approach". Springer Science & Business Media, 2012.

8- Blattmann, Hans. "Tumor therapy with heavy charged particles." *AIP Conference Proceedings*. Vol. 495. No. 1. AIP, 1999.

9- Nchodu, M. R. "Determination of energy spectra of proton therapy beams." PhD diss., University of Cape Town, 2002.

10- Jäkel, Oliver. "Heavy ion radiotherapy." *New Technologies in Radiation Oncology*. Springer, Berlin, Heidelberg, 365-377, 2006.

11- Schulz-Ertner, Daniela, and Hirohiko Tsujii. "Particle radiation therapy using proton and heavier ion beams." *Journal of clinical oncology* 25.8 ,953-964 , 2007.

12- Tolstikhina, Inga, Makoto Imai, Nicolas Winckler, and Viacheslav Shevelko. Basic Atomic Interactions of Accelerated Heavy Ions in Matter: Atomic Interactions of Heavy Ions. Vol. 98. Springer, 2018.

13- Lilley, John., "Nuclear physics: principles and applications". John Wiley & Sons, 2013. ISBN   1118723325, 9781118723326.

14- Saha, Gopal B. "Radiation biology." In Physics and Radiobiology of Nuclear Medicine, pp. 226-267. Springer, New York, NY, 2006 .

15- Meyerhof, "Elements of Nuclear Physics", McGraw-Hill, New York, 1967.

16- Evans, Robley Dunglison, and R. D. Evans. "The atomic nucleus." (1955).

17- Speight, James G. Lange's handbook of chemistry. Vol. 1. New York: McGraw-Hill, 2005.

18- Mahmoud, Insaf Jasim. "Immunohistochemical Identification And Quantification Of Brown Adipocytes In Human Adipose Tissue." Al-Kindy College Medical Journal 12.2 ,84-88, 2016.

19- International Commission on Radiation Units and Measurements, "Photon, electron, proton and neutron interaction data for body tissues". *ICRU Report No. 46* ,1992.

20- Ehrhardt p., Johanna M. Brandner and Jens-M. J." The skin:an indispensable barrier " , 2008.

21- Hall, John E. *Guyton and Hall textbook of medical physiology e-Book*. Elsevier Health Sciences, 2015.

22- "Muscle tissue" theVisualMD.com", www.thevisualmd.com. , 2015

23- Drake, Richard L.; Vogl, Wayne; Mitchell, Adam W.M. Gray's," anatomy for students (3rd ed.), Edinburgh: Churchill Livingstone/Elsevier,pp. 167–174, 2014.

24- Russo J, Russo IH.," Development of the human breast". In: Knobil E, Neill JD , Academic, New York, 1998.

25- Russo J, Russo IH." Development of the human mammary gland". In: Neville MC, Daniel C (eds) The mammary gland. Plenum, New York, pp. 67–93, 1987.

26- "Breast – Definition of breast by Merriam-Webster", merriam-webster.com. , 2015.

27- Harms, Victoria, and Lorin Elias. "Brain, Tissue." Encyclopedia of Behavioral Medicine pp. 262-263,2013.

28- Wojnar, Ryszard. "Bone and cartilage–its structure and physical properties." Biomechanics of hard tissues: 1-75, 2010.

29- Hubbell, John H., and Stephen M. Seltzer. Tables of X-ray mass attenuation coefficients and mass energy-absorption coefficients 1 keV to 20 MeV for elements Z= 1 to 92 and 48 additional substances of dosimetric interest. No. PB-95-220539/XAB; NISTIR-5632. National Inst. of Standards and Technology-PL, Gaithersburg, MD (United States). Ionizing Radiation Div., 1995.

30- E. Bonderup ," Stopping of swift protons evaluated from statistical atomic model" ,Mat.Fys.Medd.Danvid . selsk ,Vol 35,No.17, 1967.

31- Northcliffe, Lee C., and R. Fo Schilling. "Range and stopping-power tables for heavy ions." Atomic Data and Nuclear Data Tables 7.3-4 (1970): 233-463.

32- J.M.Anthony and W.A .Lanford ,"Stopping Power Of Nd Ion In Pb Determined From X-Ray Linshape", Nucl.Inst.and Math.186(1981) 647-654

33- Hubert, F., R. Bimbot, and H. Gauvin. "Range and stopping-power tables for 2.5–500 MeV/nucleon heavy ions in solids." *Atomic data and nuclear data tables* 46.1: 1-213 , 1990.

34- Y.Susuki ,M.Fritz ,K.Kimura ,M.Mannami ,N.Sakamoto, H.Ogawa ,I.Katayama , T.Noro and H.Ikegami, "Stopping power of carbon For 9.6Mev/amu H2+ ions" ,Phys. Rev. A, Vol.50 , No.4, 1994 .

35- Hiraoka, T. and Bichsel, H., "Stopping powers and ranges for heavy ions". Japanese Journal of Medical Physics, 15(2), pp.91-100, 1995.

36- Randhawa, G. S., and H. S. Virk. "Stopping power and range of heavy ions in solids: A comparative study." Radiation measurements 26.4 (1996): 541-560.

37- Ziegler, J. F. "Stopping of energetic light ions in elemental matter." Journal of applied physics 85.3 (1999): 1249-1272.

38- Paul, Helmut, and Andreas Schinner. "Empirical stopping power tables for ions from 3Li to 18Ar and from 0.001 to 1000 MeV/nucleon in solids and gases." Atomic Data and Nuclear Data Tables 85.2: 377-452. ,2003.

39- Bimbot, R. "Stopping of ions heavier than helium." Journal of the ICRU 5.1 (2005): 1-253.

40- Sun, G., et al. "Energy loss and straggling of heavy ions in silicon nitride in the low MeV energy range." Nuclear Instruments and Methods in Physics Research Section B: Beam Interactions with Materials and Atoms 256.2 (2007): 586-590.

41- K. Nakamura , "Passage of particles through matter " .Vol.37, No. 075021,2010.

42- W. N. J. Abuirqeba , "Studying of Electronic Stopping power For Heavy Charged Particles",M.Sc. Thesis, University of Kufa ,2011.

43- Lateef, Zainab W. Abdul. "Proton, Helium and Carbon Radiation Beam Targeting Reactive Oxygen, Nitrogen and Halogenated Species in TRIM-SRIM Model." Al-Nahrain Journal of Science15.1, 65-72.,2012.

44- Jin, Ke, et al. "Electronic stopping powers for heavy ions in SiC and SiO2." Journal of Applied Physics 115.4 (2014): 044903.

45- Msimanga, M., C. B. Mtshali, and C. A. Pineda-Vargas. "Stopping force of Ti for $6 \leqslant Z \leqslant 29$ ions measured by time of flight spectrometry." Nuclear Instruments and Methods in Physics Research Section B: Beam Interactions with Materials and Atoms 349 (2015): 1-5.

46- Sigmund, Peter, and A. Schinner. "Progress in understanding heavy-ion stopping." Nuclear Instruments and Methods in Physics Research Section B: Beam Interactions with Materials and Atoms 382: 15-25,(2016)

47- Usta, Metin, and Mustafa Çağatay Tufan. "Stopping power and range calculations in human tissues by using the Hartree-Fock-Roothaan wave functions." Radiation Physics and Chemistry 140: 43-50 , (2017).

48- Mohamad, Osama, et al. "Carbon ion radiotherapy: a review of clinical experiences and preclinical research, with an emphasis on DNA damage/repair." Cancers 9.6 (2017): 66.

49- Yaqoob , Saad Nafea," Interaction of some Heavy Ions (12C ,14N ,16O ,10Ne ,40Ar , 84Kr , 132Xe, 235U and 252Cf) with some tissues " Ph.D. Thesis, College of Education for Pure Science Ibn Al - Haitham, University of Baghdad ,2018.

50- Leo, W.R. and Haase, D.G., "Techniques for nuclear and particle physics experiments". *American Journal of Physics*, 1990.

51-   William L. Dunn and Richard P. Hugtenburg, "The interaction of Radiation with Matter ", IEEE Short Course ,2006.

52- Nicholas Tsoulfanidis, "Measurement and Detection of Radiation", Library of congress cataloging in publication Data , 1972.

53- D. I. Thwaites " Departures from Bragg's rule of stopping power additivity for ions in dosimetric and related materials". Nuclear instruments and methods in physics research B69, 53-63, 1992.

54- Turner, James E. "Interaction of ionizing radiation with matter." *Health Physics* 88.6 (2005): 520-544.

55- Glenn F. Knoll, "Radiation Detection and Measurement", 3th ed., (1979).

56- Joiner, M.C. and Van der Kogel, A. eds., "*Basic clinical radiobiology* " (Vol. 1). CRC press, 2016.

57- Hamza A. Mezher "Calculation of cross section for reactions induced proton with Molybdenum to product technetium isotopes". Journal of Kerbala University, Vol.14 No.2 scientific, 2016.

58- James E. Turner, "Atoms Radiation, and Radiation Protection", Wiley-VCH Verlag GmbH& Co. KGaA, Weinheim, 2007.

59- Bodansky, David. *Nuclear energy: principles, practices, and prospects*. Springer Science & Business Media, 2007.

60- S.Y. Lee, "Accelerator Design for Proton Therapy ", Indiana University, 2010.

61- McParland, Brian J. *Nuclear medicine radiation dosimetry: advanced theoretical principles*. Springer Science & Business Media, 2010.

62- Soren Mattsson and Marcus Soderberg, "Radiation Protection in Nuclear Medicine", Springer, Verlag Berlin Heidelberg,2013.

63- Thormod Henriksen &Biophysics group at UiO, "Radiation and Health", Taylor & Francis, 2003.

64- N. Bohr, LX. On the decrease of velocity of swiftly moving electrified particles in passing through matter, Philosophical Magazine Series 6, 30 (1915) 581-612.

65- P. Sigmund, Kinetic theory of particle stopping in a medium with internal motion, Physical Review A, 26 ,2497-2517, 1982.

66- A. L. Tofterup, Relativistic binary-encounter collision and stopping theory: general expressions, Journal of Physics B: Atomic and Molecular Physics, 16 (1983) 2997.

67- H. Bethe, Zur Theorie des Durchgangs schneller Korpuskularstrahlen durch Materie, Annalen der Physik, 397 (1930) 325-400.

68- W. H. Barkas, J. N. Dyer, H. H. Heckman, Resolution of the Mass Anomaly, Physical Review Letters, 26-28, 1963.

69- H. H. Andersen, H. Simonsen, H. Sørensen, An experimental investigation of chargedependent deviations from the Bethe stopping power formula, Nuclear Physics A, 125 171-175. (1969).

70- J. C. Ashley, R. H. Ritchie, W. Brandt, Z3 Effect in the Stopping Power of Matter for Charged Particles, Physical Review B, 5 (1972) 2393-2397.

71- Paul, Helmut. "A comparison of recent stopping power tables for light and medium-heavy ions with experimental data, and applications to radiotherapy dosimetry." *Nuclear Instruments and Methods in Physics Research Section B: Beam Interactions with Materials and Atoms* 247.2 (2006): 166-172.

72- J. E. Ziegler, The Stopping and Range of Ions in Solids, Pergamon Press, New York, 1985.

73- James F. Ziegler, M.D. Ziegler, J.P. Biersack, "SRIM – The stopping and range of ions in matter ", Nuclear Instruments and Methods in Physics Research Section , Volume 268, Issues 11–12, Pages 1818-1823.(2010)

74- P. L. Grande, G. Schiwietz, The unitary convolution approximation for heavy ions, Nuclear Instruments and Methods in Physics Research Section B: Beam Interactions with Materials and Atoms, 55-63,2002.

75- P. Sigmund, A. Schinner, Binary stopping theory for swift heavy ions, The European Physical Journal D, 12 (2000) 425-434

76- P. Sigmund, Particle Penetration and Radiation Effects: General Aspects and Stopping of Swift Point Charges, Springer, 2006.

77- H.Paul and A.Schinner, "An empirical approach to the stopping power of solids and gases for ions from $_3$Li to $_{18}$Ar, Part II, Nucl. Instr. Meth. Phys. Res. B 195 (2002) 166.

78- H. Paul and A. Schinner, "Empirical stopping power tables for ions from $_3$Li to $_{18}$Ar and from 0.001 to 1000 MeVnucleon in solids and gases", Atomic Data Nucl. Data Tables 85, 2003.

79- Ziegler, James F. "Comments on icru report no. 49: stopping powers and ranges for protons and alpha particles." Radiation research Vol . 152, n.2, P. 219-222, 1999.

80- Young S.K., "Human Tissues: Chemical Composition and Photon Dosimeter Data " Radiation Research. Vol. 57, P. 38–45,1974.

81- Mahalesh D., et.al., "Determination of energy loss ,range and stopping power of light ions using silicon surface barrier detector", international Journal of science, Technology& Management ,2015.

82- Getachew, Abebe. "Stopping power and range of Protons of various energies in Different materials." PhD diss., Addis Ababa University, 2007.

Appendix

Appendix

Appendix (A): Mass Stopping Power for Heavy Ions Interaction with tissues

Mass stopping power for Lithium ions interacts with the Adipose tissue using (SRIM, CasP, PASS,SRIM dictionary ,MSTAR) programs and Bethe formulae

E(MeV)	Mass Stopping power MeV/(g/cm²) For Adipose Tissue							
	Bethe	SRIM	Dic.SRIM	PASS	CasP	MSTAR	Present Work	
							Average S.P.	S.P.(P.W)
0.025	----	777.242	622.8	1372.235	97.59	721.871	707.305	766.313
0.03	----	821.881	682.5	1501.257	149.788	786.6	788.405	814.698
0.04	----	909.343	791	1710.079	227.191	899.743	907.471	909.226
0.06	----	1073.398	979.2	2045.258	380.809	1092	1114.133	1089.694
0.08	----	1220.835	1141	2311.119	529.673	1260.143	1292.554	1259.396
0.1	----	1352.342	1283	2533.429	678.537	1415.286	1452.519	1419.092
0.2	----	1892.176	1849	3291.407	1317.213	2034.429	2076.845	2089.803
0.3	----	2389.887	2358	3751.213	1808.405	2497.857	2561.072	2594.226
0.4	----	2832.16	2805	4045.233	2177.609	2868.714	2945.743	2972.936
0.6	----	3502.426	3480	4328.521	2677.865	3414.714	3480.705	3484.106
0.8	----	3917.495	3898	4395.535	3014.325	3754.857	3796.042	3778.357
1	----	4155.624	4137	4369.468	3200.707	3974.143	3967.388	3940.242
1.1	----	4226.829	4210	4338.026	3258.856	4044.143	4015.571	3987.598
1.2	----	4275.119	4259	4299.742	3295.475	4094.429	4044.753	4018.338
1.3	----	4303.404	4289	4256.676	3326.711	4122.857	4059.73	4035.654
1.4	----	4317.393	4304	4210.5	3357.947	4144	4058.453	4039.671
1.5	----	4317.485	4306	4162.592	3362.19	4144	4066.768	4042.086
1.6	----	4308.426	4298	4113.69	3366.434	4140	4045.31	4030.051
1.7	----	4291.385	4282	4064.16	3370.677	4124	4026.444	4014.565
1.8	----	4267.236	4259	4014.48	3367.118	4103.143	4002.195	3994.303
2	----	4204.533	4198	3915.833	3344.395	4046.571	3941.866	3942.88
2.25	----	4107.977	4105	3795.63	3303.164	3956.143	3853.583	3864.706
2.5	----	4000.601	4000	3680.468	3253.381	3857.714	3758.433	3777.537
2.75	----	3889.011	3891	3570.536	3203.599	3751.286	3661.086	3685.893
3	----	3776.733	3780	3466.002	3155.932	3643.143	3564.362	3592.684
3.25	----	3665.616	3670	3366.713	3108.794	3534.857	3469.196	3499.787
3.5	----	3557.962	3563	3272.268	3061.656	3427	3376.377	3408.405
3.75	----	3453.088	3459	3182.968	3014.519	3323.429	3286.601	3319.297
4	----	3352.838	3359	3098.877	2967.381	3224.571	3200.534	3232.921
4.5	----	3164.461	3172	2941.138	2875.129	3043.429	3039.231	3069.262
5	3255.05	2992.937	3001	2799.45	2784.226	2883.286	2952.658	2918.12
5.5	3060.507	2838.178	2845	2670.601	2693.323	2739.714	2807.887	2779.134
6	2865.963	2697.48	2705	2552.777	2594.178	2609	2670.733	2651.495
6.5	2716.901	2570.876	2578	2444.558	2492.972	2491.286	2549.099	2534.241
7	2567.838	2455.629	2462	2345.218	2391.766	2382	2434.075	2426.394
8	2331.306	2255.067	2261	2170.671	2201.631	2203.143	2237.136	2235.281
9	2138.556	2088.091	2093	2019.206	2037.481	2035	2068.556	2071.679
10	1978.122	1945.802	1951	1887.257	1890.181	1899	1925.227	1930.391
12	1725.601	1717.957	1722	1671.258	1663.85	1669.857	1695.087	1699.3
14	1535.14	1543.522	1547	1501.652	1487.222	1492	1517.756	1518.721
16	1385.835	1423.906	1429	1363.912	1358.208	1354.143	1385.834	1373.965
18	1265.327	1302.28	1307	1250.404	1238.385	1240.143	1267.256	1255.44
20	1165.81	1196.703	1201	1154.622	1146.134	1145.857	1168.354	1156.66
40	672.933	684.244	686.6	670.241	678.195	668.471	676.781	663.463
60	484.739	491.85	493.4	482.965	488.038	482.971	487.327	478.631
80	383.341	388.486	389.7	382.453	385.993	385.957	385.988	381.35
100	319.318	323.336	324.3	318.406	321.004	320.7	321.178	320.958
120	274.967	278.189	279.1	274.384	276.722	275.586	276.491	279.554
160	217.182	219.531	220.2	217.122	228.237	217.7	219.995	225.858
180	197.22	199.242	199.9	197.27	213.249	197.786	200.778	207.224
200	180.953	182.781	183.4	180.958	198.26	181.514	184.644	191.914
400	103.506	104.324	104.6	103.679	105.45	103.97	104.255	112.921
500	86.892	87.519	87.79	87.01	88.542	87.263	87.503	91.843
600	75.524	76.023	76.26	75.655	76.012	75.829	75.884	74.907
700	67.238	67.649	67.86	67.317	67.581	67.5	67.524	60.346
800	60.923	61.269	61.46	61.071	33.469	61.683	56.646	47.274
900	55.946	56.236	56.42	56.062	19.662	56.331	50.109	35.196
1000	51.922	52.183	52.34	51.991	19.392	52.377	46.701	23.815

Appendix

Mass stopping power for Lithium ions interacts with the Blood using (SRIM, CaSP, PASS,SRIM dictionary) programs and Bethe formulae

E(MeV)	Mass Stopping power MeV/(g/cm²) For Blood Tissue						
	Bethe	SRIM	Dic.SRIM	PASS	CasP	Average S.P.	S.P.(P.W)
						Present Work	
0.025	------	460.562	436.4	971.99	87.655	520.481	567.078
0.03	------	499.463	484.1	1121.205	110.047	583.807	607.489
0.04	------	573.76	571.4	1407.809	169.017	680.496	686.492
0.06	------	710.465	725.1	1683.672	287.183	851.605	837.542
0.08	------	835.474	861.1	1903.668	406.246	1001.622	979.888
0.1	------	952.087	985	2086.474	525.31	1137.218	1114.167
0.2	------	1458.064	1508	2716.37	1044.253	1681.672	1690.831
0.3	------	1879.008	1947	3108.927	1459.855	2098.697	2109.528
0.4	------	2232.522	2320	3378.546	1785.216	2429.071	2442.269
0.6	------	2760.009	2880	3706.487	2227.354	2893.463	2901.244
0.8	------	3096.14	3238	3861.234	2530.228	3181.4	3180.763
1	------	3306.306	3461	3914.364	2726.661	3352.083	3348.595
1.1	------	3377.789	3537	3918.954	2791.832	3406.394	3403.594
1.2	------	3434.538	3595	3913.431	2837.607	3445.144	3444.02
1.3	------	3475.695	3638	3900.343	2878.532	3473.143	3472.496
1.4	------	3507.012	3669	3881.686	2919.458	3494.289	3491.123
1.5	------	3526.641	3689	3858.932	2933.207	3504.994	3505.317
1.6	------	3539.989	3701	3832.031	2946.956	3501.945	3501.602
1.7	------	3546.53	3705	3803.028	2960.705	3503.816	3503.404
1.8	------	3547.047	3704	3772.631	2966.493	3497.543	3496.8
2	------	3533.249	3685	3707.442	2962.144	3471.959	3472.502
2.25	------	3496.551	3642	3622.649	2940.525	3425.431	3427.121
2.5	------	3444.189	3582	3536.843	2908.119	3367.788	3370.914
2.75	------	3382.81	3513	3451.748	2875.712	3305.817	3308.119
3	------	3314.053	3438	3368.546	2842.095	3240.673	3241.582
3.25	------	3240.813	3358	3287.888	2808.176	3173.719	3173.232
3.5	------	3165.79	3277	3210.039	2774.257	3106.771	3104.384
3.75	------	3089.127	3195	3134.909	2740.338	3039.844	3035.938
4	------	3012.889	3113	3062.237	2706.419	2973.636	2968.5
4.5	------	2862.867	2954	2926.61	2643.172	2846.662	2838.133
5	3039.507	2719.246	2804	2801.251	2582.985	2726.87	2715.066
5.5	2861.932	2585.921	2664	2685.288	2522.798	2614.502	2599.864
6	2684.357	2462.044	2536	2578.206	2445.205	2505.364	2492.479
6.5	2547.543	2348.586	2418	2479.25	2363.261	2402.274	2392.567
7	2410.73	2244.992	2310	2387.397	2281.316	2305.927	2299.648
8	2192.736	2063.244	2123	2221.422	2103.038	2127.676	2132.684
9	2014.515	1910.795	1965	2078.429	1947.461	1975.421	1987.503
10	1865.785	1781.41	1832	1952.298	1807.188	1847.736	1860.509
12	1630.971	1576.232	1621	1741.215	1590.347	1631.953	1649.663
14	1453.286	1420.755	1460	1571.809	1419.889	1465.148	1482.255
16	1313.645	1323.072	1356	1433.436	1297.986	1344.828	1346.409
18	1200.71	1216.663	1245	1317.875	1184.901	1233.03	1234.097
20	1107.29	1118.955	1145	1221.28	1098.267	1138.158	1139.754
40	642.427	644.329	657.6	716.544	652.451	662.67	658.638
60	463.875	464.787	473.7	518.728	470.34	478.286	473.913
80	367.391	367.845	374.7	410.979	372.686	378.72	375.65
100	306.357	306.618	312.2	343.389	310.19	315.751	314.264
120	264.019	264.173	268.8	296.11	267.58	272.136	272.01
140	232.808	232.895	236.9	261.141	235.463	239.841	240.964
160	208.782	208.781	212.4	234.236	220.986	217.037	217.057
180	189.678	189.633	192.8	212.747	206.508	198.273	197.984
200	174.1	174.037	176.9	195.422	192.031	182.498	182.342
400	99.812	99.66	101.2	111.741	102.381	102.959	104.378
500	83.844	83.688	84.93	93.785	86.043	86.458	86.224
600	72.91	72.75	73.81	81.395	73.99	74.971	73.651
700	64.936	64.777	65.71	72.375	65.597	66.679	64.849
800	58.856	58.693	59.53	65.404	59.53	60.621	58.911
900	54.063	53.901	54.67	60.021	54.57	55.664	55.33
1000	50.186	50.037	50.73	55.623	50.93	51.644	53.8

Appendix

Mass stopping power for Lithium **ions interacts with the** Brain **using (SRIM, CasP, PASS)programs and Bethe formulae**

E(MeV)	Mass Stopping power MeV/(g/cm^2) Brain Tissue					
					Present work	
	Bethe	SRIM	PASS	CasP	Average S.P.	S.P.(P.W)
0.025	------	526.776	1206.078	91.943	613.093	608.626
0.03	------	566.898	1339.532	115.862	674.097	674.719
0.04	------	644.093	1524.438	177.241	781.924	785.548
0.06	------	787.039	1819.861	300.051	968.984	968.579
0.08	------	917.45	2052.816	423.067	1131.111	1127.046
0.1	------	1038.015	2246.695	546.083	1276.931	1270.763
0.2	------	1556.403	2903.037	1079.223	1846.221	1851.124
0.3	------	1999.736	3299.495	1502.039	2267.09	2275.795
0.4	------	2378.201	3561.827	1831.534	2590.521	2594.87
0.6	------	2947.544	3853.436	2279.919	3026.966	3023.286
0.8	------	3309.99	3959.504	2585.89	3285.128	3274.394
1	------	3534.033	3973.515	2781.407	3429.652	3418.242
1.1	------	3608.775	3960.349	2846.023	3471.715	3462.931
1.2	------	3666.752	3938.981	2891.105	3498.946	3494.08
1.3	------	3707.792	3911.449	2931.304	3516.848	3514.225
1.4	------	3737.792	3879.482	2971.503	3529.593	3525.381
1.5	------	3755.252	3844.662	2984.446	3523.656	3529.163
1.6	------	3765.666	3807.912	2997.389	3528.12	3526.875
1.7	------	3768.69	3769.698	3010.332	3516.24	3519.581
1.8	------	3765.203	3730.145	3015.296	3503.548	3508.152
2	------	3742.885	3650.021	3009.266	3467.39	3475.642
2.25	------	3694.75	3549.577	2985.713	3410.014	3422.202
2.5	------	3631.062	3451.098	2951.485	3344.548	3359.829
2.75	------	3558.75	3355.629	2917.256	3277.212	3292.316
3	------	3479.898	3263.757	2882.206	3208.62	3222.171
3.25	------	3397.358	3175.646	2846.951	3139.985	3151.073
3.5	------	3313.916	3091.156	2811.696	3072.256	3080.146
3.75	------	3229.46	3010.713	2776.441	3005.538	3010.144
4	------	3146.331	2934.595	2741.186	2940.704	2941.563
4.5	------	2984.471	2791.033	2675.317	2816.94	2809.82
5	3072.347	2831.127	2660.98	2612.543	2701.55	2686.208
5.5	2892.374	2689.854	2542.095	2549.768	2593.906	2570.988
6	2712.402	2559.146	2432.933	2470.284	2487.454	2463.921
6.5	2573.831	2440.026	2332.317	2386.622	2386.322	2364.537
7	2435.26	2331.459	2239.659	2302.96	2291.359	2272.274
8	2214.574	2141.418	2076.203	2122.911	2113.511	2106.808
9	2034.221	1982.546	1933.86	1965.682	1960.696	1963.186
10	1883.757	1847.767	1809.504	1823.91	1827.06	1837.704
12	1646.29	1634.173	1605.201	1604.854	1614.743	1629.586
14	1466.666	1472.313	1444.233	1432.805	1449.784	1464.475
16	1325.543	1366.5	1313.194	1309.602	1329.765	1330.543
18	1211.435	1254.155	1205.023	1195.306	1218.162	1219.833
20	1117.064	1152.909	1113.62	1107.733	1124.754	1126.84
40	647.72	661.923	649.266	657.661	656.283	652.505
60	467.57	476.778	468.791	473.959	473.176	470.252
80	370.254	376.992	371.671	375.474	374.712	373.246
100	308.707	314.034	309.686	312.48	312.067	312.61
120	266.02	270.412	267.032	269.524	268.989	270.843
140	234.555	238.292	235.729	237.145	237.055	240.128
160	210.336	213.554	211.487	222.56	215.867	216.449
180	191.08	193.906	192.213	207.974	198.031	197.531
200	175.38	177.925	176.37	193.389	182.561	181.991
300	126.376	128.025	127.219	129.718	128.321	131.934
400	100.52	101.739	101.214	103.074	102.009	103.459
500	84.432	85.399	84.979	86.616	85.665	84.351
600	73.418	74.214	73.915	74.473	74.201	70.477
700	65.385	66.066	65.786	66.036	65.963	60.053
800	59.261	59.849	59.696	32.779	50.774	52.179
900	54.434	54.951	54.81	19.311	43.024	46.356
1000	50.529	51.005	50.839	19.037	40.294	42.282

Appendix

Mass stopping power for Lithium ions interacts with the Breast using (SRIM, CasP, PASS)programs and Bethe formulae

E(MeV)	Mass Stopping power MeV/(g/cm²) Breast Tissue					
	Bethe	SRIM	PASS	CasP	Present work	
					Average S.P.	S.P.(P.W)
0.025	------	612.164	1268.7	94.988	588.38	662.077
0.03	------	653.684	130.514	124.444	675.553	708.604
0.04	------	734.048	1481.814	190.225	802.029	799.212
0.06	------	883.416	1773.648	321.491	992.852	971.147
0.08	------	1018.751	2006.897	451.576	1159.074	1131.595
0.1	------	1142.069	2201.071	581.66	1308.267	1281.52
0.2	------	1662.29	2872.759	1145.635	1893.561	1900.528
0.3	------	2119.037	3292.286	1590.219	2333.847	2354.792
0.4	------	2514.905	3578.614	1932.349	2675.289	2694.05
0.6	------	3112.832	3911.442	2395.999	3140.091	3145.29
0.8	------	3490.699	4053.438	2711.604	3418.581	3406.637
1	------	3718.777	4090.659	2904.473	3571.303	3554.631
1.1	------	3792.267	4087.604	2966.881	3615.584	3600.111
1.2	------	3846.959	4074.909	3009.094	3643.654	3631.5
1.3	------	3883.804	4055.141	3046.259	3661.735	3651.482
1.4	------	3908.483	4030.269	3083.424	3674.059	3662.177
1.5	------	3920.261	4001.708	3093.511	3671.827	3665.277
1.6	------	3924.229	3969.531	3103.598	3665.786	3662.146
1.7	------	3920.615	3935.61	3113.685	3656.637	3653.889
1.8	------	3910.303	3900.552	3115.881	3642.245	3641.41
2	------	3874.693	3827.148	3104.49	3602.11	3606.629
2.25	------	3810.668	3733.493	3075.406	3539.855	3550.188
2.5	------	3732.757	3640.13	3036.424	3469.77	3484.766
2.75	------	3647.689	3548.595	2997.443	3397.909	3414.233
3	------	3558.137	3459.81	2958.506	3325.484	3341.139
3.25	------	3466.57	3374.241	2919.579	3253.463	3267.183
3.5	------	3375.584	3292.008	2880.653	3182.749	3193.501
3.75	------	3284.878	3212.929	2841.727	3113.178	3120.846
4	------	3196.622	3136.65	2802.8	3045.357	3049.717
4.5	------	3027.092	2994.826	2728.489	2916.802	2913.183
5	3118.415	2868.859	2864.141	2656.539	2796.513	2785.171
5.5	2934.558	2724.162	2743.791	2584.589	2684.181	2665.966
6	2750.701	2591.137	2632.97	2498.758	2574.288	2550.615
6.5	2609.363	2470.425	2530.704	2409.456	2470.195	2451.776
7	2468.024	2360.453	2435.895	2320.155	2372.167	2356.338
8	2243.194	2168.318	2264.834	2137.538	2190.23	2185.025
9	2059.624	2007.877	2117.798	1978.938	2034.871	2036.257
10	1906.591	1871.501	1988.459	1836.228	1898.729	1906.228
12	1665.278	1654.498	1772.17	1616.169	1680.946	1690.455
14	1482.912	1489.373	1598.765	1443.652	1510.597	1519.158
16	1339.738	1378.959	1457.244	1319.231	1385.145	1380.13
18	1224.037	1263.954	1339.135	1203.748	1268.945	1265.152
20	1128.394	1161.906	1240.489	1115.078	1161.467	1168.535
40	653.354	666.477	726.414	661.443	676.922	675.171
60	471.321	479.79	525.38	476.51	488.25	485.457
80	373.068	379.262	416.027	377.303	386.415	384.53
100	310.961	315.847	347.515	313.934	322.064	321.512
120	267.902	271.902	299.611	270.74	277.539	278.169
140	236.172	239.573	264.172	238.136	244.513	246.354
160	211.755	214.684	236.904	223.482	221.706	221.877
180	192.344	194.903	215.127	208.827	202.8	202.366
200	176.521	178.828	197.57	194.173	186.773	186.375
300	127.15	128.629	142.148	130.2	132.032	135.212
400	101.11	102.197	112.892	103.426	104.906	106.464
500	84.913	85.768	94.723	86.892	88.074	87.374
600	73.826	74.524	82.203	74.671	76.306	73.626
700	65.742	66.333	73.086	66.276	67.859	63.354
800	59.579	60.087	66.039	32.873	54.645	55.621
900	54.721	55.164	60.599	19.35	47.458	49.903
1000	50.792	51.197	56.16	19.079	44.307	45.885

Appendix

Mass stopping power for Lithium ions interacts with the Lung using (SRIM, CasP, PASS)programs and Bethe formulae

E(MeV)	Mass Stopping power MeV/(g/cm²) Lung Tissue					
					Present work	
	Bethe	SRIM	PASS	CasP	Average S.P.	S.P.(P.W)
0.025	----	505.676	1192.876	90.103	586.808	651.759
0.03	----	545.35	1315.115	110.64	657.035	695.568
0.04	----	621.485	1496.546	169.809	762.613	780.86
0.06	----	762.129	1786.383	288.359	945.624	942.634
0.08	----	890.456	2014.941	407.763	1104.387	1093.513
0.1	----	1009.341	2205.186	527.168	1247.232	1234.424
0.2	----	1521.499	2849.575	1047.037	1806.037	1815.538
0.3	----	1956.195	3239.419	1462.678	2219.431	2241.422
0.4	----	2325.879	3498.756	1788.056	2537.564	2559.305
0.6	----	2882.171	3791.266	2230.422	2967.953	2982.236
0.8	----	3238.193	3901.143	2533.274	3224.204	3227.694
1	----	3460.413	3919.156	2729.683	3369.751	3367.317
1.1	----	3535.4	3907.859	2794.858	3412.706	3410.498
1.2	----	3594.184	3888.252	2840.659	3441.031	3440.511
1.3	----	3636.402	3862.365	2881.616	3460.127	3459.855
1.4	----	3667.843	3831.93	2922.573	3473.938	3470.505
1.5	----	3686.938	3798.544	2936.332	3474.115	3474.038
1.6	----	3699.135	3763.145	2950.091	3470.79	3471.722
1.7	----	3703.997	3726.208	2963.849	3464.685	3464.588
1.8	----	3702.407	3687.824	2969.64	3453.29	3453.477
2	----	3683.85	3609.875	2965.286	3419.67	3421.98
2.25	----	3640.258	3511.823	2943.628	3365.236	3370.306
2.5	----	3580.754	3415.429	2911.161	3302.448	3310.038
2.75	----	3512.225	3321.816	2878.694	3237.578	3244.805
3	----	3436.705	3231.605	2845.041	3171.117	3177.007
3.25	----	3357.105	3144.991	2811.092	3104.396	3108.25
3.5	----	3276.233	3061.861	2777.143	3038.412	3039.614
3.75	----	3194.025	2982.65	2743.193	2973.29	2971.821
4	----	3112.869	2907.654	2709.244	2909.922	2905.35
4.5	----	2954.269	2766.116	2646.012	2788.799	2777.507
5	3043.155	2803.436	2637.771	2585.891	2675.699	2657.381
5.5	2865.344	2664.191	2520.371	2525.769	2570.11	2543.977
6	2687.534	2535.148	2412.519	2448.204	2465.291	2440.587
6.5	2550.543	2417.396	2313.065	2366.279	2365.58	2343.536
7	2413.552	2310.063	2221.441	2284.353	2271.952	2253.288
8	2195.281	2122.065	2059.728	2105.901	2095.898	2091.101
9	2016.837	1964.816	1918.836	1950.109	1944.587	1949.982
10	1867.922	1831.437	1795.7	1809.618	1812.251	1826.421
12	1632.821	1620.217	1593.306	1592.431	1601.985	1620.943
14	1454.921	1460.263	1433.767	1421.706	1438.579	1457.439
16	1315.115	1355.683	1303.85	1299.632	1319.722	1324.494
18	1202.046	1244.538	1196.579	1186.39	1209.169	1214.388
20	1108.517	1144.224	1105.919	1099.642	1116.595	1121.757
40	643.121	657.471	645.091	653.224	651.929	647.394
60	464.37	473.723	465.883	470.883	470.163	464.628
80	367.78	374.641	369.417	373.113	372.39	367.499
100	306.679	312.112	307.839	310.544	310.165	306.994
120	264.296	268.785	265.459	267.881	267.375	265.508
140	233.051	236.872	234.354	235.728	235.651	235.16
160	208.999	212.292	210.264	221.234	214.597	211.899
180	189.875	192.77	191.109	206.74	196.873	193.425
200	174.281	176.889	175.364	192.245	181.499	178.339
300	125.603	127.298	126.509	128.973	127.593	130.446
400	99.914	101.17	100.657	102.493	101.44	103.642
500	83.93	84.927	84.516	86.137	85.193	85.547
600	72.984	73.807	73.515	74.072	73.798	71.97
700	65.002	65.706	65.433	65.667	65.602	61.099
800	58.916	59.525	59.377	32.604	50.502	52.023
900	54.118	54.656	54.519	19.215	42.797	44.234
1000	50.237	50.732	50.57	18.942	40.081	37.426

Appendix

Mass stopping power for Lithium ions interacts with the Muscle using (SRIM, CasP, PASS,SRIM dictionary ,MSTAR)programs and Bethe formulae

E(MeV)	Mass Stopping power MeV/(g/cm²) For Muscle Tissue							
							Present Work	
	Bethe	SRIM	Dic.SRIM	PASS	CasP	MSTAR	Average S.P.	S.P. (P.W)
0.025	-------	522.076	455.9	1197.092	90.002	517.043	545.622	606.105
0.03	-------	561.987	504.7	1320.436	111.899	568.371	613.479	645.565
0.04	-------	638.66	593.9	1502.747	171.769	658.943	713.204	722.853
0.06	-------	780.382	750.5	1794.15	291.645	814.586	886.253	871.149
0.08	-------	909.475	888.4	2024.114	412.07	952.114	1037.235	1011.515
0.1	-------	1028.683	1013	2215.65	532.495	1079.143	1173.794	1144.452
0.2	-------	1540.037	1536	2865.084	1057.106	1598.429	1719.331	1712.593
0.3	-------	1976.354	1978	3258.404	1476.441	2001.714	2138.183	2151.136
0.4	-------	2348.626	2355	3519.576	1803.985	2336.857	2472.809	2492.254
0.6	-------	2909.457	2921	3811.421	2248.92	2861.857	2950.531	2967.597
0.8	-------	3268.055	3284	3918.806	2553.534	3226	3250.079	3258.097
1	-------	3490.938	3507	3934.37	2749.328	3488.143	3433.956	3431.295
1.1	-------	3565.676	3583	3921.989	2814.048	3582.714	3493.486	3487.202
1.2	-------	3623.818	3640	3901.397	2859.254	3658.143	3536.522	3527.488
1.3	-------	3665.241	3682	3874.625	2899.581	3711.714	3566.632	3554.44
1.4	-------	3695.658	3711	3843.397	2939.907	3758	3589.593	3578.368
1.5	-------	3713.681	3729	3809.295	2953.108	3780.857	3597.188	3583.974
1.6	-------	3724.644	3739	3773.243	2966.309	3799.286	3600.496	3582.901
1.7	-------	3728.232	3741	3735.708	2979.51	3804.429	3597.776	3579.362
1.8	-------	3725.336	3738	3696.802	2984.766	3800.429	3589.067	3569.89
2	-------	3704.24	3715	3617.921	2979.389	3763.429	3555.996	3539.437
2.25	-------	3657.619	3667	3518.915	2956.716	3679.429	3495.936	3485.942
2.5	-------	3595.426	3603	3421.751	2923.41	3583.143	3425.346	3421.556
2.75	-------	3524.488	3530	3327.498	2890.104	3478.857	3350.189	3350.805
3	-------	3446.975	3452	3236.748	2855.752	3375.143	3273.324	3276.699
3.25	-------	3365.718	3369	3149.677	2821.138	3273.857	3195.878	3201.257
3.5	-------	3283.484	3286	3066.156	2786.524	3176	3119.633	3125.832
3.75	-------	3200.174	3202	2986.609	2751.91	3085.286	3045.196	3051.329
4	-------	3118.135	3120	2911.319	2717.296	2998	2972.95	2978.345
4.5	-------	2958.287	2959	2769.277	2652.466	2835.714	2834.949	2838.316
5	3047.266	2806.75	2808	2640.548	2590.568	2689.857	2707.145	2707.285
5.5	2869.048	2667.069	2667	2522.835	2528.671	2558.429	2588.801	2585.562
6	2690.83	2537.797	2538	2414.723	2449.933	2438	2475.691	2472.863
6.5	2553.557	2419.937	2420	2315.05	2366.986	2329.714	2370.338	2368.638
7	2416.284	2312.512	2313	2223.241	2284.039	2230	2272.559	2272.233
8	2197.6	2124.423	2125	2061.24	2105.376	2064.286	2096.065	2100.231
9	2018.843	1967.127	1968	1920.123	1949.605	1908.429	1942.657	1951.901
10	1869.683	1833.652	1834	1796.809	1809.202	1782.143	1811.161	1823.059
12	1634.224	1622.089	1623	1594.161	1592.234	1569	1600.097	1610.947
14	1456.077	1461.728	1462	1434.448	1421.736	1404	1436.782	1444.081
16	1316.091	1356.257	1356	1304.402	1299.643	1275.286	1318.318	1309.645
18	1202.886	1244.714	1244	1197.034	1186.367	1169.571	1208.337	1199.137
20	1109.251	1144.42	1144	1106.297	1099.537	1081	1115.051	1106.74
30	808.373	828.36	828	810.036	815.173	794.314	815.177	806.179
40	643.415	657.557	657.4	645.177	653.115	634.429	649.536	641.124
60	464.538	473.756	473.5	465.901	470.793	459.657	468.721	464.166
80	367.891	374.657	374.5	369.412	373.017	368.029	371.923	369.974
100	306.759	312.116	312	307.823	310.455	306.186	309.716	310.835
120	264.356	268.778	268.7	265.439	267.802	263.414	266.827	269.823
140	233.098	236.862	236.8	234.332	235.646	232	235.128	239.418
160	209.037	212.281	212.2	210.241	221.156	208.329	212.841	215.771
180	189.906	192.756	192.7	191.085	206.666	189.386	194.519	196.707
200	174.307	176.875	176.8	175.339	192.176	173.914	179.021	180.905
400	99.92	101.154	101.1	100.637	102.448	99.886	101.045	98.747
500	83.932	84.911	84.87	84.497	86.096	83.88	84.851	78.785
600	72.985	73.792	73.75	73.498	74.03	72.927	73.599	65.136
700	65.002	65.692	65.66	65.417	65.643	64.94	65.47	56.112
800	58.915	59.511	59.48	59.362	32.589	59.363	54.061	50.868
900	54.117	54.643	54.62	54.504	19.203	54.231	47.44	48.93
1000	50.235	50.719	50.69	50.556	18.931	50.437	44.267	50.015

Appendix

Mass stopping power for Lithium ions interacts with the Bone using (SRIM, CasP, PASS, SRIM dictionary) programs and Bethe formulae

E(MeV)	Mass Stopping power MeV/(g/cm^2) For Bone Tissue						
						Present Work	
	Bethe	SRIM	Dic.SRIM	PASS	CasP	Average S.P.	S.P.(P.W)
0.025	-----	446.462	406.1	896.756	61.635	449.882	497.293
0.03	-----	485.224	449.5	975.55	74.204	496.12	529.389
0.04	-----	557.572	528.3	1114.279	119.401	579.888	592.117
0.06	-----	686.544	664.9	1338.827	209.149	724.855	711.982
0.08	-----	800.057	783.1	1518.951	296.309	849.604	824.846
0.1	-----	901.62	887.8	1670.929	383.47	960.955	931.216
0.2	-----	1301.423	1295	2194.702	763.305	1388.608	1380.368
0.3	-----	1618.516	1615	2513.49	1088.632	1708.91	1721.486
0.4	-----	1890.045	1889	2725.093	1356.32	1965.115	1983.91
0.6	-----	2310.32	2311	2963.969	1731.494	2329.196	2346.419
0.8	-----	2593.496	2596	3058.291	1996.048	2560.959	2565.372
1	-----	2779.399	2782	3080.973	2164.926	2701.825	2702.482
1.1	-----	2844.824	2848	3076.323	2223.955	2748.276	2746.212
1.2	-----	2896.58	2900	3065.027	2264.586	2781.548	2778.604
1.3	-----	2935.53	2939	3048.68	2300.618	2805.957	2801.623
1.4	-----	2964.688	2968	3028.611	2336.651	2824.487	2816.892
1.5	-----	2984.288	2989	3006.04	2350.037	2832.341	2825.736
1.6	-----	2997.363	3002	2981.692	2363.423	2836.12	2829.235
1.7	-----	3004.24	3008	2955.934	2376.809	2836.246	2828.278
1.8	-----	3005.447	3010	2928.699	2383.918	2832.016	2823.6
2	-----	2994.853	2999	2872.797	2385.579	2813.057	2805.422
2.25	-----	2963.963	2969	2801.427	2373.538	2776.982	2770.705
2.5	-----	2919.26	2924	2730.436	2352.086	2731.446	2727.269
2.75	-----	2866.214	2871	2660.963	2330.634	2682.203	2678.462
3	-----	2807.256	2812	2593.615	2309.673	2630.636	2626.542
3.25	-----	2745.057	2750	2528.657	2288.835	2578.137	2573.044
3.5	-----	2681.808	2686	2466.088	2267.997	2525.473	2519.022
3.75	-----	2617.285	2622	2406.251	2247.158	2473.174	2465.201
4	-----	2553.781	2558	2349.386	2226.32	2421.872	2412.073
4.5	-----	2429.481	2434	2241.71	2173.445	2319.659	2309.122
5	2256.237	2311.395	2316	2143.604	2113.103	2221.026	2211.664
5.5	2132.368	2202.162	2206	2053.492	2052.762	2128.604	2120.215
6	2008.498	2100.643	2105	1970.399	1985.962	2040.501	2034.793
6.5	1911.565	2007.598	2011	1893.516	1917.547	1957.415	1955.168
7	1814.633	1922.443	1926	1822.451	1849.132	1880.007	1880.993
8	1658.406	1772.267	1776	1696.411	1708.388	1738.267	1747.42
9	1529.548	1645.371	1648	1586.01	1588.173	1616.888	1630.979
10	1421.245	1536.95	1540	1489.026	1480.319	1511.574	1528.907
12	1248.857	1362.647	1365	1328.488	1312.103	1342.059	1358.996
14	1117.28	1229.028	1231	1200.89	1178.701	1209.905	1223.705
16	1013.192	1133.503	1136	1096.278	1081.7	1111.87	1113.67
18	928.568	1040.047	1042	1009.373	991.455	1020.719	1022.53
20	858.265	960.19	962.1	935.553	921.482	944.831	945.852
40	504.203	562.863	564	554.402	556.316	559.395	553.043
60	366.181	408.821	409.6	403.265	404.138	406.456	401.273
80	291.059	324.903	325.6	321.156	321.777	323.359	320.189
100	243.321	271.577	272.1	268.446	268.721	270.211	269.327
120	210.099	234.437	234.9	232.018	232.217	233.393	234.168
140	185.547	207.005	207.5	205.197	204.79	206.123	208.218
160	166.609	185.83	186.2	184.375	192.338	187.186	188.139
180	151.526	168.958	169.4	167.785	179.886	171.507	172.04
200	139.209	155.208	155.6	154.126	167.435	158.092	158.768
300	100.656	112.142	112.4	111.597	113.035	112.293	115.662
400	80.235	89.336	89.53	88.995	90.071	89.483	90.913
500	67.499	75.117	75.28	74.845	75.821	75.266	74.342
600	58.763	65.364	65.51	65.183	65.281	65.334	62.507
700	52.384	58.248	58.37	58.073	57.986	58.169	53.917
800	47.515	52.814	52.93	52.74	33.665	48.037	47.824
900	43.674	48.527	48.64	48.458	23.396	42.255	43.811
1000	40.564	45.063	45.16	44.975	22.495	39.423	41.627

Appendix

Mass stopping power for Lithium ions interacts with the Skin using (SRIM, CasP, PASS,SRIM dictionary)programs and Bethe formulae

E(MeV)	Mass Stopping power MeV/(g/cm²) For Skin Tissue						
						Present Work	
	Bethe	SRIM	Dic.SRIM	PASS	CaSP	Average S.P.	S.P. (P.W)
0.025	-------	507.166	635.8	1220.098	90.008	607.211	645.679
0.03	-------	547.784	669.8	1342.871	115.878	669.083	688.07
0.04	-------	626.203	738.8	1528.453	177.715	767.793	770.886
0.06	-------	772.253	872.42	1825.271	301.403	942.837	928.997
0.08	-------	907.074	997.48	2059.703	425.146	1097.351	1077.697
0.1	-------	1033.624	1113.97	2255.098	548.889	1237.895	1217.669
0.2	-------	1588.679	1613.6	2918.352	1087.553	1802.046	1806.481
0.3	-------	2054.71	2050.94	3320.358	1516.322	2235.583	2250.456
0.4	-------	2446.607	2429.63	3586.171	1849.392	2577.95	2589.24
0.6	-------	3025.025	3001.85	3878.091	2300.741	3051.427	3050.89
0.8	-------	3383.145	3366.73	3981.266	2609.427	3335.142	3325.722
1	-------	3598.298	3589.745	3992.181	2805.268	3496.373	3485.473
1.1	-------	3668.64	3664.001	3977.614	2869.363	3544.904	3535.833
1.2	-------	3723.079	3719.369	3954.972	2913.7	3577.78	3571.434
1.3	-------	3760.58	3758.825	3926.291	2953.098	3599.698	3595.007
1.4	-------	3787.922	3784.353	3893.297	2992.496	3614.517	3608.728
1.5	-------	3802.808	3799.937	3857.552	3004.722	3616.255	3614.352
1.6	-------	3811.28	3806.569	3819.962	3016.948	3613.69	3613.302
1.7	-------	3813.033	3806.241	3780.984	3029.175	3607.358	3606.74
1.8	-------	3808.757	3798.946	3740.772	3033.453	3595.482	3595.623
2	-------	3785.15	3770.437	3659.48	3026.116	3560.296	3562.745
2.25	-------	3736.882	3714.918	3557.863	3001.335	3502.75	3507.524
2.5	-------	3673.712	3644.495	3458.458	2966.147	3435.703	3442.448
2.75	-------	3602.71	3566.143	3362.235	2930.96	3365.512	3371.701
3	-------	3525.166	3482.844	3269.737	2895.081	3293.207	3298.053
3.25	-------	3443.919	3396.589	3181.105	2859.029	3220.161	3223.352
3.5	-------	3361.551	3310.367	3096.177	2822.977	3147.768	3148.834
3.75	-------	3278.311	3224.172	3015.364	2786.925	3076.193	3075.323
4	-------	3195.849	3139	2938.922	2750.873	3006.161	3003.361
4.5	-------	3034.646	2974.709	2794.81	2682.902	2871.767	2865.337
5	3077.423	2881.469	2821.472	2664.347	2617.686	2746.243	2736.151
5.5	2896.97	2739.451	2680.276	2545.128	2552.47	2629.331	2616.088
6	2716.516	2607.95	2550.11	2435.689	2471.281	2516.258	2504.93
6.5	2577.61	2487.53	2431.967	2334.838	2386.098	2410.108	2402.37
7	2438.703	2377.486	2323.844	2241.981	2300.915	2311.057	2308.948
8	2217.523	2184.52	2135.64	2078.212	2120.562	2129.733	2129.302
9	2036.793	2022.434	1977.479	1935.618	1963.529	1974.765	1983.951
10	1886.032	1884.69	1843.348	1811.056	1822.073	1840.292	1855.578
12	1648.129	1665.442	1630.148	1606.449	1603.654	1626.423	1642.948
14	1468.2	1498.786	1468.002	1445.259	1432.128	1461.044	1474.843
16	1326.854	1400.004	1360.8903	1314.051	1309.004	1345.987	1338.919
18	1212.575	1288.616	1247.8019	1205.746	1194.755	1234.23	1226.864
20	1118.071	1184.371	1147.7302	1114.233	1107.131	1138.366	1132.954
40	648.159	679.948	658.9931	649.438	657.345	661.431	656.77
60	467.838	490.067	474.5729	468.856	473.763	476.815	474.741
80	370.442	387.704	375.3105	371.698	375.289	377.5	377.809
100	308.85	323.102	312.672	309.695	312.319	314.447	317.052
120	266.134	278.336	269.2458	267.032	269.39	271.001	275.034
140	234.649	245.368	237.2267	235.724	237.015	238.833	243.989
160	210.415	219.947	212.6122	211.479	222.437	216.619	219.935
180	191.148	199.767	193.0008	192.203	207.859	198.208	200.618
200	175.439	183.322	177.09156	176.359	193.282	182.514	184.668
300	126.412	132.013	127.46321	127.206	129.645	129.082	132.687
400	100.544	104.956	101.24856	101.201	103.009	102.604	102.807
500	84.45	88.13	84.97957	84.966	86.559	86.159	82.983
600	73.432	76.608	73.85346	73.903	74.414	74.694	69.145
700	65.397	68.208	65.73903	65.775	66.006	66.432	59.534
800	59.271	61.801	59.55567	59.685	32.759	53.45	53.268
900	54.442	56.753	54.68303	54.799	19.296	46.383	49.853
1000	50.536	52.683	50.7409	50.829	19.024	43.319	48.994

Appendix

Mass stopping power for **Carbon** ions interacts with the **adipose tissue** using (SRIM, CasP, PASS,SRIM dictionary ,MSTAR) programs and Bethe formulae

E(MeV)	Mass Stopping power MeV/(g/cm^2) For Adipose Tissue							
							Present Work	
	Bethe	SRIM	Dic.SRIM	PASS	CaSP	MSTAR	Average S.P.	S.P. (P.W)
0.025	-----	1306.603	1285	1540.104	86.915	1207.833	1126.479	1248.552
0.03	-----	1410.873	1390	1701.241	118.092	1317	1187.441	1301.808
0.04	-----	1581.594	1558	1957.72	197.945	1503.667	1359.785	1407.002
0.06	-----	1844.118	1815	2383.477	357.65	1821	1644.249	1612.251
0.08	-----	2055.316	2022	2740.128	508.195	2084.667	1882.061	1810.923
0.1	-----	2236.871	2202	3053.156	655.687	2322.667	2094.076	2003.334
0.2	-----	2904.907	2872	4273.664	1285.308	3322.333	2931.642	2883.996
0.3	-----	3447.39	3416	5196.32	1840.481	4127	3605.438	3601.92
0.4	-----	3937.407	3905	5955.887	2415.993	4800.333	4202.924	4263.542
0.6	-----	4783.474	4751	7149.869	3606.903	5916	5241.449	5322.993
0.8	-----	5512.4	5481	8024.841	4495.609	6796	6061.97	6138.88
1	-----	6159.501	6133	8665.286	5137.208	7502.333	6719.466	6777.83
1.1	-----	6457.849	6435	8913.368	5397.606	7799.333	7000.631	7045.334
1.2	-----	6740.296	6721	9123.477	5617.736	8066	7253.702	7283.983
1.3	-----	7005.687	6990	9303.31	5837.867	8274.667	7482.306	7497.273
1.4	-----	7256.268	7245	9459.87	5997.172	8483.333	7688.329	7688.175
1.5	-----	7490.32	7483	9583.701	6156.478	8692	7881.1	7859.229
1.6	-----	7708.809	7706	9690.568	6291.131	8832.667	8045.835	8012.621
1.7	-----	7912.049	7914	9782.255	6388.805	8973.333	8194.088	8150.241
1.8	-----	8101.211	8107	9852.678	6486.479	9114	8332.274	8273.729
2	-----	8436.468	8449	9962.115	6632.689	9294.667	8554.988	8483.865
2.25	-----	8782.336	8804	10043.369	6798.741	9464.5	8778.589	8689.107
2.5	-----	9058.433	9087	10080.836	6892.013	9568.333	8937.323	8843.474
2.75	-----	9274.633	9308	10087.333	6953.1	9618.833	9048.38	8957.491
3	-----	9440.795	9479	10072.22	7018.278	9628	9127.659	9039.166
3.25	-----	9565.223	9608	10039.701	7083.456	9603.833	9160.043	9094.689
3.5	-----	9656.694	9703	9993.479	7073.417	9560.333	9188.943	9128.905
3.75	-----	9721.543	9770	9940.947	7063.378	9498.25	9197.385	9135.056
4	-----	9763.98	9814	9881.424	7045.628	9427	9198.824	9145.656
4.5	-----	9795.455	9848	9749.766	6986.992	9264.5	9186.406	9148.021
5	-----	9775.898	9830	9607.864	6928.357	9082	9044.824	9057.035
5.5	-----	9718.101	9774	9461.531	6857.435	8888.333	8939.88	8972.071
6	-----	9633.847	9690	9314.138	6778.321	8690	8821.261	8871.297
6.5	-----	9531.315	9586	9167.357	6699.208	8492.5	8695.276	8759.763
7	-----	9411.992	9468	9021.672	6620.094	8307	8565.752	8641.109
8	-----	9148.609	9202	8739.422	6461.811	7974	8305.168	8392.352
9	-----	8865.391	8916	8469.125	6303.303	7679	8046.564	8138.927
10	-----	8576.039	8625	8211.672	6144.796	7416	7794.701	7888.445
12	-----	8011.929	8055	7733.517	5840.98	6950	7318.285	7410.918
14	-----	7489.426	7528	7306.828	5561.598	6565.333	6890.237	6973.804
16	8327.71	7016.263	7050	6919.506	5325.701	6213.667	6505.027	6578.627
18	7630.03	6591.121	6622	6568.889	5109.667	5895	6157.335	6222.646
20	7050.51	6210.677	6238	6251.405	4909.902	5623.667	6047.361	5901.862
40	4133.04	4046.457	4062	4194.232	3589.58	3833.333	3976.44	3909.668
60	2996.06	3011.797	3025	3147.212	2795.239	2900	2979.218	2955.847
80	2377.21	2418.098	2431	2528.242	2205.071	2342	2383.603	2396.434
100	1983.89	2026.376	2038	2116.268	1857.7	1968.667	1998.483	2026.534
120	1710.1	1744.894	1755	1826.352	1608.719	1702	1724.511	1762.093
140	1507.72	1533.418	1542	1607.733	1419.608	1515.333	1520.969	1562.417
160	1351.58	1367.415	1375	1440.816	1273.013	1356.667	1360.748	1405.433
180	1227.18	1235.011	1241	1308.34	1155.405	1226	1232.157	1278.141
200	1125.58	1126.549	1132	1199.507	1063.033	1130	1129.445	1172.388
300	807.27	796.654	798.6	858.909	798.193	808.5	811.355	826.581
400	638.4	633.631	635.9	680.78	657.015	642.3	648.004	631.286
500	532.88	527.747	529.7	568.351	515.837	535.567	535.014	506.967
600	460.38	455.23	456.8	491.293	446.059	461.8	461.926	425.89
700	407.33	402.151	403.6	434.237	394.132	409.167	408.436	375.856
800	366.76	361.696	363	390.833	347.187	368.367	366.307	350.66
900	334.68	329.652	330.9	356.751	320.169	335.9	334.675	346.811
1000	308.65	303.735	304.9	328.868	293.15	310	308.218	362.198

Appendix

Mass stopping power for Carbon ions interacts with the Blood using (SRIM, CasP, PASS,SRIM dictionary)programs and Bethe formulae

E(MeV)	Mass Stopping power MeV/(g/cm^2) For Blood Tissue						
						Present Work	
	Bethe	SRIM	Dic.SRIM	PASS	CasP	Average S.P.	S.P.(P.W)
0.025	------	860.96	865.3	1386.486	65.493	823.13	794.988
0.03	------	949.424	954.4	1540.191	94.65	884.666	896.932
0.04	------	1071.608	1077	1770.921	156.422	1018.988	1033.455
0.06	------	1243.601	1249	2153.568	279.964	1231.533	1232.644
0.08	------	1391.372	1397	2472.599	403.576	1416.137	1403.268
0.1	------	1531.327	1538	2751.693	527.211	1587.058	1562.347
0.2	------	2149.84	2158	3822.533	1082.965	2303.335	2275.747
0.3	------	2671.254	2682	4618.122	1590.026	2890.351	2899.589
0.4	------	3127.637	3139	5264.652	2112.844	3411.033	3453.66
0.6	------	3918.986	3933	6274.824	3205.86	4333.168	4392.06
0.8	------	4618.52	4634	7021.713	4094.974	5092.302	5150.209
1	------	5256.26	5274	7587.072	4775.622	5723.238	5768.454
1.1	------	5553.938	5574	7816.726	5054.558	5999.806	6034.59
1.2	------	5838.994	5860	8016.077	5292.57	6251.91	6276.1
1.3	------	6108.839	6131	8189.031	5530.582	6489.863	6495.511
1.4	------	6364.558	6388	8339.529	5705.335	6699.356	6695.036
1.5	------	6604.761	6630	8471.367	5880.088	6896.554	6876.612
1.6	------	6829.699	6857	8588.037	6035.114	7077.462	7041.948
1.7	------	7039.844	7068	8684.183	6160.55	7238.144	7192.554
1.8	------	7236.296	7265	8768.598	6285.986	7388.97	7329.77
2	------	7584.413	7616	8903.505	6460.511	7641.107	7568.673
2.25	------	7944.281	7979	9022.046	6632.355	7894.421	7810.691
2.5	------	8231.071	8267	9095.804	6748.707	8085.645	8001.263
2.75	------	8454.867	8492	9134.875	6837.897	8229.91	8150.027
3	------	8625.684	8665	9150.201	6923.485	8341.093	8264.543
3.25	------	8752.662	8794	9146.998	7009.074	8425.683	8350.813
3.5	------	8845.806	8888	9127.903	7027.319	8472.257	8413.65
3.75	------	8910.13	8953	9098.626	7045.564	8501.83	8456.951
4	------	8952.481	8996	9061.975	7049.308	8514.941	8483.895
4.5	------	8983.948	9028	8969.899	7013.296	8498.786	8498.728
5	------	8964.705	9008	8862.852	6977.284	8453.21	8474.18
5.5	------	8909.36	8954	8746.689	6921.595	8382.911	8421.469
6	------	8830.168	8875	8625.537	6852.788	8295.873	8348.601
6.5	------	8733.306	8777	8502.241	6783.981	8199.132	8261.377
7	------	8622.013	8666	8378.499	6715.173	8095.421	8164.054
8	------	8378.172	8420	8133.048	6575.583	7876.701	7950.955
9	------	8116.92	8157	7895.549	6428.092	7649.39	7726.222
10	------	7852.656	7891	7666.896	6280.6	7422.788	7499.473
12	------	7340.094	7375	7239.507	6009.676	6991.069	7059.513
14	------	6869.184	6901	6851.326	5755.744	6594.314	6651.614
16	7848.24	6445.824	6475	6499.011	5525.626	6236.365	6280.522
18	7200.84	6067.369	6094	6178.622	5327.06	5916.763	5945.2
20	6661.83	5729.584	5754	5888.328	5135.626	5626.885	5642.616
40	3930.55	3809.143	3822	3980.059	3830.838	3874.519	3766.101
60	2857.74	2883.385	2892	3004.647	2972.796	2922.113	2871.871
80	2271.61	2345.745	2353	2415.83	2348.24	2346.885	2347.161
100	1898.2	1982.518	1989	2026.441	1982.58	1975.748	1998.657
120	1637.84	1714.752	1720	1750.136	1720.645	1708.675	1747.77
140	1445.13	1507.243	1512	1542.425	1519.742	1505.308	1556.699
160	1296.3	1341.545	1345	1384.776	1362.135	1345.951	1405.044
180	1177.63	1207.08	1210	1256.638	1237.304	1217.73	1280.835
200	1080.63	1095.413	1098	1152.027	1139.314	1113.078	1176.591
300	776.32	761.504	763.4	828.394	857.727	797.468	826.651
400	614.56	613.285	614.8	655.782	706.901	641.065	621.488
500	513.37	511.123	512.4	548.05	556.074	528.203	488.899
600	443.77	441.12	442.2	473.879	481.173	456.428	403.796
700	392.82	389.854	390.8	419.025	425.254	403.55	355.167
800	353.82	350.752	351.6	377.86	374.699	361.747	337.42
900	322.98	319.794	320.6	344.616	345.599	330.718	347.411
1000	297.95	294.735	295.5	317.573	316.499	304.451	383.239

Appendix

Mass stopping power for **Carbon** ions interacts with the **Brain using** (SRIM, CasP, PASS) programs and Bethe formulae

E(MeV)	Mass Stopping power MeV/(g/cm^2) Brain Tissue				Present work	
	Bethe	SRIM	PASS	CasP	Average S.P.	S.P.(P.W)
0.025	------	897.734	1498.765	75.789	820.578	908.777
0.03	------	987.976	1577.588	99.524	888.363	956.573
0.04	------	1113.87	1814.267	164.189	1030.775	1051.034
0.06	------	1292.258	2205.83	293.518	1263.869	1235.548
0.08	------	1444.906	2532.342	421.22	1466.156	1414.389
0.1	------	1588.6	2817.622	548.379	1651.534	1587.791
0.2	------	2216.55	3916.648	1115.579	2416.259	2380.573
0.3	------	2744.363	4732.835	1630.627	3035.942	3066.116
0.4	------	3206.645	5397.314	2162.533	3588.831	3662.79
0.6	------	4007.126	6436.948	3271.754	4571.943	4644.032
0.8	------	4713.559	7207.459	4166.99	5362.669	5406.022
1	------	5356.948	7787.994	4849.552	5998.165	5946.141
1.1	------	5657.257	8020.332	5129.024	6268.871	6339.834
1.2	------	5944.764	8221.843	5367.29	6511.299	6536.449
1.3	------	6216.911	8398.442	5605.556	6740.303	6735.831
1.4	------	6474.862	8555.709	5780.653	6937.075	6918.881
1.5	------	6717.114	8685.196	5955.75	7119.353	7085.032
1.6	------	6944.018	8799.798	6110.54	7284.785	7235.439
1.7	------	7155.98	8901.08	6234.868	7430.643	7371.489
1.8	------	7354.134	8982.982	6359.197	7565.437	7494.521
2	------	7705.335	9117.435	6533.097	7785.289	7706.303
2.25	------	8068.516	9231.829	6705	8001.782	7917.084
2.5	------	8358.097	9301.925	6819.816	8159.946	8079.622
2.75	------	8584.253	9339.256	6906.839	8276.783	8203.58
3	------	8757.089	9352.81	6990.549	8366.816	8296.383
3.25	------	8885.759	9346.457	7074.259	8435.492	8363.811
3.5	------	8980.314	9323.55	7090.722	8464.862	8410.423
3.75	------	9045.894	9292.704	7107.184	8481.927	8439.851
4	------	9089.226	9252.878	7109.266	8483.79	8455.021
4.5	------	9122.033	9155.77	7070.286	8449.363	8451.66
5	------	9103.448	9042.917	7031.307	8392.557	8414.704
5.5	------	9048.051	8921.435	6973.327	8314.271	8354.031
6	------	8968.246	8795.792	6902.679	8222.239	8276.591
6.5	------	8870.406	8668.48	6832.032	8123.639	8187.365
7	------	8757.635	8540.584	6761.385	8019.868	8089.978
8	------	8510.098	8288.363	6618.335	7805.599	7880.709
9	------	8244.436	8043.947	6468.263	7585.549	7662.971
10	------	7975.284	7809.148	6318.191	7367.541	7444.756
12	------	7452.69	7369.379	6041.98	6954.683	7023
14	------	6972.116	6973.788	5783.758	6576.554	6632.146
16	7924.595	6539.788	6613.05	5550.697	6234.512	6275.789
18	7269.719	6153.234	6285.309	5349.238	5929.26	5952.75
20	6724.635	5808.228	5987.662	5155.444	5650.445	5660.208
40	3964.674	3849.866	4043.016	3839.406	3910.763	3818.016
60	2881.569	2908.595	3043.747	2979.357	2977.233	2921.297
80	2290.076	2363.663	2449.892	2352.708	2388.754	2389.794
100	1913.353	1996.418	2053.41	1985.906	2011.911	2035.117
120	1650.731	1726.195	1773.726	1723.192	1741.037	1779.33
140	1456.379	1517.168	1562.484	1521.823	1533.825	1584.519
160	1306.294	1350.393	1400.996	1363.967	1371.785	1430.052
180	1186.637	1215.163	1272.709	1238.869	1242.247	1303.751
200	1088.841	1102.934	1167.246	1140.671	1136.95	1197.966
300	782.065	767.133	836.78	858.568	820.827	845.016
400	619.035	617.444	663.712	707.496	662.884	639.879
500	517.064	514.549	554.393	556.424	541.789	507.486
600	446.936	444.051	479.42	481.439	468.303	421.615
700	395.599	392.427	423.884	425.476	413.929	370.719
800	356.315	353.053	381.619	374.881	369.851	348.922
900	325.244	321.879	348.42	345.765	338.688	352.919
1000	300.027	296.648	321.253	316.648	311.516	380.706

Appendix

Mass stopping power for **Carbon ions** interacts with the **Breast** using (SRIM, CasP, PASS) programs and Bethe formulae

E(MeV)	Mass Stopping power MeV/(g/cm^2) Breast Tissue					
					Present work	
	Bethe	SRIM	PASS	CasP	Average S.P.	S.P.(P.W)
0.025	-------	1033.078	1480.671	69.977	780.525	777.929
0.03	-------	1127.524	1607.2	87.993	940.906	947.425
0.04	-------	1268.623	1848.783	151.399	1089.601	1109.431
0.06	-------	1476.119	2248.974	278.211	1334.435	1327.925
0.08	-------	1648.647	2583.256	403.101	1545.002	1516.794
0.1	-------	1804.664	2875.825	526.07	1735.52	1694.162
0.2	-------	2440.619	4008.088	1077.922	2508.876	2487.856
0.3	-------	2968.13	4854.789	1576.508	3133.142	3169.63
0.4	-------	3435.773	5547.302	2060.571	3681.216	3763.15
0.6	-------	4245.3	6633.707	3130.95	4669.986	4741.688
0.8	-------	4953.499	7436.65	4012.349	5467.499	5507.569
1	-------	5592.406	8035.991	4666.561	6098.319	6115.597
1.1	-------	5889.223	8273.259	4974.893	6379.125	6372.672
1.2	-------	6172.197	8477.397	5207.861	6619.152	6603.466
1.3	-------	6439.324	8654.89	5421.987	6838.734	6811.035
1.4	-------	6692.139	8811.773	5636.113	7046.675	6997.992
1.5	-------	6929.134	8939.272	5792.351	7220.252	7166.588
1.6	-------	7150.82	9051.207	5948.588	7383.538	7318.769
1.7	-------	7357.599	9149.216	6094.816	7533.877	7456.226
1.8	-------	7550.602	9227.236	6201.006	7659.615	7580.437
2	-------	7892.699	9353.27	6399.845	7881.938	7794.149
2.25	-------	8246.133	9456.58	6579.306	8094.006	8006.821
2.5	-------	8528.036	9515.833	6725.699	8256.523	8170.85
2.75	-------	8748.35	9542.988	6804.968	8365.435	8295.982
3	-------	8916.971	9547.15	6877.85	8447.324	8389.693
3.25	-------	9042.69	9532.301	6950.595	8508.529	8457.8
3.5	-------	9134.99	9501.909	7023.34	8553.413	8504.891
3.75	-------	9199.391	9464.153	7029.484	8564.343	8534.623
4	-------	9241.699	9418.119	7035.627	8565.148	8546.498
4.5	-------	9273.149	9310.291	7015.796	8533.079	8549.943
5	-------	9253.908	9188.628	6974.552	8472.362	8509.048
5.5	-------	9197.866	9059.772	6933.308	8396.982	8447.572
6	-------	9117.047	8927.799	6871.17	8305.339	8369.096
6.5	-------	9018.391	8794.914	6803.81	8205.705	8278.663
7	-------	8904.467	8661.997	6736.449	8100.971	8179.942
8	-------	8654.07	8401.503	6601.728	7885.767	7967.763
9	-------	8385.391	8150.087	6463.533	7666.337	7746.952
10	-------	8112.495	7909.251	6323.022	7448.256	7525.622
12	-------	7582.006	7459.402	6051.233	7030.881	7097.782
14	-------	7092.898	7055.736	5793.293	6647.309	6701.243
16	8022.536	6651.769	6688.117	5566.157	6302.014	6339.687
18	7356.655	6256.525	6354.463	5364.436	5991.808	6011.932
20	6802.779	5903.325	6051.692	5176.395	5710.471	5715.125
40	4003.461	3894.007	4078.01	3884.242	3964.93	3846.585
60	2907.345	2928.306	3066.604	3035.652	2984.477	2937.74
80	2309.379	2369.877	2466.546	2443.191	2397.248	2399.524
100	1928.786	1996.153	2066.347	2058.803	2012.522	2040.713
120	1663.592	1723.467	1784.288	1773.538	1736.221	1782.214
140	1467.407	1514.758	1571.38	1558.932	1528.119	1585.551
160	1315.95	1349.243	1408.699	1409.547	1370.86	1429.793
180	1195.228	1215.846	1279.512	1281.926	1243.128	1302.582
200	1096.582	1105.672	1173.338	1174.208	1137.45	1196.159
300	787.263	774.111	840.81	864.759	816.736	842.182
400	622.968	620.361	666.755	728.41	659.623	637.544
500	520.241	516.894	556.842	592.06	546.509	506.101
600	449.61	446.009	481.478	490.087	466.796	421.261
700	397.915	394.109	425.659	439.678	414.34	371.313
800	358.364	354.534	383.185	389.269	371.338	350.298
900	327.084	323.196	349.825	353.367	338.368	354.863
1000	301.701	297.838	322.528	327.137	312.301	382.978

Appendix

Mass stopping power for Carbon ions interacts with the Lung using (SRIM, CasP, PASS) programs and Bethe formulae

E(MeV)	Mass Stopping power MeV/(g/cm²) Lung Tissue					
					Present work	
	Bethe	SRIM	PASS	CasP	Average S.P.	S.P.(P.W)
0.025	---------	860.04	1349.512	70.976	759.68	844.232
0.03	---------	948.632	1556.556	95.401	866.863	891.258
0.04	---------	1070.686	1790.006	157.516	1006.069	984.213
0.06	---------	1242.255	2176.127	281.746	1233.376	1165.844
0.08	---------	1389.851	2497.985	405.81	1431.216	1341.965
0.1	---------	1529.861	2779.097	529.819	1612.926	1512.801
0.2	---------	2150.078	3860.997	1086.874	2365.983	2294.774
0.3	---------	2673.028	4663.327	1594.946	2977.1	2972.285
0.4	---------	3130.43	5316.064	2119.003	3521.832	3563.109
0.6	---------	3923.211	6337.615	3214.078	4491.635	4537.888
0.8	---------	4623.991	7096.439	4104.838	5275.089	5301.115
1	---------	5263.004	7670.352	4786.768	5906.708	5907.241
1.1	---------	5561.338	7900.897	5066.236	6176.157	6163.6
1.2	---------	5847.069	8101.342	5304.706	6417.705	6393.816
1.3	---------	6117.586	8277.417	5543.176	6646.06	6600.933
1.4	---------	6373.971	8434.555	5718.431	6842.319	6787.555
1.5	---------	6614.812	8564.411	5893.686	7024.303	6955.921
1.6	---------	6840.375	8679.591	6049.171	7189.712	7107.967
1.7	---------	7051.113	8781.638	6175.001	7335.917	7245.378
1.8	---------	7248.14	8864.501	6300.83	7471.157	7369.623
2	---------	7597.285	9001.106	6475.907	7691.433	7583.607
2.25	---------	7958.255	9118.442	6647.928	7908.208	7796.936
2.5	---------	8245.942	9191.513	6764.449	8067.301	7961.871
2.75	---------	8470.46	9231.73	6853.859	8185.35	8088.054
3	---------	8641.85	9248.032	6939.621	8276.501	8182.835
3.25	---------	8769.274	9244.259	7025.382	8346.305	8251.839
3.5	---------	8862.778	9223.727	7043.653	8376.719	8299.269
3.75	---------	8927.375	9195.137	7061.923	8394.812	8327.673
4	---------	8969.943	9157.419	7065.638	8397.666	8334.056
4.5	---------	9001.702	9064.152	7029.398	8365.084	8373.308
5	---------	8982.593	8954.702	6993.159	8310.152	8329.455
5.5	---------	8927.258	8836.269	6937.254	8233.594	8270.224
6	---------	8847.999	8713.401	6868.238	8143.212	8195.297
6.5	---------	8750.993	8588.649	6799.221	8046.288	8108.794
7	---------	8639.485	8463.155	6730.205	7944.282	8014.113
8	---------	8395.109	8215.159	6590.206	7733.491	7809.955
9	---------	8133.197	7974.497	6442.34	7516.678	7596.834
10	---------	7868.224	7743.061	6294.473	7301.92	7382.757
12	---------	7354.211	7309.121	6023.03	6895.454	6968.057
14	---------	6881.95	6918.335	5768.52	6522.935	6582.961
16	7921.233	6457.38	6561.729	5537.74	6185.616	6231.379
18	7267.153	6077.872	6237.555	5338.819	5884.749	5912.36
20	6722.665	5739.17	5943.006	5146.947	5609.708	5623.244
30	4951.072	4623.72	4798.756	4423.151	4615.209	4523.355
40	3964.807	3814.341	4016.009	3839.399	3889.916	3799.261
60	2882.095	2887.002	3024.399	2979.158	2963.52	2909.85
80	2290.704	2348.738	2434.72	2353.139	2378.866	2382.298
100	1914.001	1985.113	2040.904	1986.7	2004.239	2030.111
120	1651.371	1717.016	1763.043	1724.217	1734.759	1776.051
140	1457	1509.196	1553.154	1522.881	1528.41	1582.518
160	1306.893	1343.22	1392.688	1364.922	1366.943	1429.043
180	1187.213	1208.503	1265.205	1239.839	1237.849	1303.542
200	1089.395	1096.613	1160.398	1141.646	1132.886	1198.421
400	619.433	613.91	659.95	708.346	660.735	643.983
500	517.416	511.642	551.285	557.203	540.043	512.71
600	447.253	441.566	476.757	482.148	466.824	427.828
700	395.888	390.248	421.547	426.115	412.637	377.865
800	356.583	351.106	379.528	375.457	368.697	356.984
900	325.493	320.116	346.521	346.298	337.645	361.897
1000	300.262	295.032	319.51	317.14	310.56	390.616

Appendix

Mass stopping power for Carbon ions interacts with the Muscle using (SRIM, CasP, PASS,SRIM dictionary ,MSTAR) programs and Bethe formulae

E(MeV)	Mass Stopping power MeV/(g/cm^2) For Muscle tissue							
							Present Work	
	Bethe	SRIM	Dic.SRIM	PASS	CasP	MSTAR	Average S.P.	S.P. (P.W)
0.025	------	885.851	904.1	1403.976	71.987	842.083	809.407	983.549
0.03	------	975.068	994	1559.226	95.492	927	910.157	1025.213
0.04	------	1100.168	1121	1793.185	158.025	1073.333	1049.142	1107.811
0.06	------	1277.736	1303	2180.263	283.092	1325	1273.818	1270.13
0.08	------	1429.283	1457	2503.044	407.859	1537.333	1466.904	1428.702
0.1	------	1571.605	1601	2785.07	532.526	1730	1644.04	1583.63
0.2	------	2192.361	2222	3871.575	1091.393	2549.667	2385.399	2306.964
0.3	------	2714.56	2744	4678.53	1600.459	3223	2992.11	2952.754
0.4	------	3172.647	3202	5335.694	2125.464	3799	3526.961	3530.545
0.6	------	3966.444	3997	6364.832	3222.43	4781	4466.341	4513.561
0.8	------	4666.324	4696	7128.969	4110.221	5591.667	5238.636	5308.392
1	------	5302.873	5331	7705.875	4787.348	6273	5880.019	5954.213
1.1	------	5599.667	5627	7937.134	5064.693	6572.667	6160.232	6230.836
1.2	------	5883.628	5909	8137.884	5301.225	6847	6415.748	6480.785
1.3	------	6152.289	6176	8313.959	5537.758	7074.667	6650.934	6706.73
1.4	------	6406.808	6429	8470.871	5711.269	7302.333	6864.056	6911.03
1.5	------	6645.796	6667	8600.221	5884.78	7530	7065.559	7095.777
1.6	------	6869.543	6890	8714.779	6038.331	7699.333	7242.397	7262.826
1.7	------	7078.513	7098	8816.101	6161.942	7868.667	7404.645	7413.829
1.8	------	7273.817	7291	8898.142	6285.554	8038	7557.302	7550.262
2	------	7619.9	7635	9033.007	6458.137	8281.333	7805.475	7784.559
2.25	------	7977.606	7991	9148.118	6629.507	8528	8054.846	8016.26
2.5	------	8262.697	8273	9219.062	6744.447	8706.667	8241.175	8192.815
2.75	------	8485.199	8494	9257.321	6830.983	8829.167	8379.334	8325.044
3	------	8655.085	8663	9271.845	6913.746	8905	8481.735	8421.43
3.25	------	8781.407	8789	9266.492	6996.509	8920	8550.682	8488.687
3.5	------	8874.06	8881	9244.596	7014.58	8893.667	8581.581	8532.173
3.75	------	8938.123	8945	9214.763	7032.65	8835.5	8588.261	8556.193
4	------	8980.266	8986	9175.949	7036.091	8763	8593.207	8543.192
4.5	------	9011.499	9016	9080.837	6999.081	8597	8540.883	8564.232
5	------	8992.198	8996	8969.927	6962.071	8414.667	8466.973	8486.152
5.5	------	8936.825	8942	8850.319	6905.815	8230.333	8373.059	8404.76
6	------	8857.551	8862	8726.479	6836.73	8052	8266.952	8307.079
6.5	------	8760.651	8765	8600.9	6767.645	7885.333	8155.906	8198.754
7	------	8649.256	8655	8474.682	6698.559	7726.667	8040.833	8083.783
8	------	8405.101	8409	8225.564	6558.499	7432.667	7806.166	7844.468
9	------	8143.477	8148	7984	6410.879	7167	7570.671	7603.494
10	------	7878.677	7883	7751.823	6263.259	6928.333	7341.018	7368.164
12	------	7364.873	7370	7316.712	5990.99	6506	6909.715	6926.752
14	------	6892.514	6898	6925.042	5735.886	6152.667	6520.822	6529.824
16	7864.94	6467.587	6472	6567.706	5505.935	5829.333	6168.512	6175.618
18	7215.69	6087.545	6092	6242.92	5306.681	5536	5853.029	5859.357
20	6675.21	5748.241	5753	5947.85	5115.137	5284	5569.646	5575.919
40	3937.29	3817.529	3819	4018.047	3811.47	3620.667	3817.342	3805.149
60	2862.25	2886.963	2886	3025.374	2958.567	2749	2901.181	2913.09
80	2275	2346.744	2345	2435.216	2336.979	2225.667	2337.921	2363.615
100	1900.93	1982.294	1980	2041.147	1972.901	1873.667	1970.002	1988.455
120	1640.12	1714.064	1712	1763.151	1712.074	1622	1704.658	1715.716
140	1447.09	1506.608	1504	1553.181	1512.12	1445.333	1504.248	1508.795
160	1298.02	1341.14	1339	1392.667	1355.356	1295	1344.633	1346.85
180	1179.17	1207.014	1205	1265.155	1231.114	1171	1215.857	1217.054
200	1082.02	1095.732	1095	1160.329	1133.57	1079.667	1112.86	1111.044
300	777.25	762.694	763.1	831.869	853.3	774.2	797.033	786.144
400	615.27	613.823	613.7	659.851	703.217	615.833	641.285	625.641
500	513.95	511.558	511.5	551.191	553.133	513.833	528.243	531.997
600	444.26	441.485	441.3	476.667	478.615	443.4	456.293	468.851
700	393.24	390.17	390.1	421.461	422.99	393.067	403.558	419.512
800	354.2	351.031	350.9	379.447	372.701	354	361.616	375.235
900	323.32	320.043	320	346.444	343.755	322.9	330.628	330.993
1000	298.26	294.96	294.9	319.436	314.809	298.1	304.441	283.687

Appendix

Mass stopping power for Carbon ions interacts with the Bone using (SRIM, CasP, PASS, SRIM dictionary) programs and Bethe formulae

E(MeV)	Mass Stopping power MeV/(g/cm^2) For Bone Tissue					Present Work	
	Bethe	SRIM	Dic.SRIM	PASS	CasP	Average S.P.	S.P. (P.W)
0.025	------	701.033	701.9	1097.274	57.85	628.483	741.22
0.03	------	771.094	772.2	1208.181	69.451	705.231	777.288
0.04	------	883.471	884.8	1390.671	107.051	816.498	848.639
0.06	------	1064.315	1066	1694.67	182.251	1001.809	988.271
0.08	------	1214.661	1217	1950.025	266.409	1162.024	1123.935
0.1	------	1348.814	1351	2174.316	353.552	1306.92	1255.778
0.2	------	1901.916	1906	3044.102	748.861	1900.22	1862.335
0.3	------	2364.187	2369	3689.547	1154.618	2394.338	2391.751
0.4	------	2770.225	2776	4211.846	1587.913	2836.496	2856.158
0.6	------	3455.418	3462	5023.093	2442.184	3595.674	3627.243
0.8	------	4022.881	4031	5623.722	3144.61	4205.553	4234.357
1	------	4506.532	4515	6079.829	3672.53	4693.473	4717.819
1.1	------	4722.042	4731	6263.968	3889.908	4901.729	4922.434
1.2	------	4922.704	4932	6424.613	4076.232	5088.887	5106.155
1.3	------	5108.442	5118	6566.223	4262.556	5263.805	5271.354
1.4	------	5280.825	5291	6693.036	4394.728	5414.897	5420.079
1.5	------	5440.475	5451	6798.522	4526.9	5554.224	5554.1
1.6	------	5587.267	5598	6892.525	4644.195	5680.496	5674.96
1.7	------	5722.963	5734	6976.252	4739.174	5793.097	5784.006
1.8	------	5848.002	5859	7044.955	4834.154	5896.528	5882.42
2	------	6067.163	6079	7159.508	4971.811	6069.371	6051.39
2.25	------	6289.549	6302	7260.643	5119.31	6242.876	6218.936
2.5	------	6464.211	6477	7326.713	5221.425	6372.337	6347.589
2.75	------	6598.652	6611	7366.511	5294.329	6467.623	6445.272
3	------	6699.785	6712	7386.979	5361.724	6540.122	6518.068
3.25	------	6773.457	6786	7391.044	5429.119	6594.905	6570.713
3.5	------	6825.653	6839	7381.21	5450.508	6624.093	6606.93
3.75	------	6860.119	6873	7364.619	5471.897	6642.409	6629.68
4	------	6880.769	6894	7340.333	5483.956	6649.764	6638.724
4.5	------	6888.766	6902	7276.455	5480.082	6636.825	6641.341
5	------	6865.571	6879	7198.421	5476.208	6604.8	6610.612
5.5	------	6820.641	6834	7112.251	5452.476	6554.842	6564.839
6	------	6761.346	6774	7021.792	5415.507	6493.161	6506.837
6.5	------	6691.549	6704	6929.252	5378.538	6425.835	6440.437
7	------	6613.973	6627	6835.678	5341.568	6354.555	6368.381
8	------	6446.773	6459	6649.297	5263.499	6204.642	6214.69
9	------	6271.089	6283	6467.299	5168.909	6047.574	6056.034
10	------	6094.549	6107	6291.435	5074.319	5891.826	5897.958
12	------	5753.037	5765	5959.8	4883.098	5590.234	5594.069
14	------	5437.025	5448	5658.873	4694.432	5309.583	5313.208
16	5965.72	5149.81	5160	5382.693	4519.578	5053.02	5056.802
18	5493.1	4889.141	4900	5130.27	4360.862	4820.068	4823.406
20	5097.13	4653.299	4663	4899.758	4211.049	4606.776	4610.748
40	3056.11	3180.123	3187	3365.313	3162.928	3223.841	3214.833
60	2238.12	2427.616	2433	2557.642	2482.508	2475.191	2477.767
80	1786.98	1975.365	1980	2071.201	1978.054	2001.155	2017.981
100	1497.87	1669.596	1673	1743.781	1677.171	1690.887	1703.134
120	1295.45	1446.902	1450	1511.476	1460.6	1467.244	1474.227
140	1145.16	1276.9	1280	1335.293	1293.899	1296.523	1300.648
160	1028.79	1142.767	1145	1200.129	1162.702	1162.65	1164.831
180	935.82	1034.712	1037	1092.445	1058.357	1055.628	1055.942
200	859.69	945.422	947.6	1003.728	975.695	968.111	966.921
300	620.01	672.351	673.9	724.404	737.813	702.117	692.354
400	492.03	539.352	540.6	577.144	609.522	566.655	553.9
500	411.74	450.473	451.5	483.706	481.232	466.728	471.038
600	356.4	389.379	390.3	419.395	417.192	404.066	414.138
700	315.82	344.568	345.4	371.623	369.215	357.702	369.731
800	284.72	310.313	311	335.179	325.813	320.576	330.805
900	260.1	283.161	283.8	306.493	300.714	293.542	293.355
1000	240.1	261.157	261.8	282.978	275.615	270.388	254.921

Appendix

Mass stopping power for Carbon ions interacts with the Skin using (SRIM, CasP, PASS,SRIM dictionary)programs and Bethe formulae

E(MeV)	Mass Stopping power MeV/(g/cm²) For Skin Tissue						
						Present Work	
	Bethe	SRIM	Dic.SRIM	PASS	CasP	Average S.P.	S.P.(P.W)
0.025	------	926.423	960.7	1378.909	70.976	838.506	979.379
0.03	------	1016.764	1052	1562.297	95.146	931.551	1022.561
0.04	------	1146.395	1186	1796.881	158.183	1071.865	1108.045
0.06	------	1333.069	1380	2185.172	284.259	1295.625	1275.571
0.08	------	1490.841	1543	2509.164	409.976	1488.245	1438.643
0.1	------	1636.849	1692	2792.419	535.573	1664.21	1597.42
0.2	------	2257.73	2315	3885.411	1096.831	2388.743	2332.022
0.3	------	2777.161	2835	4699.171	1606.991	2979.581	2981.157
0.4	------	3234.591	3294	5363.013	2132.919	3506.131	3536.706
0.6	------	4027.7	4089	6403.887	3231.991	4438.144	4504.717
0.8	------	4725.608	4787	7176.414	4114.31	5200.833	5271.791
1	------	5358.626	5419	7758.125	4783.26	5829.753	5890.893
1.1	------	5653.32	5714	7990.558	5057.06	6103.735	6155.586
1.2	------	5934.857	5993	8191.831	5290.411	6352.525	6394.808
1.3	------	6200.967	6259	8367.937	5523.761	6587.916	6611.309
1.4	------	6452.918	6509	8524.521	5694.352	6795.198	6807.472
1.5	------	6689.346	6745	8653.092	5864.944	6988.095	6985.373
1.6	------	6910.577	6965	8766.684	6015.275	7164.384	7146.825
1.7	------	7117.082	7171	8866.873	6135.217	7322.543	7293.425
1.8	------	7309.961	7362	8947.622	6255.159	7468.685	7426.576
2	------	7651.741	7702	9079.744	6423.654	7714.285	7657.369
2.25	------	8004.844	8054	9191.342	6593.977	7961.041	7889.621
2.5	------	8286.254	8333	9258.924	6706.421	8146.15	8071.11
2.75	------	8505.904	8551	9294.088	6790.965	8285.489	8211.61
3	------	8673.646	8718	9305.808	6873.252	8392.676	8318.718
3.25	------	8798.4	8843	9297.972	6955.539	8473.728	8398.415
3.5	------	8889.83	8935	9273.942	6969.324	8517.024	8455.467
3.75	------	8953.121	8998	9242.172	6983.109	8544.1	8493.711
4	------	8994.627	9039	9201.657	6983.748	8554.758	8516.259
4.5	------	9025.017	9069	9103.713	6945.589	8535.83	8524.017
5	------	9005.33	9049	8990.595	6907.43	8488.089	8494.284
5.5	------	8949.765	8994	8869.237	6850.651	8415.913	8437.863
6	------	8870.316	8915	8743.97	6781.46	8327.687	8362.424
6.5	------	8773.414	8817	8617.194	6712.269	8229.969	8273.503
7	------	8662.028	8706	8489.942	6643.077	8125.262	8175.15
8	------	8417.877	8461	8239.252	6502.932	7905.265	7961.372
9	------	8156.399	8198	7996.447	6355.736	7676.646	7737.096
10	------	7891.601	7932	7763.262	6208.54	7448.851	7511.393
12	------	7377.735	7416	7326.578	5935.73	7014.011	7074.114
14	------	6904.981	6940	6933.718	5680.522	6614.805	6668.77
16	7876	6479.364	6512	6575.394	5452.422	6254.795	6299.709
18	7225.13	6098.434	6128	6249.772	5252.832	5932.259	5965.83
20	6683.38	5758.181	5786	5953.985	5062.133	5640.075	5664.157
40	3940.32	3820.299	3833	4020.215	3765.552	3859.766	3783.334
60	2863.85	2885.394	2891	3026.033	2924.553	2931.745	2881.175
80	2275.99	2342.412	2345	2435.226	2310.249	2358.222	2350.85
100	1901.58	1976.863	1977	2040.84	1950.065	1986.192	1998.81
120	1640.57	1708.584	1708	1762.695	1691.972	1717.813	1745.848
140	1447.42	1501.85	1501	1552.652	1494.307	1512.452	1553.702
160	1298.25	1337.318	1337	1392.109	1339.529	1351.489	1401.662
180	1179.33	1204.235	1204	1264.59	1216.682	1222.377	1277.545
200	1082.14	1094.004	1095	1159.769	1120.206	1117.245	1173.724
300	777.25	763.408	765.3	831.376	843.057	800.785	828.125
400	615.22	613.465	614.3	659.422	694.725	645.478	627.659
500	513.88	511.241	512	550.811	546.394	530.111	498.257
600	444.18	441.195	441.8	476.325	472.769	458.022	414.13
700	393.16	389.902	390.4	421.149	417.821	404.818	363.947
800	354.12	350.782	351.2	379.159	368.143	362.321	341.947
900	323.24	319.808	320.3	346.176	339.544	331.457	344.892
1000	298.18	294.738	295.1	319.184	310.945	304.992	370.822

Appendix

Mass stopping power for Oxygen ions interacts with the adipose tissue using (SRIM, CasP, PASS,SRIM dictionary ,MSTAR) programs and Bethe formul

E(MeV)	Mass Stopping power MeV/(g/cm²) For Adipose Tissue							
							Present Work	
	Bethe	SRIM	Dic.SRIM	PASS	CasP	MSTAR	Average S.P.	S.P.(P.W)
0.025	-------	1331.937	1313	1583.924	61.794	1105.031	1102.244	1321.365
0.03	-------	1458.976	1439	1684.242	87.324	1247.667	1183.442	1364.554
0.04	-------	1602.395	1583	1941.038	142.452	1431	1339.977	1450.388
0.06	-------	1840.434	1817	2371.916	258.13	1732.333	1603.963	1619.917
0.08	-------	2055.432	2027	2734.868	373.808	1987.222	1835.666	1786.643
0.1	-------	2245.5	2214	3054.857	514.147	2211.667	2048.034	1950.626
0.2	-------	2929.464	2897	4321.32	1206.932	3136.556	2898.254	2731.363
0.3	-------	3423.406	3396	5310.164	1745.743	3922.667	3559.596	3451.583
0.4	-------	3893.459	3868	6152.619	2214.904	4617.556	4149.308	4117.143
0.6	-------	4804.733	4778	7573.154	3045.955	5816.667	5203.702	5304.251
0.8	-------	5669.679	5642	8743.427	3889.575	6852.556	6159.447	6327.047
1	-------	6487.649	6463	9714.072	4787.982	7759.778	7042.496	7212.61
1.1	-------	6880.475	6857	10137.734	5188.25	8172.889	7447.27	7610.861
1.2	-------	7262.107	7242	10523.393	5575.007	8561	7832.701	7982.561
1.3	-------	7632.14	7615	10874.19	5961.764	8926.778	8201.974	8329.772
1.4	-------	7990.974	7978	11193.863	6315.375	9271.222	8549.887	8654.357
1.5	-------	8337.926	8328	11486.603	6619.269	9594.333	8873.226	8958.005
1.6	-------	8671.834	8667	11749.858	6923.163	9898.222	9182.016	9242.246
1.7	-------	8992.418	8994	11985.449	7227.057	10182	9476.185	9508.473
1.8	-------	9300.361	9307	12204.396	7456.716	10450	9743.695	9757.958
2	-------	9878.723	9896	12575.666	7916.032	10894.444	10232.173	10211.238
2.25	-------	10526.586	10560	12948.925	8395.491	11450	10776.2	10702.34
2.5	-------	11093.426	11140	13240.383	8827.298	11850	11230.221	11121.719
2.75	-------	11585.631	11640	13463.936	9215.448	12226.667	11626.336	11480.12
3	-------	12007.935	12080	13632.453	9518.728	12510	11949.823	11786.393
3.25	-------	12366.809	12440	13757.575	9790.927	12755.556	12222.173	12047.888
3.5	-------	12670.347	12760	13849.037	10024.088	12944.444	12449.583	12270.776
3.75	-------	12925.691	13020	13914.739	10213.417	13090	12632.769	12460.321
4	-------	13140.537	13240	13960.821	10402.747	13206.667	12790.154	12621.193
4.5	-------	13456.93	13570	13996.747	10704.047	13350	13015.545	12887.922
5	-------	13673.24	13790	13986.484	10927.988	13390	13153.542	13022.432
5.5	-------	13804.356	13930	13943.152	11039.96	13377.778	13219.049	13131.345
6	-------	13870.766	14000	13876.597	11123.94	13316.667	13237.594	13189.45
6.5	-------	13899.567	14030	13794.158	11207.919	13237.778	13233.884	13198.403
7	-------	13885.917	14020	13701.032	11245.197	13132.222	13196.874	13209.053
8	-------	13790.509	13920	13495.27	11179.647	12885.556	13054.196	13110.154
9	-------	13624.309	13760	13273.75	11114.097	12590	12872.431	12960.658
10	-------	13407.213	13540	13047.234	11048.547	12281.111	12664.821	12772.838
12	-------	12910.404	13040	12595.411	10718.442	11736.667	12200.185	12337.274
14	-------	12381.649	12500	12157.85	10369.256	11268.889	11735.529	11873.347
16	-------	11857.939	11970	11740.822	10032.194	10850	11290.191	11413.031
18	-------	11357.992	11460	11345.662	9724.332	10460	10869.597	10970.898
20	-------	10887.103	10980	10973.873	9424.226	10130.667	10479.174	10553.101
40	9196.35	7853.813	7912	8202.094	7286.107	7698.889	7790.581	7633.402
60	6696.07	6115.916	6157	6517.715	6023.353	6266	6215.997	6066.998
80	5326.33	5065.363	5100	5393.047	5175.402	5279.556	5223.282	5096.051
100	4452.16	4344.913	4377	4600.798	4461.443	4567.778	4467.348	4427.954
120	3841.86	3814.023	3844	4010.912	3943.9	4030	3914.116	3934.008
140	3389.69	3404.033	3432	3555.278	3480.775	3606.556	3478.055	3549.514
160	3040.18	3076.413	3102	3197.605	3148.033	3266.333	3138.428	3238.534
180	2761.31	2808.895	2832	2903.944	2863.631	2986	2859.297	2979.544
200	2533.24	2586.002	2607	2666.684	2627.57	2774.444	2632.489	2758.882
300	1816.73	1862.957	1874	1908.567	1896.704	2003.333	1893.714	1992.313
400	1435.15	1463.512	1470	1503.629	1583.637	1582.444	1506.396	1520.933
500	1196.11	1203.877	1211	1254.33	1367.853	1319	1258.696	1205.969
600	1031.5	1037.748	1044	1081.666	1152.07	1141.667	1081.442	998.462
700	910.86	915.765	920.9	955.128	963.476	1006.356	945.414	876.737
800	818.44	822.236	826.9	858.187	883.645	902.844	852.043	829.72
900	745.27	748.283	752.4	781.408	803.813	820.9	775.346	851.163
1000	685.83	688.149	691.9	719.626	723.982	755.489	710.829	937.275

Appendix

Mass stopping power for Oxygen ions interacts with the Blood using (SRIM, CasP, PASS,SRIM dictionary)programs and Bethe formulae

E(MeV)	Mass Stopping power MeV/(g/cm²)				For Blood Tissue	
					Present Work	
	Bethe	SRIM	Dic.SRIM	PASS	CasP	Average S.P.	S.P.(P.W)
0.025	------	871.218	873.5	1495.995	49.349	798.022	1001.882
0.03	------	954.434	956.8	1612.829	69.243	898.327	1037.673
0.04	------	1078.28	1081	1858.468	109.354	1031.775	1108.868
0.06	------	1245.183	1248	2268.213	190.011	1237.852	1249.735
0.08	------	1386.011	1389	2613.251	270.667	1414.732	1388.6
0.1	------	1517.308	1520	2916.345	380.635	1583.572	1525.5
0.2	------	2087.824	2092	4106.17	945.977	2307.993	2181.705
0.3	------	2571.597	2576	5020.278	1407.853	2893.932	2793.695
0.4	------	3016.916	3023	5791.881	1819.124	3412.73	3365.154
0.6	------	3852.051	3859	7067.578	2543.55	4330.545	4399.604
0.8	------	4644.851	4653	8101.581	3239.797	5159.807	5310.195
1	------	5407.98	5418	8953.544	3962.222	5935.437	5901.332
1.1	------	5779.563	5790	9322.86	4294.901	6296.831	6441.051
1.2	------	6143.226	6155	9660.17	4619.377	6644.443	6789.77
1.3	------	6499.014	6511	9968.728	4943.853	6980.649	7112.809
1.4	------	6846.803	6860	10252.059	5242.429	7300.323	7415.488
1.5	------	7184.899	7198	10506.587	5502.157	7597.911	7699.919
1.6	------	7512.223	7527	10739.047	5761.885	7885.039	7967.548
1.7	------	7828.606	7845	10954.785	6021.614	8162.501	8219.569
1.8	------	8134.14	8152	11151.797	6217.108	8413.761	8457.027
2	------	8710.933	8729	11495.532	6608.096	8885.89	8891.93
2.25	------	9361.889	9382	11840.357	7016.401	9400.162	9368.772
2.5	------	9934.772	9958	12117.405	7383.274	9848.363	9781.334
2.75	------	10433.227	10460	12336.974	7716.129	10236.583	10138.512
3	------	10862.073	10890	12508.915	8006.978	10566.991	10447.74
3.25	------	11226.115	11250	12642.207	8272.805	10847.782	10715.281
3.5	------	11533.534	11560	12744.676	8502.699	11085.227	10946.44
3.75	------	11790.828	11820	12822.893	8690.543	11281.066	11145.74
4	------	12004.703	12040	12877.062	8878.388	11450.038	11317.053
4.5	------	12322.648	12360	12935.678	9208.888	11706.804	11588.602
5	------	12531.307	12560	12943.951	9494.198	11882.364	11782.732
5.5	------	12657.239	12690	12918.791	9667.707	11983.434	11915.844
6	------	12723.398	12760	12869.423	9813.265	12041.521	12000.527
6.5	------	12745.165	12780	12802.913	9958.824	12071.725	12046.56
7	------	12733.542	12770	12724.345	10051.021	12069.727	12061.616
8	------	12638.638	12670	12541.387	10075.332	11981.339	12021.869
9	------	12479.927	12510	12341.753	10099.642	11857.83	11916.749
10	------	12279.773	12310	12133.137	10123.953	11711.716	11769.383
12	------	11821.002	11850	11712.622	9869.669	11313.323	11404.567
14	------	11337.556	11370	11302.061	9575.78	10896.349	11000.475
16	------	10863.659	10890	10911.044	9258.095	10480.7	10591.624
18	------	10414.382	10440	10539.178	8981.189	10093.687	10194.436
20	------	9993.808	10020	10187.274	8725.149	9731.558	9816.393
40	8724.51	7336.939	7352	7587.894	6854.885	7282.929	7141.784
60	6373.84	5781.821	5793	6013.818	5726.937	5828.894	5697.9
80	5080.42	4849.296	4857	4971.258	4925.67	4936.729	4800.792
100	4252.71	4203.628	4210	4231.555	4263.399	4232.259	4181.681
120	3673.74	3718.615	3724	3687.173	3782.3	3717.166	3722.277
140	3244.15	3335.26	3341	3268.866	3350.025	3307.861	3363.19
160	2911.72	3022.478	3028	2940.415	3032.521	2987.026	3071.479
180	2646.21	2761.951	2766	2673.003	2761.647	2721.762	2827.444
200	2428.89	2540.221	2544	2451.326	2537.402	2500.368	2618.59
300	1745.05	1800.11	1803	1757.108	1835.035	1788.061	1884.622
400	1380.12	1399.181	1401	1386.91	1532.525	1419.946	1425.352
500	1151.19	1164.941	1167	1155.878	1324.988	1192.799	1114.519
600	993.38	1004.789	1006	997.764	1117.451	1023.877	907.656
700	877.64	887.092	888.3	881.004	935.928	893.992	785.097
800	788.92	796.804	797.9	793.434	858.456	807.103	736.8
900	718.64	725.32	726.3	722.711	780.984	734.791	757.106
1000	661.53	667.236	668.1	664.999	703.513	673.075	842.579

Appendix

Mass stopping power for Oxygen ions interacts with the Brain using (SRIM, CasP, PASS) programs and Bethe formulae

E(MeV)	Mass Stopping power MeV/(g/cm^2) Brain Tissue				
				Present work	
	Bethe	SRIM	PASS	CasP	Average S.P.	S.P.(P.W)
0.025	-----	909.033	1513.75	58.579	823.131	1040.788
0.03	-----	995.851	1632.251	80.879	902.993	1079.427
0.04	-----	1122.067	1880.934	125.751	1042.917	1156.25
0.06	-----	1294.153	2295.848	215.633	1268.545	1308.101
0.08	-----	1440.242	2645.343	305.514	1463.7	1457.594
0.1	-----	1576.012	2952.447	436.793	1655.084	1604.774
0.2	-----	2158.885	4159.052	1042.241	2453.393	2307.509
0.3	-----	2648.362	5087.362	1532.995	3089.573	2958.646
0.4	-----	3099.476	5871.837	1970.222	3647.179	3562.763
0.6	-----	3946.192	7170.201	2739.073	4618.489	4645.797
0.8	-----	4749.354	8222.952	3497.701	5490.002	5584.32
1	-----	5521.511	9089.68	4274.928	6295.373	6400.671
1.1	-----	5897.28	9464.946	4626.22	6662.815	6768.853
1.2	-----	6264.934	9807.348	4977.512	7016.598	7113.042
1.3	-----	6624.539	10120.215	5314.746	7353.167	7435.012
1.4	-----	6975.984	10407.166	5595.749	7659.633	7736.378
1.5	-----	7317.616	10664.541	5876.751	7952.969	8018.613
1.6	-----	7648.33	10899.278	6157.754	8235.121	8283.06
1.7	-----	7967.913	11116.875	6369.027	8484.605	8530.951
1.8	-----	8276.514	11315.293	6580.3	8724.036	8763.414
2	-----	8859.131	11660.733	6969.88	9163.248	9186.118
2.25	-----	9516.585	12006.051	7392.679	9638.438	9644.49
2.5	-----	10095.174	12282.527	7758.67	10045.457	10036.118
2.75	-----	10598.701	12500.811	8083.357	10394.29	10370.839
3	-----	11031.957	12671.031	8377.523	10693.504	10656.804
3.25	-----	11399.841	12802.36	8637.785	10946.662	10900.814
3.5	-----	11710.667	12902.745	8838.16	11150.524	11108.578
3.75	-----	11970.98	12978.833	9038.536	11329.45	11284.915
4	-----	12187.667	13030.878	9238.911	11485.819	11433.914
4.5	-----	12509.888	13085.382	9538.95	11711.407	11663.345
5	-----	12722.305	13089.8	9779.177	11863.761	11819.237
5.5	-----	12850.954	13061.049	9929.689	11947.231	11918.24
6	-----	12918.866	13008.343	10080.201	12002.47	11972.921
6.5	-----	12942.188	12938.724	10202.439	12027.783	11985.548
7	-----	12931.134	12857.241	10211.58	11999.985	11992.885
8	-----	12836.374	12669.006	10229.861	11911.747	11910.857
9	-----	12676.222	12464.605	10248.143	11796.323	11781.912
10	-----	12473.13	12251.7	10196.346	11640.392	11619.633
12	-----	12006.631	11823.569	9882.513	11237.571	11244.506
14	-----	11513.958	11406.375	9551.306	10823.88	10847.175
16	-----	11030.295	11009.552	9208.517	10416.121	10454.801
18	-----	10571.353	10632.463	8946.004	10049.94	10079.153
20	------	10141.5	10275.849	8664.935	9694.095	9724.807
40	8802.691	7425.936	7646.777	6745.831	7272.848	7222.59
60	6428.499	5840.215	6057.962	5588.438	5828.872	5809.671
80	5122.789	4891.729	5006.665	4802.49	4900.295	4883.42
100	4287.479	4236.625	4261.172	4133.799	4210.532	4218.073
120	3703.317	3745.621	3712.715	3638.407	3698.914	3712.486
140	3269.951	3358.281	3291.363	3236.061	3295.235	3313.709
160	2934.633	3042.697	2960.571	2895.745	2966.338	2990.795
180	2666.858	2780.126	2691.277	2655.323	2708.909	2724.152
200	2447.698	2556.912	2468.052	2438.653	2487.872	2500.627
300	1758.207	1812.847	1769.026	1761.181	1781.018	1778.831
400	1390.338	1409.508	1396.263	1491.188	1432.32	1401.411
500	1159.605	1172.87	1163.625	1268.971	1201.822	1178.827
600	1000.576	1011.558	1004.411	1046.754	1020.907	1032.491
700	883.944	893.021	886.84	908.136	895.999	923.405
800	794.552	802.094	798.663	825.252	808.67	829.892
900	723.743	730.115	727.452	742.368	733.312	738.899
1000	666.198	671.625	669.343	692956	670.484	642.084

Appendix

Mass stopping power for Oxygen ions interacts with the Breast using (SRIM, CaSP, PASS)programs and Bethe formulae

E(MeV)	Mass Stopping power MeV/(g/cm^2) Breast Tissue				
				Present work	
	Bethe	SRIM	PASS	CasP	Average S.P.	S.P.(P.W)
0.025	-----	1049.221	1456.976	60.358	832.483	1065.238
0.03	-----	1149.367	1657.441	83.56	963.456	1107.556
0.04	-----	1280.565	1910.197	132.722	1107.828	1191.613
0.06	-----	1475.299	2332.209	232.425	1346.644	1357.446
0.08	-----	1645.214	2688.041	332.128	1555.128	1520.301
0.1	-----	1799.457	3001.045	470.701	1757.068	1680.251
0.2	-----	2413.083	4234.397	1107.827	2585.102	2438.51
0.3	-----	2899.037	5187.848	1618.826	3235.237	3133.718
0.4	-----	3352.203	5996.795	2071.509	3806.836	3772.354
0.6	-----	4213.772	7341.585	2869.423	4808.26	4902.698
0.8	-----	5031.682	8435.704	3673.209	5713.532	5867.887
1	-----	5813.305	9336.898	4499.776	6549.993	6697.327
1.1	-----	6191.763	9726.467	4869.614	6929.282	7068.518
1.2	-----	6561.065	10081.23	5239.453	7293.916	7413.977
1.3	-----	6921.08	10404.579	5594.028	7639.896	7735.84
1.4	-----	7271.887	10700.286	5887.546	7953.239	8036.018
1.5	-----	7612.203	10964.38	6181.064	8252.549	8316.231
1.6	-----	7940.911	11204.273	6474.582	8539.922	8578.027
1.7	-----	8257.816	11425.862	6696.049	8793.242	8822.802
1.8	-----	8563.228	11626.984	6917.516	9035.909	9051.823
2	-----	9138.672	11974.615	7325.638	9479.641	9467.088
2.25	-----	9786.318	12317.872	7768.087	9957.426	9915.919
2.5	-----	10355.099	12589.203	8152.213	10365.505	10298.471
2.75	-----	10849.676	12800.386	8482.606	10710.889	10625.029
3	-----	11274.784	12962.451	8777.957	11005.064	10903.959
3.25	-----	11635.872	13085.204	9038.565	11253.214	11142.134
3.5	-----	11941.001	13176.988	9238.517	11452.169	11345.245
3.75	-----	12196.918	13244.653	9438.469	11626.68	11518.04
4	-----	12410.653	13288.668	9638.421	11779.247	11664.513
4.5	-----	12727.259	13328.496	9915.842	11990.533	11891.49
5	-----	12938.416	13320.165	10133.962	12130.848	12047.646
5.5	-----	13066.093	13280.363	10263.129	12203.195	12148.821
6	-----	13132.223	13218.1	10392.296	12247.54	12206.908
6.5	-----	13156.746	13140.169	10494.538	12263.818	12230.976
7	-----	13144.448	13051.384	10489.075	12228.302	12228.03
8	-----	13049.859	12851.171	10478.15	12126.393	12161.844
9	-----	12888.99	12636.973	10467.225	11997.729	12039.879
10	-----	12683.199	12416.062	10394.385	11831.215	11882.365
12	-----	12211.761	11974.938	10062.964	11416.554	11509.607
14	-----	11712.883	11547.251	9723.659	10994.598	11106.201
16	-----	11221.687	11141.616	9379.097	10580.8	10701.46
18	-----	10754.601	10756.729	9104.806	10205.379	10309.257
20	-----	10316.171	10393.126	8814.192	9841.163	9935.871
40	8894.89	7521.803	7719.237	6824.911	7355.317	7262.117
60	6489.73	5900.953	6107.975	5641.062	6034.93	5786.523
80	5168.61	4924.87	5043.793	4844.607	4995.471	4859.638
100	4324.09	4251.388	4290.179	4164.976	4257.659	4217.56
120	3733.81	3749.343	3736.313	3661.722	3720.296	3741.301
140	3296.08	3356.229	3311.14	3254.541	3304.498	3370.113
160	2957.5	3038.157	2977.592	2911.41	2971.164	3069.887
180	2687.19	2775.335	2706.194	2668.628	2709.336	2820.034
200	2466	2553.545	2481.317	2450.079	2487.736	2607.403
300	1770.46	1821.634	1777.697	1768.792	1784.646	1871.635
400	1399.58	1422.245	1402.78	1497.57	1430.543	1421.662
500	1167.05	1178.495	1168.876	1273.978	1197.099	1120.973
600	1006.82	1016.239	1008.825	1050.386	1020.568	921.086
700	889.34	897.037	890.652	911.045	897.018	800.448
800	799.31	805.614	802.031	827.872	808.706	748.02
900	728	733.267	730.467	744.699	734.109	757.564
1000	670.06	674.465	672.075	670.985	679.15	825.286

Appendix

Mass stopping power for Oxygen ions interacts with the Lung using (SRIM, CasP, PASS)programs and Bethe formulae

E(MeV)	Mass Stopping power MeV/(g/cm^2) Lung Tissue					
					Present work	
	Bethe	SRIM	PASS	CasP	Average S.P.	S.P.(P.W)
0.025	------	870.205	1427.903	56.034	775.413	1023.864
0.03	------	953.326	1614.969	77.341	881.879	1062.104
0.04	------	1077.38	1860.937	120.23	1019.516	1138.131
0.06	------	1244.023	2271.233	206.147	1240.468	1288.403
0.08	------	1384.508	2616.734	292.064	1431.102	1436.335
0.1	------	1515.625	2920.234	419.624	1618.494	1581.973
0.2	------	2086.995	4111.659	1009.76	2402.805	2277.253
0.3	------	2572.369	5026.993	1491.954	3030.439	2921.358
0.4	------	3018.918	5799.613	1922.512	3580.348	3518.848
0.6	------	3855.744	7076.904	2678.642	4537.097	4589.771
0.8	------	4649.862	8112.045	3419.639	5393.849	5517.579
1	------	5414.247	8964.783	4179.39	6186.14	6324.468
1.1	------	5786.481	9334.384	4524.266	6548.377	6688.346
1.2	------	6150.801	9671.929	4869.142	6897.291	7028.493
1.3	------	6507.271	9980.684	5200.275	7229.41	7346.669
1.4	------	6855.764	10264.182	5476.438	7532.128	7644.475
1.5	------	7194.574	10518.85	5752.6	7822.008	7923.367
1.6	------	7522.617	10751.434	6028.763	8100.938	8184.68
1.7	------	7839.72	10967.285	6236.532	8347.846	8429.63
1.8	------	8145.976	11164.401	6444.301	8584.893	8659.336
2	------	8724.198	11508.324	6827.319	9019.947	9077.032
2.25	------	9376.843	11853.358	7242.795	9490.999	9529.993
2.5	------	9951.273	12130.596	7602.573	9894.814	9917.03
2.75	------	10451.115	12350.338	7924.044	10241.832	10247.866
3	------	10881.183	12522.433	8216.536	10540.051	10530.554
3.25	------	11246.273	12655.859	8475.844	10792.658	10771.812
3.5	------	11554.601	12758.44	8675.558	10996.2	10977.278
3.75	------	11812.663	12836.752	8875.272	11174.896	11151.708
4	------	12027.188	12890.994	9074.987	11331.056	11299.14
4.5	------	12346.185	12949.699	9378.828	11558.238	11526.281
5	------	12555.556	12957.997	9623.179	11712.244	11680.776
5.5	------	12682.006	12932.81	9778.292	11797.703	11779.057
6	------	12748.566	12883.374	9933.405	11855.115	11833.529
6.5	------	12770.522	12816.767	10060.108	11882.465	11853.673
7	------	12759.062	12738.079	10073.165	11856.769	11846.811
8	------	12664.148	12554.832	10099.28	11772.754	11773.683
9	------	12505.195	12354.879	10125.395	11661.823	11646.809
10	------	12304.644	12145.931	10079.808	11510.128	11486.871
12	------	11844.701	11724.761	9773.525	11114.329	11116.707
14	------	11359.869	11313.586	9447.998	10707.151	10724.292
16	------	10884.552	10922.011	9109.641	10305.401	10336.577
18	------	10433.902	10549.636	8852.079	9945.206	9965.273
20	--------	10012.048	10197.271	8575.815	9595.045	9614.958
40	8734.226	7348.404	7594.984	6688.145	7210.511	7141.213
60	6380.827	5789.399	6019.436	5544.289	5784.375	5745.508
80	5085.932	4855.387	4975.96	4765.774	4865.707	4831.018
100	4257.295	4208.961	4235.616	4104.026	4182.868	4174.138
120	3677.678	3723.431	3690.761	3613.629	3675.94	3674.85
140	3247.615	3339.641	3272.086	3214.815	3275.514	3280.888
160	2914.811	3026.463	2943.341	2877.058	2948.954	2961.743
180	2649.016	2765.556	2675.685	2638.521	2693.254	2698.12
200	2431.457	2543.458	2453.802	2423.485	2473.582	2477.066
300	1746.883	1801.904	1758.915	1750.568	1770.462	1763.191
400	1381.554	1400.345	1388.344	1482.294	1423.661	1390.53
500	1152.381	1166.129	1157.074	1261.539	1194.914	1171.474
600	994.409	1005.81	998.795	1040.784	1015.129	1027.847
700	878.544	887.991	881.913	903.038	890.981	920.693
800	789.733	797.61	794.251	820.631	804.164	828.277
900	719.38	726.053	723.454	738.225	729.244	737.475
1000	662.205	667.909	665.681	659.879	666.795	639.879

Appendix

Mass stopping power for Oxygen ions interacts with the Muscle using (SRIM, CasP, PASS,SRIM dictionary ,MSTAR)programs and Bethe formulae

E(MeV)	Mass Stopping power MeV/(g/cm²) For Muscle tissue						Present Work	
	Bethe	SRIM	Dic.SRIM	PASS	CaSP	MSTAR	Average S.P.	S.P .(P.W)
0.025	-------	897.025	916.2	1498.097	56.055	828.908	801.02	986.415
0.03	-------	982.696	1004	1617.145	77.413	885.676	890.732	1026.968
0.04	-------	1107.406	1129	1863.502	120.986	1031.441	1030.834	1107.551
0.06	-------	1278.683	1303	2274.511	208.561	1273.588	1258.835	1266.641
0.08	-------	1424.064	1452	2620.684	296.135	1482.294	1455.794	1423.017
0.1	-------	1558.866	1590	2924.84	424.74	1667.882	1644.082	1576.741
0.2	-------	2135.57	2170	4119.531	1019.564	2446.412	2430.269	2307.548
0.3	-------	2619.418	2652	5038.258	1504.962	3117.412	3070.012	2980.137
0.4	-------	3065.825	3099	5814.368	1937.962	3715.235	3633.348	3600.378
0.6	-------	3904.905	3939	7098.593	2698.827	4771.059	4618.346	4703.826
0.8	-------	4701.107	4737	8140.105	3447.536	5698.176	5496.731	5653.269
1	-------	5466.163	5502	8998.234	4216.055	6533	6303.363	6272.838
1.1	-------	5838.201	5874	9370.078	4564.292	6920.765	6673.334	6820.452
1.2	-------	6202.061	6238	9709.554	4912.53	7287.294	7027.86	7167.395
1.3	-------	6557.776	6593	10019.93	5246.783	7636.706	7365.299	7488.073
1.4	-------	6905.262	6940	10304.761	5525.099	7969.412	7676.134	7786.767
1.5	-------	7242.91	7276	10560.419	5803.415	8285.176	7972.98	8065.613
1.6	-------	7569.644	7603	10793.726	6081.732	8585.529	8257.658	8326.246
1.7	-------	7885.304	7918	11010.1	6291.346	8871	8514.437	8570.068
1.8	-------	8190.019	8222	11207.518	6500.96	9117.588	8754.021	8798.32
2	-------	8765.037	8794	11551.494	6887.309	9610.765	9203.651	9212.485
2.25	-------	9413.652	9439	11895.776	7306.267	10157.529	9693.306	9660.473
2.5	-------	9984.252	10010	12171.749	7669.252	10634.588	10114.96	10042.465
2.75	-------	10480.643	10500	12389.915	7991.433	11021.765	10470.939	10368.517
3	-------	10907.633	10930	12560.285	8283.763	11376.471	10782.038	10646.86
3.25	-------	11270.123	11290	12691.95	8542.785	11641.176	11036.509	10884.286
3.5	-------	11576.249	11590	12792.801	8742.104	11877.647	11247.2	11086.448
3.75	-------	11832.531	11850	12869.444	8941.422	12071.765	11428.791	11258.082
4	-------	12045.701	12060	12922.122	9140.741	12216.471	11581.259	11403.183
4.5	-------	12362.404	12370	12978.027	9439.374	12404.706	11796.128	11626.852
5	-------	12570.716	12580	12983.955	9678.738	12457.647	11922.764	11779.091
5.5	-------	12696.438	12710	12956.767	9829.198	12403.529	11971.483	11875.926
6	-------	12762.304	12770	12905.648	9979.657	12328.235	11993.961	11929.423
6.5	-------	12784.341	12790	12837.618	10102.04	12210.588	11983.647	11948.799
7	-------	12772.585	12780	12757.715	10112.115	12083.529	11931.486	11941.18
8	-------	12677.923	12690	12572.572	10132.264	11805.294	11797.013	11866.053
9	-------	12519.319	12530	12371.155	10152.414	11534.706	11644.398	11736.063
10	-------	12318.909	12330	12161.09	10102.685	11271.765	11463.612	11571.686
12	-------	11859.65	11870	11738.241	9793.592	10787.647	11044.783	11188.925
14	-------	11375.389	11380	11325.82	9467.294	10360	10632.126	10780.167
16	-------	10900.337	10910	10933.261	9129.526	9973.176	10234.075	10373.971
18	-------	10449.714	10460	10560.043	8870.164	9634	9878.48	9983.385
20	-------	10027.657	10040	10206.939	8592.661	9314	9535.314	9613.958
40	8740.42	7355.559	7359	7600.052	6694.336	7062.294	7178.06	7023.095
60	6384.49	5793.242	5796	6022.298	5546.987	5725.941	5772.117	5624.049
80	5088.44	4855.317	4854	4977.635	4767.633	4827.059	4856.911	4751.213
100	4259.15	4206.125	4203	4236.603	4104.783	4172.882	4180.098	4146.592
120	3679.12	3719.017	3715	3691.33	3613.596	3677.059	3675.251	3696.503
140	3248.78	3334.567	3331	3272.389	3214.412	3290.294	3277.916	3343.728
160	2915.77	3021.313	3017	2943.478	2876.562	2978.706	2955.015	3056.459
180	2649.82	2760.727	2757	2675.711	2637.89	2739.118	2703.361	2815.635
200	2432.15	2539.256	2536	2453.753	2422.779	2527.353	2485.785	2609.15
300	1747.25	1801.415	1801	1758.736	1749.995	1823	1783.287	1880.667
400	1381.78	1401.352	1402	1388.152	1481.817	1447.765	1429.771	1422.758
500	1152.54	1165.976	1166	1156.889	1261.063	1207.235	1197.791	1112.258
600	994.52	1005.654	1005	998.619	1040.308	1041.747	1021.582	905.693
700	878.62	887.838	887.6	881.747	902.587	921.794	898.492	783.81
800	789.79	797.46	797.3	794.093	820.222	828.729	810.126	736.768
900	719.42	725.91	725.7	723.303	737.856	754.553	735.406	759.017
1000	662.24	667.769	667.6	665.537	#VALUE!	694.065	675.79	847.187

Appendix

Mass stopping power for Oxygen ions interacts with the Bone using (SRIM, CasP, PASS,SRIM dictionary)programs and Bethe formulae

E(MeV)	Mass Stopping power MeV/(g/cm²)For Bone Tissue						
						Present Work	
	Bethe	SRIM	Dic.SRIM	PASS	CaSP	Average S.P.	S.P. (P.W)
0.025	------	711.073	712	1103.789	72.368	638.86	766.83
0.03	------	778.952	780	1211.699	90.733	715.346	798.67
0.04	------	875.719	876.9	1396.552	120.224	817.349	861.924
0.06	------	1037.561	1039	1706.407	175.586	989.639	986.752
0.08	------	1186.226	1188	1967.237	230.948	1143.103	1109.381
0.1	------	1319.864	1322	2197.119	321.868	1290.213	1229.865
0.2	------	1848.145	1852	3105.566	750.983	1889.173	1801.791
0.3	------	2274.673	2279	3810.399	1125.208	2372.32	2326.964
0.4	------	2670.071	2675	4405.113	1445.692	2798.969	2810.312
0.6	------	3410.871	3418	5394.498	2085.802	3577.293	3668.033
0.8	------	4095.126	4103	6201.181	2708.994	4277.075	4402.891
1	------	4727.486	4737	6871.165	3332.273	4916.981	5036.306
1.1	------	5025.004	5035	7165.649	3623.358	5212.253	5320.314
1.2	------	5310.201	5321	7435.865	3914.443	5495.377	5584.868
1.3	------	5583.436	5595	7684.183	4193.997	5764.154	5831.456
1.4	------	5845.044	5856	7913.156	4427.425	6010.406	6061.356
1.5	------	6095.007	6107	8125.483	4660.852	6247.085	6275.619
1.6	------	6333.127	6345	8319.638	4894.279	6473.011	6475.015
1.7	------	6559.773	6573	8496.678	5073.326	6675.694	6659.87
1.8	------	6775.373	6789	8663.36	5252.372	6870.026	6829.601
2	------	7174.789	7189	8954.865	5583.173	7225.456	7100.504
2.25	------	7615.851	7630	9260.934	5943.398	7612.546	7688.77
2.5	------	7996.396	8012	9512.871	6253.159	7943.607	7892.929
2.75	------	8322.155	8338	9718.191	6522.081	8225.107	8137.343
3	------	8599.282	8616	9884.183	6762.072	8465.384	8355.378
3.25	------	8832.706	8849	10017.819	6972.11	8667.909	8545.473
3.5	------	9027.979	9045	10125.324	7131.828	8832.533	8710.146
3.75	------	9190.383	9208	10212.101	7291.545	8975.507	8852.303
4	------	9324.434	9342	10282.639	7451.262	9100.084	8974.644
4.5	------	9520.939	9540	10374.965	7670.755	9276.665	9169.092
5	------	9647.832	9666	10424.934	7845.781	9396.137	9309.054
5.5	------	9721.385	9740	10442.653	7954.11	9464.537	9406.268
6	------	9755.678	9775	10436.244	8062.438	9507.34	9469.654
6.5	------	9763.607	9782	10412.181	8150.07	9511.794	9506.071
7	------	9748.883	9768	10375.378	8154.917	9526.964	9520.851
8	------	9677.592	9696	10276.389	8164.612	9453.648	9501.418
9	------	9567.495	9585	10152.831	8174.307	9369.908	9435.696
10	------	9433.181	9452	10017.671	8137.894	9260.186	9339.495
12	------	9133.212	9152	9731.802	7926.743	8985.939	9094.466
14	------	8821.044	8839	9442.402	7707.563	8702.502	8816.807
16	------	8515.071	8533	9159.21	7483.03	8422.577	8531.022
18	------	8223.655	8240	8886.168	7293.713	8160.884	8249.321
20	------	7948.101	7965	8625.656	7094.689	7908.361	7977.73
40	6742.87	6032.154	6045	6608.317	5614.744	6075.054	5966.32
60	4966.94	4846.429	4857	5326.145	4675.481	4926.264	4817.665
80	3978.87	4082.635	4091	4448.002	4036.851	4164.622	4083.543
100	3342.25	3539.866	3547	3818.607	3492.931	3599.601	3569.097
120	2894.81	3130.621	3137	3344.376	3090.043	3175.51	3184.153
140	2561.61	2809.625	2816	2974.909	2758.873	2839.852	2881.977
160	2303.03	2550.679	2556	2682.793	2475.513	2566.246	2636.065
180	2096.02	2337.282	2342	2441.761	2272.616	2348.415	2430.302
200	1926.25	2157.817	2162	2246.133	2090.206	2164.039	2254.337
300	1389.92	1566.001	1570	1616.614	1519.974	1568.147	1638.58
400	1102.24	1235.353	1238	1277.865	1289.609	1260.207	1255.777
500	921.18	1023.945	1026	1068.526	1099.789	1054.565	996.436
600	796.08	884.705	886.8	923.193	909.968	901.167	821.449
700	704.16	782.147	783.9	816.481	791.18	793.427	713.371
800	633.6	703.339	705	734.594	719.747	715.67	663.248
900	577.63	640.844	642.3	669.65	648.314	650.277	666.011
1000	532.1	589.985	591.3	617.318	608.934	597.476	718.575

Appendix

Mass stopping power for Oxygen ions interacts with the Skin using (SRIM, CasP, PASS,SRIM dictionary)programs and Bethe formulae

E(MeV)	Mass Stopping power MeV/(g/cm^2) For Skin Tissue						
						Present Work	
	Bethe	SRIM	Dic.SRIM	PASS	CaSP	Average S.P.	S.P.(P.W)
0.025	-----	939.081	974.8	1467.908	55.784	852.867	1059.11
0.03	-----	1028.748	1068	1619.757	77.124	948.407	1095.979
0.04	-----	1154.763	1195	1866.58	121.693	1084.509	1169.299
0.06	-----	1332.889	1379	2278.457	211.775	1300.53	1314.277
0.08	-----	1485.755	1538	2625.473	301.857	1487.771	1456.999
0.1	-----	1626.345	1683	2930.474	431.978	1667.949	1597.072
0.2	-----	2211.307	2277	4129.608	1033.659	2412.893	2273.112
0.3	-----	2691.742	2756	5053.18	1523.804	3006.181	2900.282
0.4	-----	3136.533	3202	5834.389	1960.308	3533.308	3484.644
0.6	-----	3976.203	4045	7128.951	2727.672	4469.456	4538.566
0.8	-----	4773.713	4846	8180.18	3487.803	5321.924	5459.114
1	-----	5538.983	5614	9046.655	4269.325	6117.241	6266.067
1.1	-----	5910.592	5986	9421.999	4622.351	6485.235	6632.13
1.2	-----	6273.753	6350	9764.497	4975.376	6840.907	6975.641
1.3	-----	6628.4	6705	10077.422	5314.062	7181.221	7298.194
1.4	-----	6974.505	7050	10364.353	5595.387	7496.061	7601.244
1.5	-----	7310.577	7386	10621.573	5876.713	7798.716	7886.122
1.6	-----	7635.537	7711	10856.022	6158.038	8090.149	8154.047
1.7	-----	7949.233	8025	11073.224	6370.319	8354.444	8406.14
1.8	-----	8251.84	8327	11271.119	6582.601	8608.14	8643.429
2	-----	8822.44	8895	11615.171	6973.735	9076.586	9077.313
2.25	-----	9465.456	9536	11958.244	7397.634	9589.334	9551.789
2.5	-----	10030.689	10100	12232.189	7765.361	10032.06	9961.057
2.75	-----	10522.227	10590	12447.83	8088.389	10412.112	10314.276
3	-----	10944.857	11010	12615.441	8380.399	10737.674	10619.089
3.25	-----	11303.673	11370	12744.291	8639.122	11014.272	10881.917
3.5	-----	11606.666	11670	12842.382	8837.938	11239.246	11108.189
3.75	-----	11860.429	11920	12916.369	9036.754	11433.388	11302.516
4	-----	12071.69	12130	12966.565	9235.57	11600.956	11468.842
4.5	-----	12385.079	12450	13018.042	9526.287	11844.852	11730.558
5	-----	12591.88	12650	13020.253	9758.115	12005.062	11915.244
5.5	-----	12716.5	12780	12989.951	9901.609	12097.015	12039.43
6	-----	12781.227	12840	12936.236	10045.103	12150.642	12115.759
6.5	-----	12803.313	12870	12866.033	10161.03	12175.094	12154.019
7	-----	12790.949	12850	12784.295	10166.686	12147.982	12161.869
8	-----	12696.357	12760	12596.34	10177.998	12057.674	12109.286
9	-----	12537.916	12600	12392.802	10189.309	11930.007	11993.185
10	-----	12337.344	12400	12181.158	10133.5	11763.001	11836.403
12	-----	11878.435	11940	11756.005	9820.52	11348.74	11456.447
14	-----	11394.473	11450	11341.915	9493.454	10919.961	11040.861
16	-----	10919.38	10980	10948.051	9156.998	10501.107	10623.082
18	-----	10468.466	10520	10573.715	8894.997	10114.295	10218.807
20	-----	10045.859	10100	10219.626	8615.626	9745.278	9835.033
40	8748.64	7361.978	7389	7606.32	6702.134	7264.858	7134.969
60	6389	5796.027	5814	6025.358	5549.709	5796.274	5683.996
80	5091.3	4852.663	4862	4978.967	4769.155	4865.696	4784.701
100	4261.11	4199.508	4204	4236.951	4104.68	4186.285	4165.44
120	3680.54	3710.18	3711	3691.103	3612.366	3681.162	3706.905
140	3249.83	3324.919	3325	3271.815	3212.71	3283.611	3349.247
160	2916.58	3011.747	3011	2942.706	2874.826	2960.07	3059.283
180	2650.45	2751.857	2751	2674.822	2635.996	2703.419	2817.17
200	2432.63	2531.548	2531	2452.797	2420.818	2484.041	2610.33
300	1747.38	1800.18	1803	1757.771	1748.47	1777.355	1886.302
400	1381.78	1402.636	1406	1387.29	1480.545	1419.118	1435.121
500	1152.46	1165.32	1167	1156.121	1259.863	1187.076	1129.685
600	994.41	1005.047	1007	997.927	1039.18	1012.289	925.233
700	878.5	887.273	888.5	881.115	901.544	889.608	801.965
800	789.66	796.932	798	793.509	819.272	801.928	749.775
900	719.28	725.417	726.4	722.76	737	727.894	762.965
1000	662.09	667.301	668.1	665.028	649.357	659.357	638.076

Appendix

Mass stopping power for Fluorine ions interacts with the adipose tissue using (SRIM, CasP, PASS,SRIM dictionary ,MSTAR)programs and Bethe formulae

E(MeV)	Mass Stopping power MeV/(g/cm²) For Adipose Tissue						Present Work	
	Bethe	SRIM	Dic.SRIM	PASS	CaSP	MSTAR	Average S.P.	S.P.(P.W)
0.025	----	1111.794	1097	1494.029	44.319	981.152	938.566	1006.501
0.03	----	1217.86	1201	1602.214	66.24	1073.343	1032.132	1130.551
0.04	----	1471.666	1452	1847.902	110.082	1232.143	1222.759	1318.532
0.06	----	1808.185	1786	2259.487	228.385	1497.429	1515.897	1584.14
0.08	----	1890.496	1865	2607.065	346.688	1718.571	1685.564	1788.902
0.1	----	2006.349	1978	2914.382	464.991	1915.143	1855.773	1966.927
0.2	----	2916.084	2880	4130.824	1036.199	2727.19	2738.059	2715.68
0.3	----	3675.363	3641	5082.759	1535.519	3426.857	3472.3	3374.003
0.4	----	4247.155	4215	5901.244	1979.835	4064.952	4081.637	3984.928
0.6	----	5142.503	5111	7302.957	2780.967	5206.429	5108.771	5100.813
0.8	----	5903.08	5872	8495.012	3496.949	6222.333	5997.875	6099.292
1	----	6624.546	6593	9533.692	4199.671	7148.571	6819.896	6997.27
1.1	----	6979.864	6950	10002.604	4568.873	7581.429	7216.554	7412.518
1.2	----	7333.863	7306	10439.538	4938.076	7996.143	7602.724	7807.056
1.3	----	7686.341	7660	10846.248	5308.401	8393.667	7978.931	8182.077
1.4	----	8037.011	8013	11225.093	5678.726	8774.333	8345.633	8538.684
1.5	----	8383.824	8364	11579.04	6049.051	9138.714	8702.926	8877.896
1.6	----	8727.743	8711	11911.642	6419.376	9487.048	9051.362	9200.661
1.7	----	9067.603	9054	12219.919	6712.953	9819.619	9374.819	9507.862
1.8	----	9402.24	9393	12502.547	7006.531	10135.714	9688.006	9800.323
2	----	10049.52	10050	13015.991	7593.685	10733.81	10288.601	10344.057
2.25	----	10815.984	10830	13564.774	8168.297	11361.429	10948.097	10953.536
2.5	----	11526.431	11550	14009.868	8697.832	11947.143	11546.255	11493.808
2.75	----	12174.094	12210	14380.274	9159.752	12463.81	12077.586	11973.012
3	----	12759.107	12810	14687.311	9569.01	12911.429	12547.371	12398.164
3.25	----	13286.085	13350	14941.704	9947.756	13311.429	12967.395	12775.343
3.5	----	13747.863	13820	15150.489	10257.111	13640	13323.092	13109.832
3.75	----	14151.857	14240	15314.969	10540.315	13940	13637.428	13406.247
4	----	14506.846	14600	15450.954	10806.085	14173.333	13907.444	13668.627
4.5	----	15083.71	15190	15650.887	11242.35	14554.286	14344.247	14105.065
5	----	15502.144	15620	15774.707	11678.616	14820.476	14679.189	14442.827
5.5	----	15795.368	15930	15839.679	11920.628	14991.905	14895.516	14700.496
6	----	16003.107	16140	15863.41	12162.639	15090	15051.831	14892.792
6.5	----	16133.843	16280	15855.022	12300.392	15130	15139.851	15031.481
7	----	16207.08	16350	15824.125	12438.144	15130	15189.87	15126.035
8	----	16222.191	16380	15718.872	12713.65	15055.714	15218.085	15197.063
9	----	16129.235	16290	15572.373	12759.945	14895.714	15129.454	15212.064
10	----	15964.509	16120	15403.765	12806.241	14684.286	14995.76	15112.406
12	----	15521.761	15670	15032.463	12898.833	14192.857	14663.183	14814.481
14	----	15007.979	15150	14646.552	12661.437	13733.333	14239.86	14425.965
16	----	14478.106	14620	14262.399	12424.042	13310	13818.909	14001.854
18	----	13973.146	14100	13889.085	12138.526	12922.857	13404.723	13570.929
20	----	13490.738	13610	13528.27	11853.01	12561.429	13008.689	13148.278
40	13285.178	10201.59	10280	10650.626	9382.966	9928.19	10088.675	9956.954
60	9702.538	8406.359	8464	8738.71	7911.961	8262	8356.606	8138.415
80	7731.28	7141.117	7188	7391.222	6850.924	7097.81	7233.392	6977.538
100	6469.791	6221.929	6265	6403.497	6138.217	6222.429	6286.811	6158.983
120	5587.372	5510.818	5551	5643.485	5425.511	5543.429	5543.602	5539.667
140	4932.612	4937.494	4976	5044	4938.317	5001	4971.571	5046.725
160	4425.905	4465.51	4502	4560.019	4451.122	4557.19	4493.625	4639.414
180	4021.203	4069.307	4103	4162.102	4100.015	4188.571	4107.366	4293.234
200	3689.933	3734.836	3766	3832.712	3748.907	3877.095	3774.914	3992.594
300	2647.413	2641.254	2660	2758.543	2731.488	2855.714	2715.735	2900.042
400	2090.921	2073.174	2084	2175.749	2161.514	2268.714	2142.345	2186.958
500	1741.74	1741.341	1749	1812.711	1930.353	1893.143	1811.381	1694.045
600	1500.979	1513.557	1522	1561.437	1699.193	1632.143	1571.551	1365.045
700	1324.343	1334.294	1342	1377.513	1468.033	1444.333	1381.753	1175.037
800	1188.913	1196.394	1203	1236.178	1236.873	1295.714	1226.179	1111.286
900	1081.598	1087.814	1094	1124.854	1123.091	1178	1114.893	1166.609
1000	994.357	999.253	1005	1034.939	1009.309	1082.333	1020.865	1336.644

Appendix

Mass stopping power for Flourier ions interacts with the Blood using (SRIM, CasP, PASS,SRIM dictionary)programs and Bethe formulae

E(MeV)	Mass Stopping power MeV/(g/cm²) For Blood Tissue						
	Bethe	SRIM	Dic.SRIM	PASS	CaSP	Present Work Average S.P.	Present Work S.P.(P.W)
0.025	------	727.341	690.2	1410.911	48.34	720.863	1004.839
0.03	------	796.814	756.1	1543.963	54.44	791.219	1035.883
0.04	------	971.629	921.4	1779.752	86.434	939.804	1097.745
0.06	------	1225.157	1160	2175.208	171.781	1183.036	1220.572
0.08	------	1276.903	1214	2507.729	257.128	1313.94	1342.213
0.1	------	1352.826	1289	2800.585	342.475	1446.221	1462.68
0.2	------	2037.58	1950	3953.884	796.721	2184.546	2047.823
0.3	------	2700.221	2586	4847.372	1215.788	2837.345	2605.364
0.4	------	3233.264	3095	5604.975	1592.295	3381.384	3136.676
0.6	------	4067.303	3893	6884.146	2316.727	4290.294	4125.751
0.8	------	4773.998	4568	7956.419	2921.599	5055.004	5024.65
1	------	5448.366	5211	8872.605	3487.488	5754.865	5841.986
1.1	------	5783.084	5530	9284.236	3774.151	6092.868	6222.516
1.2	------	6118.413	5849	9667.539	4060.813	6423.941	6585.489
1.3	------	6453.564	6168	10024.868	4353.853	6750.071	6931.75
1.4	------	6788.326	6486	10358.932	4646.893	7070.038	7262.096
1.5	------	7122.329	6804	10672.763	4939.932	7384.756	7577.285
1.6	------	7454.231	7119	10959.957	5232.972	7691.54	7878.036
1.7	------	7783	7431	11229.351	5480.166	7980.879	8165.028
1.8	------	8109.132	7739	11485.771	5727.36	8265.316	8438.907
2	------	8742.194	8340	11939.318	6221.749	8810.815	8949.745
2.25	------	9497.793	9055	12426.98	6694.447	9418.555	9524.793
2.5	------	10202.703	9721	12840.494	7135.436	9974.908	10036.588
2.75	------	10849.707	10330	13188.542	7528.86	10474.277	10492.051
3	------	11435.373	10890	13480.026	7865.181	10917.645	10897.277
3.25	------	11960.012	11380	13723.693	8175.407	11309.778	11257.636
3.5	------	12424.5	11820	13927.922	8438.36	11652.695	11577.871
3.75	------	12832.179	12210	14100.217	8678.87	11955.317	11862.176
4	------	13188.229	12550	14247.017	8904.419	12222.416	12114.265
4.5	------	13760.224	13090	14455.064	9297.749	12650.759	12534.609
5	------	14175.245	13490	14593.511	9691.079	12987.459	12861.121
5.5	------	14470.093	13770	14677.462	9953.373	13217.732	13111.439
6	------	14666.264	13960	14719.771	10215.666	13390.425	13299.651
6.5	------	14793.93	14080	14730.741	10401.601	13501.568	13437.07
7	------	14861.454	14150	14718.435	10587.537	13579.356	13532.829
8	------	14876.058	14180	14642.162	10959.407	13664.407	13627.643
9	------	14788.135	14100	14521.635	11101.942	13627.928	**13628.535**
10	------	14632.929	13960	14373.307	11244.477	13552.678	13565.495
12	------	14211.422	13570	14037.701	11529.547	13337.168	13323.478
14	------	13739.582	13130	13681.586	11441.689	12998.214	13001.834
16	------	13259.02	12680	13324.209	11353.831	12654.265	12650.23
18	------	12797.186	12250	12973.706	11121.09	12285.496	12293.756
20	------	12361.569	11840	12634.649	10888.35	11931.142	11945.037
40	12583.203	9472.341	9112	9929.853	8685.883	9300.019	9307.007
60	9223.183	7900.2	7611	8138.109	7433.6	7770.727	7737.413
80	7365.527	6783.48	6542	6878.748	6483.869	6810.725	6670.992
100	6173.201	5970.418	5763	5947.783	5819.44	5934.768	5875.782
120	5337.418	5333.478	5150	5239.106	5155.011	5243.003	5248.367
140	4716.281	4810.405	4647	4680.512	4709.77	4712.794	4735.426
160	4234.991	4370.856	4225	4233.586	4264.53	4265.792	4306.131
180	3850.192	3994.916	3864	3864.012	3938.502	3902.324	3941.017
200	3534.94	3671.094	3553	3553.907	3612.475	3585.083	3626.922
300	2541.094	2575.394	2500	2560.935	2639.602	2563.405	2562.321
400	2009.388	1990.672	1937	2021.442	2091.776	2010.055	1988.884
500	1675.271	1666.101	1622	1682.286	1868.971	1702.926	1665.413
600	1444.654	1464.599	1425	1450.279	1646.165	1486.139	1471.551
700	1275.323	1291.519	1258	1279.675	1423.36	1305.575	1337.398
800	1145.409	1158.985	1129	1150.771	1200.554	1156.944	1218.739
900	1042.409	1053.919	1027	1047.393	1090.624	1052.269	1085.965
1000	958.638	968.439	943.5	962.959	980.694	962.846	918.404

Appendix

Mass stopping power for Fluorine ions interacts with the Brain using (SRIM, CasP, PASS)programs and Bethe formulae

| E(MeV) | Mass Stopping power MeV/(g/cm²) Brain Tissue | | | | | |
| | | | | | Present work | |
	Bethe	SRIM	PASS	CasP	Average S.P.	S.P.(P.W)
0.025	----	758.899	1425.821	42.298	742.339	984.914
0.03	----	831.38	1560.316	61.121	817.606	1021.237
0.04	----	1012.948	1798.687	100.699	970.778	1093.513
0.06	----	1273.612	2198.56	195.315	1222.496	1236.598
0.08	----	1327.041	2534.893	289.93	1383.955	1377.753
0.1	----	1405.674	2831.188	385.651	1540.838	1517.014
0.2	----	2110.219	3998.942	876.665	2328.609	2186.05
0.3	----	2785.57	4904.797	1323.043	3004.47	2812.434
0.4	----	3326.364	5673.779	1729.762	3576.635	3399.649
0.6	----	4171.594	6973.898	2472.504	4539.332	4468.791
0.8	----	4886.95	8065.006	3114.398	5355.451	5414.904
1	----	5569.061	8997.626	3727.747	6098.145	6255.465
1.1	----	5907.475	9416.557	4038.269	6454.1	6640.763
1.2	----	6246.449	9806.52	4352.326	6801.765	7004.866
1.3	----	6585.254	10169.88	4668.739	7141.291	7349.198
1.4	----	6923.636	10509.383	4985.153	7472.724	7675.061
1.5	----	7261.135	10828.122	5301.567	7796.941	7983.648
1.6	----	7596.574	11119.505	5576.75	8097.61	8276.058
1.7	----	7928.871	11392.603	5841.627	8387.7	8553.298
1.8	----	8258.431	11652.374	6106.504	8672.436	8816.299
2	----	8898.182	12111.042	6574.472	9194.565	9302.953
2.25	----	9661.706	12603.094	7082.2	9782.333	9845.157
2.5	----	10374.009	13019.271	7514.083	10302.454	10323.242
2.75	----	11027.72	13368.631	7908.313	10768.221	10745.634
3	----	11619.534	13660.425	8253.989	11177.983	11119.411
3.25	----	12149.957	13903.693	8545.782	11533.144	11450.56
3.5	----	12619.368	14107.047	8814.423	11846.946	11744.175
3.75	----	13031.38	14278.153	9055.675	12121.736	12004.617
4	----	13391.446	14423.555	9271.289	12362.097	12235.637
4.5	----	13970.545	14628.364	9689.699	12762.869	12621.965
5	----	14391.113	14763.424	10036.762	13063.766	12924.383
5.5	----	14689.94	14844.012	10312.478	13282.144	13159.151
6	----	14889.971	14883.076	10538.28	13437.109	13338.905
6.5	----	15020.252	14890.952	10730.806	13547.337	13473.594
7	----	15089.786	14875.709	10923.332	13629.609	13571.132
8	----	15106.413	14794.026	11211.601	13704.013	13679.004
9	----	15018.662	14668.641	11354.695	13680.666	13700.48
10	----	14862.111	14515.919	11497.789	13625.273	13661.203
12	----	14435.583	14172.518	11666.739	13424.947	13466.209
14	----	13955.611	13809.589	11562.132	13109.111	13183.009
16	----	13465.749	13446.193	11398.914	12770.285	12858.333
18	----	12994.864	13090.212	11147.779	12410.951	12517.739
20	----	12549.98	12746.18	10875.481	12057.214	12175.507
40	12698.316	9593.145	10008.059	8637.863	9413.022	9400.385
60	9303.706	7986.746	8198.379	7355.072	7846.732	7699.5
80	7427.965	6848.191	6927.877	6402.523	6726.197	6581.759
100	6224.442	6021.346	5989.313	5695.728	5902.129	5785.922
120	5381.012	5375.188	5275.177	5058.6	5236.322	5184.009
140	4754.305	4845.59	4712.45	4584.03	4714.023	4707.753
160	4268.769	4401.368	4262.312	4160.497	4274.726	4317.747
180	3880.621	4021.905	3890.135	3813.521	3908.52	3989.736
200	3562.656	3695.462	3577.877	3513.343	3595.561	3708.003
300	2560.46	2592.835	2578.146	2546.601	2572.527	2712.87
400	2024.423	2005.17	2035.009	2059.521	2033.233	2086.039
500	1687.641	1678.32	1693.548	1823.198	1731.689	1656.35
600	1455.213	1474.561	1459.955	1586.875	1507.13	1362.157
700	1284.567	1300.248	1288.179	1350.552	1312.993	1175.835
800	1153.655	1166.734	1158.389	1162.132	1162.418	1083.159
900	1049.869	1060.942	1054.301	1045.568	1053.604	1076.059
1000	965.463	974.859	969.286	929.004	957.716	1149.616

Appendix

Mass stopping power for Flourier ions interacts with the Breast using (SRIM, CasP, PASS)programs and Bethe formulae

E(MeV)	Mass Stopping power MeV/(g/cm²) Breast Tissue					
					Present work	
	Bethe	SRIM	PASS	CasP	Average S.P.	S.P.(P.W)
0.025	------	875.878	1443.938	38.528	796.115	771.126
0.03	------	959.488	1580.205	57.172	875.622	871.78
0.04	------	1164.742	1821.779	94.461	1026.994	1036.617
0.06	------	1450.322	2227.235	191.679	1289.745	1287.892
0.08	------	1514.27	2568.525	288.897	1457.231	1488.774
0.1	------	1605.926	2869.432	386.115	1620.491	1664.707
0.2	------	2377.562	4058.122	881.756	2439.146	2398.623
0.3	------	3076.048	4983.871	1328.632	3129.517	3033.756
0.4	------	3622.257	5772.634	1728.599	3707.83	3617.182
0.6	------	4476.842	7112.157	2489.901	4692.967	4671.843
0.8	------	5201.722	8241.433	3136.68	5526.612	5605.676
1	------	5891.811	9209.413	3754.292	6285.172	6438.642
1.1	------	6233.262	9644.628	4072.193	6650.027	6821.82
1.2	------	6574.577	10049.754	4390.093	7004.808	7184.79
1.3	------	6915.203	10427.07	4712.462	7351.578	7528.862
1.4	------	7254.905	10779.313	5034.832	7689.683	7855.231
1.5	------	7592.655	11109.648	5357.201	8019.835	8164.99
1.6	------	7928.006	11410.977	5679.57	8339.518	8459.141
1.7	------	8259.895	11692.836	5944.418	8632.383	8738.609
1.8	------	8588.159	11960.497	6209.266	8919.307	9004.248
2	------	9224.517	12430.845	6738.962	9464.775	9497.144
2.25	------	9981.755	12932.048	7250.113	10054.639	10048.403
2.5	------	10686.489	13352.538	7724.509	10587.845	10536.318
2.75	------	11331.689	13702.365	8143.769	11059.274	10968.831
3	------	11915.32	13991.783	8507.87	11471.658	11352.68
3.25	------	12439.345	14230.721	8844.216	11838.094	11693.612
3.5	------	12901.487	14428.505	9124.701	12151.564	11996.563
3.75	------	13306.639	14593.299	9381.383	12427.107	12265.787
4	------	13661.342	14731.944	9622.196	12671.827	12504.974
4.5	------	14233.827	14922.814	10031.778	13062.806	12905.679
5	------	14649.143	15044.433	10441.359	13378.312	13219.864
5.5	------	14942.686	15112.575	10695.303	13583.522	13463.936
6	------	15142.91	15140.379	10949.247	13744.179	13650.761
6.5	------	15271.43	15138.168	11116.438	13842.012	13790.542
7	------	15341.118	15113.893	11283.628	13912.88	13891.453
8	------	15356.02	15016.981	11618.01	13997.004	14001.859
9	------	15266.524	14879.329	11723.232	13956.362	14021.603
10	------	15108.345	14716.659	11828.455	13884.486	13977.625
12	------	14680.498	14357.638	12038.901	13692.346	13767.953
14	------	14194.509	13982.671	11893.411	13356.864	13466.886
16	------	13696.955	13609.534	11747.921	13018.137	13123.785
18	------	13220.339	13245.07	11495.391	12653.6	12765.516
20	------	12768.459	12893.548	11242.861	12301.623	12406.954
40	12837.142	9734.814	10105.633	8941.808	9594.085	9541.6
60	9395.873	8081.326	8268.561	7607.696	7985.861	7815.413
80	7496.919	6910.305	6981.277	6616.607	6836.063	6689.519
100	6279.52	6057.911	6031.651	5934.543	6008.035	5889.84
120	5426.866	5393.337	5309.926	5252.479	5318.581	5284.803
140	4793.587	4851.594	4741.728	4791.608	4794.977	4805.124
160	4303.132	4400.114	4287.558	4330.736	4339.469	4411.167
180	3911.165	4016.878	3912.265	3995.448	3974.864	4078.703
200	3590.149	3689.43	3597.543	3660.16	3649.044	3792.114
300	2578.834	2596.595	2590.902	2671.435	2619.644	2770.211
400	2038.261	2019.714	2044.584	2115.826	2060.041	2118.554
500	1698.767	1693.075	1701.268	1890.106	1761.483	1670.29
600	1464.536	1481.642	1466.457	1664.387	1537.495	1365.681
700	1292.606	1306.401	1293.805	1438.667	1346.291	1178.054
800	1160.732	1171.962	1163.363	1212.947	1182.757	1093.706
900	1056.2	1065.671	1058.758	1101.683	1075.371	1104.875
1000	971.198	979.109	973.325	990.419	980.951	1206.838

Appendix

Mass stopping power for Flourier ions interacts with the Lung using (SRIM, CasP, PASS)programs and Bethe formulae

E(MeV)	Mass Stopping power MeV/(g/cm²) Lung Tissue					
					Present work	
	Bethe	SRIM	PASS	CasP	Average S.P.	S.P.(P.W)
0.025	--------	726.497	1450.785	35.965	757.749	725.318
0.03	--------	795.89	1587.714	53.03	812.211	815.497
0.04	--------	970.614	1830.649	87.158	962.807	967.158
0.06	--------	1224.134	2236.508	172.895	1211.179	1204.977
0.08	--------	1275.626	2578.908	258.632	1371.056	1398.062
0.1	--------	1351.338	2880.352	344.37	1525.353	1567.896
0.2	--------	2036.205	4068.237	799.905	2301.449	2275.646
0.3	--------	2700.262	4986.647	1219.942	2968.95	2885.801
0.4	--------	3234.764	5768.25	1597.265	3533.427	3445.339
0.6	--------	4070.798	7083.743	2320.997	4491.846	4456.236
0.8	--------	4778.833	8180.816	2926.509	5295.386	5351.625
1	--------	5454.345	9118.633	3492.969	6021.983	6150.942
1.1	--------	5789.625	9535.316	3779.886	6368.276	6518.905
1.2	--------	6125.529	9922.922	4066.803	6705.085	6867.636
1.3	--------	6461.276	10284.123	4359.98	7035.126	7198.379
1.4	--------	6796.644	10616.917	4653.157	7355.573	7512.267
1.5	--------	7131.281	10925.278	4946.334	7667.631	7810.333
1.6	--------	7463.838	11213.879	5239.511	7972.41	8093.529
1.7	--------	7793.272	11486.404	5486.739	8255.472	8362.729
1.8	--------	8120.098	11732.203	5733.968	8528.756	8618.741
2	--------	8754.554	12182.724	6228.424	9055.234	9094.143
2.25	--------	9511.921	12658.422	6701.183	9623.842	9626.462
2.5	--------	10218.571	13053.849	7142.29	10138.237	10098.234
2.75	--------	10867.242	13384.9	7535.92	10596.021	10516.995
3	--------	11454.457	13660.842	7872.167	10995.822	10889.145
3.25	--------	11980.474	13890.615	8182.287	11351.125	11220.149
3.5	--------	12446.239	14082.475	8445.28	11657.998	11514.701
3.75	--------	12855.068	14239.023	8685.787	11926.626	11776.858
4	--------	13212.124	14362.494	8911.305	12161.974	12010.136
4.5	--------	13785.731	14552.209	9304.638	12547.526	12401.933
5	--------	14202.012	14664.49	9697.971	12854.824	12710.337
5.5	--------	14497.848	14724.973	9960.629	13061.15	12951.05
6	--------	14694.67	14747.668	10223.288	13221.875	13136.406
6.5	--------	14822.877	14741.925	10409.544	13324.782	13276.2
7	--------	14890.734	14712.697	10595.801	13399.744	13378.287
8	--------	14905.771	14607.45	10968.315	13493.845	13493.6
9	--------	14817.945	14464.846	11111.391	13464.727	**13520.546**
10	--------	14662.563	14299.661	11254.467	13405.564	13485.158
12	--------	14240.173	13934.74	11540.619	13238.511	13294.675
14	--------	13767.145	13555.935	11453.377	12925.486	13013.491
16	--------	13285.278	13180.553	11366.135	12610.656	12689.781
18	--------	12822.049	12816.188	11133.169	12257.135	12349.898
20	--------	12385.073	12465.017	10900.202	11916.764	12008.533
40	12597.332	9487.286	9705.166	8695.097	9295.85	9259.673
60	9233.359	7911.219	7901.165	7441.695	7751.36	7593.842
80	7373.566	6792.149	6653.561	6491.041	6645.584	6504.812
100	6179.888	5977.9	5739.982	5825.914	5847.932	5730.361
120	5343.167	5340.246	5044.738	5160.787	5181.924	5143.969
140	4721.338	4816.617	4501.888	4715.068	4677.857	4678.838
160	4239.514	4376.588	4060.488	4269.348	4235.475	4296.695
180	3854.292	4000.188	3706.863	3942.964	3883.338	3974.114
200	3538.693	3675.919	3409.909	3616.58	3567.469	3695.985
300	2543.766	2578.331	2449.162	2642.592	2556.695	2703.756
400	2011.488	1992.461	1935.068	2094.129	2007.219	2070.367
500	1677.014	1667.512	1611.847	1871.069	1716.809	1633.928
600	1446.152	1466.09	1389.587	1648.009	1501.229	1336.434
700	1276.642	1292.829	1227.767	1424.949	1315.182	1151.973
800	1146.591	1160.162	1101.869	1201.888	1154.64	1067.227
900	1043.483	1054.986	1004.664	1091.835	1050.495	1074.654
1000	959.623	969.419	#VALUE!	981.781	950.4	1169.662

Appendix

Mass stopping power for Flourier ions interacts with the Muscle using (SRIM, CasP, PASS,SRIM dictionary ,MSTAR)programs and Bethe formulae

E(MeV)	Mass Stopping power MeV/(g/cm²) For Muscle						Present Work	
	Bethe	SRIM	Dic.SRIM	PASS	CaSP	MSTAR	Average S.P.	S.P. (P.W)
0.025	-------	748.877	764.9	1452.089	35.914	700.463	740.449	713.085
0.03	-------	820.398	838	1589.159	53.005	774.058	814.924	818.066
0.04	-------	999.541	1020	1832.358	87.187	902.121	968.241	978.185
0.06	-------	1257.737	1282	2238.708	173.908	1118.263	1214.123	1207.411
0.08	-------	1311.591	1337	2581.582	260.629	1302.684	1358.697	1386.673
0.1	-------	1390.021	1417	2883.494	347.35	1467.947	1501.163	1544.027
0.2	-------	2087.588	2124	4073.778	805.861	2166.789	2251.603	2214.655
0.3	-------	2755.221	2794	4994.788	1227.399	2782.474	2910.776	2810.061
0.4	-------	3290.025	3329	5779.179	1605.965	3347.632	3470.36	3365.202
0.6	-------	4127.107	4166	7100.578	2338.608	4371.632	4420.785	4384.054
0.8	-------	4836.452	4876	8203.586	2949.197	5302.526	5233.552	5300.411
1	-------	5512.718	5553	9146.982	3522.316	6163.895	5979.782	6128.153
1.1	-------	5848.072	5888	9566.219	3813.342	6571.579	6337.442	6512.071
1.2	-------	6183.835	6224	9956.193	4104.368	6965.053	6686.69	6877.515
1.3	-------	6519.273	6559	10319.56	4401.482	7344.579	7028.779	7225.494
1.4	-------	6854.177	6894	10654.269	4698.597	7710.474	7362.303	7556.943
1.5	-------	7188.092	7228	10964.3	4995.711	8062.316	7687.684	7872.732
1.6	-------	7519.817	7559	11254.36	5292.825	8402.316	8005.664	8173.673
1.7	-------	7848.331	7887	11528.165	5542.456	8728.579	8306.906	8460.527
1.8	-------	8174.03	8211	11774.937	5792.087	9042.368	8598.884	8734.005
2	-------	8806.056	8842	12226.917	6291.348	9609.737	9155.212	9243.472
2.25	-------	9559.964	9594	12703.436	6769.442	10276.579	9780.684	9816.166
2.5	-------	10262.965	10290	13098.836	7215.086	10875.789	10348.535	10325.327
2.75	-------	10907.922	10940	13429.278	7612.055	11407.368	10859.325	10778.176
3	-------	11491.643	11520	13704.202	7952.248	11872.632	11308.145	11180.985
3.25	-------	12014.701	12040	13932.699	8266.12	12293.684	11709.441	11539.223
3.5	-------	12477.503	12500	14123.133	8531.479	12641.053	12054.634	11857.674
3.75	-------	12883.621	12900	14278.171	8774.231	12956.842	12358.573	12140.536
4	-------	13238.422	13260	14400.126	9001.91	13213.684	12622.829	12391.506
4.5	-------	13808.784	13820	14586.898	9397.225	13631.579	13048.897	12810.439
5	-------	14222.566	14240	14696.504	9792.54	13905.263	13371.375	13136.346
5.5	-------	14516.276	14530	14754.621	10053.193	14046.316	13580.081	13386.507
6	-------	14712.385	14720	14775.242	10313.846	14073.684	13719.032	13574.687
6.5	-------	14839.697	14850	14767.692	10496.605	14063.158	13803.431	13711.937
7	-------	14907.26	14920	14736.918	10679.364	14004.737	13849.656	13807.19
8	-------	14921.689	14930	14629.189	11044.883	13825.789	13870.31	13895.29
9	-------	14833.645	14840	14484.677	11181.401	13610.526	13790.05	**13899.454**
10	-------	14678.361	14680	14318.002	11317.92	13389.474	13676.751	13824.563
12	-------	14257.075	14270	13950.945	11590.957	12943.684	13402.532	13560.073
14	-------	13784.535	13790	13570.659	11494.361	12522.632	13032.437	13208.761
16	-------	13302.902	13310	13194.126	11397.766	12128.421	12666.643	12823.111
18	-------	12840.262	12850	12828.826	11162.467	11768.947	12290.1	12430.533
20	-------	12403.54	12410	12476.845	10927.168	11442.105	11931.932	12045.353
40	12607.083	9500.262	9506	9711.851	8714.352	8961.211	9278.735	9146.967
60	9239.163	7918.247	7921	7905.147	7451.422	7421.263	7723.416	7504.729
80	7377.55	6795.031	6795	6656.004	6496.653	6340.947	6616.727	6457.5
100	6182.847	5976.993	5976	5741.491	5830.405	5543.316	5813.641	5717.786
120	5345.477	5336.53	5333	5045.655	5164.157	4926.895	5161.247	5156.309
140	4723.206	4811.152	4806	4502.424	4717.131	4437.053	4654.752	4707.633
160	4241.065	4370.234	4364	4060.765	4270.104	4037.947	4220.61	4335.324
180	3855.603	3993.579	3988	3706.971	3943.082	3706.842	3867.695	4017.547
200	3539.82	3669.56	3664	3409.898	3616.06	3445.789	3561.061	3740.44
300	2544.382	2575.664	2573	2448.925	2641.862	2518.579	2551.606	2723.446
400	2011.877	1993.014	1994	1934.808	2093.435	2001.842	2003.42	2051.232
500	1677.281	1668.653	1669	1611.595	1870.414	1671.632	1698.259	1583.453
600	1446.345	1465.899	1465	1389.349	1647.393	1446.737	1482.876	1270.686
700	1276.785	1292.656	1292	1227.543	1424.372	1277.263	1302.767	1091.073
800	1146.7	1159.956	1160	1101.657	1201.351	1146.947	1153.982	1033.458
900	1043.566	1054.8	1055	1004.462	1091.324	1043.6	1049.837	1091.553
1000	959.688	969.233	969	978.096	981.297	959.442	969.795	1261.542

Appendix

Mass stopping power for Fluorine ions interacts with the Bone using (SRIM, CasP, PASS,SRIM dictionary)programs and Bethe formulae

E(MeV)	Mass Stopping power MeV/(g/cm²) For Bone Tissue					Present Work	
	Bethe	SRIM	Dic.SRIM	PASS	CaSP	Average S.P.	S.P.(P.W)
0.025	----	593.621	594.5	1119.818	58.207	591.537	795.873
0.03	----	650.286	651.2	1225.597	77.659	651.185	790.902
0.04	----	790.767	791.9	1414.977	116.564	778.552	863.078
0.06	----	1005.812	1007	1732.401	184.091	982.326	983.418
0.08	----	1075.841	1077	1998.625	251.617	1100.771	1100.482
0.1	----	1162.786	1164	2237.747	319.144	1220.919	1215.6
0.2	----	1802.178	1805	3182.396	640.937	1857.628	1766.471
0.3	----	2389.47	2394	3937.396	920.507	2410.343	2279.844
0.4	----	2860.182	2865	4558.451	1217.109	2875.186	2759.204
0.6	----	3602.119	3609	5615.973	1887.851	3678.736	3627.323
0.8	----	4222.975	4231	6490.431	2400.089	4336.124	4390.624
1	----	4796.359	4806	7236.56	2878.651	4929.393	5064.951
1.1	----	5073.421	5083	7563.977	3155.668	5219.016	5372.864
1.2	----	5345.535	5356	7867.289	3432.685	5500.377	5663.16
1.3	----	5612.867	5624	8149.061	3673.395	5764.831	5937.09
1.4	----	5875.526	5887	8408.192	3914.104	6021.206	6195.791
1.5	----	6133.11	6145	8648.247	4154.814	6270.293	6440.301
1.6	----	6385.081	6398	8873.058	4395.524	6512.916	6671.568
1.7	----	6631.653	6645	9085.53	4599.031	6740.304	6890.459
1.8	----	6872.469	6885	9277.652	4802.538	6959.415	7097.77
2	----	7332.529	7347	9641.577	5209.553	7382.665	7480.519
2.25	----	7868.589	7884	10036.471	5610.918	7849.994	7905.673
2.5	----	8358.241	8374	10364.809	5982.083	8269.783	8279.455
2.75	----	8799.885	8817	10640.196	6307.949	8641.257	8608.871
3	----	9194.358	9212	10870.93	6592.653	8967.485	8899.759
3.25	----	9544.489	9562	11064.592	6857.449	9257.133	9157.017
3.5	----	9851.174	9870	11228.036	7083.774	9508.246	9384.785
3.75	----	10118.244	10140	11363.296	7314.809	9734.087	9586.586
4	----	10350.025	10370	11472.258	7548.984	9935.317	9765.434
4.5	----	10719.633	10740	11649.961	7861.327	10242.73	10064.284
5	----	10984.031	11010	11763.331	8173.669	10482.758	10298.183
5.5	----	11168.135	11190	11832.252	8387.983	10644.593	10479.935
6	----	11288.769	11310	11869.006	8602.298	10767.518	10619.421
6.5	----	11363.312	11380	11881.694	8728.823	10838.457	10724.371
7	----	11399.285	11420	11874.358	8855.348	10887.248	10800.91
8	----	11392.04	11420	11816.68	9108.399	10891.955	10887.408
9	----	11320.566	11340	11724.71	9182.542	10934.28	10908.018
10	----	11208.235	11230	11612.369	9256.686	10826.822	10882.294
12	----	10920.559	10940	11355.842	9404.972	10655.343	10741.838
14	----	10608.574	10630	11084.416	9306.926	10407.479	10533.493
16	----	10295.739	10320	10813.095	9208.88	10159.428	10292.646
18	----	9998.828	10020	10547.978	9049.252	9904.014	10038.689
20	----	9719.747	9739	10287.364	8889.624	9658.934	9782.517
40	9686.177	7791.048	7808	8183.211	7212.099	7748.59	7677.718
60	7163.602	6580.701	6595	6727.676	6136.394	6509.943	6363.849
80	5751.735	5700.288	5712	5699.253	5297.653	5602.299	5488.325
100	4838.725	5028.308	5039	4928.504	4777.721	4943.383	4857.459
120	4195.384	4491.362	4501	4346.643	4257.788	4399.198	4375.17
140	3715.384	4050.127	4059	3893.924	3908.09	3977.785	3989.811
160	3342.299	3680.989	3689	3526.388	3558.391	3613.692	3671.406
180	3043.254	3368.193	3376	3231.974	3298.293	3318.615	3401.432
200	2797.733	3101.351	3108	2979.755	3038.194	3056.825	3167.848
300	2020.409	2214.756	2220	2140.597	2246.952	2205.576	2329.99
400	1602.261	1744.984	1749	1703.42	1674.367	1717.943	1794.513
500	1338.578	1471.318	1475	1423.111	1505.188	1468.654	1428.81
600	1156.116	1287.366	1290	1230.774	1336.009	1286.037	1184.954
700	1021.881	1137.018	1140	1090.262	1166.83	1133.527	1041.423
800	918.733	1021.507	1024	976.66	997.651	1004.954	987.117
900	836.848	929.902	932.1	889.043	910.709	915.438	1015.734
1000	770.178	855.191	857.2	877.117	823.767	842.837	1123.429

Appendix

 Mass stopping power for **Flourier** ions interacts with the **Skin** using (SRIM, CasP, PASS,SRIM dictionary)programs and Bethe formulae

E(MeV)	Mass Stopping power MeV/(g/cm^2) For Skin Tissue						
						Present Work	
	Bethe	SRIM	Dic.SRIM	PASS	CaSP	Average S.P.	S.P.(P.W)
0.025	-----	783.969	813.3	1453.602	35.665	781.634	1031.3
0.03	-----	858.827	891	1590.83	52.759	848.354	1065.568
0.04	-----	1045.033	1083	1834.329	86.946	1012.327	1133.797
0.06	-----	1310.497	1355	2241.244	175.081	1270.455	1269.041
0.08	-----	1367.741	1415	2584.674	263.216	1407.658	1402.688
0.1	-----	1450.349	1500	2887.154	351.351	1547.214	1534.763
0.2	-----	2167.874	2235	4080.585	814.371	2324.458	2172.366
0.3	-----	2840.371	2914	5005.242	1238.327	2999.485	2774.081
0.4	-----	3374.393	3449	5793.657	1619	3559.013	3342.59
0.6	-----	4210.167	4287	7123.751	2363.742	4496.165	4390.894
0.8	-----	4919.137	4998	8235.658	2981.605	5283.6	5369.887
1	-----	5595.18	5675	9187.552	3564.407	6005.535	6124.342
1.1	-----	5930.265	6011	9610.714	3861.554	6353.383	6520.882
1.2	-----	6265.587	6347	10004.342	4158.701	6693.907	6891.868
1.3	-----	6600.452	6683	10371.064	4461.676	7029.048	7242.431
1.4	-----	6934.653	7017	10708.748	4764.65	7356.263	7574.697
1.5	-----	7267.526	7350	11021.381	5067.625	7676.633	7890.069
1.6	-----	7598.105	7681	11313.715	5370.6	7990.855	8189.667
1.7	-----	7925.375	8008	11589.519	5623.723	8286.654	8474.46
1.8	-----	8249.536	8331	11837.805	5876.846	8573.797	8745.314
2	-----	8878.271	8960	12292.057	6383.093	9128.355	9248.31
2.25	-----	9627.447	9708	12769.828	6868.802	9743.519	9811.516
2.5	-----	10325.404	10400	13165.137	7320.924	10302.866	10310.535
2.75	-----	10965.159	11040	13494.562	7722.667	10805.597	10753.252
3	-----	11543.976	11620	13767.824	8068.83	11250.158	11146.38
3.25	-----	12062.918	12140	13994.249	8388.404	11646.393	11495.677
3.5	-----	12521.53	12590	14182.374	8657.198	11987.775	11806.104
3.75	-----	12923.783	13000	14334.98	8903.245	12290.502	12081.961
4	-----	13275.384	13350	14454.497	9134.128	12553.502	12326.986
4.5	-----	13841.209	13910	14636.55	9532.592	12980.088	12737.201
5	-----	14251.422	14320	14741.895	9931.055	13311.093	13058.377
5.5	-----	14542.012	14610	14796.259	10188.605	13534.219	13307.341
6	-----	14737.139	14810	14813.613	10446.155	13701.727	13497.335
6.5	-----	14863.05	14930	14803.236	10623.754	13805.01	13638.893
7	-----	14930.155	15000	14770.06	10801.353	13875.392	13740.467
8	-----	14943.432	15010	14658.523	11156.551	13942.127	13849.757
9	-----	14854.713	14920	14511.134	11283.29	13892.284	**13866.269**
10	-----	14699.242	14770	14342.256	11410.029	13805.382	13817.918
12	-----	14278.981	14350	13972.13	11663.507	13566.155	13598.453
14	-----	13806.497	13870	13589.794	11552.965	13204.814	13288.292
16	-----	13324.628	13390	13211.703	11442.423	12842.188	12937.883
18	-----	12862.406	12920	12845.154	11203.817	12457.844	12574.349
20	-----	12425.708	12490	12492.094	10965.211	12093.253	12212.475
40	12620.366	9513.218	9550	9720.014	8741.501	9381.183	9372.062
60	9246.551	7924.553	7949	7909.422	7464.745	7811.93	7693.837
80	7382.311	6795.866	6811	6658.052	6503.885	6692.201	6607.695
100	6186.173	5972.467	5982	5742.206	5836.003	5883.169	5838.006
120	5347.92	5327.956	5332	5045.553	5168.121	5218.408	5255.268
140	4725.062	4800.109	4801	4501.816	4719.089	4705.504	4792.176
160	4242.508	4358.041	4357	4059.835	4270.058	4261.233	4410.577
180	3856.745	3981.219	3979	3705.85	3942.057	3902.031	4087.303
200	3540.734	3657.813	3656	3408.66	3614.056	3584.132	3807.494
300	2544.699	2570.603	2571	2447.595	2639.766	2557.241	2798.48
400	2011.958	1993.453	1997	1933.612	2091.599	2003.916	2143.7
500	1677.248	1670.049	1673	1610.532	1868.714	1705.574	1687.306
600	1446.25	1465.079	1467	1388.394	1645.829	1491.576	1373.816
700	1276.654	1291.921	1294	1226.673	1422.944	1308.885	1178.539
800	1146.547	1159.211	1161	1100.858	1200.059	1155.282	1088.818
900	1043.4	1054.122	1055	1003.718	1090.114	1050.739	1097.496
1000	959.514	968.585	969.7	975.6	980.17	994.539	1200.221

Appendix

Appendix (B): Range, thickness, linear energy transfer, absorbed dose, equivalent dose, effective dose, and Stopping Time

for Lithium ioninteract with Adipose tissue

E(MeV)	Range ($\frac{g}{cm^2}$)	Thickness (cm)	LET MeV ($\frac{MeV}{cm}$)	Absorbed Dose × 10^{-6} (rad)	Equivalent Dose× 10^{-5} (rem)	Effective Dose× 10^{-7} (rem)	Stopping Time (nm)
0.025	0.0017	0.00185	712.671	0.0004	0.0008	0.0096	0.037
0.03	0.00433	0.0047	757.669	0.0005	0.0010	0.0012	0.086
0.04	0.00801	0.00871	845.581	0.0006	0.0013	0.0015	0.138
0.06	0.0124	0.01348	1013.416	0.0010	0.0019	0.0023	0.174
0.08	0.01502	0.01632	1171.239	0.0013	0.0026	0.0031	0.182
0.1	0.01681	0.01827	1319.756	0.0016	0.0032	0.0038	0.183
0.2	0.02126	0.02311	1943.517	0.0032	0.0064	0.0077	0.163
0.3	0.02324	0.02527	2412.63	0.0048	0.0096	0.0115	0.146
0.4	0.02443	0.02655	2764.831	0.0064	0.0128	0.0154	0.133
0.6	0.02584	0.02808	3240.218	0.0096	0.0192	0.0230	0.115
0.8	0.02668	0.029	3513.872	0.0128	0.0256	0.0307	0.102
1	0.02725	0.02962	3664.425	0.0160	0.0320	0.0384	0.094
1.1	0.02748	0.02987	3708.466	0.0176	0.0352	0.0422	0.090
1.2	0.02768	0.03008	3737.054	0.0192	0.0384	0.0461	0.087
1.3	0.02785	0.03027	3753.158	0.0208	0.0416	0.0499	0.084
1.4	0.02801	0.03044	3756.894	0.0224	0.0448	0.0538	0.081
1.5	0.02815	0.03059	3759.14	0.0240	0.0480	0.0576	0.079
1.6	0.02749	0.02988	3747.948	0.0256	0.0512	0.0614	0.075
1.7	0.02759	0.02999	3733.545	0.0272	0.0544	0.0653	0.073
1.8	0.02769	0.0301	3714.702	0.0288	0.0576	0.0691	0.071
2	0.02788	0.03031	3666.878	0.0320	0.0640	0.0768	0.068
2.25	0.02812	0.03057	3594.176	0.0360	0.0720	0.0864	0.064
2.5	0.02835	0.03082	3513.109	0.0400	0.0800	0.0960	0.062
2.75	0.02858	0.03106	3427.88	0.0440	0.0880	0.1056	0.059
3	0.0288	0.0313	3341.196	0.0480	0.0960	0.1152	0.057
3.25	0.02902	0.03154	3254.802	0.0520	0.1040	0.1248	0.055
3.5	0.02923	0.03177	3169.817	0.0560	0.1120	0.1344	0.054
3.75	0.02944	0.032	3086.946	0.0600	0.1200	0.1440	0.052
4	0.02964	0.03222	3006.616	0.0640	0.1280	0.1536	0.051
4.5	0.03005	0.03266	2854.413	0.0720	0.1440	0.1728	0.049
5	0.03044	0.03308	2713.852	0.0800	0.1600	0.1920	0.047
5.5	0.03082	0.0335	2584.594	0.0880	0.1760	0.2112	0.045
6	0.0312	0.03391	2465.89	0.0960	0.1920	0.2304	0.044
6.5	0.03156	0.03431	2356.844	0.1040	0.2080	0.2496	0.043
7	0.03192	0.0347	2256.546	0.1120	0.2240	0.2688	0.041
8	0.03263	0.03546	2078.812	0.1280	0.2560	0.3072	0.040
9	0.03331	0.0362	1926.661	0.1440	0.2880	0.3456	0.038
10	0.03397	0.03693	1795.263	0.1600	0.3200	0.3840	0.037
12	0.03526	0.03832	1580.349	0.1920	0.3840	0.4608	0.035
14	0.03649	0.03966	1412.41	0.2240	0.4480	0.5376	0.034
16	0.03768	0.04096	1277.787	0.2560	0.5120	0.6144	0.032
18	0.03884	0.04221	1167.56	0.2880	0.5760	0.6912	0.031
20	0.03996	0.04344	1075.694	0.3200	0.6400	0.7680	0.031
40	0.05011	0.05447	617.021	0.6400	1.2800	1.5360	0.027
60	0.05906	0.0642	445.127	0.9600	1.9200	2.3040	0.026
80	0.06732	0.07317	354.656	1.2800	2.5600	3.0720	0.026
100	0.07508	0.08161	298.491	1.6000	3.2000	3.8400	0.026
160	0.09647	0.10486	210.048	2.5600	5.1200	6.1440	0.026
180	0.10314	0.1121	192.718	2.8800	5.7600	6.9120	0.026
200	0.10963	0.11916	178.48	3.2000	6.4000	7.6800	0.027
300	0.14009	0.15228	132.277	4.8000	9.6000	11.5200	0.028
400	0.16818	0.1828	105.017	6.4000	12.8000	15.3600	0.029
500	0.19461	0.21153	85.414	8.0000	16.0000	19.2000	0.030
600	0.2198	0.23892	69.664	9.6000	19.2000	23.0400	0.031
700	0.24401	0.26522	56.122	11.2000	22.4000	26.8800	0.032
800	0.26739	0.29064	43.965	12.8000	25.6000	30.7200	0.032
900	0.29009	0.31532	32.732	14.4000	28.8000	34.5600	0.033
1000	0.31219	0.3357	22.148	16.0000	32.0000	38.4000	0.034

129

Appendix

Lithium ions interact with Blood tissue

E(MeV)	Range ($\frac{g}{cm^2}$)	Thickness (cm)	LET ($\frac{MeV}{cm}$)	Absorbed Dose $\times$ 10^{-6} (rad)	Equivalent Dose $\times$ 10^{-5} (rem)	Effective Dose $\times$ 10^{-7} (rem)	Stopping Time (nm)
0.025	0.0023	0.0021	601.103	0.0004	0.0008	0.0096	0.043
0.03	0.0058	0.0055	643.938	0.0005	0.0010	0.0115	0.100
0.04	0.0108	0.0101	727.681	0.0006	0.0013	0.0154	0.160
0.06	0.0165	0.0156	887.794	0.0010	0.0019	0.0230	0.201
0.08	0.0199	0.0188	1038.681	0.0013	0.0026	0.0307	0.210
0.1	0.0222	0.021	1181.017	0.0016	0.0032	0.0384	0.210
0.2	0.0278	0.0263	1792.281	0.0032	0.0064	0.0768	0.186
0.3	0.0303	0.0285	2236.100	0.0048	0.0096	0.1152	0.165
0.4	0.0317	0.0299	2588.806	0.0064	0.0128	0.1536	0.149
0.6	0.0334	0.0315	3075.319	0.0096	0.0192	0.2304	0.128
0.8	0.0343	0.0324	3371.608	0.0128	0.0256	0.3072	0.115
1	0.035	0.033	3549.511	0.0160	0.0320	0.3840	0.104
1.1	0.0353	0.0333	3607.810	0.0176	0.0352	0.4224	0.100
1.2	0.0355	0.0335	3650.661	0.0192	0.0384	0.4608	0.097
1.3	0.0357	0.0337	3680.845	0.0208	0.0416	0.4992	0.093
1.4	0.0359	0.0338	3700.590	0.0224	0.0448	0.5376	0.090
1.5	0.036	0.034	3715.636	0.0240	0.0480	0.5760	0.088
1.6	0.0371	0.035	3713.609	0.0256	0.0512	0.6144	0.087
1.7	0.0372	0.0351	3711.698	0.0272	0.0544	0.6528	0.085
1.8	0.0373	0.0352	3706.608	0.0288	0.0576	0.6912	0.083
2	0.0375	0.0354	3680.852	0.0320	0.0640	0.7680	0.079
2.25	0.0377	0.0356	3632.749	0.0360	0.0720	0.8640	0.075
2.5	0.038	0.0358	3573.169	0.0400	0.0800	0.9600	0.072
2.75	0.0382	0.036	3506.606	0.0440	0.0880	1.0560	0.069
3	0.0384	0.0362	3436.077	0.0480	0.0960	1.1520	0.066
3.25	0.0386	0.0364	3363.626	0.0520	0.1040	1.2480	0.064
3.5	0.0388	0.0366	3290.648	0.0560	0.1120	1.3440	0.062
3.75	0.039	0.0368	3218.094	0.0600	0.1200	1.4400	0.060
4	0.0392	0.037	3146.610	0.0640	0.1280	1.5360	0.059
4.5	0.0396	0.0374	3008.421	0.0720	0.1440	1.7280	0.056
5	0.04	0.0378	2877.970	0.0800	0.1600	1.9200	0.053
5.5	0.0404	0.0381	2755.855	0.0880	0.1760	2.1120	0.051
6	0.0408	0.0385	2642.027	0.0960	0.1920	2.3040	0.050
6.5	0.0412	0.0388	2536.121	0.1040	0.2080	2.4960	0.048
7	0.0415	0.0392	2437.627	0.1120	0.2240	2.6880	0.047
8	0.0422	0.0398	2260.646	0.1280	0.2560	3.0720	0.045
9	0.0429	0.0405	2106.754	0.1440	0.2880	3.4560	0.043
10	0.0435	0.0411	1972.140	0.1600	0.3200	3.8400	0.041
12	0.0448	0.0423	1748.643	0.1920	0.3840	4.6080	0.039
14	0.0461	0.0434	1571.190	0.2240	0.4480	5.3760	0.037
16	0.0472	0.0446	1427.193	0.2560	0.5120	6.1440	0.035
18	0.0484	0.0457	1308.143	0.2880	0.5760	6.9120	0.034
20	0.0495	0.0467	1208.139	0.3200	0.6400	7.6800	0.033
40	0.0596	0.0563	698.156	0.6400	1.2800	15.3600	0.028
60	0.0686	0.0647	502.348	0.9600	1.9200	23.0400	0.026
80	0.0768	0.0725	398.189	1.2800	2.5600	30.7200	0.026
100	0.0846	0.0798	333.120	1.6000	3.2000	38.4000	0.025
120	0.092	0.0868	288.331	1.9200	3.8400	46.0800	0.025
140	0.0991	0.0935	255.422	2.2400	4.4800	53.7600	0.025
160	0.106	0.1	230.081	2.5600	5.1200	61.4400	0.025
180	0.1127	0.1063	209.863	2.8800	5.7600	69.1200	0.025
200	0.1192	0.1125	193.282	3.2000	6.4000	76.8000	0.025
300	0.1498	0.1413	140.232	4.8000	9.6000	115.2000	0.026
400	0.178	0.1679	110.640	6.4000	12.8000	153.6000	0.027
500	0.2045	0.1929	91.398	8.0000	16.0000	192.0000	0.027
600	0.2298	0.2168	78.070	9.6000	19.2000	230.4000	0.028
700	0.2541	0.2398	68.740	11.2000	22.4000	268.8000	0.029
800	0.2777	0.2619	62.446	12.8000	25.6000	307.2000	0.029
900	0.3005	0.2835	58.650	14.4000	28.8000	345.6000	0.030
1000	0.3227	0.3045	57.028	16.0000	32.0000	384.0000	0.030

Appendix

Lithium ions interact with Brain

E(MeV)	Range ($\frac{g}{cm^2}$)	Thickness (cm)	LET MeV ($\frac{MeV}{cm}$)	Absorbed Dose × 10^{-6} (rad)	Equivalent Dose× 10^{-5} (rem)	Effective Dose× 10^{-7} (rem)	Stopping Time (nm)
0.025	0.002	0.00193	63297	0.0004	0.0008	0.0008	0.039
0.03	0.005	0.00484	70171	0.0005	0.0010	0.0010	0.088
0.04	0.0093	0.00892	81697	0.0006	0.0013	0.0013	0.141
0.06	0.0143	0.01377	100732	0.0010	0.0019	0.0019	0.178
0.08	0.0173	0.01665	117213	0.0013	0.0026	0.0026	0.186
0.1	0.0194	0.01862	132159	0.0016	0.0032	0.0032	0.186
0.2	0.0244	0.02351	192517	0.0032	0.0064	0.0064	0.166
0.3	0.0267	0.02567	236683	0.0048	0.0096	0.0096	0.148
0.4	0.028	0.02696	269866	0.0064	0.0128	0.0128	0.135
0.6	0.0296	0.02849	314422	0.0096	0.0192	0.0192	0.116
0.8	0.0306	0.0294	340537	0.0128	0.0256	0.0256	0.104
1	0.0312	0.03002	355497	0.0160	0.0320	0.0320	0.095
1.1	0.0315	0.03026	360145	0.0176	0.0352	0.0352	0.091
1.2	0.0317	0.03048	363384	0.0192	0.0384	0.0384	0.088
1.3	0.0319	0.03066	365479	0.0208	0.0416	0.0416	0.085
1.4	0.0321	0.03083	36664	0.0224	0.0448	0.0448	0.082
1.5	0.0322	0.03098	367033	0.0240	0.0480	0.0480	0.080
1.6	0.0332	0.03188	366795	0.0256	0.0512	0.0512	0.080
1.7	0.0333	0.03197	366036	0.0272	0.0544	0.0544	0.078
1.8	0.0334	0.03207	364848	0.0288	0.0576	0.0576	0.076
2	0.0336	0.03226	361467	0.0320	0.0640	0.0640	0.072
2.25	0.0338	0.03249	355909	0.0360	0.0720	0.0720	0.069
2.5	0.034	0.03272	349422	0.0400	0.0800	0.0800	0.065
2.75	0.0343	0.03294	342401	0.0440	0.0880	0.0880	0.063
3	0.0345	0.03315	335106	0.0480	0.0960	0.0960	0.061
3.25	0.0347	0.03336	327712	0.0520	0.1040	0.1040	0.059
3.5	0.0349	0.03357	320335	0.0560	0.1120	0.1120	0.057
3.75	0.0351	0.03377	313055	0.0600	0.1200	0.1200	0.055
4	0.0353	0.03397	305923	0.0640	0.1280	0.1280	0.054
4.5	0.0357	0.03437	292221	0.0720	0.1440	0.1440	0.051
5	0.0361	0.03475	279366	0.0800	0.1600	0.1600	0.049
5.5	0.0365	0.03512	267383	0.0880	0.1760	0.1760	0.047
6	0.0369	0.03549	256248	0.0960	0.1920	0.1920	0.046
6.5	0.0373	0.03585	245912	0.1040	0.2080	0.2080	0.045
7	0.0376	0.0362	236316	0.1120	0.2240	0.2240	0.043
8	0.0384	0.03689	219108	0.1280	0.2560	0.2560	0.041
9	0.0391	0.03756	204171	0.1440	0.2880	0.2880	0.040
10	0.0397	0.03821	191121	0.1600	0.3200	0.3200	0.038
12	0.041	0.03947	169477	0.1920	0.3840	0.3840	0.036
14	0.0423	0.04068	152305	0.2240	0.4480	0.4480	0.034
16	0.0435	0.04185	138376	0.2560	0.5120	0.5120	0.033
18	0.0447	0.04298	126863	0.2880	0.5760	0.5760	0.032
20	0.0459	0.04409	117191	0.3200	0.6400	0.6400	0.031
40	0.0563	0.0541	67860	0.6400	1.2800	1.2800	0.027
60	0.0655	0.06296	48906	0.9600	1.9200	1.9200	0.026
80	0.074	0.07113	38818	1.2800	2.5600	2.5600	0.025
100	0.082	0.07884	32511	1.6000	3.2000	3.2000	0.025
120	0.0896	0.0862	28168	1.9200	3.8400	3.8400	0.025
140	0.097	0.09327	24973	2.2400	4.4800	4.4800	0.025
160	0.1041	0.10011	22511	2.5600	5.1200	5.1200	0.025
180	0.111	0.10676	20543	2.8800	5.7600	5.7600	0.025
200	0.1178	0.11323	18927	3.2000	6.4000	6.4000	0.025
300	0.1494	0.14364	13721	4.8000	9.6000	9.6000	0.026
400	0.1786	0.17173	10760	6.4000	12.8000	12.8000	0.027
500	0.2061	0.19821	8773	8.0000	16.0000	16.0000	0.028
600	0.2324	0.22348	7330	9.6000	19.2000	19.2000	0.029
700	0.2577	0.24777	6245	11.2000	22.4000	22.4000	0.030
800	0.2821	0.27127	5427	12.8000	25.6000	25.6000	0.030
900	0.3058	0.29409	4821	14.4000	28.8000	28.8000	0.031
1000	0.329	0.31632	4397	16.0000	32.0000	32.0000	0.032

Appendix

Lithium ions interact with Breast tissue

E(MeV)	Range ($\frac{g}{cm^2}$)	Thickness (cm)	LET ($\frac{MeV}{cm}$)	Absorbed Dose × 10^{-6} (rad)	Equivalent Dose× 10^{-5} (rem)	Effective Dose× 10^{-7} (rem)	Stopping Time (nm)
0.025	0.0021	0.002	675.319	0.0004	0.0008	0.0096	0.0407
0.03	0.0051	0.005	722.776	0.0005	0.0010	0.0115	0.0907
0.04	0.0093	0.0091	815.196	0.0006	0.0013	0.0154	0.1434
0.06	0.0142	0.0139	990.570	0.0010	0.0019	0.0230	0.1797
0.08	0.0171	0.0168	1154.227	0.0013	0.0026	0.0307	0.1878
0.1	0.0191	0.0188	1307.150	0.0016	0.0032	0.0384	0.1875
0.2	0.0241	0.0236	1938.539	0.0032	0.0064	0.0768	0.1667
0.3	0.0262	0.0257	2401.887	0.0048	0.0096	0.1152	0.1484
0.4	0.0275	0.027	2747.931	0.0064	0.0128	0.1536	0.1348
0.6	0.029	0.0285	3208.196	0.0096	0.0192	0.2304	0.1162
0.8	0.0299	0.0293	3474.770	0.0128	0.0256	0.3072	0.1037
1	0.0305	0.0299	3625.724	0.0160	0.0320	0.3840	0.0947
1.1	0.0308	0.0302	3672.114	0.0176	0.0352	0.4224	0.0910
1.2	0.031	0.0304	3704.130	0.0192	0.0384	0.4608	0.0877
1.3	0.0312	0.0306	3724.512	0.0208	0.0416	0.4992	0.0848
1.4	0.0313	0.0307	3735.420	0.0224	0.0448	0.5376	0.0821
1.5	0.0315	0.0309	3738.583	0.0240	0.0480	0.5760	0.0797
1.6	0.0328	0.0322	3735.389	0.0256	0.0512	0.6144	0.0805
1.7	0.0329	0.0323	3726.967	0.0272	0.0544	0.6528	0.0783
1.8	0.033	0.0324	3714.238	0.0288	0.0576	0.6912	0.0763
2	0.0332	0.0326	3678.762	0.0320	0.0640	0.7680	0.0728
2.25	0.0334	0.0328	3621.192	0.0360	0.0720	0.8640	0.0691
2.5	0.0336	0.033	3554.462	0.0400	0.0800	0.9600	0.0659
2.75	0.0338	0.0332	3482.518	0.0440	0.0880	1.0560	0.0633
3	0.034	0.0334	3407.962	0.0480	0.0960	1.1520	0.0609
3.25	0.0342	0.0336	3332.527	0.0520	0.1040	1.2480	0.0589
3.5	0.0344	0.0338	3257.371	0.0560	0.1120	1.3440	0.0571
3.75	0.0346	0.034	3183.263	0.0600	0.1200	1.4400	0.0554
4	0.0348	0.0341	3110.712	0.0640	0.1280	1.5360	0.0540
4.5	0.0352	0.0345	2971.447	0.0720	0.1440	1.7280	0.0514
5	0.0356	0.0349	2840.874	0.0800	0.1600	1.9200	0.0493
5.5	0.0359	0.0352	2719.285	0.0880	0.1760	2.1120	0.0475
6	0.0363	0.0355	2601.627	0.0960	0.1920	2.3040	0.0459
6.5	0.0366	0.0359	2500.812	0.1040	0.2080	2.4960	0.0445
7	0.0369	0.0362	2403.465	0.1120	0.2240	2.6880	0.0433
8	0.0376	0.0369	2228.726	0.1280	0.2560	3.0720	0.0412
9	0.0382	0.0375	2076.982	0.1440	0.2880	3.4560	0.0395
10	0.0388	0.0381	1944.353	0.1600	0.3200	3.8400	0.0381
12	0.0401	0.0393	1724.264	0.1920	0.3840	4.6080	0.0358
14	0.0412	0.0404	1549.542	0.2240	0.4480	5.3760	0.0341
16	0.0423	0.0415	1407.733	0.2560	0.5120	6.1440	0.0328
18	0.0434	0.0426	1290.455	0.2880	0.5760	6.9120	0.0317
20	0.0445	0.0436	1191.905	0.3200	0.6400	7.6800	0.0308
40	0.0542	0.0532	688.675	0.6400	1.2800	15.3600	0.0266
60	0.0629	0.0616	495.167	0.9600	1.9200	23.0400	0.0252
80	0.0709	0.0695	392.220	1.2800	2.5600	30.7200	0.0246
100	0.0785	0.0769	327.942	1.6000	3.2000	38.4000	0.0243
120	0.0857	0.0841	283.733	1.9200	3.8400	46.0800	0.0243
140	0.0927	0.0909	251.281	2.2400	4.4800	53.7600	0.0243
160	0.0995	0.0976	226.315	2.5600	5.1200	61.4400	0.0244
180	0.1061	0.104	206.413	2.8800	5.7600	69.1200	0.0245
200	0.1125	0.1103	190.102	3.2000	6.4000	76.8000	0.0247
300	0.1429	0.1401	137.917	4.8000	9.6000	115.2000	0.0256
400	0.171	0.1677	108.594	6.4000	12.8000	153.6000	0.0265
500	0.1977	0.1938	89.122	8.0000	16.0000	192.0000	0.0274
600	0.2231	0.2187	75.099	9.6000	19.2000	230.4000	0.0282
700	0.2477	0.2428	64.621	11.2000	22.4000	268.8000	0.0290
800	0.2715	0.2661	56.733	12.8000	25.6000	307.2000	0.0297
900	0.2946	0.2888	50.901	14.4000	28.8000	345.6000	0.0304
1000	0.3172	0.3109	46.803	16.0000	32.0000	384.0000	0.0311

Appendix

Lithium ions interact with Lung tissue

E(MeV)	Range ($\frac{g}{cm^2}$)	Thickness (cm)	LET ($\frac{MeV}{cm}$)	Absorbed Dose × 10^{-6} (rad)	Equivalent Dose× 10^{-5} (rem)	Effective Dose× 10^{-7} (rem)	Stopping Time (nm)
0.025	0.00203	0.00194	684.347	0.0004	0.0008	0.0096	0.0387
0.03	0.00516	0.00492	730.346	0.0005	0.0010	0.0115	0.0898
0.04	0.00955	0.00909	819.903	0.0006	0.0013	0.0154	0.1437
0.06	0.01473	0.01402	989.766	0.0010	0.0019	0.0230	0.1810
0.08	0.0178	0.01695	1148.189	0.0013	0.0026	0.0307	0.1895
0.1	0.0199	0.01895	1296.145	0.0016	0.0032	0.0384	0.1895
0.2	0.02507	0.02388	1906.315	0.0032	0.0064	0.0768	0.1688
0.3	0.02735	0.02605	2353.493	0.0048	0.0096	0.1152	0.1504
0.4	0.02871	0.02734	2687.271	0.0064	0.0128	0.1536	0.1367
0.6	0.03031	0.02887	3131.348	0.0096	0.0192	0.2304	0.1178
0.8	0.03126	0.02977	3389.079	0.0128	0.0256	0.3072	0.1052
1	0.03191	0.03039	3535.683	0.0160	0.0320	0.3840	0.0961
1.1	0.03216	0.03063	3581.023	0.0176	0.0352	0.4224	0.0923
1.2	0.03238	0.03084	3612.536	0.0192	0.0384	0.4608	0.0890
1.3	0.03258	0.03103	3632.848	0.0208	0.0416	0.4992	0.0860
1.4	0.03275	0.03119	3644.031	0.0224	0.0448	0.5376	0.0833
1.5	0.03291	0.03134	3647.74	0.0240	0.0480	0.5760	0.0809
1.6	0.03455	0.0329	3645.308	0.0256	0.0512	0.6144	0.0822
1.7	0.03464	0.03299	3637.817	0.0272	0.0544	0.6528	0.0800
1.8	0.03473	0.03308	3626.151	0.0288	0.0576	0.6912	0.0779
2	0.03491	0.03325	3593.079	0.0320	0.0640	0.7680	0.0743
2.25	0.03513	0.03346	3538.822	0.0360	0.0720	0.8640	0.0705
2.5	0.03535	0.03366	3475.54	0.0400	0.0800	0.9600	0.0673
2.75	0.03556	0.03386	3407.045	0.0440	0.0880	1.0560	0.0646
3	0.03576	0.03406	3335.857	0.0480	0.0960	1.1520	0.0622
3.25	0.03597	0.03425	3263.663	0.0520	0.1040	1.2480	0.0601
3.5	0.03616	0.03444	3191.595	0.0560	0.1120	1.3440	0.0582
3.75	0.03636	0.03463	3120.412	0.0600	0.1200	1.4400	0.0565
4	0.03655	0.03481	3050.618	0.0640	0.1280	1.5360	0.0550
4.5	0.03693	0.03517	2916.382	0.0720	0.1440	1.7280	0.0524
5	0.0373	0.03553	2790.25	0.0800	0.1600	1.9200	0.0502
5.5	0.03766	0.03587	2671.175	0.0880	0.1760	2.1120	0.0484
6	0.03802	0.03621	2562.616	0.0960	0.1920	2.3040	0.0467
6.5	0.03837	0.03654	2460.713	0.1040	0.2080	2.4960	0.0453
7	0.03871	0.03687	2365.953	0.1120	0.2240	2.6880	0.0441
8	0.03938	0.03751	2195.657	0.1280	0.2560	3.0720	0.0419
9	0.04004	0.03813	2047.481	0.1440	0.2880	3.4560	0.0402
10	0.04067	0.03874	1917.742	0.1600	0.3200	3.8400	0.0387
12	0.04191	0.03991	1701.99	0.1920	0.3840	4.6080	0.0364
14	0.0431	0.04105	1530.311	0.2240	0.4480	5.3760	0.0347
16	0.04425	0.04215	1390.719	0.2560	0.5120	6.1440	0.0333
18	0.04538	0.04322	1275.108	0.2880	0.5760	6.9120	0.0322
20	0.04648	0.04426	1177.845	0.3200	0.6400	7.6800	0.0313
40	0.05648	0.05379	679.764	0.6400	1.2800	15.3600	0.0269
60	0.0654	0.06229	487.859	0.9600	1.9200	23.0400	0.0254
80	0.0737	0.07019	385.874	1.2800	2.5600	30.7200	0.0248
100	0.08156	0.07767	322.344	1.6000	3.2000	38.4000	0.0246
120	0.08908	0.08484	278.783	1.9200	3.8400	46.0800	0.0245
140	0.09633	0.09175	246.918	2.2400	4.4800	53.7600	0.0245
160	0.10337	0.09845	222.494	2.5600	5.1200	61.4400	0.0246
180	0.11022	0.10497	203.097	2.8800	5.7600	69.1200	0.0247
200	0.1169	0.11134	187.256	3.2000	6.4000	76.8000	0.0249
300	0.14846	0.14139	136.969	4.8000	9.6000	115.2000	0.0258
400	0.17779	0.16933	108.824	6.4000	12.8000	153.6000	0.0268
500	0.20556	0.19578	89.824	8.0000	16.0000	192.0000	0.0277
600	0.23216	0.2211	75.568	9.6000	19.2000	230.4000	0.0285
700	0.25781	0.24553	64.154	11.2000	22.4000	268.8000	0.0293
800	0.28268	0.26922	54.624	12.8000	25.6000	307.2000	0.0301
900	0.30689	0.29227	46.446	14.4000	28.8000	345.6000	0.0308
1000	0.33052	0.31478	39.297	16.0000	32.0000	384.0000	0.0315

Appendix

Lithium ions interact with muscle tissue

E(MeV)	Range ($\frac{g}{cm^2}$)	Thickness (cm)	LET MeV ($\frac{MeV}{cm}$)	Absorbed Dose $\times$ 10^{-6} (rad)	Equivalent Dose$\times$ 10^{-5} (rem)	Effective Dose$\times$ 10^{-7} (rem)	Stopping Time (nm)
0.025	0.00215	0.00205	642.411	0.0004	0.0008	0.0096	0.0410
0.03	0.00553	0.00527	684.235	0.0005	0.0010	0.0115	0.0962
0.04	0.01024	0.00976	766.152	0.0006	0.0013	0.0154	0.1542
0.06	0.01578	0.01503	923.330	0.0010	0.0019	0.0230	0.1940
0.08	0.01906	0.01815	1072.105	0.0013	0.0026	0.0307	0.2029
0.1	0.02128	0.02026	1213.004	0.0016	0.0032	0.0384	0.2026
0.2	0.02672	0.02545	1815.177	0.0032	0.0064	0.0768	0.1799
0.3	0.02909	0.02771	2279.989	0.0048	0.0096	0.1152	0.1599
0.4	0.0305	0.02905	2641.540	0.0064	0.0128	0.1536	0.1452
0.6	0.03215	0.03062	3145.356	0.0096	0.0192	0.2304	0.1250
0.8	0.03312	0.03155	3453.257	0.0128	0.0256	0.3072	0.1115
1	0.03378	0.03218	3636.829	0.0160	0.0320	0.3840	0.1017
1.1	0.03404	0.03242	3696.085	0.0176	0.0352	0.4224	0.0977
1.2	0.03427	0.03264	3738.785	0.0192	0.0384	0.4608	0.0942
1.3	0.03447	0.03283	3767.351	0.0208	0.0416	0.4992	0.0910
1.4	0.03464	0.03299	3792.713	0.0224	0.0448	0.5376	0.0882
1.5	0.0348	0.03315	3797.517	0.0240	0.0480	0.5760	0.0856
1.6	0.03603	0.03432	3798.654	0.0256	0.0512	0.6144	0.0858
1.7	0.03613	0.03441	3793.766	0.0272	0.0544	0.6528	0.0834
1.8	0.03623	0.0345	3783.727	0.0288	0.0576	0.6912	0.0813
2	0.03641	0.03468	3751.449	0.0320	0.0640	0.7680	0.0775
2.25	0.03664	0.0349	3694.749	0.0360	0.0720	0.8640	0.0736
2.5	0.03687	0.03511	3626.507	0.0400	0.0800	0.9600	0.0702
2.75	0.03708	0.03532	3551.518	0.0440	0.0880	1.0560	0.0673
3	0.0373	0.03552	3472.973	0.0480	0.0960	1.1520	0.0648
3.25	0.03751	0.03572	3393.012	0.0520	0.1040	1.2480	0.0626
3.5	0.03771	0.03592	3313.069	0.0560	0.1120	1.3440	0.0607
3.75	0.03792	0.03611	3234.104	0.0600	0.1200	1.4400	0.0590
4	0.03812	0.0363	3156.748	0.0640	0.1280	1.5360	0.0574
4.5	0.03851	0.03668	3008.331	0.0720	0.1440	1.7280	0.0547
5	0.03889	0.03704	2869.452	0.0800	0.1600	1.9200	0.0524
5.5	0.03926	0.0374	2740.437	0.0880	0.1760	2.1120	0.0504
6	0.03963	0.03774	2620.988	0.0960	0.1920	2.3040	0.0487
6.5	0.03999	0.03809	2510.519	0.1040	0.2080	2.4960	0.0472
7	0.04034	0.03842	2408.340	0.1120	0.2240	2.6880	0.0459
8	0.04103	0.03908	2226.035	0.1280	0.2560	3.0720	0.0437
9	0.0417	0.03972	2068.820	0.1440	0.2880	3.4560	0.0419
10	0.04236	0.04034	1932.260	0.1600	0.3200	3.8400	0.0403
12	0.04363	0.04155	1707.442	0.1920	0.3840	4.6080	0.0379
14	0.04485	0.04271	1530.581	0.2240	0.4480	5.3760	0.0361
16	0.04603	0.04383	1388.093	0.2560	0.5120	6.1440	0.0346
18	0.04718	0.04493	1270.965	0.2880	0.5760	6.9120	0.0335
20	0.0483	0.046	1173.034	0.3200	0.6400	7.6800	0.0325
40	0.05846	0.05567	679.527	0.6400	1.2800	15.3600	0.0278
60	0.06749	0.06428	491.969	0.9600	1.9200	23.0400	0.0262
80	0.07586	0.07224	392.135	1.2800	2.5600	30.7200	0.0255
100	0.08376	0.07977	329.454	1.6000	3.2000	38.4000	0.0252
120	0.09132	0.08697	283.733	1.9200	3.8400	46.0800	0.0251
140	0.09859	0.0939	251.281	2.2400	4.4800	53.7600	0.0251
160	0.10564	0.10061	226.315	2.5600	5.1200	61.4400	0.0251
180	0.11249	0.10713	206.413	2.8800	5.7600	69.1200	0.0252
200	0.11917	0.1135	190.102	3.2000	6.4000	76.8000	0.0254
300	0.15064	0.14346	136.651	4.8000	9.6000	115.2000	0.0262
400	0.17979	0.17123	104.662	6.4000	12.8000	153.6000	0.0271
500	0.20733	0.19746	83.504	8.0000	16.0000	192.0000	0.0279
600	0.23366	0.22253	69.037	9.6000	19.2000	230.4000	0.0287
700	0.25901	0.24668	59.474	11.2000	22.4000	268.8000	0.0295
800	0.28356	0.27006	53.915	12.8000	25.6000	307.2000	0.0302
900	0.30743	0.29279	51.861	14.4000	28.8000	345.6000	0.0309
1000	0.33071	0.31496	53.011	16.0000	32.0000	384.0000	0.0315

Appendix

Lithium ions interact with Bone tissue

E(MeV)	Range ($\frac{g}{cm^2}$)	Thickness (cm)	LET MeV ($\frac{MeV}{cm}$)	Absorbed Dose × 10^{-6} (rad)	Equivalent Dose× 10^{-5} (rem)	Effective Dose× 10^{-7} (rem)	Stopping Time (nm)
0.025	0.0027	0.0025	954.802	0.0004	0.0008	0.0008	0.0286
0.03	0.0068	0.0063	1016.426	0.0005	0.0010	0.0010	0.0650
0.04	0.0126	0.0115	1136.866	0.0006	0.0013	0.0013	0.1040
0.06	0.0193	0.0177	1367.005	0.0010	0.0019	0.0019	0.1300
0.08	0.0234	0.0214	1583.704	0.0013	0.0026	0.0026	0.1360
0.1	0.0261	0.0239	1787.934	0.0016	0.0032	0.0032	0.1360
0.2	0.0328	0.0301	2650.307	0.0032	0.0064	0.0064	0.1210
0.3	0.0358	0.0328	3305.253	0.0048	0.0096	0.0096	0.1080
0.4	0.0376	0.0344	3809.108	0.0064	0.0128	0.0128	0.0978
0.6	0.0396	0.0363	4505.125	0.0096	0.0192	0.0192	0.0843
0.8	0.0409	0.0374	4925.514	0.0128	0.0256	0.0256	0.0752
1	0.0417	0.0382	5188.765	0.0160	0.0320	0.0320	0.0687
1.1	0.0420	0.0385	5272.728	0.0176	0.0352	0.0352	0.0660
1.2	0.0423	0.0388	5334.919	0.0192	0.0384	0.0384	0.0636
1.3	0.0426	0.0390	5379.116	0.0208	0.0416	0.0416	0.0615
1.4	0.0428	0.0392	5408.433	0.0224	0.0448	0.0448	0.0596
1.5	0.0430	0.0394	5425.412	0.0240	0.0480	0.0480	0.0578
1.6	0.0448	0.0410	5432.13	0.0256	0.0512	0.0512	0.0583
1.7	0.0449	0.0411	5430.294	0.0272	0.0544	0.0544	0.0567
1.8	0.0450	0.0412	5421.313	0.0288	0.0576	0.0576	0.0553
2	0.0453	0.0414	5386.41	0.0320	0.0640	0.0640	0.0527
2.25	0.0455	0.0417	5319.755	0.0360	0.0720	0.0720	0.0500
2.5	0.0458	0.0419	5236.357	0.0400	0.0800	0.0800	0.0477
2.75	0.0461	0.0422	5142.648	0.0440	0.0880	0.0880	0.0457
3	0.0463	0.0424	5042.96	0.0480	0.0960	0.0960	0.0440
3.25	0.0466	0.0426	4940.244	0.0520	0.1040	0.1040	0.0425
3.5	0.0468	0.0429	4836.523	0.0560	0.1120	0.1120	0.0412
3.75	0.0470	0.0431	4733.185	0.0600	0.1200	0.1200	0.0400
4	0.0473	0.0433	4631.18	0.0640	0.1280	0.1280	0.0389
4.5	0.0478	0.0437	4433.514	0.0720	0.1440	0.1440	0.0371
5	0.0482	0.0441	4246.395	0.0800	0.1600	0.1600	0.0355
5.5	0.0486	0.0445	4070.813	0.0880	0.1760	0.1760	0.0342
6	0.0491	0.0449	3906.803	0.0960	0.1920	0.1920	0.0330
6.5	0.0495	0.0453	3753.923	0.1040	0.2080	0.2080	0.0320
7	0.0499	0.0457	3611.506	0.1120	0.2240	0.2240	0.0311
8	0.0507	0.0465	3355.046	0.1280	0.2560	0.2560	0.0295
9	0.0515	0.0472	3131.479	0.1440	0.2880	0.2880	0.0283
10	0.0523	0.0479	2935.501	0.1600	0.3200	0.3200	0.0272
12	0.0538	0.0493	2609.273	0.1920	0.3840	0.3840	0.0256
14	0.0552	0.0499	2349.513	0.2240	0.4480	0.4480	0.0243
16	0.0566	0.0518	2138.247	0.2560	0.5120	0.5120	0.0233
18	0.0579	0.0524	1963.257	0.2880	0.5760	0.5760	0.0225
20	0.0592	0.0543	1816.036	0.3200	0.6400	0.6400	0.0218
40	0.0710	0.0651	1061.843	0.6400	1.2800	1.2800	0.0185
60	0.0815	0.0675	770.443	0.9600	1.9200	1.9200	0.0173
80	0.0911	0.0746	614.763	1.2800	2.5600	2.5600	0.0168
100	0.1002	0.0769	517.108	1.6000	3.2000	3.2000	0.0165
120	0.1088	0.0917	449.602	1.9200	3.8400	3.8400	0.0164
140	0.1171	0.0957	399.778	2.2400	4.4800	4.4800	0.0163
160	0.1252	0.1110	361.228	2.5600	5.1200	5.1200	0.0163
180	0.1330	0.1218	330.317	2.8800	5.7600	5.7600	0.0163
200	0.1406	0.1287	304.834	3.2000	6.4000	6.4000	0.0164
300	0.1762	0.2200	222.071	4.8000	9.6000	9.6000	0.0168
400	0.2092	0.2337	174.553	6.4000	12.8000	12.8000	0.0172
500	0.2402	0.2471	142.737	8.0000	16.0000	16.0000	0.0177
600	0.2698	0.2602	120.013	9.6000	19.2000	19.2000	0.0181
700	0.2982	0.2731	103.52	11.2000	22.4000	22.4000	0.0186
800	0.3257	0.2983	91.823	12.8000	25.6000	25.6000	0.0190
900	0.3524	0.3227	84.118	14.4000	28.8000	28.8000	0.0193
1000	0.3784	0.3466	79.924	16.0000	32.0000	32.0000	0.0197

Appendix

Lithium ions interact with Skin tissue

E(MeV)	Range ($\frac{g}{cm^2}$)	Thickness (cm)	LET ($\frac{MeV}{cm}$)	Absorbed Dose $\times$ 10^{-6} (rad)	Equivalent Dose$\times 10^{-5}$ (rem)	Effective Dose$\times$ 10^{-7} (rem)	Stopping Time (nm)
0.025	0.00189	0.00173	703.790	0.0004	0.0008	0.0008	0.0197
0.03	0.00502	0.00461	749.997	0.0005	0.0010	0.0010	0.0477
0.04	0.00941	0.00863	840.266	0.0006	0.0013	0.0013	0.0775
0.06	0.01459	0.01338	1012.606	0.0010	0.0019	0.0019	0.0981
0.08	0.01767	0.01621	1174.690	0.0013	0.0026	0.0026	0.1028
0.1	0.01976	0.01813	1327.259	0.0016	0.0032	0.0032	0.1029
0.2	0.02492	0.02287	1969.064	0.0032	0.0064	0.0064	0.0918
0.3	0.0272	0.02495	2452.997	0.0048	0.0096	0.0096	0.0818
0.4	0.02855	0.02619	2822.272	0.0064	0.0128	0.0128	0.0743
0.6	0.03014	0.02765	3325.470	0.0096	0.0192	0.0192	0.0641
0.8	0.03109	0.02852	3625.037	0.0128	0.0256	0.0256	0.0572
1	0.03173	0.02911	3799.166	0.0160	0.0320	0.0320	0.0522
1.1	0.03198	0.02934	3854.058	0.0176	0.0352	0.0352	0.0502
1.2	0.03221	0.02955	3892.864	0.0192	0.0384	0.0384	0.0484
1.3	0.0324	0.02972	3918.557	0.0208	0.0416	0.0416	0.0468
1.4	0.03257	0.02988	3933.513	0.0224	0.0448	0.0448	0.0453
1.5	0.03273	0.03003	3939.643	0.0240	0.0480	0.0480	0.0440
1.6	0.03406	0.03124	3938.499	0.0256	0.0512	0.0512	0.0443
1.7	0.03415	0.03133	3931.347	0.0272	0.0544	0.0544	0.0431
1.8	0.03424	0.03141	3919.229	0.0288	0.0576	0.0576	0.0420
2	0.03442	0.03158	3883.392	0.0320	0.0640	0.0640	0.0401
2.25	0.03465	0.03178	3823.201	0.0360	0.0720	0.0720	0.0380
2.5	0.03486	0.03198	3752.268	0.0400	0.0800	0.0800	0.0363
2.75	0.03507	0.03218	3675.154	0.0440	0.0880	0.0880	0.0348
3	0.03528	0.03237	3594.878	0.0480	0.0960	0.0960	0.0335
3.25	0.03548	0.03255	3513.454	0.0520	0.1040	0.1040	0.0324
3.5	0.03568	0.03274	3432.229	0.0560	0.1120	0.1120	0.0314
3.75	0.03588	0.03292	3352.102	0.0600	0.1200	0.1200	0.0305
4	0.03607	0.0331	3273.664	0.0640	0.1280	0.1280	0.0297
4.5	0.03646	0.03345	3123.217	0.0720	0.1440	0.1440	0.0283
5	0.03683	0.03379	2982.405	0.0800	0.1600	0.1600	0.0271
5.5	0.03719	0.03412	2851.536	0.0880	0.1760	0.1760	0.0261
6	0.03754	0.03444	2730.374	0.0960	0.1920	0.1920	0.0252
6.5	0.03789	0.03477	2618.583	0.1040	0.2080	0.2080	0.0245
7	0.03824	0.03508	2516.753	0.1120	0.2240	0.2240	0.0238
8	0.03891	0.0357	2320.939	0.1280	0.2560	0.2560	0.0227
9	0.03956	0.0363	2162.507	0.1440	0.2880	0.2880	0.0217
10	0.0402	0.03688	2022.580	0.1600	0.3200	0.3200	0.0209
12	0.04143	0.03801	1790.814	0.1920	0.3840	0.3840	0.0197
14	0.04262	0.0391	1607.579	0.2240	0.4480	0.4480	0.0188
16	0.04377	0.04016	1459.421	0.2560	0.5120	0.5120	0.0180
18	0.0449	0.04119	1337.282	0.2880	0.5760	0.5760	0.0174
20	0.04599	0.04219	1234.920	0.3200	0.6400	0.6400	0.0169
40	0.05593	0.05131	715.879	0.6400	1.2800	1.2800	0.0146
60	0.06478	0.05943	517.468	0.9600	1.9200	1.9200	0.0138
80	0.07299	0.06696	411.812	1.2800	2.5600	2.5600	0.0134
100	0.08076	0.07409	345.586	1.6000	3.2000	3.2000	0.0133
120	0.08818	0.0809	299.787	1.9200	3.8400	3.8400	0.0133
140	0.09534	0.08747	265.949	2.2400	4.4800	4.4800	0.0133
160	0.10228	0.09383	239.729	2.5600	5.1200	5.1200	0.0133
180	0.10903	0.10002	218.674	2.8800	5.7600	5.7600	0.0134
200	0.11561	0.10606	201.288	3.2000	6.4000	6.4000	0.0135
300	0.14665	0.13454	144.629	4.8000	9.6000	9.6000	0.0139
400	0.17544	0.16096	112.060	6.4000	12.8000	12.8000	0.0144
500	0.20268	0.18594	90.451	8.0000	16.0000	16.0000	0.0149
600	0.22873	0.20984	75.368	9.6000	19.2000	19.2000	0.0154
700	0.25383	0.23287	64.892	11.2000	22.4000	22.4000	0.0158
800	0.27816	0.25519	58.062	12.8000	25.6000	25.6000	0.0162
900	0.30182	0.2769	54.340	14.4000	28.8000	28.8000	0.0166
1000	0.32491	0.29808	53.403	16.0000	32.0000	32.0000	0.0169

Appendix

Carbon ions interact with Adipose tissue

E(MeV)	Range ($\frac{g}{cm^2}$)	Thickness (cm)	LET ($\frac{MeV}{cm}$)	Absorbed Dose × 10^{-6} (rad)	Equivalent Dose× 10^{-5} (rem)	Effective Dose× 10^{-7} (rem)	Stopping Time (nm)
0.025	0.00099	0.00107	1161.153	0.0004	0.0008	0.0096	0.0282
0.03	0.00276	0.003	1210.682	0.0005	0.0010	0.0115	0.0721
0.04	0.00527	0.00572	1308.511	0.0006	0.0013	0.0154	0.1190
0.06	0.00825	0.00897	1499.394	0.0010	0.0019	0.0230	0.1523
0.08	0.01004	0.01091	1684.158	0.0013	0.0026	0.0307	0.1605
0.1	0.01127	0.01224	1863.100	0.0016	0.0032	0.0384	0.1610
0.2	0.01433	0.01557	2682.116	0.0032	0.0064	0.0768	0.1448
0.3	0.0157	0.01706	3349.786	0.0048	0.0096	0.1152	0.1295
0.4	0.01652	0.01795	3965.094	0.0064	0.0128	0.1536	0.1180
0.6	0.01749	0.01902	4950.384	0.0096	0.0192	0.2304	0.1021
0.8	0.01808	0.01965	5709.158	0.0128	0.0256	0.3072	0.0914
1	0.01848	0.02009	6303.382	0.0160	0.0320	0.3840	0.0835
1.1	0.01864	0.02026	6552.161	0.0176	0.0352	0.4224	0.0803
1.2	0.01878	0.02041	6774.104	0.0192	0.0384	0.4608	0.0775
1.3	0.0189	0.02055	6972.464	0.0208	0.0416	0.4992	0.0749
1.4	0.01901	0.02066	7150.002	0.0224	0.0448	0.5376	0.0726
1.5	0.01911	0.02077	7309.083	0.0240	0.0480	0.5760	0.0705
1.6	0.0192	0.02087	7451.738	0.0256	0.0512	0.6144	0.0686
1.7	0.01928	0.02096	7579.724	0.0272	0.0544	0.6528	0.0668
1.8	0.01935	0.02104	7694.568	0.0288	0.0576	0.6912	0.0652
2	0.01949	0.02118	7889.994	0.0320	0.0640	0.7680	0.0623
2.25	0.01963	0.02133	8080.870	0.0360	0.0720	0.8640	0.0591
2.5	0.01974	0.02146	8224.431	0.0400	0.0800	0.9600	0.0564
2.75	0.01985	0.02157	8330.467	0.0440	0.0880	1.0560	0.0541
3	0.01993	0.02167	8406.425	0.0480	0.0960	1.1520	0.0520
3.25	0.02001	0.02175	8458.061	0.0520	0.1040	1.2480	0.0502
3.5	0.02008	0.02183	8480.746	0.0560	0.1120	1.3440	0.0485
3.75	0.02063	0.02243	8489.881	0.0600	0.1200	1.4400	0.0482
4	0.02067	0.02247	8505.460	0.0640	0.1280	1.5360	0.0467
4.5	0.02074	0.02255	8507.659	0.0720	0.1440	1.7280	0.0442
5	0.02081	0.02262	8423.043	0.0800	0.1600	1.9200	0.0421
5.5	0.02088	0.02269	8344.026	0.0880	0.1760	2.1120	0.0402
6	0.02094	0.02276	8250.306	0.0960	0.1920	2.3040	0.0386
6.5	0.02101	0.02283	8146.579	0.1040	0.2080	2.4960	0.0372
7	0.02107	0.0229	8036.231	0.1120	0.2240	2.6880	0.0360
8	0.02119	0.02303	7804.887	0.1280	0.2560	3.0720	0.0339
9	0.02131	0.02316	7569.202	0.1440	0.2880	3.4560	0.0321
10	0.02142	0.02329	7336.254	0.1600	0.3200	3.8400	0.0306
12	0.02164	0.02353	6892.154	0.1920	0.3840	4.6080	0.0282
14	0.02186	0.02376	6485.638	0.2240	0.4480	5.3760	0.0264
16	0.02206	0.02398	6118.123	0.2560	0.5120	6.1440	0.0249
18	0.02226	0.02419	5787.060	0.2880	0.5760	6.9120	0.0237
20	0.02245	0.0244	5488.732	0.3200	0.6400	7.6800	0.0227
40	0.02417	0.02627	3635.992	0.6400	1.2800	15.3600	0.0173
60	0.02567	0.0279	2748.938	0.9600	1.9200	23.0400	0.0150
80	0.02704	0.02939	2228.684	1.2800	2.5600	30.7200	0.0137
100	0.02833	0.03079	1884.676	1.6000	3.2000	38.4000	0.0128
120	0.02955	0.03212	1638.747	1.9200	3.8400	46.0800	0.0122
140	0.03073	0.0334	1453.048	2.2400	4.4800	53.7600	0.0117
160	0.03185	0.03462	1307.053	2.5600	5.1200	61.4400	0.0114
180	0.03295	0.03581	1188.671	2.8800	5.7600	69.1200	0.0111
200	0.03401	0.03697	1090.321	3.2000	6.4000	76.8000	0.0109
300	0.03897	0.04236	768.720	4.8000	9.6000	115.2000	0.0102
400	0.04352	0.0473	587.096	6.4000	12.8000	153.6000	0.0098
500	0.04778	0.05193	471.479	8.0000	16.0000	192.0000	0.0097
600	0.05182	0.05633	396.078	9.6000	19.2000	230.4000	0.0096
700	0.0557	0.06054	349.546	11.2000	22.4000	268.8000	0.0095
800	0.05943	0.0646	326.114	12.8000	25.6000	307.2000	0.0095
900	0.06305	0.06853	322.535	14.4000	28.8000	345.6000	0.0095
1000	0.06656	0.07235	336.844	16.0000	32.0000	384.0000	0.0095

Appendix

Carbon ions interact with Blood tissue

E(MeV)	Range ($\frac{g}{cm^2}$)	Thickness (cm)	LET MeV ($\frac{MeV}{cm}$)	Absorbed Dose × 10^{-6} (rad)	Equivalent Dose× 10^{-5} (rem)	Effective Dose× 10^{-7} (rem)	Stopping Time (nm)
0.025	0.0013	0.00107	842.687	0.0004	0.0008	0.0096	0.03191
0.03	0.0037	0.003	950.748	0.0005	0.0010	0.0115	0.08423
0.04	0.0071	0.0057	1095.463	0.0006	0.0013	0.0154	0.13955
0.06	0.0111	0.00887	1306.603	0.0010	0.0019	0.0230	0.17794
0.08	0.0135	0.01074	1487.465	0.0013	0.0026	0.0307	0.18687
0.1	0.0151	0.01201	1656.088	0.0016	0.0032	0.0384	0.18703
0.2	0.0190	0.01511	2412.292	0.0032	0.0064	0.0768	0.16678
0.3	0.0207	0.01647	3073.564	0.0048	0.0096	0.1152	0.14850
0.4	0.0217	0.01726	3660.879	0.0064	0.0128	0.1536	0.13492
0.6	0.0229	0.0182	4655.584	0.0096	0.0192	0.2304	0.11622
0.8	0.0237	0.01876	5459.222	0.0128	0.0256	0.3072	0.10376
1	0.0241	0.01913	6114.561	0.0160	0.0320	0.3840	0.09469
1.1	0.0243	0.01928	6396.666	0.0176	0.0352	0.4224	0.09099
1.2	0.0245	0.01941	6652.665	0.0192	0.0384	0.4608	0.08770
1.3	0.0246	0.01952	6885.242	0.0208	0.0416	0.4992	0.08476
1.4	0.0248	0.01962	7096.738	0.0224	0.0448	0.5376	0.08210
1.5	0.0249	0.01971	7289.208	0.0240	0.0480	0.5760	0.07969
1.6	0.0250	0.01979	7464.465	0.0256	0.0512	0.6144	0.07748
1.7	0.0251	0.01987	7624.107	0.0272	0.0544	0.6528	0.07545
1.8	0.0252	0.01993	7769.557	0.0288	0.0576	0.6912	0.07358
2	0.0253	0.02005	8022.794	0.0320	0.0640	0.7680	0.07023
2.25	0.0255	0.02018	8279.333	0.0360	0.0720	0.8640	0.06663
2.5	0.0256	0.02028	8481.339	0.0400	0.0800	0.9600	0.06355
2.75	0.0257	0.02037	8639.029	0.0440	0.0880	1.0560	0.06087
3	0.0258	0.02045	8760.416	0.0480	0.0960	1.1520	0.05851
3.25	0.0259	0.02052	8851.862	0.0520	0.1040	1.2480	0.05641
3.5	0.0260	0.02058	8918.469	0.0560	0.1120	1.3440	0.05452
3.75	0.0261	0.02064	8964.368	0.0600	0.1200	1.4400	0.05282
4	0.0261	0.02069	8992.929	0.0640	0.1280	1.5360	0.05127
4.5	0.0267	0.02078	9008.652	0.0720	0.1440	1.7280	0.04943
5	0.0268	0.02085	8982.631	0.0800	0.1600	1.9200	0.04702
5.5	0.0269	0.02091	8926.757	0.0880	0.1760	2.1120	0.04494
6	0.0269	0.02097	8849.517	0.0960	0.1920	2.3040	0.04314
6.5	0.0270	0.02102	8757.059	0.1040	0.2080	2.4960	0.04154
7	0.0271	0.02106	8653.898	0.1120	0.2240	2.6880	0.04013
8	0.0272	0.02113	8428.013	0.1280	0.2560	3.0720	0.03771
9	0.0273	0.02135	8189.795	0.1440	0.2880	3.4560	0.03571
10	0.0274	0.02139	7949.441	0.1600	0.3200	3.8400	0.03402
12	0.0276	0.02147	7483.084	0.1920	0.3840	4.6080	0.03132
14	0.0279	0.02155	7050.711	0.2240	0.4480	5.3760	0.02922
16	0.0281	0.02162	6657.354	0.2560	0.5120	6.1440	0.02754
18	0.0283	0.02169	6301.912	0.2880	0.5760	6.9120	0.02615
20	0.0285	0.02176	5981.173	0.3200	0.6400	7.6800	0.02498
40	0.0302	0.02234	3992.067	0.6400	1.2800	15.3600	0.01875
60	0.0318	0.02283	3044.184	0.9600	1.9200	23.0400	0.01608
80	0.0332	0.02327	2487.991	1.2800	2.5600	30.7200	0.01454
100	0.0345	0.02367	2118.577	1.6000	3.2000	38.4000	0.01352
120	0.0357	0.02405	1852.636	1.9200	3.8400	46.0800	0.01279
140	0.0369	0.02441	1650.100	2.2400	4.4800	53.7600	0.01223
160	0.0380	0.02475	1489.346	2.5600	5.1200	61.4400	0.01180
180	0.0392	0.02508	1357.686	2.8800	5.7600	69.1200	0.01145
200	0.0402	0.02539	1247.186	3.2000	6.4000	76.8000	0.01116
300	0.0453	0.02684	876.250	4.8000	9.6000	115.2000	0.01025
400	0.0499	0.02813	658.777	6.4000	12.8000	153.6000	0.00978
500	0.0542	0.02932	518.233	8.0000	16.0000	192.0000	0.00951
600	0.0583	0.03043	428.024	9.6000	19.2000	230.4000	0.00934
700	0.0622	0.03148	376.477	11.2000	22.4000	268.8000	0.00922
800	0.0660	0.03249	357.665	12.8000	25.6000	307.2000	0.00915
900	0.0696	0.03345	368.255	14.4000	28.8000	345.6000	0.00911
1000	0.0732	0.03438	406.233	16.0000	32.0000	384.0000	0.00908

Appendix

Carbon ions interact with Brain tissue

E(MeV)	Range $(\frac{g}{cm^2})$	Thickness (cm)	LET $\frac{MeV}{cm}$	Absorbed Dose × 10^{-6} (rad)	Equivalent Dose× 10^{-5} (rem)	Effective Dose× 10^{-7} (rem)	Stopping Time (nm)
0.025	0.00138	0.001324	945.128	0.0004	0.0008	0.0008	0.0348
0.03	0.00375	0.00361	994.836	0.0005	0.0010	0.0010	0.0867
0.04	0.00707	0.006796	1093.075	0.0006	0.0013	0.0013	0.1413
0.06	0.01096	0.010535	1284.970	0.0010	0.0019	0.0019	0.1789
0.08	0.01325	0.01274	1470.964	0.0013	0.0026	0.0026	0.1873
0.1	0.01480	0.014233	1651.302	0.0016	0.0032	0.0032	0.1872
0.2	0.01860	0.017886	2475.796	0.0032	0.0064	0.0064	0.1663
0.3	0.02026	0.019477	3188.760	0.0048	0.0096	0.0096	0.1479
0.4	0.02123	0.020415	3809.302	0.0064	0.0128	0.0128	0.1342
0.6	0.02238	0.021515	4829.794	0.0096	0.0192	0.0192	0.1155
0.8	0.02305	0.022164	5622.263	0.0128	0.0256	0.0256	0.1031
1	0.02351	0.022604	6183.986	0.0160	0.0320	0.0320	0.0940
1.1	0.02369	0.022776	6593.427	0.0176	0.0352	0.0352	0.0903
1.2	0.02384	0.022926	6797.907	0.0192	0.0384	0.0384	0.0870
1.3	0.02398	0.023058	7005.265	0.0208	0.0416	0.0416	0.0841
1.4	0.02410	0.023175	7195.637	0.0224	0.0448	0.0448	0.0815
1.5	0.02421	0.02328	7368.434	0.0240	0.0480	0.0480	0.0791
1.6	0.02431	0.023375	7524.856	0.0256	0.0512	0.0512	0.0769
1.7	0.02440	0.023462	7666.348	0.0272	0.0544	0.0544	0.0748
1.8	0.02448	0.02354	7794.302	0.0288	0.0576	0.0576	0.0730
2	0.02463	0.023679	8014.555	0.0320	0.0640	0.0640	0.0696
2.25	0.02478	0.023826	8233.767	0.0360	0.0720	0.0720	0.0661
2.5	0.02491	0.023949	8402.807	0.0400	0.0800	0.0800	0.0630
2.75	0.02502	0.024055	8531.723	0.0440	0.0880	0.0880	0.0603
3	0.02511	0.024148	8628.238	0.0480	0.0960	0.0960	0.0580
3.25	0.02520	0.024229	8698.364	0.0520	0.1040	0.1040	0.0559
3.5	0.02527	0.024301	8746.840	0.0560	0.1120	0.1120	0.0540
3.75	0.02534	0.024365	8777.445	0.0600	0.1200	0.1200	0.0523
4	0.02540	0.024424	8793.222	0.0640	0.1280	0.1280	0.0508
4.5	0.02554	0.024558	8789.727	0.0720	0.1440	0.1440	0.0481
5	0.02561	0.024624	8751.293	0.0800	0.1600	0.1600	0.0458
5.5	0.02568	0.024688	8688.192	0.0880	0.1760	0.1760	0.0438
6	0.02574	0.024751	8607.655	0.0960	0.1920	0.1920	0.0420
6.5	0.02581	0.024813	8514.860	0.1040	0.2080	0.2080	0.0405
7	0.02587	0.024873	8413.577	0.1120	0.2240	0.2240	0.0391
8	0.02599	0.024991	8195.937	0.1280	0.2560	0.2560	0.0368
9	0.02611	0.025105	7969.490	0.1440	0.2880	0.2880	0.0348
10	0.02622	0.025215	7742.546	0.1600	0.3200	0.3200	0.0332
12	0.02645	0.025428	7303.920	0.1920	0.3840	0.3840	0.0305
14	0.02666	0.025632	6897.431	0.2240	0.4480	0.4480	0.0285
16	0.02686	0.025828	6526.821	0.2560	0.5120	0.5120	0.0269
18	0.02706	0.026018	6190.860	0.2880	0.5760	0.5760	0.0255
20	0.02725	0.026203	5886.616	0.3200	0.6400	0.6400	0.0244
40	0.02897	0.027851	3970.736	0.6400	1.2800	1.2800	0.0183
60	0.03046	0.029288	3038.149	0.9600	1.9200	1.9200	0.0157
80	0.03183	0.030603	2485.386	1.2800	2.5600	2.5600	0.0142
100	0.03311	0.031834	2116.521	1.6000	3.2000	3.2000	0.0132
120	0.03432	0.033002	1850.504	1.9200	3.8400	3.8400	0.0125
140	0.03549	0.03412	1647.900	2.2400	4.4800	4.4800	0.0120
160	0.03661	0.035197	1487.254	2.5600	5.1200	5.1200	0.0116
180	0.03769	0.03624	1355.901	2.8800	5.7600	5.7600	0.0112
200	0.03874	0.037253	1245.885	3.2000	6.4000	6.4000	0.0110
300	0.04366	0.041976	878.817	4.8000	9.6000	9.6000	0.0101
400	0.04815	0.046299	665.474	6.4000	12.8000	12.8000	0.0096
500	0.05236	0.050346	527.786	8.0000	16.0000	16.0000	0.0094
600	0.05635	0.054185	438.479	9.6000	19.2000	19.2000	0.0092
700	0.06018	0.057861	385.548	11.2000	22.4000	22.4000	0.0091
800	0.06386	0.061402	362.879	12.8000	25.6000	25.6000	0.0090
900	0.06742	0.064828	367.036	14.4000	28.8000	28.8000	0.0090
1000	0.07088	0.068157	395.934	16.0000	32.0000	32.0000	0.0090

Appendix

<div align="center">

Carbon ions interact with **Breast** tissue

</div>

E(MeV)	Range ($\frac{g}{cm^2}$)	Thickness (cm)	LET ($\frac{MeV}{cm}$)	Absorbed Dose $\times$ 10^{-6} (rad)	Equivalent Dose$\times$ 10^{-5} (rem)	Effective Dose$\times$ 10^{-7} (rem)	Stopping Time (nm)
0.025	0.0014	0.0014	793.488	0.0004	0.0008	0.0096	0.0368
0.03	0.00359	0.00359	966.374	0.0005	0.0010	0.0115	0.0863
0.04	0.00666	0.00666	1131.620	0.0006	0.0013	0.0154	0.1386
0.06	0.01028	0.01028	1354.483	0.0010	0.0019	0.0230	0.1745
0.08	0.01241	0.01241	1547.130	0.0013	0.0026	0.0307	0.1825
0.1	0.01386	0.01386	1728.046	0.0016	0.0032	0.0384	0.1823
0.2	0.01743	0.01743	2537.613	0.0032	0.0064	0.0768	0.1621
0.3	0.01899	0.01899	3233.022	0.0048	0.0096	0.1152	0.1442
0.4	0.01991	0.01991	3838.413	0.0064	0.0128	0.1536	0.1310
0.6	0.021	0.021	4836.522	0.0096	0.0192	0.2304	0.1128
0.8	0.02164	0.02164	5617.720	0.0128	0.0256	0.3072	0.1006
1	0.02208	0.02208	6237.909	0.0160	0.0320	0.3840	0.0918
1.1	0.02225	0.02225	6500.125	0.0176	0.0352	0.4224	0.0882
1.2	0.0224	0.0224	6735.535	0.0192	0.0384	0.4608	0.0850
1.3	0.02253	0.02253	6947.255	0.0208	0.0416	0.4992	0.0822
1.4	0.02265	0.02265	7137.952	0.0224	0.0448	0.5376	0.0796
1.5	0.02276	0.02276	7309.920	0.0240	0.0480	0.5760	0.0773
1.6	0.02285	0.02285	7465.144	0.0256	0.0512	0.6144	0.0751
1.7	0.02294	0.02294	7605.350	0.0272	0.0544	0.6528	0.0732
1.8	0.02302	0.02302	7732.046	0.0288	0.0576	0.6912	0.0713
2	0.02315	0.02315	7950.032	0.0320	0.0640	0.7680	0.0681
2.25	0.0233	0.0233	8166.958	0.0360	0.0720	0.8640	0.0646
2.5	0.02342	0.02342	8334.267	0.0400	0.0800	0.9600	0.0616
2.75	0.02353	0.02353	8461.902	0.0440	0.0880	1.0560	0.0590
3	0.02362	0.02362	8557.487	0.0480	0.0960	1.1520	0.0567
3.25	0.02371	0.02371	8626.956	0.0520	0.1040	1.2480	0.0547
3.5	0.02378	0.02378	8674.989	0.0560	0.1120	1.3440	0.0529
3.75	0.02384	0.02384	8705.315	0.0600	0.1200	1.4400	0.0512
4	0.0239	0.0239	8717.428	0.0640	0.1280	1.5360	0.0497
4.5	**0.02454**	**0.02454**	**8720.942**	**0.0720**	**0.1440**	**1.7280**	**0.0481**
5	0.02461	0.02461	8679.229	0.0800	0.1600	1.9200	0.0458
5.5	0.02468	0.02468	8616.523	0.0880	0.1760	2.1120	0.0438
6	0.02474	0.02474	8536.478	0.0960	0.1920	2.3040	0.0420
6.5	0.02481	0.02481	8444.236	0.1040	0.2080	2.4960	0.0405
7	0.02487	0.02487	8343.541	0.1120	0.2240	2.6880	0.0391
8	0.02499	0.02499	8127.119	0.1280	0.2560	3.0720	0.0367
9	0.02511	0.02511	7901.891	0.1440	0.2880	3.4560	0.0348
10	0.02522	0.02522	7676.135	0.1600	0.3200	3.8400	0.0332
12	0.02544	0.02544	7239.738	0.1920	0.3840	4.6080	0.0305
14	0.02565	0.02565	6835.268	0.2240	0.4480	5.3760	0.0285
16	0.02585	0.02585	6466.480	0.2560	0.5120	6.1440	0.0269
18	0.02605	0.02605	6132.171	0.2880	0.5760	6.9120	0.0255
20	0.02624	0.02624	5829.428	0.3200	0.6400	7.6800	0.0244
40	0.02793	0.02793	3923.516	0.6400	1.2800	15.3600	0.0184
60	0.0294	0.0294	2996.495	0.9600	1.9200	23.0400	0.0158
80	0.03075	0.03075	2447.515	1.2800	2.5600	30.7200	0.0143
100	0.03201	0.03201	2081.528	1.6000	3.2000	38.4000	0.0133
120	0.0332	0.0332	1817.858	1.9200	3.8400	46.0800	0.0126
140	0.03435	0.03435	1617.262	2.2400	4.4800	53.7600	0.0121
160	0.03545	0.03545	1458.388	2.5600	5.1200	61.4400	0.0117
180	0.03651	0.03651	1328.634	2.8800	5.7600	69.1200	0.0113
200	0.03755	0.03755	1220.082	3.2000	6.4000	76.8000	0.0110
300	0.04237	0.04237	859.026	4.8000	9.6000	115.2000	0.0102
400	0.04678	0.04678	650.295	6.4000	12.8000	153.6000	0.0097
500	0.0509	0.0509	516.224	8.0000	16.0000	192.0000	0.0095
600	0.05482	0.05482	429.686	9.6000	19.2000	230.4000	0.0093
700	0.05856	0.05856	378.739	11.2000	22.4000	268.8000	0.0092
800	0.06216	0.06216	357.304	12.8000	25.6000	307.2000	0.0091
900	0.06565	0.06565	361.960	14.4000	28.8000	345.6000	0.0091
1000	0.06904	0.06904	390.637	16.0000	32.0000	384.0000	0.0091

Appendix

Carbon ions interact with Lung tissue

E(MeV)	Range $(\frac{g}{cm^2})$	Thickness (cm)	LET MeV $(\frac{MeV}{cm})$	Absorbed Dose × 10^{-6} (rad)	Equivalent Dose× 10^{-5} (rem)	Effective Dose× 10^{-7} (rem)	Stopping Time (nm)
0.025	0.0013	0.00127	886.443	0.0004	0.0008	0.0096	0.0276
0.03	0.0038	0.00361	935.821	0.0005	0.0010	0.0115	0.0678
0.04	0.0072	0.00686	1033.424	0.0006	0.0013	0.0154	0.1100
0.06	0.0112	0.01065	1224.137	0.0010	0.0019	0.0230	0.1389
0.08	0.0135	0.01287	1409.064	0.0013	0.0026	0.0307	0.1453
0.1	0.0151	0.01437	1588.441	0.0016	0.0032	0.0384	0.1451
0.2	0.0189	0.018	2409.513	0.0032	0.0064	0.0768	0.1287
0.3	0.0205	0.01957	3120.899	0.0048	0.0096	0.1152	0.1144
0.4	0.0215	0.02049	3741.265	0.0064	0.0128	0.1536	0.1037
0.6	0.0226	0.02156	4764.783	0.0096	0.0192	0.2304	0.0892
0.8	0.0233	0.02218	5566.171	0.0128	0.0256	0.3072	0.0796
1	0.0237	0.02261	6202.603	0.0160	0.0320	0.3840	0.0726
1.1	0.0239	0.02277	6471.78	0.0176	0.0352	0.4224	0.0697
1.2	0.0241	0.02292	6713.507	0.0192	0.0384	0.4608	0.0672
1.3	0.0242	0.02304	6930.98	0.0208	0.0416	0.4992	0.0649
1.4	0.0243	0.02315	7126.932	0.0224	0.0448	0.5376	0.0628
1.5	0.0244	0.02325	7303.717	0.0240	0.0480	0.5760	0.0610
1.6	0.0245	0.02334	7463.366	0.0256	0.0512	0.6144	0.0593
1.7	0.0246	0.02343	7607.647	0.0272	0.0544	0.6528	0.0577
1.8	0.0247	0.0235	7738.104	0.0288	0.0576	0.6912	0.0563
2	0.0248	0.02363	7962.788	0.0320	0.0640	0.7680	0.0537
2.25	0.0250	0.02377	8186.782	0.0360	0.0720	0.8640	0.0509
2.5	0.0251	0.02389	8359.964	0.0400	0.0800	0.9600	0.0486
2.75	0.0252	0.02399	8492.457	0.0440	0.0880	1.0560	0.0465
3	0.0253	0.02407	8591.976	0.0480	0.0960	1.1520	0.0447
3.25	0.0254	0.02415	8664.431	0.0520	0.1040	1.2480	0.0431
3.5	0.0254	0.02422	8714.233	0.0560	0.1120	1.3440	0.0416
3.75	0.0255	0.02428	8744.057	0.0600	0.1200	1.4400	0.0403
4	0.0256	0.02433	8750.759	0.0640	0.1280	1.5360	0.0391
4.5	0.0257	0.02443	8791.973	0.0720	0.1440	1.7280	0.0379
5	0.0257	0.02451	8745.928	0.0800	0.1600	1.9200	0.0360
5.5	0.0258	0.02458	8683.736	0.0880	0.1760	2.1120	0.0344
6	0.0259	0.02464	8605.062	0.0960	0.1920	2.3040	0.0330
6.5	0.0263	0.02501	8514.234	0.1040	0.2080	2.4960	0.0318
7	0.0263	0.02505	8414.819	0.1120	0.2240	2.6880	0.0307
8	0.0264	0.02511	8200.453	0.1280	0.2560	3.0720	0.0289
9	0.0264	0.02517	7976.675	0.1440	0.2880	3.4560	0.0274
10	0.0265	0.02523	7751.895	0.1600	0.3200	3.8400	0.0261
12	0.0266	0.02535	7316.46	0.1920	0.3840	4.6080	0.0240
14	0.0267	0.02546	6912.109	0.2240	0.4480	5.3760	0.0224
16	0.0268	0.02556	6542.948	0.2560	0.5120	6.1440	0.0211
18	0.0269	0.02566	6207.978	0.2880	0.5760	6.9120	0.0200
20	0.0270	0.02576	5904.406	0.3200	0.6400	7.6800	0.0191
40	0.0279	0.02661	3989.224	0.6400	1.2800	15.3600	0.0144
60	0.0287	0.02733	3055.342	0.9600	1.9200	23.0400	0.0123
80	0.0294	0.02799	2501.413	1.2800	2.5600	30.7200	0.0111
100	0.0300	0.02859	2131.617	1.6000	3.2000	38.4000	0.0103
120	0.0306	0.02916	1864.854	1.9200	3.8400	46.0800	0.0098
140	0.0312	0.02969	1661.644	2.2400	4.4800	53.7600	0.0094
160	0.0317	0.03021	1500.496	2.5600	5.1200	61.4400	0.0090
180	0.0322	0.03071	1368.719	2.8800	5.7600	69.1200	0.0087
200	0.0327	0.03119	1258.342	3.2000	6.4000	76.8000	0.0085
300	0.0351	0.03339	890.083	4.8000	9.6000	115.2000	0.0078
400	0.0372	0.03538	676.182	6.4000	12.8000	153.6000	0.0074
500	0.0391	0.03722	538.345	8.0000	16.0000	192.0000	0.0072
600	0.0418	0.03895	449.219	9.6000	19.2000	230.4000	0.0071
700	0.0426	0.04059	396.759	11.2000	22.4000	268.8000	0.0070
800	0.0443	0.04217	374.833	12.8000	25.6000	307.2000	0.0069
900	0.0459	0.04368	379.992	14.4000	28.8000	345.6000	0.0069
1000	0.0474	0.04514	410.146	16.0000	32.0000	384.0000	0.0069

Appendix

Carbon ions interact with Muscle tissue

E(MeV)	Range ($\frac{g}{cm^2}$)	Thickness (cm)	LET ($\frac{MeV}{cm}$)	Absorbed Dose × 10^{-6} (rad)	Equivalent Dose× 10^{-5} (rem)	Effective Dose× 10^{-7} (rem)	Stopping Time (nm)
0.025	0.00132	0.00126	1042.464	0.0004	0.0008	0.0096	0.0331
0.03	0.00368	0.0035	1086.623	0.0005	0.0010	0.0115	0.0841
0.04	0.00696	0.00663	1174.169	0.0006	0.0013	0.0154	0.1379
0.06	0.01083	0.01031	1346.210	0.0010	0.0019	0.0230	0.1751
0.08	0.01311	0.01249	1514.281	0.0013	0.0026	0.0307	0.1837
0.1	0.01467	0.01397	1678.489	0.0016	0.0032	0.0384	0.1837
0.2	0.01847	0.01759	2445.152	0.0032	0.0064	0.0768	0.1636
0.3	0.02014	0.01918	3129.624	0.0048	0.0096	0.1152	0.1456
0.4	0.02112	0.02012	3742.025	0.0064	0.0128	0.1536	0.1323
0.6	0.02228	0.02122	4783.923	0.0096	0.0192	0.2304	0.1139
0.8	0.02297	0.02187	5626.365	0.0128	0.0256	0.3072	0.1017
1	0.02343	0.02232	6310.871	0.0160	0.0320	0.3840	0.0928
1.1	0.02361	0.02249	6604.063	0.0176	0.0352	0.4224	0.0892
1.2	0.02377	0.02264	6868.984	0.0192	0.0384	0.4608	0.0860
1.3	0.02391	0.02277	7108.463	0.0208	0.0416	0.4992	0.0831
1.4	0.02404	0.02289	7325.001	0.0224	0.0448	0.5376	0.0805
1.5	0.02415	0.023	7520.814	0.0240	0.0480	0.5760	0.0781
1.6	0.02425	0.02309	7697.869	0.0256	0.0512	0.6144	0.0759
1.7	0.02434	0.02318	7857.917	0.0272	0.0544	0.6528	0.0739
1.8	0.02442	0.02326	8002.523	0.0288	0.0576	0.6912	0.0721
2	0.02457	0.0234	8250.854	0.0320	0.0640	0.7680	0.0688
2.25	0.02473	0.02355	8496.434	0.0360	0.0720	0.8640	0.0653
2.5	0.02486	0.02368	8683.565	0.0400	0.0800	0.9600	0.0623
2.75	0.02497	0.02378	8823.714	0.0440	0.0880	1.0560	0.0596
3	0.02507	0.02388	8925.873	0.0480	0.0960	1.1520	0.0573
3.25	0.02516	0.02396	8997.159	0.0520	0.1040	1.2480	0.0553
3.5	0.02523	0.02403	9043.250	0.0560	0.1120	1.3440	0.0534
3.75	0.0253	0.0241	9054.929	0.0600	0.1200	1.4400	0.0518
4	0.02537	0.02416	9068.709	0.0640	0.1280	1.5360	0.0502
4.5	0.02596	0.02472	9077.230	0.0720	0.1440	1.7280	0.0485
5	0.02603	0.02479	8994.472	0.0800	0.1600	1.9200	0.0461
5.5	0.0261	0.02486	8908.205	0.0880	0.1760	2.1120	0.0441
6	0.02617	0.02492	8804.673	0.0960	0.1920	2.3040	0.0423
6.5	0.02623	0.02498	8689.860	0.1040	0.2080	2.4960	0.0408
7	0.0263	0.02505	8568.001	0.1120	0.2240	2.6880	0.0394
8	0.02643	0.02517	8314.352	0.1280	0.2560	3.0720	0.0370
9	0.02655	0.02528	8058.943	0.1440	0.2880	3.4560	0.0351
10	0.02667	0.0254	7809.517	0.1600	0.3200	3.8400	0.0334
12	0.0269	0.02562	7341.664	0.1920	0.3840	4.6080	0.0308
14	0.02712	0.02582	6920.961	0.2240	0.4480	5.3760	0.0287
16	0.02733	0.02603	6545.538	0.2560	0.5120	6.1440	0.0271
18	0.02753	0.02622	6210.333	0.2880	0.5760	6.9120	0.0257
20	0.02773	0.02641	5909.916	0.3200	0.6400	7.6800	0.0246
40	0.0295	0.0281	4033.077	0.6400	1.2800	15.3600	0.0185
60	0.03104	0.02957	3087.584	0.9600	1.9200	23.0400	0.0159
80	0.03245	0.03091	2505.196	1.2800	2.5600	30.7200	0.0144
100	0.03377	0.03216	2107.563	1.6000	3.2000	38.4000	0.0134
120	0.03502	0.03335	1818.488	1.9200	3.8400	46.0800	0.0127
140	0.03622	0.03449	1599.172	2.2400	4.4800	53.7600	0.0121
160	0.03737	0.03559	1427.526	2.5600	5.1200	61.4400	0.0117
180	0.03848	0.03665	1289.956	2.8800	5.7600	69.1200	0.0114
200	0.03956	0.03768	1177.595	3.2000	6.4000	76.8000	0.0111
300	0.04461	0.04248	833.234	4.8000	9.6000	115.2000	0.0102
400	0.04921	0.04687	663.117	6.4000	12.8000	153.6000	0.0097
500	0.05352	0.05098	563.864	8.0000	16.0000	192.0000	0.0095
600	0.05761	0.05487	496.935	9.6000	19.2000	230.4000	0.0093
700	0.06152	0.05859	444.641	11.2000	22.4000	268.8000	0.0092
800	0.06529	0.06218	397.712	12.8000	25.6000	307.2000	0.0091
900	0.06893	0.06565	350.819	14.4000	28.8000	345.6000	0.0091
1000	0.07247	0.06902	300.680	16.0000	32.0000	384.0000	0.0091

Appendix

Carbon ions interact with Bone tissue

E(MeV)	Range ($\frac{g}{cm^2}$)	Thickness (cm)	LET ($\frac{MeV}{cm}$)	Absorbed Dose × 10^{-6} (rad)	Equivalent Dose× 10^{-5} (rem)	Effective Dose× 10^{-7} (rem)	Stopping Time (nm)
0.025	0.00176	0.0016	1423.143	0.0004	0.0008	0.0008	0.0242
0.03	0.00477	0.0044	1492.393	0.0005	0.0010	0.0010	0.0597
0.04	0.00897	0.0082	1629.387	0.0006	0.0013	0.0013	0.0971
0.06	0.01389	0.0127	1897.48	0.0010	0.0019	0.0019	0.1228
0.08	0.01679	0.0154	2157.955	0.0013	0.0026	0.0026	0.1286
0.1	0.01875	0.0172	2411.094	0.0016	0.0032	0.0032	0.1284
0.2	0.02356	0.0216	3575.683	0.0032	0.0064	0.0064	0.1141
0.3	0.02565	0.0235	4592.162	0.0048	0.0096	0.0096	0.1014
0.4	0.02688	0.0246	5483.823	0.0064	0.0128	0.0128	0.0921
0.6	0.02833	0.0259	6964.307	0.0096	0.0192	0.0192	0.0792
0.8	0.02918	0.0267	8129.966	0.0128	0.0256	0.0256	0.0707
1	0.02976	0.0272	9058.212	0.0160	0.0320	0.0320	0.0645
1.1	0.02998	0.0275	9451.073	0.0176	0.0352	0.0352	0.0619
1.2	0.03018	0.0276	9803.818	0.0192	0.0384	0.0384	0.0597
1.3	0.03035	0.0278	10121.001	0.0208	0.0416	0.0416	0.0577
1.4	0.03051	0.0279	10406.551	0.0224	0.0448	0.0448	0.0558
1.5	0.03064	0.0281	10663.872	0.0240	0.0480	0.0480	0.0542
1.6	0.03077	0.0282	10895.923	0.0256	0.0512	0.0512	0.0527
1.7	0.03088	0.0283	11105.291	0.0272	0.0544	0.0544	0.0513
1.8	0.03099	0.0284	11294.246	0.0288	0.0576	0.0576	0.0500
2	0.03117	0.0285	11618.668	0.0320	0.0640	0.0640	0.0477
2.25	0.03136	0.0287	11940.358	0.0360	0.0720	0.0720	0.0453
2.5	0.03152	0.0289	12187.371	0.0400	0.0800	0.0800	0.0432
2.75	0.03166	0.0290	12374.922	0.0440	0.0880	0.0880	0.0414
3	0.03178	0.0291	12514.692	0.0480	0.0960	0.0960	0.0397
3.25	0.03189	0.0292	12615.769	0.0520	0.1040	0.1040	0.0383
3.5	0.03198	0.0293	12685.305	0.0560	0.1120	0.1120	0.0370
3.75	0.03289	0.0301	12728.986	0.0600	0.1200	0.1200	0.0368
4	0.03294	0.0302	12746.35	0.0640	0.1280	0.1280	0.0357
4.5	0.03303	0.0302	12751.374	0.0720	0.1440	0.1440	0.0337
5	0.03311	0.0303	12692.376	0.0800	0.1600	0.1600	0.0321
5.5	0.03320	0.0304	12604.491	0.0880	0.1760	0.1760	0.0307
6	0.03328	0.0305	12493.126	0.0960	0.1920	0.1920	0.0294
6.5	0.03336	0.0306	12365.639	0.1040	0.2080	0.2080	0.0283
7	0.03344	0.0306	12227.292	0.1120	0.2240	0.2240	0.0274
8	0.03360	0.0308	11932.204	0.1280	0.2560	0.2560	0.0257
9	0.03375	0.0309	11627.585	0.1440	0.2880	0.2880	0.0244
10	0.03389	0.0310	11324.079	0.1600	0.3200	0.3200	0.0232
12	0.03417	0.0313	10740.612	0.1920	0.3840	0.3840	0.0214
14	0.03443	0.0315	10201.359	0.2240	0.4480	0.4480	0.0199
16	0.03469	0.0318	9709.061	0.2560	0.5120	0.5120	0.0188
18	0.03493	0.0320	9260.939	0.2880	0.5760	0.5760	0.0178
20	0.03517	0.0322	8852.637	0.3200	0.6400	0.6400	0.0170
40	0.03728	0.0341	6172.479	0.6400	1.2800	1.2800	0.0128
60	0.03909	0.0358	4757.312	0.9600	1.9200	1.9200	0.0109
80	0.04074	0.0373	3874.523	1.2800	2.5600	2.5600	0.0099
100	0.04228	0.0387	3270.018	1.6000	3.2000	3.2000	0.0092
120	0.04373	0.0400	2830.517	1.9200	3.8400	3.8400	0.0086
140	0.04512	0.0413	2497.244	2.2400	4.4800	4.4800	0.0083
160	0.04645	0.0425	2236.475	2.5600	5.1200	5.1200	0.0080
180	0.04773	0.0437	2027.408	2.8800	5.7600	5.7600	0.0077
200	0.04898	0.0449	1856.487	3.2000	6.4000	6.4000	0.0075
300	0.05475	0.0501	1329.319	4.8000	9.6000	9.6000	0.0068
400	0.06000	0.0549	1063.489	6.4000	12.8000	12.8000	0.0065
500	0.06488	0.0594	904.393	8.0000	16.0000	16.0000	0.0063
600	0.06950	0.0636	795.146	9.6000	19.2000	19.2000	0.0061
700	0.07390	0.0677	709.883	11.2000	22.4000	22.4000	0.0060
800	0.07813	0.0715	635.146	12.8000	25.6000	25.6000	0.0060
900	0.08221	0.0753	563.242	14.4000	28.8000	28.8000	0.0059
1000	0.08616	0.0789	489.449	16.0000	32.0000	32.0000	0.0059

Appendix

Carbon ions interact with Skin tissue

E(MeV)	Range ($\frac{g}{cm^2}$)	Thickness (cm)	LET ($\frac{MeV}{cm}$)	Absorbed Dose × 10^{-6} (rad)	Equivalent Dose× 10^{-5} (rem)	Effective Dose× 10^{-7} (rem)	Stopping Time (nm)
0.025	0.00128	0.00117	1067.523	0.0004	0.0008	0.0008	0.0202
0.03	0.00358	0.00328	1114.591	0.0005	0.0010	0.0010	0.0516
0.04	0.00679	0.00623	1207.770	0.0006	0.0013	0.0013	0.0849
0.06	0.01059	0.00972	1390.373	0.0010	0.0019	0.0019	0.1081
0.08	0.01284	0.01178	1568.121	0.0013	0.0026	0.0026	0.1135
0.1	0.01438	0.01319	1741.187	0.0016	0.0032	0.0032	0.1136
0.2	0.01816	0.01666	2541.904	0.0032	0.0064	0.0064	0.1015
0.3	0.01982	0.01818	3249.461	0.0048	0.0096	0.0096	0.0905
0.4	0.0208	0.01909	3855.009	0.0064	0.0128	0.0128	0.0822
0.6	0.02197	0.02015	4910.141	0.0096	0.0192	0.0192	0.0709
0.8	0.02266	0.02079	5746.252	0.0128	0.0256	0.0256	0.0633
1	0.02313	0.02122	6421.073	0.0160	0.0320	0.0320	0.0578
1.1	0.02331	0.02139	6709.589	0.0176	0.0352	0.0352	0.0556
1.2	0.02347	0.02154	6970.341	0.0192	0.0384	0.0384	0.0536
1.3	0.02362	0.02167	7206.327	0.0208	0.0416	0.0416	0.0518
1.4	0.02374	0.02178	7420.145	0.0224	0.0448	0.0448	0.0502
1.5	0.02386	0.02189	7614.056	0.0240	0.0480	0.0480	0.0487
1.6	0.02396	0.02198	7790.040	0.0256	0.0512	0.0512	0.0474
1.7	0.02405	0.02207	7949.833	0.0272	0.0544	0.0544	0.0461
1.8	0.02414	0.02214	8094.968	0.0288	0.0576	0.0576	0.0450
2	0.02429	0.02228	8346.533	0.0320	0.0640	0.0640	0.0429
2.25	0.02445	0.02243	8599.686	0.0360	0.0720	0.0720	0.0407
2.5	0.02458	0.02255	8797.510	0.0400	0.0800	0.0800	0.0389
2.75	0.0247	0.02266	8950.655	0.0440	0.0880	0.0880	0.0372
3	0.0248	0.02275	9067.402	0.0480	0.0960	0.0960	0.0358
3.25	0.02489	0.02283	9154.272	0.0520	0.1040	0.1040	0.0345
3.5	0.02497	0.0229	9216.459	0.0560	0.1120	0.1120	0.0334
3.75	0.02504	0.02297	9258.145	0.0600	0.1200	0.1200	0.0323
4	0.0251	0.02303	9282.722	0.0640	0.1280	0.1280	0.0314
4.5	0.02567	0.02355	9291.179	0.0720	0.1440	0.1440	0.0303
5	0.02574	0.02362	9258.769	0.0800	0.1600	0.1600	0.0288
5.5	0.02581	0.02368	9197.270	0.0880	0.1760	0.1760	0.0275
6	0.02588	0.02374	9115.042	0.0960	0.1920	0.1920	0.0264
6.5	0.02594	0.0238	9018.118	0.1040	0.2080	0.2080	0.0254
7	0.02601	0.02386	8910.913	0.1120	0.2240	0.2240	0.0246
8	0.02613	0.02397	8677.895	0.1280	0.2560	0.2560	0.0231
9	0.02625	0.02409	8433.434	0.1440	0.2880	0.2880	0.0219
10	0.02637	0.02419	8187.418	0.1600	0.3200	0.3200	0.0208
12	0.0266	0.0244	7710.784	0.1920	0.3840	0.3840	0.0192
14	0.02681	0.0246	7268.960	0.2240	0.4480	0.4480	0.0179
16	0.02702	0.02479	6866.682	0.2560	0.5120	0.5120	0.0169
18	0.02723	0.02498	6502.755	0.2880	0.5760	0.5760	0.0160
20	0.02742	0.02516	6173.931	0.3200	0.6400	0.6400	0.0153
40	0.02917	0.02676	4123.835	0.6400	1.2800	1.2800	0.0115
60	0.0307	0.02817	3140.480	0.9600	1.9200	1.9200	0.0099
80	0.0321	0.02945	2562.427	1.2800	2.5600	2.5600	0.0090
100	0.03341	0.03065	2178.703	1.6000	3.2000	3.2000	0.0084
120	0.03465	0.03179	1902.974	1.9200	3.8400	3.8400	0.0079
140	0.03583	0.03287	1693.536	2.2400	4.4800	4.4800	0.0076
160	0.03698	0.03392	1527.811	2.5600	5.1200	5.1200	0.0073
180	0.03808	0.03494	1392.524	2.8800	5.7600	5.7600	0.0071
200	0.03916	0.03593	1279.360	3.2000	6.4000	6.4000	0.0069
300	0.04417	0.04053	902.656	4.8000	9.6000	9.6000	0.0064
400	0.04876	0.04473	684.149	6.4000	12.8000	12.8000	0.0061
500	0.05305	0.04867	543.100	8.0000	16.0000	16.0000	0.0059
600	0.05712	0.05241	451.402	9.6000	19.2000	19.2000	0.0058
700	0.06102	0.05598	396.702	11.2000	22.4000	22.4000	0.0058
800	0.06478	0.05943	372.722	12.8000	25.6000	25.6000	0.0057
900	0.06841	0.06276	375.932	14.4000	28.8000	28.8000	0.0057
1000	0.07194	0.066	404.196	16.0000	32.0000	32.0000	0.0057

Appendix

Oxygen ions interact with Adipose tissue

E(MeV)	Range ($\frac{g}{cm^2}$)	Thickness (cm)	LET ($\frac{MeV}{cm}$)	Absorbed Dose × 10^{-6} (rad)	Equivalent Dose × 10^{-5} (rem)	Effective Dose × 10^{-7} (rem)	Stopping Time (nm)
0.025	0.00091	0.00099	1228.870	0.0004	0.0008	0.0096	0.0302
0.03	0.00276	0.003	1269.035	0.0005	0.0010	0.0115	0.0831
0.04	0.00534	0.00581	1348.861	0.0006	0.0013	0.0154	0.1390
0.06	0.00841	0.00914	1506.523	0.0010	0.0019	0.0230	0.1790
0.08	0.01023	0.01112	1661.578	0.0013	0.0026	0.0307	0.1890
0.1	0.01148	0.01248	1814.082	0.0016	0.0032	0.0384	0.1890
0.2	0.01456	0.01583	2540.168	0.0032	0.0064	0.0768	0.1700
0.3	0.01593	0.01732	3209.972	0.0048	0.0096	0.1150	0.1520
0.4	0.01674	0.0182	3828.943	0.0064	0.0128	0.1540	0.1380
0.6	0.01771	0.01925	4932.953	0.0096	0.0192	0.2300	0.1190
0.8	0.01828	0.01987	5884.153	0.0128	0.0256	0.3070	0.1070
1	0.01868	0.0203	6707.727	0.0160	0.0320	0.3840	0.0974
1.1	0.01883	0.02047	7078.101	0.0176	0.0352	0.4220	0.0937
1.2	0.01896	0.02061	7423.781	0.0192	0.0384	0.4610	0.0903
1.3	0.01908	0.02074	7746.688	0.0208	0.0416	0.4990	0.0873
1.4	0.01919	0.02086	8048.552	0.0224	0.0448	0.5380	0.0846
1.5	0.01928	0.02096	8330.944	0.0240	0.0480	0.5760	0.0821
1.6	0.01937	0.02105	8595.288	0.0256	0.0512	0.6140	0.0799
1.7	0.01945	0.02114	8842.880	0.0272	0.0544	0.6530	0.0778
1.8	0.01952	0.02122	9074.901	0.0288	0.0576	0.6910	0.0759
2	0.01965	0.02135	9496.451	0.0320	0.0640	0.7680	0.0725
2.25	0.01978	0.0215	9953.177	0.0360	0.0720	0.8640	0.0688
2.5	0.01989	0.02162	10343.198	0.0400	0.0800	0.9600	0.0656
2.75	0.01999	0.02173	10676.512	0.0440	0.0880	1.0600	0.0629
3	0.02008	0.02182	10961.345	0.0480	0.0960	1.1500	0.0605
3.25	0.02015	0.0219	11204.536	0.0520	0.1040	1.2500	0.0583
3.5	0.02022	0.02198	11411.822	0.0560	0.1120	1.3400	0.0564
3.75	0.02028	0.02204	11588.098	0.0600	0.1200	1.4400	0.0546
4	0.02033	0.0221	11737.710	0.0640	0.1280	1.5400	0.0530
4.5	0.02043	0.0222	11985.767	0.0720	0.1440	1.7300	0.0502
5	0.02051	0.02229	12110.862	0.0800	0.1600	1.9200	0.0478
5.5	0.02058	0.02236	12212.151	0.0880	0.1760	2.1100	0.0458
6	0.02064	0.02243	12266.188	0.0960	0.1920	2.3000	0.0440
6.5	0.02091	0.02273	12274.515	0.1040	0.2080	2.5000	0.0428
7	0.02095	0.02277	12284.419	0.1120	0.2240	2.6900	0.0413
8	0.02101	0.02284	12192.443	0.1280	0.2560	3.0700	0.0388
9	0.02107	0.0229	12053.412	0.1440	0.2880	3.4600	0.0366
10	0.02113	0.02297	11878.739	0.1600	0.3200	3.8400	0.0349
12	0.02124	0.02309	11473.665	0.1920	0.3840	4.6100	0.0320
14	0.02135	0.0232	11042.213	0.2240	0.4480	5.3800	0.0298
16	0.02145	0.02331	10614.119	0.2560	0.5120	6.1400	0.0280
18	0.02155	0.02342	10202.935	0.2880	0.5760	6.9100	0.0265
20	0.02164	0.02352	9814.384	0.3200	0.6400	7.6800	0.0252
40	0.02248	0.02443	7099.064	0.6400	1.2800	15.4000	0.0185
60	0.02319	0.0252	5642.308	0.9600	1.9200	23.0000	0.0156
80	0.02383	0.0259	4739.327	1.2800	2.5600	30.7000	0.0139
100	0.02442	0.02654	4117.997	1.6000	3.2000	38.4000	0.0127
120	0.02498	0.02715	3658.628	1.9200	3.8400	46.1000	0.0119
140	0.02551	0.02772	3301.048	2.2400	4.4800	53.8000	0.0112
160	0.02601	0.02827	3011.836	2.5600	5.1200	61.4000	0.0107
180	0.0265	0.02881	2770.976	2.8800	5.7600	69.1000	0.0103
200	0.02697	0.02932	2565.761	3.2000	6.4000	76.8000	0.0100
300	0.02915	0.03169	1852.851	4.8000	9.6000	115.0000	0.0088
400	0.03111	0.03382	1414.468	6.4000	12.8000	154.0000	0.0081
500	0.03293	0.0358	1121.551	8.0000	16.0000	192.0000	0.0077
600	0.03464	0.03766	928.570	9.6000	19.2000	230.0000	0.0074
700	0.03627	0.03942	815.366	11.2000	22.4000	269.0000	0.0072
800	0.03783	0.04111	771.640	12.8000	25.6000	307.0000	0.0070
900	0.03932	0.04274	791.581	14.4000	28.8000	346.0000	0.0068
1000	0.04077	0.04432	871.665	16.0000	32.0000	384.0000	0.0067

Appendix

Oxygen ions interact with Blood tissue

E(MeV)	Range ($\frac{g}{cm^2}$)	Thickness (cm)	LET ($\frac{MeV}{cm}$)	Absorbed Dose $\times 10^{-6}$ (rad)	Equivalent Dose $\times 10^{-5}$ (rem)	Effective Dose $\times 10^{-7}$ (rem)	Stopping Time (nm)
0.025	0.0012	0.00117	1061.995	0.0004	0.0008	0.0096	0.0354
0.03	0.0037	0.00347	1099.933	0.0005	0.0010	0.0115	0.0962
0.04	0.0071	0.00669	1175.400	0.0006	0.0013	0.0154	0.1605
0.06	0.0111	0.01046	1324.719	0.0010	0.0019	0.0230	0.2049
0.08	0.0134	0.01268	1471.916	0.0013	0.0026	0.0307	0.2151
0.1	0.0150	0.01418	1617.030	0.0016	0.0032	0.0384	0.2153
0.2	0.0189	0.01786	2312.608	0.0032	0.0064	0.0768	0.1917
0.3	0.0206	0.01946	2961.317	0.0048	0.0096	0.1152	0.1705
0.4	0.0216	0.0204	3567.063	0.0064	0.0128	0.1536	0.1548
0.6	0.0228	0.02151	4663.580	0.0096	0.0192	0.2304	0.1333
0.8	0.0235	0.02216	5628.807	0.0128	0.0256	0.3072	0.1189
1	0.0240	0.0226	6255.412	0.0160	0.0320	0.3840	0.1085
1.1	0.0241	0.02278	6827.514	0.0176	0.0352	0.4224	0.1042
1.2	0.0243	0.02293	7197.156	0.0192	0.0384	0.4608	0.1005
1.3	0.0244	0.02306	7539.577	0.0208	0.0416	0.4992	0.0971
1.4	0.0246	0.02318	7860.418	0.0224	0.0448	0.5376	0.0940
1.5	0.0247	0.02328	8161.914	0.0240	0.0480	0.5760	0.0912
1.6	0.0248	0.02338	8445.601	0.0256	0.0512	0.6144	0.0887
1.7	0.0249	0.02347	8712.744	0.0272	0.0544	0.6528	0.0864
1.8	0.0250	0.02354	8964.448	0.0288	0.0576	0.6912	0.0842
2	0.0251	0.02368	9425.446	0.0320	0.0640	0.7680	0.0804
2.25	0.0253	0.02383	9930.899	0.0360	0.0720	0.8640	0.0763
2.5	0.0254	0.02395	10368.214	0.0400	0.0800	0.9600	0.0727
2.75	0.0255	0.02406	10746.822	0.0440	0.0880	1.0560	0.0696
3	0.0256	0.02415	11074.604	0.0480	0.0960	1.1520	0.0669
3.25	0.0257	0.02423	11358.198	0.0520	0.1040	1.2480	0.0645
3.5	0.0258	0.02431	11603.226	0.0560	0.1120	1.3440	0.0624
3.75	0.0258	0.02437	11814.484	0.0600	0.1200	1.4400	0.0604
4	0.0259	0.02443	11996.077	0.0640	0.1280	1.5360	0.0586
4.5	0.0260	0.02453	12283.918	0.0720	0.1440	1.7280	0.0555
5	0.0261	0.02462	12489.696	0.0800	0.1600	1.9200	0.0528
5.5	0.0262	0.02469	12630.795	0.0880	0.1760	2.1120	0.0505
6	0.0262	0.02476	12720.559	0.0960	0.1920	2.3040	0.0485
6.5	0.0265	0.02504	12769.354	0.1040	0.2080	2.4960	0.0471
7	0.0266	0.02507	12785.313	0.1120	0.2240	2.6880	0.0455
8	0.0266	0.02513	12743.181	0.1280	0.2560	3.0720	0.0427
9	0.0267	0.02519	12631.754	0.1440	0.2880	3.4560	0.0403
10	0.0268	0.02525	12475.546	0.1600	0.3200	3.8400	0.0383
12	0.0269	0.02536	12088.841	0.1920	0.3840	4.6080	0.0351
14	0.0270	0.02547	11660.503	0.2240	0.4480	5.3760	0.0327
16	0.0271	0.02557	11227.122	0.2560	0.5120	6.1440	0.0307
18	0.0272	0.02567	10806.102	0.2880	0.5760	6.9120	0.0290
20	0.0273	0.02577	10405.376	0.3200	0.6400	7.6800	0.0277
40	0.0282	0.0266	7570.291	0.6400	1.2800	15.3600	0.0202
60	0.0289	0.02731	6039.775	0.9600	1.9200	23.0400	0.0169
80	0.0296	0.02795	5088.839	1.2800	2.5600	30.7200	0.0150
100	0.0302	0.02854	4432.582	1.6000	3.2000	38.4000	0.0137
120	0.0308	0.02909	3945.613	1.9200	3.8400	46.0800	0.0127
140	0.0314	0.02962	3564.982	2.2400	4.4800	53.7600	0.0120
160	0.0319	0.03013	3255.768	2.5600	5.1200	61.4400	0.0114
180	0.0325	0.03062	2997.090	2.8800	5.7600	69.1200	0.0110
200	0.0330	0.03109	2775.705	3.2000	6.4000	76.8000	0.0106
300	0.0353	0.03326	1997.700	4.8000	9.6000	115.2000	0.0092
400	0.0373	0.03522	1510.873	6.4000	12.8000	153.6000	0.0085
500	0.0393	0.03703	1181.390	8.0000	16.0000	192.0000	0.0079
600	0.0411	0.03874	962.116	9.6000	19.2000	230.4000	0.0076
700	0.0428	0.04036	832.203	11.2000	22.4000	268.8000	0.0073
800	0.0444	0.04192	781.008	12.8000	25.6000	307.2000	0.0071
900	0.0460	0.04341	802.532	14.4000	28.8000	345.6000	0.0069
1000	0.0475	0.04486	893.133	16.0000	32.0000	384.0000	0.0068

Appendix

Oxygen ions interact with Brain tissue

E(MeV)	Range ($\frac{g}{cm^2}$)	Thickness (cm)	LET ($\frac{MeV}{cm}$)	Absorbed Dose $\times 10^{-6}$ (rad)	Equivalent Dose $\times 10^{-5}$ (rem)	Effective Dose $\times 10^{-7}$ (rem)	Stopping Time (nm)
0.025	0.00126	0.001213	1082.419	0.0004	0.0008	0.0008	0.03681
0.03	0.00366	0.003519	1122.604	0.0005	0.0010	0.0010	0.09752
0.04	0.00699	0.006722	1202.500	0.0006	0.0013	0.0013	0.16132
0.06	0.01088	0.01046	1360.425	0.0010	0.0019	0.0019	0.20497
0.08	0.01316	0.012653	1515.897	0.0013	0.0026	0.0026	0.21472
0.1	0.0147	0.014131	1668.965	0.0016	0.0032	0.0032	0.21449
0.2	0.01843	0.017726	2399.809	0.0032	0.0064	0.0064	0.19025
0.4	0.02099	0.020187	3076.992	0.0064	0.0128	0.0128	0.1532
0.6	0.0221	0.021249	3705.273	0.0096	0.0192	0.0192	0.13167
0.8	0.02275	0.021871	4831.629	0.0128	0.0256	0.0256	0.11737
1	0.02318	0.022291	5807.693	0.0160	0.0320	0.0320	0.107
1.1	0.02335	0.022456	6656.698	0.0176	0.0352	0.0352	0.10277
1.2	0.0235	0.022598	7039.607	0.0192	0.0384	0.0384	0.09902
1.3	0.02363	0.022724	7397.564	0.0208	0.0416	0.0416	0.09566
1.4	0.02375	0.022835	7732.413	0.0224	0.0448	0.0448	0.09263
1.5	0.02385	0.022935	8045.834	0.0240	0.0480	0.0480	0.08988
1.6	0.02395	0.023025	8339.357	0.0256	0.0512	0.0512	0.08737
1.7	0.02403	0.023106	8614.382	0.0272	0.0544	0.0544	0.08506
1.8	0.02411	0.023181	8872.189	0.0288	0.0576	0.0576	0.08293
2	0.02424	0.023312	9113.951	0.0320	0.0640	0.0640	0.07912
2.25	0.02439	0.023451	9553.563	0.0360	0.0720	0.0720	0.07504
2.5	0.02451	0.023567	10030.270	0.0400	0.0800	0.0800	0.07154
2.75	0.02461	0.023666	10437.563	0.0440	0.0880	0.0880	0.0685
3	0.0247	0.023753	10785.672	0.0480	0.0960	0.0960	0.06582
3.25	0.02478	0.023829	11083.076	0.0520	0.1040	0.1040	0.06344
3.5	0.02485	0.023896	11336.847	0.0560	0.1120	0.1120	0.06131
3.75	0.02492	0.023957	11552.921	0.0600	0.1200	0.1200	0.05938
4	0.02497	0.024011	11736.312	0.0640	0.1280	0.1280	0.05763
4.5	0.02507	0.024106	11891.271	0.0720	0.1440	0.1440	0.05454
5	0.02515	0.024186	12129.879	0.0800	0.1600	0.1600	0.05192
5.5	0.02522	0.024254	12292.007	0.0880	0.1760	0.1760	0.04964
6	0.02529	0.024313	12394.969	0.0960	0.1920	0.1920	0.04764
6.5	0.02534	0.024365	12451.838	0.1040	0.2080	0.2080	0.04587
7	0.02539	0.024411	12472.601	0.1120	0.2240	0.2240	0.04429
8	0.02564	0.024653	12464.970	0.1280	0.2560	0.2560	0.04184
9	0.0257	0.024714	12387.291	0.1440	0.2880	0.2880	0.03954
10	0.02576	0.024773	12253.188	0.1600	0.3200	0.3200	0.0376
12	0.02588	0.024887	12084.418	0.1920	0.3840	0.3840	0.03448
14	0.02599	0.024994	11694.286	0.2240	0.4480	0.4480	0.03206
16	0.0261	0.025097	11281.062	0.2560	0.5120	0.5120	0.03012
18	0.0262	0.025196	10872.993	0.2880	0.5760	0.5760	0.02851
20	0.0263	0.025292	10482.319	0.3200	0.6400	0.6400	0.02715
40	0.02718	0.026135	10113.799	0.6400	1.2800	1.2800	0.01983
60	0.02793	0.026855	7511.493	0.9600	1.9200	1.9200	0.01664
80	0.0286	0.027505	6042.058	1.2800	2.5600	2.5600	0.01476
100	0.02923	0.028107	5078.757	1.6000	3.2000	3.2000	0.01349
120	0.02982	0.028674	4386.796	1.9200	3.8400	3.8400	0.01256
140	0.03038	0.029213	3860.985	2.2400	4.4800	4.4800	0.01185
160	0.03092	0.029729	3446.258	2.5600	5.1200	5.1200	0.01128
180	0.03144	0.030226	3110.426	2.8800	5.7600	5.7600	0.01081
200	0.03194	0.030707	2833.118	3.2000	6.4000	6.4000	0.01042
300	0.03424	0.032927	2600.652	4.8000	9.6000	9.6000	0.00912
400	0.03633	0.034931	1849.984	6.4000	12.8000	12.8000	0.00838
500	0.03826	0.036788	1457.467	8.0000	16.0000	16.0000	0.0079
600	0.04008	0.038537	1225.980	9.6000	19.2000	19.2000	0.00755
700	0.04181	0.040199	1073.790	11.2000	22.4000	22.4000	0.00729
800	0.04346	0.041792	960.341	12.8000	25.6000	25.6000	0.00709
900	0.04506	0.043326	863.088	14.4000	28.8000	28.8000	0.00693
1000	0.0466	0.044809	768.455	16.0000	32.0000	32.0000	0.0068

147

Appendix

Oxygen ions interact with Breast tissue

E(MeV)	Range ($\frac{g}{cm^2}$)	Thickness (cm)	LET ($\frac{MeV}{cm}$)	Absorbed Dose $\times$ 10^{-6} (rad)	Equivalent Dose$\times$ 10^{-5} (rem)	Effective Dose$\times$ 10^{-7} (rem)	Stopping Time (nm)
0.025	0.00126	0.00123	1086.543	0.0004	0.0008	0.0096	0.0374
0.03	0.0035	0.00343	1129.707	0.0005	0.0010	0.0115	0.0952
0.04	0.00663	0.0065	1215.445	0.0006	0.0013	0.0154	0.1560
0.06	0.01028	0.01008	1384.595	0.0010	0.0019	0.0230	0.1976
0.08	0.01243	0.01219	1550.707	0.0013	0.0026	0.0307	0.2069
0.1	0.01389	0.01361	1713.856	0.0016	0.0032	0.0384	0.2066
0.2	0.01743	0.01709	2487.280	0.0032	0.0064	0.0768	0.1834
0.3	0.01896	0.01859	3196.392	0.0048	0.0096	0.1152	0.1629
0.4	0.01986	0.01947	3847.801	0.0064	0.0128	0.1536	0.1478
0.6	0.02092	0.02051	5000.752	0.0096	0.0192	0.2304	0.1271
0.8	0.02154	0.02112	5985.244	0.0128	0.0256	0.3072	0.1133
1	0.02196	0.02153	6831.273	0.0160	0.0320	0.3840	0.1033
1.1	0.02212	0.02169	7209.888	0.0176	0.0352	0.4224	0.0993
1.2	0.02226	0.02183	7562.257	0.0192	0.0384	0.4608	0.0956
1.3	0.02239	0.02195	7890.556	0.0208	0.0416	0.4992	0.0924
1.4	0.0225	0.02206	8196.738	0.0224	0.0448	0.5376	0.0895
1.5	0.0226	0.02216	8482.556	0.0240	0.0480	0.5760	0.0868
1.6	0.02269	0.02225	8749.587	0.0256	0.0512	0.6144	0.0844
1.7	0.02277	0.02233	8999.258	0.0272	0.0544	0.6528	0.0822
1.8	0.02285	0.0224	9232.859	0.0288	0.0576	0.6912	0.0801
2	0.02298	0.02253	9656.430	0.0320	0.0640	0.7680	0.0765
2.25	0.02312	0.02266	10114.237	0.0360	0.0720	0.8640	0.0725
2.5	0.02323	0.02278	10504.441	0.0400	0.0800	0.9600	0.0691
2.75	0.02333	0.02288	10837.529	0.0440	0.0880	1.0560	0.0662
3	0.02342	0.02296	11122.039	0.0480	0.0960	1.1520	0.0636
3.25	0.0235	0.02304	11364.977	0.0520	0.1040	1.2480	0.0613
3.5	0.02357	0.0231	11572.149	0.0560	0.1120	1.3440	0.0593
3.75	0.02363	0.02316	11748.401	0.0600	0.1200	1.4400	0.0574
4	0.02368	0.02322	11897.803	0.0640	0.1280	1.5360	0.0557
4.5	0.02378	0.02331	12129.319	0.0720	0.1440	1.7280	0.0527
5	0.02386	0.02339	12288.599	0.0800	0.1600	1.9200	0.0502
5.5	0.02393	0.02346	12391.798	0.0880	0.1760	2.1120	0.0480
6	0.02399	0.02352	12451.047	0.0960	0.1920	2.3040	0.0461
6.5	0.02437	0.02389	12475.595	0.1040	0.2080	2.4960	0.0450
7	0.0244	0.02392	12472.590	0.1120	0.2240	2.6880	0.0434
8	0.02447	0.02399	12405.081	0.1280	0.2560	3.0720	0.0407
9	0.02453	0.02405	12280.676	0.1440	0.2880	3.4560	0.0385
10	0.02459	0.02411	12120.012	0.1600	0.3200	3.8400	0.0366
12	0.02471	0.02422	11739.799	0.1920	0.3840	4.6080	0.0336
14	0.02482	0.02433	11328.325	0.2240	0.4480	5.3760	0.0312
16	0.02493	0.02444	10915.490	0.2560	0.5120	6.1440	0.0293
18	0.02503	0.02454	10515.442	0.2880	0.5760	6.9120	0.0278
20	0.02513	0.02464	10134.588	0.3200	0.6400	7.6800	0.0264
40	0.026	0.02549	7407.360	0.6400	1.2800	15.3600	0.0193
60	0.02675	0.02622	5902.253	0.9600	1.9200	23.0400	0.0162
80	0.02742	0.02688	4956.831	1.2800	2.5600	30.7200	0.0144
100	0.02804	0.02749	4301.911	1.6000	3.2000	38.4000	0.0132
120	0.02863	0.02807	3816.127	1.9200	3.8400	46.0800	0.0123
140	0.02919	0.02862	3437.516	2.2400	4.4800	53.7600	0.0116
160	0.02972	0.02914	2876.435	2.5600	5.1200	61.4400	0.0111
180	0.03024	0.02964	3131.285	2.8800	5.7600	69.1200	0.0106
200	0.03073	0.03013	2659.551	3.2000	6.4000	76.8000	0.0102
300	0.03303	0.03238	1909.068	4.8000	9.6000	115.2000	0.0090
400	0.0351	0.03442	1450.095	6.4000	12.8000	153.6000	0.0083
500	0.03703	0.0363	1143.392	8.0000	16.0000	192.0000	0.0078
600	0.03883	0.03807	939.507	9.6000	19.2000	230.4000	0.0075
700	0.04055	0.03976	816.457	11.2000	22.4000	268.8000	0.0072
800	0.0422	0.04137	762.981	12.8000	25.6000	307.2000	0.0070
900	0.04379	0.04293	772.715	14.4000	28.8000	345.6000	0.0069
1000	0.04532	0.04443	841.792	16.0000	32.0000	384.0000	0.0067

Appendix

Oxygen ions interact with Muscle tissue

E(MeV)	Range $(\frac{g}{cm^2})$	Thickness (cm)	LET $(\frac{MeV}{cm})$	Absorbed Dose × 10^{-6} (rad)	Equivalent Dose× 10^{-5} (rem)	Effective Dose× 10^{-7} (rem)	Stopping Time (nm)
0.025	0.0013	0.00124	1045.501	0.0004	0.0008	0.0096	0.0376
0.03	0.0037	0.00355	1088.484	0.0005	0.0010	0.0115	0.0985
0.04	0.0071	0.00676	1173.893	0.0006	0.0013	0.0154	0.1624
0.06	0.0110	0.01051	1342.513	0.0010	0.0019	0.0230	0.2059
0.08	0.0133	0.0127	1508.256	0.0013	0.0026	0.0307	0.2155
0.1	0.0149	0.01418	1671.188	0.0016	0.0032	0.0384	0.2152
0.2	0.0186	0.01776	2445.770	0.0032	0.0064	0.0768	0.1906
0.3	0.0203	0.0193	3158.647	0.0048	0.0096	0.1152	0.1691
0.4	0.0212	0.0202	3816.041	0.0064	0.0128	0.1536	0.1533
0.6	0.0223	0.02126	4985.585	0.0096	0.0192	0.2304	0.1317
0.8	0.0230	0.02187	5991.900	0.0128	0.0256	0.3072	0.1174
1	0.0234	0.02229	6648.581	0.0160	0.0320	0.3840	0.1070
1.1	0.0236	0.02245	7228.997	0.0176	0.0352	0.4224	0.1028
1.2	0.0237	0.02259	7596.722	0.0192	0.0384	0.4608	0.0990
1.3	0.0239	0.02272	7936.608	0.0208	0.0416	0.4992	0.0956
1.4	0.0240	0.02283	8253.195	0.0224	0.0448	0.5376	0.0926
1.5	0.0241	0.02293	8548.743	0.0240	0.0480	0.5760	0.0898
1.6	0.0242	0.02301	8824.988	0.0256	0.0512	0.6144	0.0873
1.7	0.0242	0.02309	9083.415	0.0272	0.0544	0.6528	0.0850
1.8	0.0243	0.02317	9325.339	0.0288	0.0576	0.6912	0.0829
2	0.0245	0.0233	9764.312	0.0320	0.0640	0.7680	0.0791
2.25	0.0246	0.02343	10239.136	0.0360	0.0720	0.8640	0.0750
2.5	0.0247	0.02355	10644.008	0.0400	0.0800	0.9600	0.0715
2.75	0.0248	0.02365	10989.592	0.0440	0.0880	1.0560	0.0684
3	0.0249	0.02373	11284.607	0.0480	0.0960	1.1520	0.0658
3.25	0.0250	0.02381	11536.255	0.0520	0.1040	1.2480	0.0634
3.5	0.0251	0.02387	11750.526	0.0560	0.1120	1.3440	0.0612
3.75	0.0251	0.02393	11932.441	0.0600	0.1200	1.4400	0.0593
4	0.0252	0.02399	12086.234	0.0640	0.1280	1.5360	0.0576
4.5	0.0253	0.02408	12323.301	0.0720	0.1440	1.7280	0.0545
5	0.0254	0.02416	12484.659	0.0800	0.1600	1.9200	0.0519
5.5	0.0258	0.02456	12587.294	0.0880	0.1760	2.1120	0.0503
6	0.0258	0.0246	12643.996	0.0960	0.1920	2.3040	0.0482
6.5	0.0259	0.02463	12664.532	0.1040	0.2080	2.4960	0.0464
7	0.0259	0.02467	12656.456	0.1120	0.2240	2.6880	0.0448
8	0.0260	0.02473	12576.829	0.1280	0.2560	3.0720	0.0420
9	0.0260	0.0248	12439.053	0.1440	0.2880	3.4560	0.0397
10	0.0261	0.02486	12264.829	0.1600	0.3200	3.8400	0.0377
12	0.0262	0.02498	11859.141	0.1920	0.3840	4.6080	0.0346
14	0.0263	0.02509	11425.899	0.2240	0.4480	5.3760	0.0322
16	0.0265	0.02519	10995.372	0.2560	0.5120	6.1440	0.0302
18	0.0266	0.0253	10581.390	0.2880	0.5760	6.9120	0.0286
20	0.0267	0.02539	10189.834	0.3200	0.6400	7.6800	0.0273
40	0.0276	0.02625	7443.778	0.6400	1.2800	15.3600	0.0199
60	0.0283	0.02698	5960.929	0.9600	1.9200	23.0400	0.0167
80	0.0290	0.02764	5035.811	1.2800	2.5600	30.7200	0.0148
100	0.0297	0.02824	4394.973	1.6000	3.2000	38.4000	0.0136
120	0.0303	0.02881	3917.924	1.9200	3.8400	46.0800	0.0126
140	0.0308	0.02935	3544.017	2.2400	4.4800	53.7600	0.0119
160	0.0314	0.02987	3239.541	2.5600	5.1200	61.4400	0.0113
180	0.0319	0.03036	2984.292	2.8800	5.7600	69.1200	0.0109
200	0.0324	0.03084	2765.439	3.2000	6.4000	76.8000	0.0105
300	0.0347	0.03304	1993.319	4.8000	9.6000	115.2000	0.0092
400	0.0368	0.03502	1507.981	6.4000	12.8000	153.6000	0.0084
500	0.0387	0.03684	1178.882	8.0000	16.0000	192.0000	0.0079
600	0.0405	0.03856	959.944	9.6000	19.2000	230.4000	0.0076
700	0.0422	0.04019	830.760	11.2000	22.4000	268.8000	0.0073
800	0.0438	0.04174	780.900	12.8000	25.6000	307.2000	0.0071
900	0.0454	0.04324	804.482	14.4000	28.8000	345.6000	0.0069
1000	0.0469	0.04468	897.934	16.0000	32.0000	384.0000	0.0068

Appendix

Oxygen ions interact with Bone tissue

E(MeV)	Range ($\frac{g}{cm^2}$)	Thickness (cm)	LET ($\frac{MeV}{cm}$)	Absorbed Dose $\times 10^{-6}$ (rad)	Equivalent Dose $\times 10^{-5}$ (rem)	Effective Dose $\times 10^{-7}$ (rem)	Stopping Time (nm)
0.025	0.0016	0.0014	1472.313	0.0004	0.0008	0.0008	0.0376
0.03	0.0046	0.0043	1533.446	0.0005	0.0010	0.0010	0.0985
0.04	0.0089	0.0082	1654.895	0.0006	0.0013	0.0013	0.1624
0.06	0.0139	0.0127	1894.563	0.0010	0.0019	0.0019	0.2059
0.08	0.0168	0.0164	2130.012	0.0013	0.0026	0.0026	0.2155
0.1	0.0188	0.0172	2361.340	0.0016	0.0032	0.0032	0.2152
0.2	0.0236	0.0216	3459.439	0.0032	0.0064	0.0064	0.1906
0.3	0.0257	0.0244	4467.771	0.0048	0.0096	0.0096	0.1691
0.4	0.0269	0.0246	5395.799	0.0064	0.0128	0.0128	0.1533
0.6	0.0283	0.0259	7042.624	0.0096	0.0192	0.0192	0.1317
0.8	0.0292	0.0270	8453.550	0.0128	0.0256	0.0256	0.1174
1	0.0297	0.0272	9669.708	0.0160	0.0320	0.0320	0.1070
1.1	0.0299	0.0274	10215.003	0.0176	0.0352	0.0352	0.1028
1.2	0.0301	0.0276	10722.947	0.0192	0.0384	0.0384	0.0990
1.3	0.0303	0.0278	11196.396	0.0208	0.0416	0.0416	0.0956
1.4	0.0305	0.0279	11637.803	0.0224	0.0448	0.0448	0.0926
1.5	0.0306	0.0280	12049.189	0.0240	0.0480	0.0480	0.0898
1.6	0.0307	0.0281	12432.030	0.0256	0.0512	0.0512	0.0873
1.7	0.0308	0.0282	12786.951	0.0272	0.0544	0.0544	0.0850
1.8	0.0309	0.0283	13112.833	0.0288	0.0576	0.0576	0.0829
2	0.0311	0.0285	13632.968	0.0320	0.0640	0.0640	0.0791
2.25	0.0313	0.0286	14762.439	0.0360	0.0720	0.0720	0.0750
2.5	0.0314	0.0288	15154.423	0.0400	0.0800	0.0800	0.0715
2.75	0.0316	0.0289	15623.698	0.0440	0.0880	0.0880	0.0684
3	0.0317	0.0290	16042.325	0.0480	0.0960	0.0960	0.0658
3.25	0.0318	0.0291	16407.307	0.0520	0.1040	0.1040	0.0634
3.5	0.0319	0.0292	16723.479	0.0560	0.1120	0.1120	0.0612
3.75	0.0320	0.0293	16996.423	0.0600	0.1200	0.1200	0.0593
4	0.0320	0.0293	17231.316	0.0640	0.1280	0.1280	0.0576
4.5	0.0322	0.0295	17604.656	0.0720	0.1440	0.1440	0.0545
5	0.0323	0.0296	17873.383	0.0800	0.1600	0.1600	0.0519
5.5	0.0324	0.0296	18060.034	0.0880	0.1760	0.1760	0.0503
6	0.0324	0.0297	18181.736	0.0960	0.1920	0.1920	0.0482
6.5	0.0329	0.0301	18251.656	0.1040	0.2080	0.2080	0.0464
7	0.0329	0.0302	18280.035	0.1120	0.2240	0.2240	0.0448
8	0.0330	0.0302	18242.723	0.1280	0.2560	0.2560	0.0420
9	0.0331	0.0303	18116.537	0.1440	0.2880	0.2880	0.0397
10	0.0332	0.0304	17931.830	0.1600	0.3200	0.3200	0.0377
12	0.0333	0.0305	17461.374	0.1920	0.3840	0.3840	0.0346
14	0.0335	0.0307	16928.270	0.2240	0.4480	0.4480	0.0322
16	0.0336	0.0307	16379.562	0.2560	0.5120	0.5120	0.0302
18	0.0337	0.0309	15838.697	0.2880	0.5760	0.5760	0.0286
20	0.0339	0.0310	15317.242	0.3200	0.6400	0.6400	0.0273
40	0.0349	0.0320	11455.334	0.6400	1.2800	1.2800	0.0199
60	0.0358	0.0328	9249.917	0.9600	1.9200	1.9200	0.0167
80	0.0366	0.0339	7840.403	1.2800	2.5600	2.5600	0.0148
100	0.0374	0.0342	6852.665	1.6000	3.2000	3.2000	0.0136
120	0.0380	0.0348	6113.573	1.9200	3.8400	3.8400	0.0126
140	0.0387	0.0354	5533.395	2.2400	4.4800	4.4800	0.0119
160	0.0393	0.0360	5061.244	2.5600	5.1200	5.1200	0.0113
180	0.0399	0.0366	4666.179	2.8800	5.7600	5.7600	0.0109
200	0.0405	0.0371	4328.328	3.2000	6.4000	6.4000	0.0105
300	0.0431	0.0395	3146.074	4.8000	9.6000	9.6000	0.0092
400	0.0455	0.0417	2411.091	6.4000	12.8000	12.8000	0.0084
500	0.0477	0.0427	1913.157	8.0000	16.0000	16.0000	0.0079
600	0.0497	0.0455	1577.181	9.6000	19.2000	19.2000	0.0076
700	0.0517	0.0473	1369.672	11.2000	22.4000	22.4000	0.0073
800	0.0535	0.0490	1273.436	12.8000	25.6000	25.6000	0.0071
900	0.0553	0.0506	1278.741	14.4000	28.8000	28.8000	0.0069
1000	0.0570	0.0522	1379.663	16.0000	32.0000	32.0000	0.0068

Appendix

Oxygen ions interact with Skin tissue

E(MeV)	Range ($\frac{g}{cm^2}$)	Thickness (cm)	LET ($\frac{MeV}{cm}$)	Absorbed Dose $\times 10^{-6}$ (rad)	Equivalent Dose$\times 10^{-5}$ (rem)	Effective Dose$\times 10^{-7}$ (rem)	Stopping Time (nm)
0.025	0.0012	0.00108	1154.430	0.0004	0.0008	0.0008	0.0185
0.03	0.0035	0.0032	1194.617	0.0005	0.0010	0.0010	0.0503
0.04	0.0067	0.00615	1274.536	0.0006	0.0013	0.0013	0.0839
0.06	0.0105	0.00963	1432.562	0.0010	0.0019	0.0019	0.1072
0.08	0.0127	0.01169	1588.129	0.0013	0.0026	0.0026	0.1126
0.1	0.0143	0.01308	1740.808	0.0016	0.0032	0.0032	0.1127
0.2	0.0180	0.01651	2477.692	0.0032	0.0064	0.0064	0.1006
0.3	0.0196	0.018	3161.307	0.0048	0.0096	0.0096	0.0895
0.4	0.0206	0.01888	3798.262	0.0064	0.0128	0.0128	0.0814
0.6	0.0217	0.01992	4947.037	0.0096	0.0192	0.0192	0.0701
0.8	0.0224	0.02053	5950.434	0.0128	0.0256	0.0256	0.0626
1	0.0228	0.02095	6830.013	0.0160	0.0320	0.0320	0.0571
1.1	0.0230	0.02111	7229.022	0.0176	0.0352	0.0352	0.0549
1.2	0.0232	0.02125	7603.449	0.0192	0.0384	0.0384	0.0529
1.3	0.0233	0.02138	7955.031	0.0208	0.0416	0.0416	0.0511
1.4	0.0234	0.02149	8285.356	0.0224	0.0448	0.0448	0.0495
1.5	0.0235	0.02159	8595.873	0.0240	0.0480	0.0480	0.0480
1.6	0.0236	0.02168	8887.912	0.0256	0.0512	0.0512	0.0467
1.7	0.0237	0.02176	9162.693	0.0272	0.0544	0.0544	0.0455
1.8	0.0238	0.02184	9421.338	0.0288	0.0576	0.0576	0.0444
2	0.0239	0.02197	9894.271	0.0320	0.0640	0.0640	0.0423
2.25	0.0241	0.02211	10411.450	0.0360	0.0720	0.0720	0.0402
2.5	0.0242	0.02223	10857.553	0.0400	0.0800	0.0800	0.0383
2.75	0.0243	0.02233	11242.561	0.0440	0.0880	0.0880	0.0367
3	0.0244	0.02242	11574.807	0.0480	0.0960	0.0960	0.0353
3.25	0.0245	0.02249	11861.290	0.0520	0.1040	0.1040	0.0340
3.5	0.0246	0.02256	12107.926	0.0560	0.1120	0.1120	0.0329
3.75	0.0247	0.02262	12319.743	0.0600	0.1200	0.1200	0.0318
4	0.0247	0.02268	12501.038	0.0640	0.1280	0.1280	0.0309
4.5	0.0248	0.02278	12786.308	0.0720	0.1440	0.1440	0.0293
5	0.0249	0.02286	12987.616	0.0800	0.1600	0.1600	0.0279
5.5	0.0250	0.02293	13122.978	0.0880	0.1760	0.1760	0.0266
6	0.0251	0.02299	13206.177	0.0960	0.1920	0.1920	0.0256
6.5	0.0253	0.02325	13247.881	0.1040	0.2080	0.2080	0.0248
7	0.0254	0.02328	13256.44	0.1120	0.2240	0.2240	0.0240
8	0.0254	0.02334	13199.122	0.1280	0.2560	0.2560	0.0225
9	0.0255	0.0234	13072.572	0.1440	0.2880	0.2880	0.0213
10	0.0256	0.02346	12901.680	0.1600	0.3200	0.3200	0.0202
12	0.0257	0.02357	12487.527	0.1920	0.3840	0.3840	0.0185
14	0.0258	0.02367	12034.539	0.2240	0.4480	0.4480	0.0172
16	0.0259	0.02377	11579.159	0.2560	0.5120	0.5120	0.0162
18	0.0260	0.02387	11138.500	0.2880	0.5760	0.5760	0.0153
20	0.0261	0.02396	10720.186	0.3200	0.6400	0.6400	0.0146
40	0.0270	0.02478	7777.116	0.6400	1.2800	1.2800	0.0107
60	0.0278	0.02548	6195.555	0.9600	1.9200	1.9200	0.0090
80	0.0285	0.0261	5215.324	1.2800	2.5600	2.5600	0.0080
100	0.0291	0.02668	4540.329	1.6000	3.2000	3.2000	0.0073
120	0.0297	0.02723	4040.527	1.9200	3.8400	3.8400	0.0068
140	0.0302	0.02775	3650.680	2.2400	4.4800	4.4800	0.0064
160	0.0308	0.02824	3334.618	2.5600	5.1200	5.1200	0.0061
180	0.0313	0.02872	3070.715	2.8800	5.7600	5.7600	0.0058
200	0.0318	0.02918	2845.260	3.2000	6.4000	6.4000	0.0056
300	0.0341	0.03131	2056.069	4.8000	9.6000	9.6000	0.0049
400	0.0362	0.03323	1564.282	6.4000	12.8000	12.8000	0.0045
500	0.0382	0.035	1231.357	8.0000	16.0000	16.0000	0.0043
600	0.0400	0.03667	1008.504	9.6000	19.2000	19.2000	0.0041
700	0.0417	0.03826	874.142	11.2000	22.4000	22.4000	0.0039
800	0.0434	0.03978	817.255	12.8000	25.6000	25.6000	0.0038
900	0.0449	0.04124	831.632	14.4000	28.8000	28.8000	0.0037
1000	0.0465	0.04265	913.503	16.0000	32.0000	32.0000	0.0037

Appendix

Fluorine ions interact with Adipose tissue

E(MeV)	Range $(\frac{g}{cm^2})$	Thickness (cm)	LET MeV $(\frac{}{cm})$	Absorbed Dose × 10^{-6} (rad)	Equivalent Dose× 10^{-5} (rem)	Effective Dose× 10^{-7} (rem)	Stopping Time (nm)
0.025	0.001135	0.00123	936.046	0.0004	0.0008	0.00960	0.0408
0.03	0.003185	0.00346	1051.413	0.0005	0.0010	0.01152	0.1045
0.04	0.006044	0.00657	1226.234	0.0006	0.0013	0.01536	0.1718
0.06	0.009402	0.01022	1473.250	0.0010	0.0019	0.02304	0.2182
0.08	0.011384	0.01237	1663.679	0.0013	0.0026	0.03072	0.2288
0.1	0.012727	0.01383	1829.242	0.0016	0.0032	0.03840	0.2288
0.2	0.016018	0.01741	2525.582	0.0032	0.0064	0.07680	0.2036
0.3	0.017453	0.01897	3137.823	0.0048	0.0096	0.11520	0.1812
0.4	0.018300	0.01989	3705.983	0.0064	0.0128	0.15360	0.1645
0.6	0.019295	0.02097	4743.756	0.0096	0.0192	0.23040	0.1416
0.8	0.019882	0.02161	5672.341	0.0128	0.0256	0.30720	0.1264
1	0.020280	0.02204	6507.461	0.0160	0.0320	0.38400	0.1153
1.1	0.020436	0.02221	6893.642	0.0176	0.0352	0.42240	0.1108
1.2	0.020572	0.02236	7260.562	0.0192	0.0384	0.46080	0.1068
1.3	0.020692	0.02249	7609.332	0.0208	0.0416	0.49920	0.1032
1.4	0.020798	0.02261	7940.976	0.0224	0.0448	0.53760	0.0999
1.5	0.020893	0.02271	8256.443	0.0240	0.0480	0.57600	0.0970
1.6	0.020979	0.0228	8556.615	0.0256	0.0512	0.61440	0.0943
1.7	0.021057	0.02289	8842.312	0.0272	0.0544	0.65280	0.0918
1.8	0.021129	0.02297	9114.301	0.0288	0.0576	0.69120	0.0895
2	0.021255	0.0231	9619.973	0.0320	0.0640	0.76800	0.0854
2.25	0.021388	0.02325	10186.788	0.0360	0.0720	0.86400	0.0811
2.5	0.021500	0.02337	10689.242	0.0400	0.0800	0.96000	0.0773
2.75	0.021597	0.02347	11134.901	0.0440	0.0880	1.05600	0.0740
3	0.021680	0.02357	11530.293	0.0480	0.0960	1.15200	0.0712
3.25	0.021754	0.02365	11881.069	0.0520	0.1040	1.24800	0.0686
3.5	0.021819	0.02372	12192.144	0.0560	0.1120	1.34400	0.0663
3.75	0.021878	0.02378	12467.810	0.0600	0.1200	1.44000	0.0642
4	0.021931	0.02384	12711.824	0.0640	0.1280	1.53600	0.0623
4.5	0.022023	0.02394	13117.710	0.0720	0.1440	1.72800	0.0590
5	0.022101	0.02402	13431.829	0.0800	0.1600	1.92000	0.0562
5.5	0.022168	0.0241	13671.461	0.0880	0.1760	2.11200	0.0537
6	0.022226	0.02416	13850.297	0.0960	0.1920	2.30400	0.0516
6.5	0.022277	0.02421	13979.277	0.1040	0.2080	2.49600	0.0497
7	0.022322	0.02426	14067.213	0.1120	0.2240	2.68800	0.0480
8	0.022584	0.02455	14133.269	0.1280	0.2560	3.07200	0.0454
9	0.022630	0.0246	14147.220	0.1440	0.2880	3.45600	0.0429
10	0.022675	0.02465	14054.537	0.1600	0.3200	3.84000	0.0408
12	0.022760	0.02474	13777.467	0.1920	0.3840	4.60800	0.0374
14	0.022841	0.02483	13416.147	0.2240	0.4480	5.37600	0.0347
16	0.022918	0.02491	13021.724	0.2560	0.5120	6.14400	0.0326
18	0.022992	0.02499	12620.964	0.2880	0.5760	6.91200	0.0308
20	0.023063	0.02507	12227.898	0.3200	0.6400	7.68000	0.0293
40	0.023682	0.02574	9259.967	0.6400	1.2800	15.36000	0.0213
60	0.024201	0.02631	7568.726	0.9600	1.9200	23.04000	0.0178
80	0.024666	0.02681	6489.110	1.2800	2.5600	30.72000	0.0157
100	0.025094	0.02728	5727.854	1.6000	3.2000	38.40000	0.0143
120	0.025494	0.02771	5151.890	1.9200	3.8400	46.08000	0.0132
140	0.025873	0.02812	4693.455	2.2400	4.4800	53.76000	0.0124
160	0.026234	0.02852	4314.655	2.5600	5.1200	61.44000	0.0118
180	0.026581	0.02889	3992.707	2.8800	5.7600	69.12000	0.0113
200	0.026915	0.02926	3713.113	3.2000	6.4000	76.80000	0.0108
300	0.028447	0.03092	2697.039	4.8000	9.6000	115.20000	0.0093
400	0.029817	0.03241	2033.871	6.4000	12.8000	153.60000	0.0085
500	0.031077	0.03378	1575.462	8.0000	16.0000	192.00000	0.0079
600	0.032256	0.03506	1269.492	9.6000	19.2000	230.40000	0.0075
700	0.033372	0.03627	1092.784	11.2000	22.4000	268.80000	0.0072
800	0.034437	0.03743	1033.496	12.8000	25.6000	307.20000	0.0069
900	0.035459	0.03854	1084.947	14.4000	28.8000	345.60000	0.0067
1000	0.036444	0.03961	1243.079	16.0000	32.0000	384.00000	0.0066

Appendix

Fluorine ions interact with **Blood tissue**

E(MeV)	Range $(\frac{g}{cm^2})$	Thickness (cm)	LET $(\frac{MeV}{cm})$	Absorbed Dose × 10^{-6} (rad)	Equivalent Dose× 10^{-5} (rem)	Effective Dose× 10^{-7} (rem)	Stopping Time (nm)
0.025	0.00113	0.00107	1065.130	0.0004	0.0008	0.0096	0.0354
0.03	0.00318	0.003	1098.036	0.0005	0.0010	0.0115	0.0907
0.04	0.00604	0.0057	1163.610	0.0006	0.0013	0.0154	0.1491
0.06	0.0094	0.00887	1293.806	0.0010	0.0019	0.0230	0.1894
0.08	0.01138	0.01074	1422.745	0.0013	0.0026	0.0307	0.1986
0.1	0.01273	0.01201	1550.440	0.0016	0.0032	0.0384	0.1986
0.2	0.01602	0.01511	2170.692	0.0032	0.0064	0.0768	0.1767
0.3	0.01745	0.01647	2761.685	0.0048	0.0096	0.1152	0.1572
0.4	0.0183	0.01726	3324.877	0.0064	0.0128	0.1536	0.1428
0.6	0.01929	0.0182	4373.296	0.0096	0.0192	0.2304	0.1229
0.8	0.01988	0.01876	5326.129	0.0128	0.0256	0.3072	0.1097
1	0.02028	0.01913	6192.505	0.0160	0.0320	0.3840	0.1001
1.1	0.02044	0.01928	6595.867	0.0176	0.0352	0.4224	0.0961
1.2	0.02057	0.01941	6980.619	0.0192	0.0384	0.4608	0.0927
1.3	0.02069	0.01952	7347.655	0.0208	0.0416	0.4992	0.0895
1.4	0.0208	0.01962	7697.822	0.0224	0.0448	0.5376	0.0867
1.5	0.02089	0.01971	8031.922	0.0240	0.0480	0.5760	0.0842
1.6	0.02098	0.01979	8350.718	0.0256	0.0512	0.6144	0.0818
1.7	0.02106	0.01987	8654.929	0.0272	0.0544	0.6528	0.0797
1.8	0.02113	0.01993	8945.242	0.0288	0.0576	0.6912	0.0777
2	0.02126	0.02005	9486.730	0.0320	0.0640	0.7680	0.0742
2.25	0.02139	0.02018	10096.281	0.0360	0.0720	0.8640	0.0704
2.5	0.0215	0.02028	10638.783	0.0400	0.0800	0.9600	0.0671
2.75	0.0216	0.02037	11121.574	0.0440	0.0880	1.0560	0.0643
3	0.02168	0.02045	11551.114	0.0480	0.0960	1.1520	0.0618
3.25	0.02175	0.02052	11933.094	0.0520	0.1040	1.2480	0.0595
3.5	0.02182	0.02058	12272.543	0.0560	0.1120	1.3440	0.0575
3.75	0.02188	0.02064	12573.906	0.0600	0.1200	1.4400	0.0557
4	0.02193	0.02069	12841.120	0.0640	0.1280	1.5360	0.0541
4.5	0.02202	0.02078	13286.686	0.0720	0.1440	1.7280	0.0512
5	0.0221	0.02085	13632.788	0.0800	0.1600	1.9200	0.0488
5.5	0.02217	0.02091	13898.126	0.0880	0.1760	2.1120	0.0466
6	0.02223	0.02097	14097.630	0.0960	0.1920	2.3040	0.0448
6.5	0.02228	0.02102	14243.294	0.1040	0.2080	2.4960	0.0431
7	0.02232	0.02106	14344.799	0.1120	0.2240	2.6880	0.0416
8	0.0224	0.02113	14445.302	0.1280	0.2560	3.0720	0.0391
9	0.02263	0.02135	14446.247	0.1440	0.2880	3.4560	0.0372
10	0.02268	0.02139	14379.424	0.1600	0.3200	3.8400	0.0354
12	0.02276	0.02147	14122.887	0.1920	0.3840	4.6080	0.0324
14	0.02284	0.02155	13781.944	0.2240	0.4480	5.3760	0.0301
16	0.02292	0.02162	13409.244	0.2560	0.5120	6.1440	0.0283
18	0.02299	0.02169	13031.382	0.2880	0.5760	6.9120	0.0267
20	0.02306	0.02176	12661.740	0.3200	0.6400	7.6800	0.0254
40	0.02368	0.02234	9865.427	0.6400	1.2800	15.3600	0.0185
60	0.0242	0.02283	8201.658	0.9600	1.9200	23.0400	0.0154
80	0.02467	0.02327	7071.251	1.2800	2.5600	30.7200	0.0136
100	0.02509	0.02367	6228.329	1.6000	3.2000	38.4000	0.0124
120	0.02549	0.02405	5563.269	1.9200	3.8400	46.0800	0.0115
140	0.02587	0.02441	5019.551	2.2400	4.4800	53.7600	0.0108
160	0.02623	0.02475	4564.499	2.5600	5.1200	61.4400	0.0102
180	0.02658	0.02508	4177.478	2.8800	5.7600	69.1200	0.0098
200	0.02692	0.02539	3844.537	3.2000	6.4000	76.8000	0.0094
300	0.02845	0.02684	2716.061	4.8000	9.6000	115.2000	0.0081
400	0.02982	0.02813	2108.217	6.4000	12.8000	153.6000	0.0074
500	0.03108	0.02932	1765.337	8.0000	16.0000	192.0000	0.0069
600	0.03226	0.03043	1559.844	9.6000	19.2000	230.4000	0.0065
700	0.03337	0.03148	1417.642	11.2000	22.4000	268.8000	0.0062
800	0.03444	0.03249	1291.863	12.8000	25.6000	307.2000	0.0060
900	0.03546	0.03345	1151.123	14.4000	28.8000	345.6000	0.0058
1000	0.03644	0.03438	973.509	16.0000	32.0000	384.0000	0.0057

Appendix

Fluorine ions interact with Breast tissue

E(MeV)	Range ($\frac{g}{cm^2}$)	Thickness (cm)	LET ($\frac{MeV}{cm}$)	Absorbed Dose $\times 10^{-6}$ (rad)	Equivalent Dose$\times 10^{-5}$ (rem)	Effective Dose$\times 10^{-7}$ (rem)	Stopping Time (nm)
0.025	0.00133	0.00131	786.548	0.0004	0.0008	0.0096	0.0432
0.03	0.00377	0.0037	889.215	0.0005	0.0010	0.0115	0.1117
0.04	0.00716	0.00702	1057.350	0.0006	0.0013	0.0154	0.1835
0.06	0.01109	0.01088	1313.649	0.0010	0.0019	0.0230	0.2322
0.08	0.0134	0.01313	1518.549	0.0013	0.0026	0.0307	0.2429
0.1	0.01494	0.01465	1698.001	0.0016	0.0032	0.0384	0.2423
0.2	0.01869	0.01833	2446.595	0.0032	0.0064	0.0768	0.2143
0.3	0.0203	0.0199	3094.432	0.0048	0.0096	0.1152	0.1901
0.4	0.02124	0.02083	3689.525	0.0064	0.0128	0.1536	0.1722
0.6	0.02234	0.0219	4765.279	0.0096	0.0192	0.2304	0.1479
0.8	0.02298	0.02253	5717.790	0.0128	0.0256	0.3072	0.1317
1	0.02341	0.02295	6567.415	0.0160	0.0320	0.3840	0.1200
1.1	0.02358	0.02311	6958.257	0.0176	0.0352	0.4224	0.1153
1.2	0.02372	0.02326	7328.485	0.0192	0.0384	0.4608	0.1111
1.3	0.02385	0.02338	7679.439	0.0208	0.0416	0.4992	0.1073
1.4	0.02397	0.0235	8012.336	0.0224	0.0448	0.5376	0.1039
1.5	0.02407	0.0236	8328.290	0.0240	0.0480	0.5760	0.1008
1.6	0.02416	0.02368	8628.324	0.0256	0.0512	0.6144	0.0979
1.7	0.02424	0.02377	8913.381	0.0272	0.0544	0.6528	0.0953
1.8	0.02432	0.02384	9184.333	0.0288	0.0576	0.6912	0.0929
2	0.02445	0.02397	9687.087	0.0320	0.0640	0.7680	0.0887
2.25	0.02459	0.02411	10249.371	0.0360	0.0720	0.8640	0.0841
2.5	0.02471	0.02423	10747.044	0.0400	0.0800	0.9600	0.0801
2.75	0.02481	0.02432	11188.208	0.0440	0.0880	1.0560	0.0767
3	0.0249	0.02441	11579.734	0.0480	0.0960	1.1520	0.0737
3.25	0.02498	0.02449	11927.485	0.0520	0.1040	1.2480	0.0710
3.5	0.02504	0.02455	12236.494	0.0560	0.1120	1.3440	0.0686
3.75	0.02511	0.02461	12511.102	0.0600	0.1200	1.4400	0.0665
4	0.02516	0.02467	12755.073	0.0640	0.1280	1.5360	0.0645
4.5	0.02526	0.02476	13163.792	0.0720	0.1440	1.7280	0.0611
5	0.02534	0.02484	13484.262	0.0800	0.1600	1.9200	0.0581
5.5	0.02541	0.02491	13733.215	0.0880	0.1760	2.1120	0.0556
6	0.02547	0.02497	13923.776	0.0960	0.1920	2.3040	0.0533
6.5	0.02552	0.02502	14066.353	0.1040	0.2080	2.4960	0.0513
7	0.02556	0.02506	14169.282	0.1120	0.2240	2.6880	0.0495
8	0.02564	0.02514	14281.896	0.1280	0.2560	3.0720	0.0465
9	0.02595	0.02544	14302.035	0.1440	0.2880	3.4560	0.0444
10	0.02599	0.02548	14257.177	0.1600	0.3200	3.8400	0.0422
12	0.02609	0.02557	14043.312	0.1920	0.3840	4.6080	0.0386
14	0.02617	0.02566	13736.223	0.2240	0.4480	5.3760	0.0359
16	0.02625	0.02574	13386.261	0.2560	0.5120	6.1440	0.0337
18	0.02633	0.02581	13020.826	0.2880	0.5760	6.9120	0.0318
20	0.02641	0.02589	12655.093	0.3200	0.6400	7.6800	0.0303
40	0.02706	0.02653	9732.432	0.6400	1.2800	15.3600	0.0219
60	0.0276	0.02706	7971.721	0.9600	1.9200	23.0400	0.0183
80	0.02809	0.02754	6823.309	1.2800	2.5600	30.7200	0.0161
100	0.02854	0.02798	6007.637	1.6000	3.2000	38.4000	0.0146
120	0.02896	0.02839	5390.499	1.9200	3.8400	46.0800	0.0136
140	0.02935	0.02877	4901.226	2.2400	4.4800	53.7600	0.0127
160	0.02973	0.02914	4499.390	2.5600	5.1200	61.4400	0.0121
180	0.03009	0.0295	4160.277	2.8800	5.7600	69.1200	0.0115
200	0.03043	0.02984	3867.956	3.2000	6.4000	76.8000	0.0110
300	0.03202	0.03139	2825.615	4.8000	9.6000	115.2000	0.0095
400	0.03344	0.03278	2160.925	6.4000	12.8000	153.6000	0.0086
500	0.03474	0.03406	1703.696	8.0000	16.0000	192.0000	0.0080
600	0.03596	0.03525	1392.995	9.6000	19.2000	230.4000	0.0075
700	0.0371	0.03638	1201.616	11.2000	22.4000	268.8000	0.0072
800	0.0382	0.03745	1115.580	12.8000	25.6000	307.2000	0.0069
900	0.03925	0.03848	1126.973	14.4000	28.8000	345.6000	0.0067
1000	0.04026	0.03947	1230.975	16.0000	32.0000	384.0000	0.0065

Appendix

Fluorine ions interact with Brain tissue

E(MeV)	Range ($\frac{g}{cm^2}$)	Thickness (cm)	LET ($\frac{MeV}{cm}$)	Absorbed Dose $\times$ 10^{-6} (rad)	Equivalent Dose$\times$ 10^{-5} (rem)	Effective Dose$\times$ 10^{-7} (rem)	Stopping Time (nm)
0.025	0.00145	0.001395	1024.310	0.0004	0.0008	0.0008	0.04613
0.03	0.00404	0.003887	1062.087	0.0005	0.0010	0.0010	0.11739
0.04	0.00763	0.007335	1137.254	0.0006	0.0013	0.0013	0.19184
0.06	0.01179	0.011337	1286.061	0.0010	0.0019	0.0019	0.24208
0.08	0.01422	0.01367	1432.863	0.0013	0.0026	0.0026	0.25279
0.1	0.01585	0.015236	1577.695	0.0016	0.0032	0.0032	0.25201
0.2	0.01978	0.019015	2273.492	0.0032	0.0064	0.0064	0.2224
0.3	0.02146	0.020631	2924.931	0.0048	0.0096	0.0096	0.19701
0.4	0.02244	0.021573	3535.635	0.0064	0.0128	0.0128	0.17841
0.6	0.02357	0.022666	4647.543	0.0096	0.0192	0.0192	0.15305
0.8	0.02424	0.023303	5631.500	0.0128	0.0256	0.0256	0.13627
1	0.02468	0.023731	6505.684	0.0160	0.0320	0.0320	0.12412
1.1	0.02485	0.023898	6906.393	0.0176	0.0352	0.0352	0.11918
1.2	0.025	0.024043	7285.061	0.0192	0.0384	0.0384	0.1148
1.3	0.02514	0.02417	7643.166	0.0208	0.0416	0.0416	0.11088
1.4	0.02525	0.024282	7982.063	0.0224	0.0448	0.0448	0.10734
1.5	0.02536	0.024383	8302.994	0.0240	0.0480	0.0480	0.10413
1.6	0.02545	0.024474	8607.100	0.0256	0.0512	0.0512	0.1012
1.7	0.02554	0.024556	8895.430	0.0272	0.0544	0.0544	0.09851
1.8	0.02562	0.024631	9168.951	0.0288	0.0576	0.0576	0.09603
2	0.02575	0.024763	9675.071	0.0320	0.0640	0.0640	0.09159
2.25	0.0259	0.024902	10238.964	0.0360	0.0720	0.0720	0.08683
2.5	0.02602	0.025018	10736.172	0.0400	0.0800	0.0800	0.08276
2.75	0.02612	0.025118	11175.459	0.0440	0.0880	0.0880	0.07922
3	0.02621	0.025204	11564.187	0.0480	0.0960	0.0960	0.07611
3.25	0.02629	0.02528	11908.582	0.0520	0.1040	0.1040	0.07335
3.5	0.02636	0.025347	12213.942	0.0560	0.1120	0.1120	0.07087
3.75	0.02642	0.025407	12484.801	0.0600	0.1200	0.1200	0.06863
4	0.02648	0.025462	12725.063	0.0640	0.1280	0.1280	0.06659
4.5	0.02658	0.025555	13126.844	0.0720	0.1440	0.1440	0.06301
5	0.02666	0.025634	13441.358	0.0800	0.1600	0.1600	0.05996
5.5	0.02673	0.025702	13685.517	0.0880	0.1760	0.1760	0.05732
6	0.02679	0.02576	13872.461	0.0960	0.1920	0.1920	0.05501
6.5	0.02684	0.025811	14012.537	0.1040	0.2080	0.2080	0.05295
7	0.02689	0.025857	14113.977	0.1120	0.2240	0.2240	0.05112
8	0.02697	0.025934	14226.164	0.1280	0.2560	0.2560	0.04796
9	0.02704	0.026	14248.499	0.1440	0.2880	0.2880	0.04533
10	0.02707	0.026033	14207.651	0.1600	0.3200	0.3200	0.04306
12	0.02714	0.026094	14004.858	0.1920	0.3840	0.3840	0.0394
14	0.0272	0.026153	13710.329	0.2240	0.4480	0.4480	0.03656
16	0.02726	0.026208	13372.667	0.2560	0.5120	0.5120	0.03427
18	0.02731	0.026262	13018.449	0.2880	0.5760	0.5760	0.03238
20	0.02737	0.026313	12662.528	0.3200	0.6400	0.6400	0.03078
40	0.02783	0.026759	9776.401	0.6400	1.2800	1.2800	0.02213
60	0.02822	0.027134	8007.480	0.9600	1.9200	1.9200	0.01832
80	0.02857	0.027468	6845.030	1.2800	2.5600	2.5600	0.01606
100	0.02889	0.027776	6017.359	1.6000	3.2000	3.2000	0.01453
120	0.02919	0.028064	5391.369	1.9200	3.8400	3.8400	0.0134
140	0.02947	0.028336	4896.063	2.2400	4.4800	4.4800	0.01253
160	0.02974	0.028596	4490.457	2.5600	5.1200	5.1200	0.01182
180	0.03	0.028845	4149.326	2.8800	5.7600	5.7600	0.01125
200	0.03025	0.029086	3856.323	3.2000	6.4000	6.4000	0.01076
300	0.03139	0.030186	2821.385	4.8000	9.6000	9.6000	0.00912
400	0.03242	0.031168	2169.481	6.4000	12.8000	12.8000	0.00815
500	0.03335	0.032072	1722.604	8.0000	16.0000	16.0000	0.0075
600	0.03423	0.032918	1416.643	9.6000	19.2000	19.2000	0.00703
700	0.03507	0.033717	1222.868	11.2000	22.4000	22.4000	0.00667
800	0.03586	0.03448	1126.486	12.8000	25.6000	25.6000	0.00638
900	0.03662	0.035212	1119.102	14.4000	28.8000	28.8000	0.00614
1000	0.03735	0.035918	1195.600	16.0000	32.0000	32.0000	0.00594

Appendix

Fluorine ions interact with Lung tissue

E(MeV)	Range ($\frac{g}{cm^2}$)	Thickness (cm)	LET MeV ($\frac{MeV}{cm}$)	Absorbed Dose × 10^{-6} (rad)	Equivalent Dose× 10^{-5} (rem)	Effective Dose× 10^{-7} (rem)	Stopping Time (nm)
0.025	0.00142	0.00135	761.584	0.0004	0.0008	0.0096	0.0447
0.03	0.00403	0.00384	856.272	0.0005	0.0010	0.0115	0.1160
0.04	0.00765	0.00729	1015.516	0.0006	0.0013	0.0154	0.1906
0.06	0.01185	0.01129	1265.225	0.0010	0.0019	0.0230	0.2410
0.08	0.0143	0.01362	1467.965	0.0013	0.0026	0.0307	0.2519
0.1	0.01595	0.01519	1646.291	0.0016	0.0032	0.0384	0.2512
0.2	0.01992	0.01897	2389.428	0.0032	0.0064	0.0768	0.2219
0.3	0.02162	0.02059	3030.091	0.0048	0.0096	0.1152	0.1966
0.4	0.02261	0.02153	3617.606	0.0064	0.0128	0.1536	0.1781
0.6	0.02376	0.02263	4679.048	0.0096	0.0192	0.2304	0.1528
0.8	0.02443	0.02327	5619.206	0.0128	0.0256	0.3072	0.1361
1	0.02488	0.0237	6458.489	0.0160	0.0320	0.3840	0.1239
1.1	0.02506	0.02386	6844.851	0.0176	0.0352	0.4224	0.1190
1.2	0.02521	0.02401	7211.018	0.0192	0.0384	0.4608	0.1146
1.3	0.02534	0.02414	7558.298	0.0208	0.0416	0.4992	0.1107
1.4	0.02546	0.02425	7887.88	0.0224	0.0448	0.5376	0.1072
1.5	0.02557	0.02435	8200.85	0.0240	0.0480	0.5760	0.1040
1.6	0.02566	0.02444	8498.205	0.0256	0.0512	0.6144	0.1011
1.7	0.02575	0.02452	8780.865	0.0272	0.0544	0.6528	0.0984
1.8	0.02583	0.0246	9049.678	0.0288	0.0576	0.6912	0.0959
2	0.02597	0.02473	9548.85	0.0320	0.0640	0.7680	0.0915
2.25	0.02611	0.02487	10107.785	0.0360	0.0720	0.8640	0.0867
2.5	0.02624	0.02499	10603.145	0.0400	0.0800	0.9600	0.0827
2.75	0.02634	0.02509	11042.845	0.0440	0.0880	1.0560	0.0791
3	0.02643	0.02517	11433.603	0.0480	0.0960	1.1520	0.0760
3.25	0.02651	0.02525	11781.156	0.0520	0.1040	1.2480	0.0733
3.5	0.02658	0.02532	12090.436	0.0560	0.1120	1.3440	0.0708
3.75	0.02665	0.02538	12365.701	0.0600	0.1200	1.4400	0.0685
4	0.0267	0.02543	12610.643	0.0640	0.1280	1.5360	0.0665
4.5	0.0268	0.02553	13022.029	0.0720	0.1440	1.7280	0.0629
5	0.02689	0.02561	13345.854	0.0800	0.1600	1.9200	0.0599
5.5	0.02696	0.02567	13598.603	0.0880	0.1760	2.1120	0.0573
6	0.02702	0.02573	13793.226	0.0960	0.1920	2.3040	0.0549
6.5	0.02707	0.02578	13940.01	0.1040	0.2080	2.4960	0.0529
7	0.02712	0.02583	14047.202	0.1120	0.2240	2.6880	0.0511
8	0.0272	0.02591	14168.28	0.1280	0.2560	3.0720	0.0479
9	0.02753	0.02622	14196.574	0.1440	0.2880	3.4560	0.0457
10	0.02758	0.02627	14159.416	0.1600	0.3200	3.8400	0.0434
12	0.02767	0.02635	13959.409	0.1920	0.3840	4.6080	0.0398
14	0.02776	0.02644	13664.166	0.2240	0.4480	5.3760	0.0370
16	0.02784	0.02652	13324.27	0.2560	0.5120	6.1440	0.0347
18	0.02793	0.0266	12967.393	0.2880	0.5760	6.9120	0.0328
20	0.028	0.02667	12608.959	0.3200	0.6400	7.6800	0.0312
40	0.02867	0.02731	9722.657	0.6400	1.2800	15.3600	0.0226
60	0.02924	0.02784	7973.534	0.9600	1.9200	23.0400	0.0188
80	0.02974	0.02832	6830.053	1.2800	2.5600	30.7200	0.0166
100	0.0302	0.02876	6016.879	1.6000	3.2000	38.4000	0.0150
120	0.03062	0.02917	5401.167	1.9200	3.8400	46.0800	0.0139
140	0.03103	0.02955	4912.78	2.2400	4.4800	53.7600	0.0131
160	0.03142	0.02992	4511.529	2.5600	5.1200	61.4400	0.0124
180	0.03179	0.03027	4172.82	2.8800	5.7600	69.1200	0.0118
200	0.03214	0.03061	3880.784	3.2000	6.4000	76.8000	0.0113
300	0.03377	0.03216	2838.944	4.8000	9.6000	115.2000	0.0097
400	0.03522	0.03355	2173.886	6.4000	12.8000	153.6000	0.0088
500	0.03656	0.03481	1715.625	8.0000	16.0000	192.0000	0.0081
600	0.0378	0.036	1403.256	9.6000	19.2000	230.4000	0.0077
700	0.03898	0.03712	1209.571	11.2000	22.4000	268.8000	0.0073
800	0.0401	0.03819	1120.588	12.8000	25.6000	307.2000	0.0071
900	0.04117	0.03921	1128.387	14.4000	28.8000	345.6000	0.0068
1000	0.04221	0.0402	1228.145	16.0000	32.0000	384.0000	0.0066

Appendix

Fluorine ions interact with Muscle tissue

E(MeV)	Range ($\frac{g}{cm^2}$)	Thickness (cm)	LET ($\frac{MeV}{cm}$)	Absorbed Dose × 10^{-6} (rad)	Equivalent Dose× 10^{-5} (rem)	Effective Dose× 10^{-7} (rem)	Stopping Time (nm)
0.025	0.0014	0.00133	755.798	0.0004	0.0008	0.0096	0.0442
0.03	0.00402	0.00383	867.069	0.0005	0.0010	0.0115	0.1158
0.04	0.00766	0.00729	1036.779	0.0006	0.0013	0.0154	0.1907
0.06	0.01188	0.01132	1279.735	0.0010	0.0019	0.0230	0.2416
0.08	0.01435	0.01366	1469.735	0.0013	0.0026	0.0307	0.2527
0.1	0.01601	0.01524	1636.514	0.0016	0.0032	0.0384	0.2521
0.2	0.02002	0.01906	2347.313	0.0032	0.0064	0.0768	0.2230
0.3	0.02174	0.0207	2978.383	0.0048	0.0096	0.1152	0.1977
0.4	0.02274	0.02166	3566.778	0.0064	0.0128	0.1536	0.1791
0.6	0.02391	0.02277	4646.658	0.0096	0.0192	0.2304	0.1537
0.8	0.02459	0.02342	5617.905	0.0128	0.0256	0.3072	0.1369
1	0.02505	0.02385	6495.229	0.0160	0.0320	0.3840	0.1248
1.1	0.02523	0.02402	6902.144	0.0176	0.0352	0.4224	0.1198
1.2	0.02538	0.02417	7289.478	0.0192	0.0384	0.4608	0.1154
1.3	0.02552	0.0243	7658.302	0.0208	0.0416	0.4992	0.1115
1.4	0.02564	0.02442	8009.604	0.0224	0.0448	0.5376	0.1079
1.5	0.02575	0.02452	8344.309	0.0240	0.0480	0.5760	0.1047
1.6	0.02584	0.02461	8663.276	0.0256	0.0512	0.6144	0.1018
1.7	0.02593	0.0247	8967.312	0.0272	0.0544	0.6528	0.0991
1.8	0.02601	0.02477	9257.172	0.0288	0.0576	0.6912	0.0966
2	0.02616	0.02491	9797.156	0.0320	0.0640	0.7680	0.0921
2.25	0.0263	0.02505	10404.154	0.0360	0.0720	0.8640	0.0874
2.5	0.02643	0.02517	10943.814	0.0400	0.0800	0.9600	0.0833
2.75	0.02654	0.02527	11423.789	0.0440	0.0880	1.0560	0.0797
3	0.02663	0.02536	11850.726	0.0480	0.0960	1.1520	0.0766
3.25	0.02671	0.02544	12230.422	0.0520	0.1040	1.2480	0.0738
3.5	0.02678	0.02551	12567.948	0.0560	0.1120	1.3440	0.0713
3.75	0.02685	0.02557	12867.755	0.0600	0.1200	1.4400	0.0691
4	0.02691	0.02563	13133.758	0.0640	0.1280	1.5360	0.0670
4.5	0.02701	0.02572	13577.784	0.0720	0.1440	1.7280	0.0634
5	0.02709	0.0258	13923.213	0.0800	0.1600	1.9200	0.0604
5.5	0.02717	0.02587	14188.359	0.0880	0.1760	2.1120	0.0577
6	0.02723	0.02593	14387.811	0.0960	0.1920	2.3040	0.0554
6.5	0.02729	0.02599	14533.282	0.1040	0.2080	2.4960	0.0533
7	0.02734	0.02603	14634.241	0.1120	0.2240	2.6880	0.0515
8	0.02742	0.02611	14727.618	0.1280	0.2560	3.0720	0.0483
9	0.02768	0.02636	14732.031	0.1440	0.2880	3.4560	0.0460
10	0.02773	0.02641	14652.655	0.1600	0.3200	3.8400	0.0437
12	0.02782	0.0265	14372.321	0.1920	0.3840	4.6080	0.0400
14	0.02791	0.02658	13999.966	0.2240	0.4480	5.3760	0.0372
16	0.02799	0.02666	13591.216	0.2560	0.5120	6.1440	0.0349
18	0.02807	0.02674	13175.122	0.2880	0.5760	6.9120	0.0330
20	0.02815	0.02681	12766.869	0.3200	0.6400	7.6800	0.0314
40	0.02882	0.02745	9694.870	0.6400	1.2800	15.3600	0.0227
60	0.02938	0.02799	7954.263	0.9600	1.9200	23.0400	0.0189
80	0.02989	0.02846	6844.304	1.2800	2.5600	30.7200	0.0166
100	0.03035	0.0289	6060.281	1.6000	3.2000	38.4000	0.0151
120	0.03078	0.02931	5465.172	1.9200	3.8400	46.0800	0.0140
140	0.03118	0.0297	4989.620	2.2400	4.4800	53.7600	0.0131
160	0.03157	0.03007	4595.010	2.5600	5.1200	61.4400	0.0124
180	0.03194	0.03042	4258.198	2.8800	5.7600	69.1200	0.0119
200	0.0323	0.03076	3964.492	3.2000	6.4000	76.8000	0.0114
300	0.03394	0.03232	2886.580	4.8000	9.6000	115.2000	0.0098
400	0.0354	0.03371	2174.101	6.4000	12.8000	153.6000	0.0088
500	0.03673	0.03499	1678.302	8.0000	16.0000	192.0000	0.0082
600	0.03799	0.03618	1346.800	9.6000	19.2000	230.4000	0.0077
700	0.03917	0.0373	1156.428	11.2000	22.4000	268.8000	0.0074
800	0.0403	0.03838	1095.362	12.8000	25.6000	307.2000	0.0071
900	0.04138	0.03941	1156.937	14.4000	28.8000	345.6000	0.0069
1000	0.04242	0.0404	1337.108	16.0000	32.0000	384.0000	0.0067

Appendix

Fluorine ions interact with Bone tissue

E(MeV)	Range ($\frac{g}{cm^2}$)	Thickness (cm)	LET ($\frac{MeV}{cm}$)	Absorbed Dose × 10^{-6} (rad)	Equivalent Dose× 10^{-5} (rem)	Effective Dose× 10^{-7} (rem)	Stopping Time (nm)
0.025	0.00181	0.00166	1393.677	0.0004	0.0008	0.0008	0.03122
0.03	0.00507	0.00464	1518.531	0.0005	0.0010	0.0010	0.07969
0.04	0.00957	0.00876	1657.109	0.0006	0.0013	0.0013	0.13029
0.06	0.01478	0.01354	1888.163	0.0010	0.0019	0.0019	0.16440
0.08	0.01782	0.01632	2112.924	0.0013	0.0026	0.0026	0.17164
0.1	0.01986	0.01733	2333.952	0.0016	0.0032	0.0032	0.17108
0.2	0.02477	0.01819	3391.623	0.0032	0.0064	0.0064	0.15091
0.3	0.02687	0.02269	4377.300	0.0048	0.0096	0.0096	0.13365
0.4	0.02809	0.02461	5297.672	0.0064	0.0128	0.0128	0.12100
0.6	0.02951	0.02573	6964.461	0.0096	0.0192	0.0192	0.10378
0.8	0.03033	0.02702	8429.999	0.0128	0.0256	0.0256	0.09239
1	0.03089	0.02778	9724.707	0.0160	0.0320	0.0320	0.08415
1.1	0.03110	0.02829	10315.899	0.0176	0.0352	0.0352	0.08079
1.2	0.03129	0.02848	10873.267	0.0192	0.0384	0.0384	0.07782
1.3	0.03146	0.02865	11399.213	0.0208	0.0416	0.0416	0.07516
1.4	0.03160	0.02881	11895.919	0.0224	0.0448	0.0448	0.07276
1.5	0.03173	0.02894	12365.378	0.0240	0.0480	0.0480	0.07058
1.6	0.03185	0.02906	12809.410	0.0256	0.0512	0.0512	0.06859
1.7	0.03195	0.02917	13229.681	0.0272	0.0544	0.0544	0.06677
1.8	0.03205	0.02926	13627.718	0.0288	0.0576	0.0576	0.06508
2	0.03222	0.02935	14362.597	0.0320	0.0640	0.0640	0.06207
2.25	0.03240	0.02951	15178.891	0.0360	0.0720	0.0720	0.05885
2.5	0.03255	0.02967	15896.553	0.0400	0.0800	0.0800	0.05609
2.75	0.03268	0.02981	16529.033	0.0440	0.0880	0.0880	0.05369
3	0.03279	0.02993	17087.537	0.0480	0.0960	0.0960	0.05158
3.25	0.03289	0.03003	17581.472	0.0520	0.1040	0.1040	0.04970
3.5	0.03298	0.03012	18018.787	0.0560	0.1120	0.1120	0.04802
3.75	0.03305	0.03020	18406.246	0.0600	0.1200	0.1200	0.04650
4	0.03312	0.03027	18749.633	0.0640	0.1280	0.1280	0.04512
4.5	0.03325	0.03033	19323.424	0.0720	0.1440	0.1440	0.04269
5	0.03335	0.03044	19772.512	0.0800	0.1600	0.1600	0.04063
5.5	0.03343	0.03054	20121.476	0.0880	0.1760	0.1760	0.03884
6	0.03351	0.03062	20389.288	0.0960	0.1920	0.1920	0.03727
6.5	0.03357	0.03069	20590.793	0.1040	0.2080	0.2080	0.03588
7	0.03363	0.03075	20737.746	0.1120	0.2240	0.2240	0.03463
8	0.03373	0.03080	20903.823	0.1280	0.2560	0.2560	0.03249
9	0.03414	0.03089	20943.394	0.1440	0.2880	0.2880	0.03101
10	0.03421	0.03127	20894.005	0.1600	0.3200	0.3200	0.02947
12	0.03432	0.03132	20624.328	0.1920	0.3840	0.3840	0.02699
14	0.03443	0.03153	20224.308	0.2240	0.4480	0.4480	0.02507
16	0.03453	0.03162	19761.880	0.2560	0.5120	0.5120	0.02352
18	0.03472	0.03171	19274.283	0.2880	0.5760	0.5760	0.02223
20	0.03553	0.03180	18782.433	0.3200	0.6400	0.6400	0.02115
40	0.03621	0.03254	14741.218	0.6400	1.2800	1.2800	0.01531
60	0.03680	0.03316	12218.590	0.9600	1.9200	1.9200	0.01273
80	0.03735	0.03370	10537.583	1.2800	2.5600	2.5600	0.01121
100	0.03786	0.03396	9326.321	1.6000	3.2000	3.2000	0.01017
120	0.03879	0.03467	8400.326	1.9200	3.8400	3.8400	0.00941
140	0.03833	0.03510	7660.437	2.2400	4.4800	4.4800	0.00883
160	0.03922	0.03572	7049.100	2.5600	5.1200	5.1200	0.00835
180	0.03964	0.03592	6530.750	2.8800	5.7600	5.7600	0.00796
200	0.04155	0.03630	6082.269	3.2000	6.4000	6.4000	0.00764
300	0.04324	0.03805	4473.580	4.8000	9.6000	9.6000	0.00653
400	0.04403	0.03959	3445.464	6.4000	12.8000	12.8000	0.00589
500	0.04478	0.04101	2743.315	8.0000	16.0000	16.0000	0.00546
600	0.04691	0.04233	2275.112	9.6000	19.2000	19.2000	0.00514
700	0.04758	0.04357	1999.531	11.2000	22.4000	22.4000	0.00490
800	0.04887	0.04475	1895.264	12.8000	25.6000	25.6000	0.00471
900	0.05010	0.04588	1950.208	14.4000	28.8000	28.8000	0.00455
1000	0.05128	0.04696	2156.983	16.0000	32.0000	32.0000	0.00442

Appendix

Fluorine ions interact with Skin tissue

E(MeV)	Range ($\frac{g}{cm^2}$)	Thickness (cm)	LET ($\frac{MeV}{cm}$)	Absorbed Dose × 10^{-6} (rad)	Equivalent Dose× 10^{-5} (rem)	Effective Dose× 10^{-7} (rem)	Stopping Time (nm)
0.025	0.00135	0.00124	1124.117	0.0004	0.0008	0.0008	0.0233
0.03	0.00385	0.00354	1161.469	0.0005	0.0010	0.0010	0.0606
0.04	0.00732	0.00672	1235.838	0.0006	0.0013	0.0013	0.0997
0.06	0.01137	0.01043	1383.255	0.0010	0.0019	0.0019	0.1264
0.08	0.01374	0.01261	1528.930	0.0013	0.0026	0.0026	0.1323
0.1	0.01534	0.01407	1672.892	0.0016	0.0032	0.0032	0.1321
0.2	0.01922	0.01764	2367.879	0.0032	0.0064	0.0064	0.1171
0.3	0.0209	0.01917	3023.748	0.0048	0.0096	0.0096	0.1039
0.4	0.02188	0.02007	3643.423	0.0064	0.0128	0.0128	0.0943
0.6	0.02303	0.02113	4786.075	0.0096	0.0192	0.0192	0.0810
0.8	0.0237	0.02174	5853.177	0.0128	0.0256	0.0256	0.0722
1	0.02415	0.02216	6675.533	0.0160	0.0320	0.0320	0.0658
1.1	0.02433	0.02232	7107.761	0.0176	0.0352	0.0352	0.0632
1.2	0.02448	0.02246	7512.136	0.0192	0.0384	0.0384	0.0609
1.3	0.02462	0.02258	7894.250	0.0208	0.0416	0.0416	0.0588
1.4	0.02474	0.02269	8256.420	0.0224	0.0448	0.0448	0.0570
1.5	0.02484	0.02279	8600.175	0.0240	0.0480	0.0480	0.0553
1.6	0.02494	0.02288	8926.737	0.0256	0.0512	0.0512	0.0537
1.7	0.02503	0.02296	9237.161	0.0272	0.0544	0.0544	0.0523
1.8	0.02511	0.02304	9532.392	0.0288	0.0576	0.0576	0.0510
2	0.02525	0.02317	10080.658	0.0320	0.0640	0.0640	0.0486
2.25	0.0254	0.0233	10694.553	0.0360	0.0720	0.0720	0.0461
2.5	0.02552	0.02342	11238.484	0.0400	0.0800	0.0800	0.0440
2.75	0.02563	0.02352	11721.045	0.0440	0.0880	0.0880	0.0421
3	0.02572	0.0236	12149.554	0.0480	0.0960	0.0960	0.0405
3.25	0.02581	0.02368	12530.288	0.0520	0.1040	0.1040	0.0390
3.5	0.02588	0.02374	12868.654	0.0560	0.1120	0.1120	0.0377
3.75	0.02594	0.0238	13169.338	0.0600	0.1200	0.1200	0.0365
4	0.026	0.02386	13436.415	0.0640	0.1280	0.1280	0.0354
4.5	0.0261	0.02395	13883.549	0.0720	0.1440	0.1440	0.0335
5	0.02619	0.02403	14233.631	0.0800	0.1600	0.1600	0.0319
5.5	0.02626	0.02409	14505.001	0.0880	0.1760	0.1760	0.0305
6	0.02633	0.02415	14712.095	0.0960	0.1920	0.1920	0.0293
6.5	0.02638	0.0242	14866.394	0.1040	0.2080	0.2080	0.0282
7	0.02643	0.02425	14977.109	0.1120	0.2240	0.2240	0.0272
8	0.02652	0.02433	15096.235	0.1280	0.2560	0.2560	0.0255
9	0.02676	0.02455	15114.233	0.1440	0.2880	0.2880	0.0243
10	0.02681	0.0246	15061.531	0.1600	0.3200	0.3200	0.0231
12	0.0269	0.02468	14822.314	0.1920	0.3840	0.3840	0.0212
14	0.02699	0.02476	14484.239	0.2240	0.4480	0.4480	0.0197
16	0.02707	0.02484	14102.292	0.2560	0.5120	0.5120	0.0184
18	0.02715	0.02491	13706.041	0.2880	0.5760	0.5760	0.0174
20	0.02723	0.02498	13311.597	0.3200	0.6400	0.6400	0.0166
40	0.02789	0.02559	10215.548	0.6400	1.2800	1.2800	0.0120
60	0.02845	0.0261	8386.283	0.9600	1.9200	1.9200	0.0100
80	0.02895	0.02656	7202.388	1.2800	2.5600	2.5600	0.0088
100	0.0294	0.02697	6363.427	1.6000	3.2000	3.2000	0.0080
120	0.02983	0.02737	5728.242	1.9200	3.8400	3.8400	0.0074
140	0.03023	0.02774	5223.472	2.2400	4.4800	4.4800	0.0070
160	0.03062	0.02809	4807.529	2.5600	5.1200	5.1200	0.0066
180	0.03099	0.02843	4455.160	2.8800	5.7600	5.7600	0.0063
200	0.03134	0.02875	4150.169	3.2000	6.4000	6.4000	0.0060
300	0.03297	0.03025	3050.343	4.8000	9.6000	9.6000	0.0052
400	0.03442	0.03158	2336.633	6.4000	12.8000	12.8000	0.0047
500	0.03575	0.0328	1839.163	8.0000	16.0000	16.0000	0.0044
600	0.037	0.03395	1497.460	9.6000	19.2000	19.2000	0.0041
700	0.03818	0.03503	1284.608	11.2000	22.4000	22.4000	0.0039
800	0.0393	0.03606	1186.811	12.8000	25.6000	25.6000	0.0038
900	0.04038	0.03705	1196.270	14.4000	28.8000	28.8000	0.0037
1000	0.04142	0.038	1308.241	16.0000	32.0000	32.0000	0.0036

الخلاصة

ساهمت علوم الفيزياء النووية بشكل كبير في تطوير استخدام الأيونات الثقيلة في علاج الأورام بسبب قدرتها على قتل الأنسجة المصابة بدقة عالية دون التأثير على الأنسجة السليمة المحيطة بالورم كذلك قدرتها على تأين الأنسجة المصابة وبالتالي تدمير الخلايا السرطانية بأقل جرعة تم امتصاصها من الإشعاع . لذا يتوجب تقديم وصف دقيق لفقدان طاقة الايونات الثقيلة ومداها داخل الانسجة .

في هذه الدراسة ، تم حساب قدرة الايقاف والمدى للأيونات الثقيلة (^7Li ، ^{12}C ، ^{16}O، ^{19}F) التي تتفاعل مع ثمانية انسجة بشرية وهي (الانسجة الدهنية ، الدم ، الثدي ، الدماغ ، الرئة ، العضلات ، العظام ، الجلد) باستخدام ستة طرق (SRIM، SRIM Dictionary ، برنامج CasP ، برنامج PASS ، برنامج MSATR ، ومعادلة Bethe) ضمن مدى الطاقة (1000-0.025) MeV . وقد تم ملاحظة فروقات طفيفة في قدرة الايقاف الكتلية المحسوبة بواسطة الست طرق وقد تم تفسير هذه الاختلافات وبيان اسبابها . ومن خلال استخدام برنامج الماتلاب ، تم التوصل الى صيغة شبة تجريبية لحساب قدرة الايقاف الكتلية للايونات الثقيلة ومداها داخل هذه الانسجة من خلال معرفة طاقة هذه الايونات . كما تم حساب مقدار الطاقة الخطية المنتقلة (LET) وسمك هذة الانسجة وزمن ايقاف الايون الثقيل داخل هذه الانسجة . بالاضافة الى حساب الجرعة والجرعة المكافئة والجرعة الفعالة لهذه الايونات الثقيلة .

اظهرت النتائج زيادة قيم فقدان الطاقة الكلية مع زيادة العدد الذري للجسيم الساقط ويعزى ذلك الى ان قدرة الايقاف تتناسب تناسبا طرديا مع مربع العدد الذري للجسيم الساقط ، كذلك عند استخدام جسيمات مشحونة ثقيلة يمكن تشكيل قمة Bragg الحادة اللازمة لايداع معظم طاقة الجسيمات المشحونة الثقيلة في كتلة الورم من اجل تحقيق افضل علاج وتقليل احداث ضرر في الانسجة المحيطة بالورم.

بمقارنة النتائج التي تم التوصل إليها من حساب قدرة الايقاف الكتلية للأنسجة الدهنية والأنسجة العظمية مع ICRU-73 نجد انها كانت متفقة جدا والى حد كبير معها .

جمهورية العراق
وزارة التعليم العالي والبحث العلمي
جامعة بغداد
كلية التربية للعلوم الصرفة ابن الهيثم

قدرة الايقاف ومدى الايونات الثقيلة في انسجة جسم الانسان

اطروحة مقدمة

الى كلية التربية – ابن الهيثم – جامعة بغداد كجزء من متطلبات نيل درجة دكتوراه فلسفة في علوم الفيزياء

من قبل

زينة جميل رحيم

بكلوريوس في الفيزياء ، كلية التربية للعلوم الصرفة/ ابن الهيثمـ جامعة بغداد 2007

ماجستير في علوم الفيزياء ، كلية التربية للعلوم الصرفة / ابن الهيثمـ جامعة بغداد 2010

بأشراف
أ. د. بشائر محمد سعيد

1440 هـ   2019 م